

MODELING OF VISCOELASTIC EFFECTS ON
WEB HANDLING SYSTEM BEHAVIOR

By

XIAOFENG GUAN

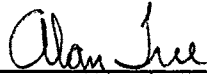
Bachelor of Science
Dalian University of Technology
Dalian, Liaoning, PRC
1982

Master of Science
Dalian University of Technology
Dalian, Liaoning, PRC
1984

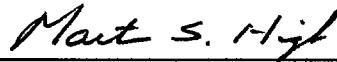
Submitted to the Faculty of the
Graduate College of the
Oklahoma State University
in partial fulfillment of
the requirements for
the Degree of
DOCTOR OF PHILOSOPHY
May, 1995

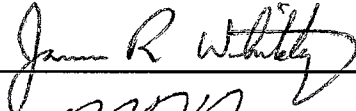
MODELING OF VISCOELASTIC EFFECTS ON
WEB HANDLING SYSTEM BEHAVIOR

Thesis Approved:



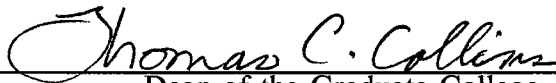
Thesis Advisor











Dean of the Graduate College

ACKNOWLEDGEMENTS

I wish to express my special appreciation to my major advisor, Dr. D. Alan Tree for his intelligent guidance, invaluable helpfulness, inspiration and friendship throughout my Ph.D. program.

I also express my sincere gratitude to Dr. Martin S. High, Dr. Kenneth J. Bell, Dr. Khaled A. M. Gasem, Dr. Rob Whiteley and Dr. R. D. Delahoussaye for serving as my thesis committee members and giving me assistance and suggestions for this study.

Many thanks are expressed to Dr. Karl N. Reid, Dr. K.-C. Lin and Dr. Y.-C. Shiau for their encouragement and constructive discussions. Members of the Tree group have helped me in innumerable ways and I must make special mention of T.-C. Tsai, S. Ma, M. Rajasekhar, and S. Balasubramaniam.

I would like to take this opportunity to thank my parents for their encouragement and sacrifice; my wife, Xiaoping Shi and my daughter, Yang Guan for their understanding, sacrifice and help during my study.

Finally, I thank the School of Chemical Engineering for providing me the opportunity by accepting me into the Graduate Program. Financial support from the Oklahoma Center for Integrated Design and Manufacture for this work is greatly acknowledged.

TABLE OF CONTENTS

Chapter	Page
I. INTRODUCTION	1
II. BACKGROUND	6
2.1 Web Handling System Models	7
2.2 Viscoelastic Properties and Behavior	11
2.3 Rheological Equations of State	16
2.4 Modeling of Extensional Deformation in Transporting Processes	23
2.5 Numerical Methods and Techniques	27
2.6 Summary	28
III. MODEL DEVELOPMENT	30
3.1 System Analysis	30
3.2 Assumptions	36
3.3 Governing Equations	39
3.3.1 Mass Conservation	39
3.3.2 Force Balance	40
3.3.3 The Rheological Equation of State	41
3.3.4 Strain in the Web Material	46
3.3.5 Elastic Response in the Contact Region	48
3.3.6 Initial and Boundary Conditions	50
3.3.7 Summary of the Governing Equations	51
3.4 Non-Dimensionalization	51
3.4.1 Dimensionless Governing Equations	52
3.4.2 Initial and Boundary Conditions	53
3.5 Governing Equation in Steady State	54
3.6 Chapter Review	57
IV. NUMERICAL METHODS AND TECHNIQUES	59
4.1 Steady State	59

4.2	Transient State	63
4.2.1	Discretization of Governing Equations	67
4.2.1.1	Discretization of Eq. (4.18)	68
4.2.1.2	Discretization of Eq. (4.19)	69
4.2.1.3	Discretization of Eq. (4.20)	69
4.2.1.4	Discretization of Eq. (4.21)	70
4.2.2	Treatment of the Boundary Conditions	71
4.2.3	Solution Strategy	73
4.3	Special Concerns	75
4.3.1	Consistency	75
4.3.2	Stability	76
4.3.3	Convergence	78
4.3.4	Numerical Testing	79
4.4	Chapter Review	83
V.	NUMERICAL RESULTS AND DISCUSSION	85
5.1	Verification	86
5.1.1	Example: Fiber Spinning	87
5.1.2	Purely Elastic Model Case	90
5.1.3	Transient Procedure	93
5.2	Estimation of Model Parameters	96
5.3	Steady-State Analysis	98
5.3.1	Single-Span Behavior	99
5.3.2	Irrecoverable Deformation	101
5.3.3	Effects of the Power Law Exponent, n	104
5.3.4	Stress Ratio	106
5.3.5	Effects of Irrecoverable Deformation	107
5.3.6	Effects of Slackness in Multi-Span Systems	113
5.3.7	Tension Transfer	116
5.3.8	Summary	117
5.4	Unsteady-State Analysis	119
5.4.1	Start-Up Procedure	120
5.4.1.1	Effect of Deborah Number on Tension Variation	120

5.4.1.2	Viscoelastic Behavior in a Three-Span System . . .	123
5.4.1.3	Summary	132
5.4.2	Transition from One Steady State to Another	132
5.4.2.1	Effect of Deborah Number on Tension Variation .	134
5.4.2.2	Effect of Transient Time of Velocity on Tension Variation	137
5.4.2.3	Summary	137
5.4.3	Sinusoidal Disturbance about a Steady State	139
5.4.3.1	Effects of Deborah Number and Disturbance Parameters on Tension	139
5.4.3.2	Viscoelastic Behavior in a Three-Span System . .	148
5.4.3.3	Summary	152
5.5	Chapter Review	153
VI.	CONCLUSIONS AND RECOMMENDATIONS	154
6.1	Conclusions	154
6.2	Recommendations	156
	REFERENCES	159
	APPENDIXES	167
APPENDIX A	TRANSFORMATION OF EQS. (3.50)-(3.53) TO EQS. (4.18)-(4.21)	168
APPENDIX B	AN ANALYTICAL SOLUTION OF THE PURELY ELASTIC MODEL	170
APPENDIX C	IRRECOVERABLE DEFORMATION	176
APPENDIX D	EFFECT OF n ON ϵ_p/ϵ_t AT VERY HIGH D_{Rs}	178
APPENDIX E	MINIMUM REQUIRED DRAW RATIO	181
APPENDIX F	SIMULATION FOR MULTI-SPAN SYSTEMS IN TRANSITION BETWEEN TWO STEADY STATES . .	183
F.1	Viscoelastic Behavior in a Three-Span System	183
F.2	Transition between Two Steady States in a Four-Span System	187
F.3	Summary	189

APPENDIX G	ADDITIONAL SIMULATION FOR SINUSOIDAL DISTURBANCE CASES	194
G.1	Sinusoidal Disturbance in a Single-Span System	194
G.2	Sinusoidal Disturbance in a Four-Span System	194
APPENDIX H	COMPUTER CODES	200
APPENDIX I	AN EXAMPLE PROBLEM	222

LIST OF TABLES

Table	Page
4.1 Steady-State Tensions with Different $\Delta\xi$	81
4.2 Stable Conditions for Different $\Delta\xi$ and $\Delta\theta$	83
5.1 Estimation of m and n	98
5.2 Strain Ratio in a Single-Span System	101
5.3 Tension Predictions in the Second and Third Spans	115
5.4 Tension in the Second Span	116

LIST OF FIGURES

Figure	Page
2.1 Turntable Problem	19
2.2 Schematic Illustration of Tension Transfer Mechanism	24
2.3 Schematic Illustration of Strain Variations in a Span	26
3.1 A Typical Web Handling System	31
3.2 An Isolated Span with a Coordinate System	35
3.3 A Control Volume Cut from a Web Line	37
3.4 A Schematic Showing Strain at Three Different Positions	47
4.1 Shooting Procedure	64
4.2 Solution Procedure	74
4.3 A Single-Span System at Steady State	80
4.4 A Single-Span System Subjected to a Start-Up Procedure	82
5.1 Velocity Profile for a Polystyrene Melt in a Fiber Spinning Process	89
5.2 An Example in Modeling Web Handling Systems	91
5.3 A Two-Span System with an Elastic Material Undergoing a Start-Up Procedure	94
5.4 Comparison of Numerical and Analytical Simulation for the Elastic Model in the Start-Up Procedure (a) First Span, (b) Second Span with $v_{s3} = 2.51$ m/s, (c) Second Span with $v_{s3} = 2.52$ m/s, and (d) Second Span with $v_{s3} = 2.53$ m/s	95
5.5 A Case Study of a Single Span	100

5.6	Permanent Deformation as a Function of Deborah Number with Draw Ratio as a Parameter for a Single Span	103
5.7	Permanent Deformation as a Function of Deborah Number with the Power Law Exponent as a Parameter	105
5.8	Dimensionless Inverse Tension as a Function of Deborah Number with Draw Ratio as a Parameter for a Single Span	108
5.9	A Two-Span System Studied for the Effect of the Irrecoverable Deformation	109
5.10	Minimum Required Draw Ratio to Prevent Slackness in the Second Span as a Function of the Draw Ratio in the First Span with Deborah Number as a Parameter	112
5.11	A Three-Span System at Steady State	114
5.12	Deviations of Hookean Results from Viscoelastic Results as a Function of Roller's Velocity at the Third Roller Set of a Two-Span System	118
5.13	Velocity Function in the Start-Up Procedure	121
5.14	A Single-Span System Subjected to a Start-Up Procedure	122
5.15	Dimensionless Tension as a Function of Dimensionless Time with De as a Parameter During Start-Up	124
5.16	A Three-Span System Subjected to a Start-Up Procedure	126
5.17	Tension in the First Span of a Three-Span System	127
5.18	Tension in the Second Span of a Three-Span System (a) $v_{s3} = 2.501$ m/s, (b) $v_{s3} = 2.51$ m/s, (c) $v_{s3} = 2.52$ m/s, and (d) $v_{s3} = 2.53$ m/s	128
5.19	Tension in the Third Span of a Three-Span System, $v_{s3} = 2.51$ m/s	131
5.20	Velocity Function from One Steady State to Another	133
5.21	A Single-Span System Subjected to a Variation in v_2	135
5.22	Effect of Deborah Number on Tension Variation During the Transition from One Steady State to Another	136

5.23	Effect of Transient Time of Velocity on Tension Variation in a Single-Span System	138
5.24	A Single-Span System with v_2 Changing Sinusoidally	140
5.25	An Eccentrically Mounted Roller	142
5.26	Tension variation in a Single-Span System due to a Disturbance in v_2 , $D_{Rs} = 1.00222$, $\delta_e/R_{avg} = 0.05\%$, $\omega_1 = 10.0222$, and $n = 1$	144
5.27	Δf as a Function of (a) De , (b) δ_e/R_{avg} , and (c) ω_1 for a Single-Span System with $D_{Rs} = 1.00222$ and $n = 1$	145
5.28	ψ as a Function of De for a Single-Span System with $D_{Rs} = 1.00222$, $\delta_e/R_{avg} = 0.05\%$, $\omega_1 = 10.0222$, and $n = 1$	147
5.29	ψ as a Function of ω_1 for a Single-Span System with $D_{Rs} = 1.00222$, $De = 13.5$, $\delta_e/R_{avg} = 0.05\%$, and $n = 1$	149
5.30	A Three-Span System with v_3 Changing Sinusoidally	150
5.31	Tension Variations in a Three-Span System due to a Disturbance in v_3 (a) First Span, (b) Second Span, and (c) Third Span	151
B.1	A Two-Span System with Purely Elastic Material Properties Subjected to a Start-Up Procedure	171
D.1	ϵ_p/ϵ_t as a Function of n with D_{Rs} as a Parameter (for $De = 10$)	179
D.2	ϵ_p/ϵ_t as a Function of n with D_{Rs} as a Parameter (for $De = 1$)	180
F.1	A Three-Span System Subjected to a Variation in v_3	184
F.2	Tension in a Three-Span System During the Transition between Two Steady States due to the Variation in v_3 (a) First Span, (b) Second Span, and (c) Third Span	185
F.3	Tension in a Three-Span System During the Transition between Two Steady States due to the Variations in v_3 and v_4 (a) First Span, (b) Second span, and (c) Third Span	188
F.4	A Four-Span System Subjected to a Variation in v_3	190
F.5	Tension in a Four-Span System Subjected to a Variation in v_3 , simulated by the Elastic Model	191

F.6	Tension in a Four-Span System Subjected to a Variation in v_3 , simulated by the Viscoelastic Model	192
G.1	Tension Variations in a Single-Span System with $De = 13.5$ by Changing v_1 or v_2	195
G.2	A Four-Span System with v_3 Changing Sinusoidally	196
G.3	Tension Variations in a Four-Span System Subjected to a Disturbance in v_3 (Viscoelastic Simulation)	198
G.4	Tension Variations in a Four-Span System Subjected to a Disturbance in v_3 (Elastic Simulation)	199

NOMENCLATURE

a	dimensionless cross-sectional area of web
a_s	dimensionless cross-sectional area of web at steady state
A	cross-sectional area of web
A_s	cross-sectional area of web at steady state
A_i	cross-sectional area of web at labeled position ($i = u, 1$ or 2)
c	tension transfer parameter
De	Deborah number
D_R	draw ratio
D_{Rs}	draw ratio at steady state
E	Young's modulus
f	dimensionless tension
F	tension
F_s	tension at steady state
G	elastic modulus
L	length of span
m	power law coefficient
n	power law exponent
N	dimensionless inverse tension or stress ratio
p	isotropic pressure

p_a	ambient pressure
R_{avg}	average radius of an eccentric roller or roll
R_{max}	maximum radius of an eccentric roller or roll
R_{min}	minimum radius of an eccentric roller or roll
t	time
T_{ij}	dimensionless viscous stress tensor (i and j = x, y or z)
T_{ijs}	T_{ij} at steady state
v_{amp}	amplitude of velocity
v_i or \underline{v}	velocity vector (i = x, y or z)
v_{zs}	v_z at steady state
$v_1, v_2 \dots$	tangential velocities of roller 1, roller 2 ...
$v_{s1}, v_{s2} \dots$	$v_1, v_2 \dots$ at steady state

Greek Symbols

α, β	incline angles of web surfaces
γ_{ij} or $\underline{\gamma}$	strain tensor (i, j = x, y or z)
$\underline{\gamma}^{(1)}$	first-order contravariant convected time derivative of $\underline{\gamma}$ or strain rate tensor $\underline{\dot{\gamma}}$
$\dot{\gamma}$	magnitude (second invariant) of the strain rate tensor
δ_{ij}	Kronecker delta
δ_e	center offset of an eccentric roller or roll
Δ	difference operator
ϵ_e	elastic component of ϵ_z across web/roller contact region
$\Delta\epsilon_e$	recovered elastic component of ϵ_t in unloading
ϵ_p	irrecoverable component of ϵ_t

ϵ_t	total amount of ϵ_z at $z = L$
ϵ_{ve}	viscoelastic component of ϵ_z in open span
ϵ_z	strain in z-direction
$(\epsilon_z)_i$	strain in z-direction at labeled position ($i = 1$ or 2)
ϵ_{zs}	ϵ_z at steady state
η	viscosity
η_c	characteristic viscosity
θ	dimensionless time
λ_0	zero-shear-rate relaxation time
ξ	dimensionless length
ρ	density
σ_{ij}	total stress tensor (i and $j = x, y$ or z)
τ_{ij} or $\underline{\tau}$	viscous stress tensor (i and $j = x, y$ or z)
$\underline{\tau}^{(1)}$	contravariant convected time derivative of $\underline{\tau}$
ϕ	dimensionless velocity in z-direction
ϕ_s	ϕ at steady state
ϕ_1	ϕ at $\xi = 1$
$(\phi_s)_1$	ϕ_s at $\xi = 1$
ω	angular velocity
ω_1	dimensionless angular velocity
ψ	phase angle difference
Subscripts	
i	point in space
L	position at the end of a span

x, y, z	indicating x-, y- and z-directions, respectively
ξ	derivative with respect to ξ
$0^-, 0^+$	positions just before and after the entry roller of a span, respectively
00	initial value
$1, 2, 3, \dots$	roller number or span number

Superscripts

j	time step
T	transpose

Mathematical Symbols

∇	gradient operator
'	first-order direct derivative with respect to ξ
"	second-order direct derivative with respect to ξ
overline	predicted value

CHAPTER I

INTRODUCTION

The manufacture and treatment of web materials, which include polymer films, paper, metallic foils, and fabrics, present a unique challenge. These materials are usually very long, thin, and highly flexible. Since the webs are flexible and moving at high speeds, controlling the processing is difficult without a precise model. The goal of this thesis is to develop a web handling model which captures the viscoelastic behavior of materials to give more confident control of the web handling process.

Among the concerns for the web handling systems, tension control is paramount since the product qualities and the stable operations of web handling systems rely on the tension levels in the webs. For example, a coating procedure requires the proper tension in the substrate in order to obtain a product with acceptable interaction between the substrate and the coating layer. Improper tension may also result in slackness of the web line, breakage of the web materials, slippage between the web and the rollers, or wrinkling of the web.

The tension in the web is a function of the operating conditions, the system configuration and the web material response. A slight variation in the speed difference between the rollers at the ends of a span will result in a large change in the tension level in the system. Tension in a free span depends not only on the velocity

difference at the two ends of the span but also on the tension level in the upstream span. This phenomenon, referred to as "tension transfer" (Shin, 1991), is closely related to the system configuration.

The material response is also an important factor in the tension control. Most web materials, especially polymer films at higher temperatures or wet paper, exhibit viscoelastic behavior, i.e., the material response to the applied force can be attributed to the combination of the present time conditions as well as past rheological events. This time-dependent, partially viscous and partially elastic deformation behavior makes the tension control very difficult.

The control strategy is another significant issue. There have been two major control methods in the web handling systems: open-loop and closed-loop (Shin, 1991; Reid and Lin, 1993). The open-loop control measures and controls the speed. Closed-loop control directly measures the tension level in the span and adjusts the roller speed in order to maintain the desired tension value. Practical difficulties associated with measuring the tension on line have hampered the use of closed-loop control. As expected, open-loop control is more sensitive to the material response than the closed-loop control since the tension level in the span is a strong function of the material properties. Therefore, the roller speeds must be controlled with extreme accuracy and the relationship of roller speed to tension known with a high degree of precision.

Due to the complexity of web handling systems, modeling of the system is not an easy task, especially when viscoelasticity is incorporated into the model. Some

models have been developed which use a purely elastic material response (Hooke's Law). However, a realistic model must include the viscoelastic properties of the web. In fact, the purely elastic model is a limiting case of the viscoelastic response exhibited by most web materials and would be included in a realistic viscoelastic model.

In a viscoelastic material, the deformation is continuous, although not produced at a constant rate, throughout a free span. The viscous component of the deformation allows the stress to relax to some extent. In contrast, a purely elastic model allows only for a step change in the deformation to occur at the beginning of the span. Thereafter, the deformation remains constant meaning that there is no possibility to model stress relaxation. Moreover, the permanent deformation due to the viscoelasticity will affect the tension distribution in the subsequent spans and may result in undesired operating conditions.

In addition, the interaction of the web line and rolls or rollers may severely affect the system behavior. Rolls and rollers apply the driving forces, provide the moving velocities, and serve as supports to the web line by direct contact. In the contact region, the web material undergoes a rapid change of kinematic conditions. For the viscoelastic material, this rapid change may seriously influence the tension transfer from the upstream span to the downstream span as well as the viscoelastic responses in the subsequent spans.

Under transient operating conditions such as start-up or shut-down of the system, viscoelasticity is even more significant since relaxation will affect the system

behavior. Purely elastic models cannot predict the dynamic response resulting from the relaxation.

This study was motivated by the need for a viscoelastic model. Also, the study provides a means for evaluating the effects of the viscoelasticity. Open-loop control problems are major concerns, but the methods and techniques are essentially the same for the closed-loop control problems.

In Chapter II, the background in the field is introduced and the relevant literature is reviewed. Considerable attention is drawn to the previous studies of viscoelastic models and constitutive equations.

In Chapter III, the viscoelastic model is developed through system analysis, appropriate assumptions, and the establishment of governing equations. The White-Metzner rheological equation of state was used to model viscoelastic behavior. Non-dimensionalization is further carried out to enable the model to be suitable to general analysis. In addition, boundary and initial conditions are set for the governing equations.

Chapter IV describes and develops the numerical methods and the formulations. As an analytical solution to the model was not possible, two different numerical methods were used for the steady-state and unsteady-state analyses, respectively.

Chapter V presents the numerical simulation results and discussions for both steady state and unsteady state. Parameter studies were performed to investigate the effects of the viscoelasticity by varying the viscoelastic properties. The tension

distribution is the major concern, and is examined in several significantly different cases. Also, the viscoelastic results are compared to the purely elastic simulation in order to emphasize the significance of the viscoelastic model.

Finally, in Chapter VI, conclusions are drawn, and recommendations are made for future studies.

CHAPTER II

BACKGROUND

Significant attention has been given to the modeling of web handling systems during the past several decades. Current models capture the behavior of complex multi-span systems under the assumption that the web materials behave as Hookean solids. However, the literature also shows that nearly all web materials have some degree of viscoelastic character. This chapter reviews the development of web handling models and presents the essential elements of viscoelastic modeling and numerical solutions to systems of differential equations.

In spite of extensive studies on web handling systems, the effect of viscoelasticity on tension control is still somewhat of a mystery in multi-span systems. Undesired operations could result from influence of viscoelastic behavior of materials. Modern web handling industries require precise control of web tensions since significant economic loss and unacceptable product quality result from malfunctions of the operating systems. Thus, even though the incorporation of viscoelasticity may significantly complicate the modeling, a realistic and rigorous model which includes viscoelastic response is essential for the accurate tension control.

2.1 Web Handling System Models

Work on modeling web handling systems can be traced to the late 1950's. Campbell (1958) related the tension of the moving web material in a free span to the deformation of the web by assuming that the material obeyed Hooke's law. The dynamic change of the tension was also modeled for a free span. Campbell clearly recognized the need to include viscoelasticity in his model and made an initial attempt to account for viscoelastic effects in the formulation by adding one more term to the elastic model. However, the model was not fully examined for details of the viscoelastic behavior of web handling systems and did not consider the effect of tension transfer from the previous span.

Models have also been proposed by Grenfell (1963), Brandenburg (1976) and Taguchi et al. (1985). Grenfell also assumed Hookean behavior but introduced the tension transfer effect into the mathematical model which allowed the model to simulate the interaction of adjacent spans in multi-span systems. Steady-state system behavior as well as dynamic responses with step change and sinusoidal variation of the end speeds were formulated in the model. Grenfell noted, from the simulation results, that the tension did not instantaneously respond to step changes in roller speeds even though the material was purely elastic. The delay in tension response could be correlated by a time constant that reflected the residence time of a material particle in the span.

Based on a purely elastic analysis, Brandenburg (1976) also conducted mathematical simulation for the dynamic behavior of web handling systems. The

purely elastic analysis revealed that the stress, strain and velocity in a free span at steady state and under transient conditions do not vary with position. This conclusion is true for Hookean materials since all deformation occurs at the beginning of the span when the web enters the current span, and the tension is constant in the span if the inertial forces can be neglected due to very small mass of the web. However, real web handling systems show continuous deformation through out the span due to the viscoelastic nature of the material.

Brandenburg's model also showed that the velocity of the web in contact with a roller is not instantly identical to the surface velocity of the roller. The web velocity gradually changes from the value of the previous span to the value of the current span going through an adhesion zone and a sliding zone. This phenomenon has also been reported and modeled by Whitworth and Harrison (1983) and Shin (1991).

The interaction of tensions in multi-span systems was also studied by Taguchi et al. (1985), who related the tension difference before and after the drag (driven) roller to the friction force in the web/roller contact region. An actual measurement showed that the tension transfer was significantly affected by the slippage between the web and the drag roller. Although Taguchi et al. acknowledged that viscoelastic effects might influence their system (wet paper), only an elastic analysis was given.

In later work, Shin (1991) produced a systematic method to model a multi-span system. In his model, the systems were assembled from six primitive elements: unwinding roll, free span, driven roller, idle roller, dancer-type device and winding

roll. These elements could be combined to any desired configuration to simulate even the most complex web handling operation. Shin also considered tension transfer in his model.

The results of Shin's model showed that the tension level in the current span of interest depends on the operating conditions in the current span as well as the conditions in the previous span. The tension transfer between spans makes tension control more difficult since the effect of change in one operating parameter (such as roller speed) will propagate through the subsequent spans. Therefore, accurate control of the operating conditions in the current span of interest cannot be maintained to give the desired tension level without controlling the operating conditions in the upstream spans by using some systematic control scheme.

Although viscoelastic effects were not incorporated into his model, Shin pointed out the viscoelastic behavior in the web handling systems and showed that the effect of viscoelasticity on the tension decreases as transport speed increases.

By extending Shin's work, Reid and Lin (1993) conducted simulation for multi-span systems during start up. The variation of the tension during the start-up procedure was fully investigated for systems with simple fixed-gain PID controllers. The elastic analysis indicated that web breakage and instability could occur during the start-up procedure if the system is not properly controlled.

In an experimental investigation, Whitworth and Harrison (1983) reported that the materials (Melinex and HDPE) exhibited typically viscoelastic behavior in tensile tests. In an attempt to account for the effect of the viscoelasticity, the authors

suggested that a viscoelastic dynamic modulus be used to replace the elastic modulus in their model, which was developed to predict the tension variations due to disturbance. However, the formulation was still based on Hooke's law in essence and showed no significant effects from the "viscoelasticity" of the materials.

Another model dealing with longitudinal tension was proposed by Akatsuka (1990) whose mathematical model employs linear viscoelastic equations to simulate the steady-state responses of the web systems. Unfortunately, the model did not include the effect of irrecoverable strains. Calculation results for several two-span systems indicated that no matter what the speed of the third roller, the total strain at the end of the second span is always identical to the strain predicted from the elastic model. Actually, it is expected that the irrecoverable deformation is accumulated in the subsequent spans so that the total strain will be larger than the elastic strain.

Other models for web handling systems, which are based on elastic analyses, can also be found in multi-span systems (Dunn, 1969; Soong and Li, 1979; Young et al., 1989; Young et al., 1989; Parant et al., 1992), tension control (Martin, 1973; Henderson et al., 1979), tension measurements (Horst and Negin, 1992), tension oscillations (Veits et al., 1981), lateral dynamics (Shelton and Reid, 1971a; Shelton and Reid, 1971b), winding mechanism (Pfeiffer, 1966; Pfeiffer, 1968; Rand and Eriksson, 1973; Pfeiffer, 1977), and wrinkles (Gehlbach et al., 1989).

Several viscoelastic studies are also available in winding mechanics (Tramposch, 1967; Mukherjee, 1974; Lin and Westmann, 1989; Kalker, 1991), and single span behavior of paper handling system (Hauptmann and Cutshall, 1977).

2.2 Viscoelastic Properties and Behavior

Most web materials are viscoelastic. The degree of viscoelasticity varies from one material to another and depends on the micro-structures of materials and processing conditions such as temperature, pressure, geometry of deformation, type of force, operating condition, time and prehistory. The viscoelastic properties of web materials as well as viscoelastic behavior of systems are discussed in this section.

The viscoelastic response of a real material exhibits both elastic (recoverable) and viscous (irrecoverable) components. The ratio of viscous to elastic response depends on the manner of deformation, the temperature and the time scale (Ward, 1983). A viscoelastic material will respond to a sudden change in stress with an instant elastic deformation and reacts to a gradual change in stress with both elastic and viscous deformations. Since the viscous deformation requires a finite amount of time, the material response is highly time-dependent. The longer the time over which a stress is applied, the greater viscous component of the deformation. Therefore, a viscoelastic material may respond to an applied stress like a purely elastic solid (governed by Hooke's law) if the time over which the stress is applied is short enough, or like a purely viscous fluid if the time is long enough.

To quantify the viscoelastic behavior, a dimensionless group, the Deborah number, (Bird et al., 1987) may be employed. The Deborah number is defined as the ratio of the characteristic time of the material response to the characteristic time of the process. A zero Deborah number means that viscous fluid behavior is obtained while an infinite Deborah number indicates that the system behaves like a Hookean

elastic solid. Any intermediate Deborah number indicates some degree of viscoelasticity.

In practice, many commercial web handling systems are operated with larger Deborah numbers and, therefore, the elastic analyses for these systems may result in reasonable predictions. However, there are many other systems in which viscoelastic behavior may be so important that the operation and product quality can be significantly affected. The relatively small Deborah number systems consist of either more viscoelastic materials or long residence times and should be analyzed using more rigorous models that include viscoelasticity.

Two types of common web materials have short relaxation times. One is polymeric materials at higher temperatures, and the other is wet paper. An effort has been made to study the viscoelastic properties of the two types of materials (Halsey et al., 1945; Akker, 1970; Smith, 1973; Titomanlio et al., 1976; Rendell et al., 1987). The emphasis has been on relaxation and creep that are typical characteristics of viscoelasticity, though few of the studies have been directly related to the applications in web handling.

Polymeric materials exhibit viscoelastic behavior provided that the operating temperature is high enough. For amorphous or partially crystallized polymers, the amorphous part of the structure undergoes a sharp and dramatic transition of deformation response at a temperature called the glass transition temperature, T_g (Aklonis et al., 1972). Above this temperature (actually a narrow region of temperature), the short range diffusional motions of the polymer segments begin to

occur so that the viscoelastic behavior increases. In this rubbery region, the degree of viscoelasticity may be several orders of magnitude higher than that in the glassy region ($T < T_g$) in which the chain segments are "frozen" in fixed positions with slight vibrating.

Indeed, the organization of the macromolecules plays a critical role in the viscoelastic behavior of polymeric materials. As relaxation takes place over chain distances with time, the relaxation times are strongly dependent on the chain architecture. Thus the molecular weight (related to the structures) and temperature (reflects the thermal activity) are very important in the rheological properties of the polymers (Mark et al., 1984).

Orientation also affects the viscoelastic responses of the polymer materials since the further viscous deformation is restrained, for example in elongational deformation, by the aligned chain structures. Flow-induced crystallization and anisotropy are also typical consequences of the orientation, which influence the viscoelastic behavior (Ericksen, 1962; Perkins and Porter, 1977; Cogswell, 1981; Tree, 1990; McHugh et al., 1991; McHugh et al., 1992).

Since the molecular motions of the polymers are largely restricted in the glassy region, the materials are hard and brittle (Aklonis et al., 1972). But, the polymers in this region are still capable of flowing with a comparatively small degree of viscoelasticity (Lockett, 1972). However, the viscoelastic response of linear polymers will increase rapidly as temperature increases above T_g since the entire polymer molecule can undergo large scale movement. For some other structural types of

polymers such as highly crystalline polymers or lightly cross-linked polymers, the mechanisms of molecular motions are different. However, viscoelasticity will generally increase as the processing temperature increases (Ferry, 1970; Aklonis et al., 1972; Ward, 1983).

Wet paper, as another typical viscoelastic material, is composed of porous, fibrous structures. Although the paper sheet is constructed by macromolecules from natural or synthetic fibers, the deformation mechanism is quite different from that of common polymers.

Structurally, the paper sheet can be considered as fiber network. A fiber in the network is linked to a number of crossing fibers by hydrogen bonds (Nissan, 1977; Hollmark et al., 1978; Page et al., 1979). When the network undergoes straining, the stresses are propagated through fibers and their contact points. Since the distribution of fiber length and direction are random, the stress distribution is microscopically nonuniform and highly dependent on the local structure of the network. The strain in a fiber is dependent on the local network strains and the strain transfer process through the crossing fibers (Hollmark et al., 1978).

The fiber to fiber bonds that are under highly concentrated stresses usually break earlier and the stress will redistribute. Therefore, paper exhibits plastic deformations (Rance, 1956; Sanborn, 1962; Perez, 1970). The weaker the bond is, the more ready it will break.

In a wet paper web, however, the bonds are very weak compared to the fiber strength since the interface between two crossing fibers is formed by water. Since the

bonds cannot withstand any significant shear stress, the fiber has less tendency to break (Williams, 1983). When the sheet is strained, the fibers tend to slide frictionally over the crossing fibers after the bond failure. This mechanical response is typically viscoelastic since the process is highly time-dependent (Brezinski, 1956; Schulz, 1961) and results in permanent deformation.

Viscoelastic behavior of wet paper can be affected by several factors. Typical viscoelastic response of wet paper can appear at high stress level before failure but is still not negligible at low stress level (Hauptmann and Cutshall, 1977; Baum et al., 1984). Also, the water content of paper can greatly influence the viscoelasticity. Experiments have indicated that the viscoelastic response of the wet paper increases with increasing relative humidity (Brezinski, 1956; Byrd, 1972).

Even though the deformation mechanisms of polymer and paper are different, their viscoelastic behavior is essentially the same and can be characterized by the same macroscopic models (Brezinski, 1956). Actually, there has been a great amount of work successfully done regarding the viscoelastic behavior of paper using the same mathematical models as those for polymer materials. The work in this field can be found in stress analysis (Agbezuge, 1981a; Agbezuge, 1981b; Pecht and Johnson, Jr., 1985), creep (Pecht et al., 1984), single-span web behavior (Hauptmann and Cutshall, 1977), and dynamic response (Roylance et al., 1980).

Theoretically, the viscoelastic behavior of web handling systems with those materials should be taken into account. The viscoelastic responses of the systems in some conditions will behave quite differently from those modeled by Hooke's law that

can only characterize the limiting properties of the materials, i.e., purely elastic responses.

2.3 Rheological Equations of State

Historically, rheological equations of state have been developed over more than a hundred years from primary forms to more sophisticated ones, from non-objective to objective, and are still under development. Extensive applications have revealed that no single rheological equation of state can universally predict the viscoelastic responses in various applied situations (Spriggs et al., 1966; Tanner, 1983; Bird et al, 1987).

The selection of a model should be made based on the understanding of the essence of the model, particular applications, and equation solving techniques. A more systematic and thorough review can be found in Bird et al. (1987). Here only some relative context is given for the purpose of this study.

Generally speaking, the rheological equations of state fall into five major categories that characterize the viscoelastic responses of the processes. Each of those equations has found specific applications.

The Generalized Newtonian Fluids (GNF) are the simplest constitutive equations. The stress tensor, $\underline{\tau}$, is linearly related to the strain rate tensor, $\underline{\dot{\gamma}}$, by the viscosity, η . The viscosity may be a function of the second invariant of the strain rate tensor, II , or its equivalent, the magnitude of the strain rate tensor, $\dot{\gamma}$

$$\underline{\underline{\tau}} = \eta(I)\underline{\underline{\dot{\gamma}}} = \eta(\dot{\gamma})\underline{\underline{\dot{\gamma}}}. \quad (2.1)$$

This viscosity function is commonly chosen to be a power law relationship to account for the non-Newtonian viscosity. A typical power law relationship can be expressed as

$$\eta = m\dot{\gamma}^{n-1} \quad (2.2)$$

where m and n are parameters.

An essential limitation of the generalized Newtonian fluid is that it cannot predict elastic effects so that the use of GNFs must be restricted to systems with very small Deborah numbers. However, in the common web handling systems especially with solid materials, the Deborah numbers are quite large and the elastic effects are very important. Therefore the generalized Newtonian fluid is not suitable in modeling web handling operations.

General Linear Viscoelastic Fluids are a large group of rheological equations of state, which linearly combine Hooke's law and Newton's law of viscosity. A typical example is the Maxwell model

$$\underline{\underline{\tau}} + \lambda_1 \frac{\partial}{\partial t} \underline{\underline{\tau}} = -\eta_0 \underline{\underline{\dot{\gamma}}} \quad (2.3)$$

where λ_1 and η_0 are the time constant and zero-shear-rate viscosity, respectively (Ferry, 1970; Aklonis et al., 1972; Lockett, 1972; Han, 1976; Ward, 1983). Other members of this group include the Voigt model, the generalized Maxwell model, and the Jeffreys model.

The linear viscoelastic models do not meet the requirement of material objectivity. The concept of material objectivity or admissibility (proposed by Oldroyd) was well explained by Bird et al. (1987), that is, the relationship of stress and strain should be independent of the coordinate system, position in space, translational and rotational motions of the material element, and effects of the neighboring elements.

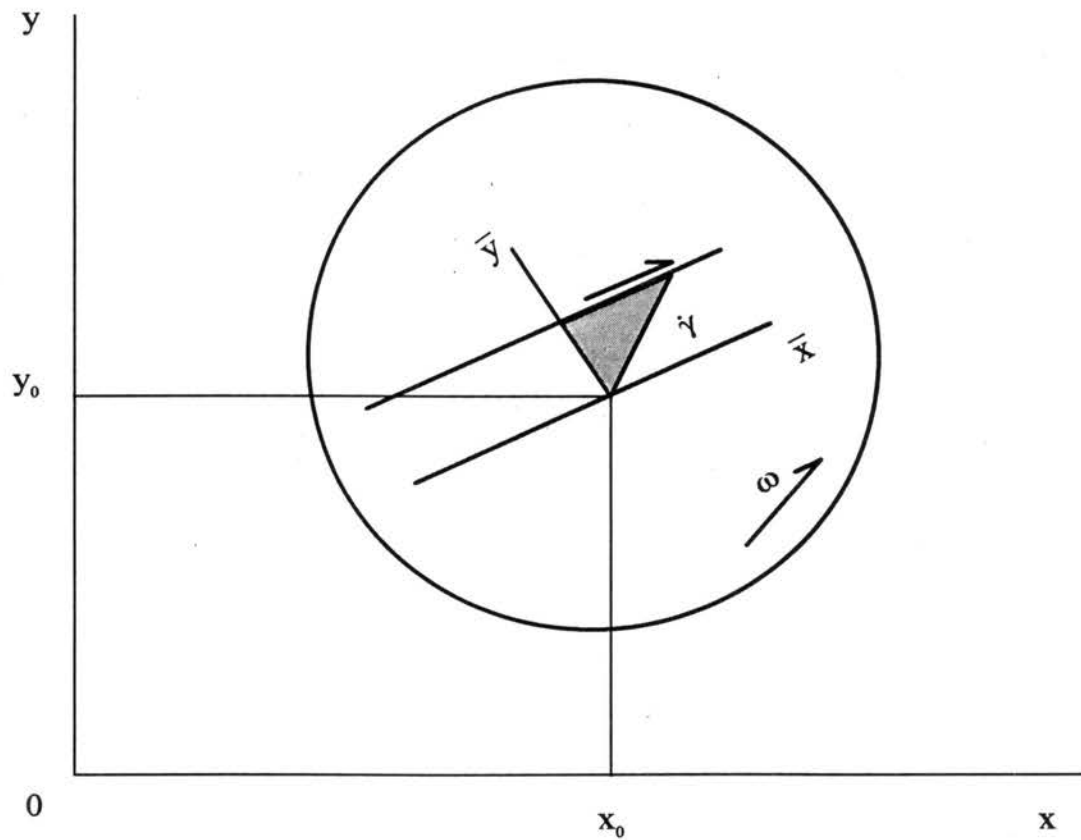
To illustrate material objectivity, the turntable problem is shown here. A shearing flow with constant strain rate, $\dot{\gamma}$, between two parallel plates is on the turntable as shown in Figure 2.1. If one views the flow on the turntable and uses the general linear viscoelastic model to determine the viscosity, the zero-shear-rate viscosity, η_0 is

$$\eta_0 = \int_0^{\infty} H(s) ds \quad (2.4)$$

where H is the relaxation modulus. If one views the flow in a laboratory coordinate reference (off the turntable), the viscosity, when the parallel plate is lined up with the x-axis, is given by

$$\eta_0 = \int_0^{\infty} H(s) \cos 2\omega s ds. \quad (2.5)$$

In the second case, η_0 is dependent on the angular velocity, ω . Physically, however, the viscosity must be a definite value no matter how one views it. Obviously, the general linear model gives different results based on the different coordinate



In \bar{x}, \bar{y} coordinates:

$$v_{\bar{x}} = \dot{\gamma}\bar{y}, \quad v_{\bar{y}} = 0.$$

In x, y coordinates:

$$x = \bar{x}\cos\omega t - \bar{y}\sin\omega t + x_0$$

$$y = \bar{x}\sin\omega t + \bar{y}\cos\omega t + y_0$$

$$v_x = \dot{\gamma}[-(x-x_0)\sin\omega t\cos\omega t + (y-y_0)\cos^2\omega t] - \omega(y-y_0)$$

$$v_y = \dot{\gamma}[-(x-x_0)\sin^2\omega t + (y-y_0)\sin\omega t\cos\omega t] + \omega(x-x_0)$$

Figure 2.1 Turntable Problem

references. The coordinate dependence of the interpretation in this example clearly illustrates the non-objectivity of the general linear models.

Although the rotational motion is generally absent in web material, the translational motion is significant since the web materials may be stretched to such an extent in some operations that the relative translation will affect the objectivity. The linear viscoelastic models are restricted to small-displacement-gradient flows and therefore are incapable of accounting for material objectivity.

Another inconvenience of using the linear viscoelastic models in modeling web handling systems arises from the conveying movement of the webs, especially in transient analysis. Usually, a web enters a free span with variables changing over position and time. The partial derivatives of the variables in the linear viscoelastic models require moving coordinates unless a translation between the moving coordinates and fixed coordinates is involved. However, in transient analysis, this translation is too cumbersome to consider.

Both the effect of the translational motion and the inconvenience of using moving coordinates in web handling systems require a more sophisticated constitutive equation that is objective (admissible), and can be conveniently constructed in a fixed coordinate system.

The Differential Constitutive Equations can meet the requirements by introducing convected derivatives to replace the partial derivatives. The equation may be generated by changing the convected derivatives for the partial derivatives in the linear viscoelastic model which results in a quasi-linear model, or by including

nonlinear terms. The kinematic quantities in these models are defined in the convected coordinate system but expressed in terms of Cartesian components in a fixed coordinate system. Generally speaking, the nonlinear models are more accurate than the quasi-linear models since they can predict real material data such as shear-rate-dependent viscosity that the linear models cannot.

As an equivalent approach to the differential models, the Integral Constitutive Equations allow more general equations to be generated by taking advantage of integration. A simple integral constitutive equation can be expressed as

$$\underline{\underline{\tau}}(t) = \int_{-\infty}^t Q(t-t') \underline{\underline{\gamma}}(t, t') dt' \quad (2.6)$$

where $Q(t-t')$ is the memory function. Although the integral models are particularly useful in some applications, the general forms of the integral models prohibit more accurate numerical evaluations in practice since the material functions are difficult to determine. Furthermore, unless convected coordinates are introduced, integral models involve in the problem of tracking the position of particles making the computational time significantly longer than that of the equivalent differential models (Crochet et al., 1984).

Actually, the choice of using the differential model or the integral model is arbitrary as long as they are equivalent in theory. Practical uses of the models rely on a number of factors such as the material, the accuracy required and the computing techniques.

The Retarded-Motion Expansion (RME), in the last category of constitutive

equations, is based not on empiricism but rather a purely mathematical treatment.

The RME is an expansion about Newton's law of viscosity, and practically used in truncated forms

$$\begin{aligned} \underline{\tau} = & -[b_1 \underline{\dot{\gamma}}_{(1)} + b_2 \underline{\dot{\gamma}}_{(2)} + b_{11} \{\underline{\dot{\gamma}}_{(1)} \cdot \underline{\dot{\gamma}}_{(1)}\} + b_3 \underline{\dot{\gamma}}_{(3)} \\ & + b_{12} \{\underline{\dot{\gamma}}_{(1)} \cdot \underline{\dot{\gamma}}_{(2)} + \underline{\dot{\gamma}}_{(2)} \cdot \underline{\dot{\gamma}}_{(1)}\} + b_{1:11} (\underline{\dot{\gamma}}_{(1)} : \underline{\dot{\gamma}}_{(1)}) \underline{\dot{\gamma}}_{(1)} + \dots] \end{aligned} \quad (2.7)$$

where b_1 , b_2 , b_{11} , etc. are constants and subscripts (1), (2) and (3) indicate first-, second- and third-order convected derivatives, respectively. The elastic effect has been accounted for since the successive terms in the expansion reflect the deviations from the Newtonian behavior, and those deviations are due to the elastic responses as mentioned previously. However, the retarded-motion expansion is restricted to applications with small Deborah numbers. The applications of the RME outside the small Deborah number range will result in undesired consequences such as negative viscosity and no stress relaxation. As a result, the retarded-motion expansion is not recommended for modeling web handling systems that commonly exhibit large Deborah numbers.

In summary, among the many rheological equations of state available, the nonlinear models are particularly suitable and useful for the modeling of the viscoelastic behavior of the web handling systems. Therefore, in this study, a White-Metzner equation (Bird et al., 1987) in the category of Differential Constitutive

Equations

$$\underline{\underline{\tau}} + \frac{\eta(\dot{\gamma})}{G} \underline{\underline{\tau}}_{(1)} = -\eta(\dot{\gamma}) \underline{\underline{\gamma}}_{(1)} \quad (2.8)$$

was used since it allows for stress relaxation through viscous deformation; preserves material objectivity, independence of selection of coordinate system; provides the flexibility to model diverse materials such as polymer and paper; and has sufficient mathematical simplicity to allow for a solution.

2.4 Modeling of Extensional Deformation in Transporting Processes

In modeling of the longitudinal tensions in the web handling systems, the web may be considered as a strip of material which is primarily in uniaxial extension, as shown schematically in Figure 2.2. As the web is moving from the upstream span into the current span, mass and momentum (if heat effects are neglected) are transferred under different conditions in the two spans. Therefore, the tensions are interactive at the transient point (the roller that separates the two spans). This phenomenon is called tension transfer.

In elastic analyses, Shin (1991) and other authors (Spielbauer and Walker, 1993; Reid and Lin, 1993) treated the web as a perfectly elastic material. This treatment required a step change in strain at the span entrance and no further strain occurring in the free span resulting in a one-dimensional (time) approach.

However, in a viscoelastic analysis, the web behavior is different from that of the elastic analysis. As the web particle enters the span, part of the strain is produced

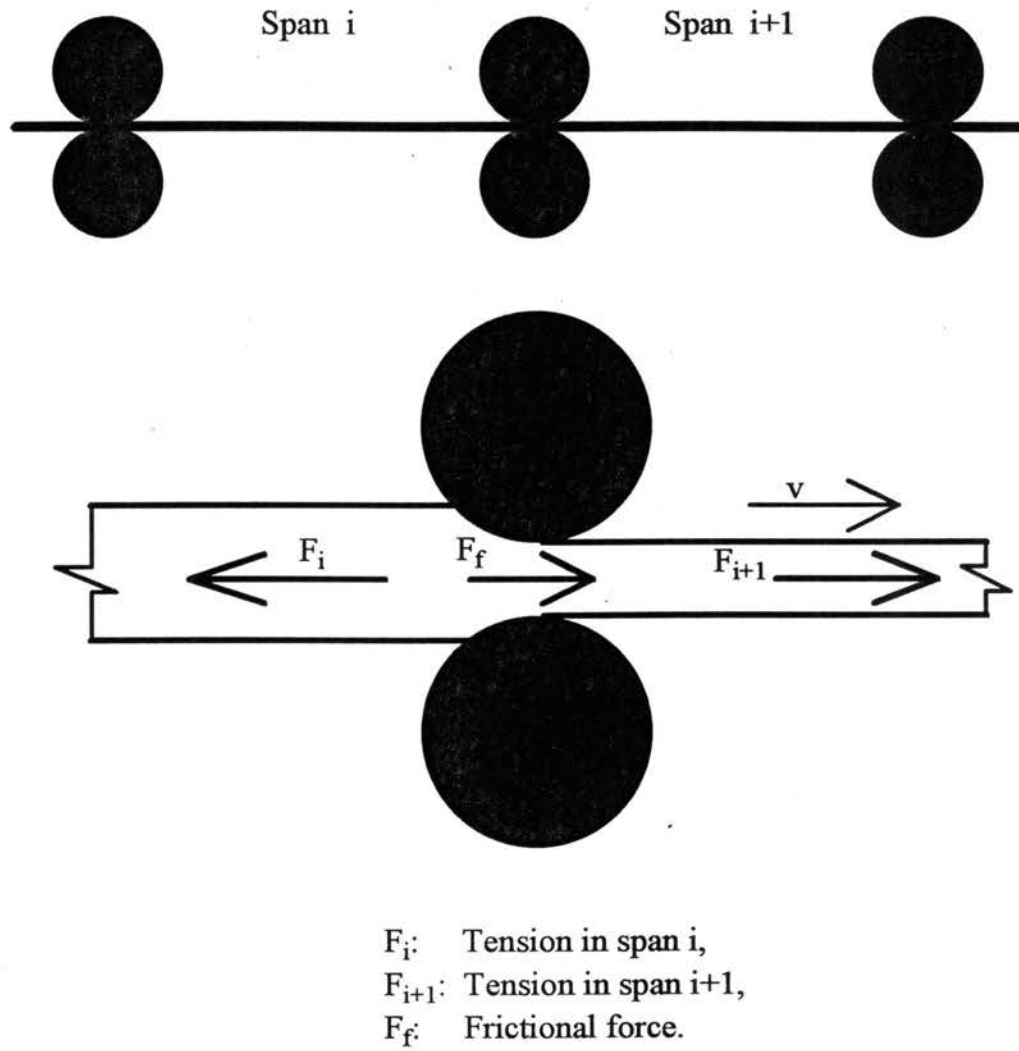


Figure 2.2 Schematic Illustration of Tension Transfer Mechanism

in the roller region due to the elastic effect. Elastic deformation and the viscous deformation will continuously occur throughout the free span. Thus, the total strain is no longer a constant with position as shown in Figure 2.3. Certainly, a two-dimensional (position and time) approach must be involved in the modeling so that the necessary boundary and initial conditions can be specified for the mixed value problem.

Since tension is only transferred downstream (Shin, 1991), the tension interaction occurs between the upstream span and the current span of interest. Obviously, the tension interaction should be embedded into the boundary conditions for the viscoelastic response in the free span. Moreover, the elastic response in the roller region and the viscoelastic response in the free span must be balanced in order to determine the tension level.

Due to the lack of viscoelastic analysis for multi-span web handling systems, quantitative viscoelastic behavior is unclear. However, a number of viscoelastic analyses can be found in other applications that are analogous to the web handling systems such as fiber spinning (Spearot and Metzner, 1972), thin film casting (Alaie and Papanastasiou, 1991), paper making (Hauptmann and Cutshall, 1977), and liquid stretching (Denn and Marrucci, 1971). Although these applications involve only one span without tension transfer, the viscoelastic responses in the free span are of interest in modeling of the web handling systems since they are subjected to the same type of deformation.

Fisher and Denn's (1976) modeling of the fiber spinning process should be

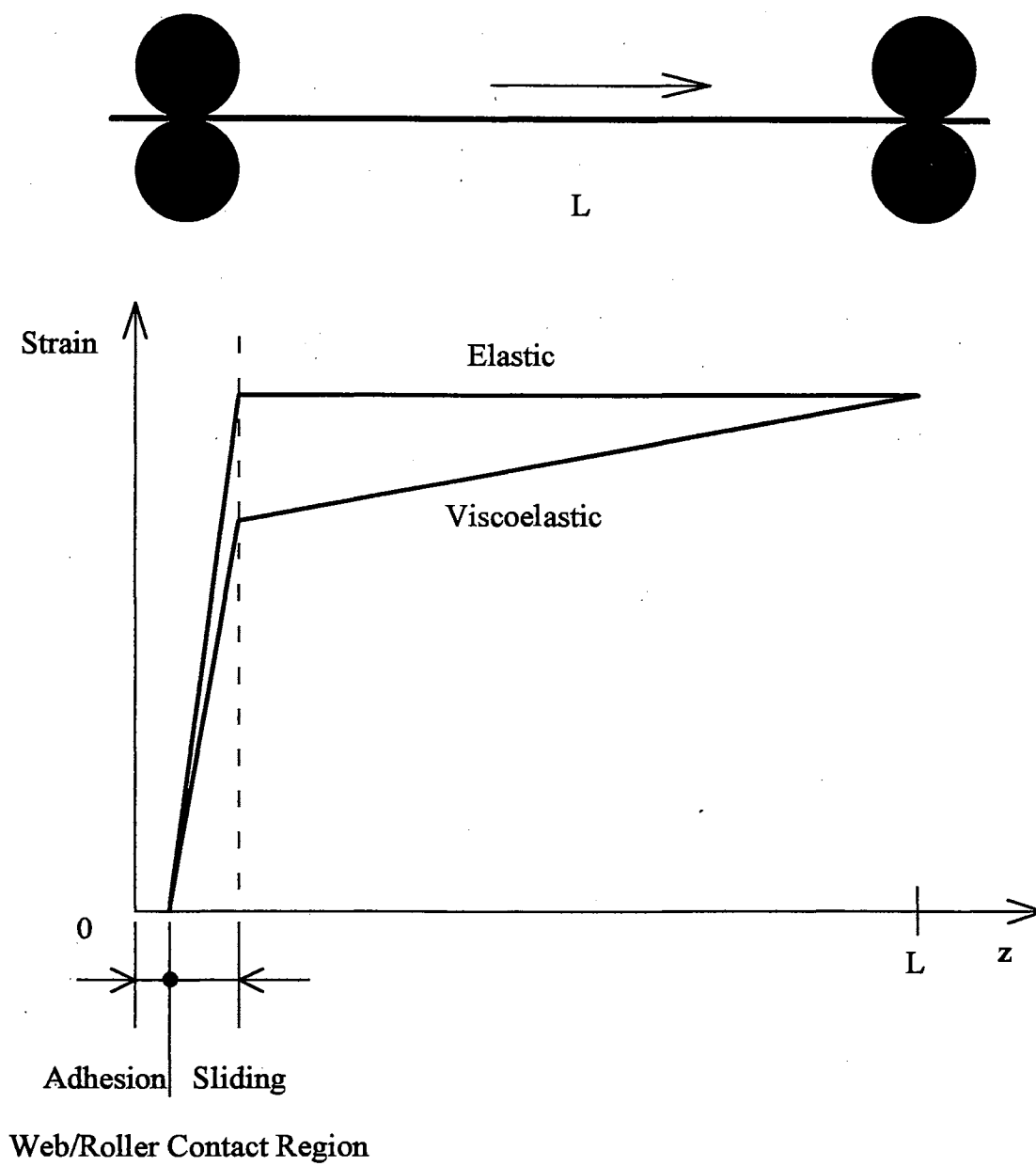


Figure 2.3 Schematic Illustration of Strain Variations in a Span

particularly noted since their model was similar to the model developed in this study in terms of viscoelastic deformations. Fisher and Dunn used the White-Metzner equation and simultaneously solved the mass and momentum conservation equations for both steady-state and transient operations. Their work showed that the tension level is closely related to the Deborah number.

Other modeling work of viscoelasticity in extensional deformation can also be found in steady state (Matovich and Pearson, 1969; Kase, 1974; Keunings et al., 1983), dynamic and stability analysis (Kase and Matsuo, 1965; Pearson, 1971; Pearson and Shah, 1972; Shah and Pearson, 1972a; Shah and Pearson, 1972b; Kase, 1974; Schultz and Davis, 1984; Kase and Katsui, 1985), and wet spinning (Han and Segal, 1970a; Han and Segal, 1970b).

2.5 Numerical Methods and Techniques

The viscoelastic problem cannot be solved analytically without oversimplifying the complex governing rheological equations. Consequently, most researchers have preferred numerical methods in their studies of the extensional deformation.

Usually, the models consist of a set of partial differential equations that involve two-dimensional independent variables (position and time). The equations are often highly coupled, and the boundary conditions are incomplete or unknown before the solution. These difficulties require special techniques to decouple the equations and to get the solutions iteratively.

Many numerical methods can be found in the literature regarding extensional deformation. The examples include series expansion (Kase, 1974), finite element method (Keunings et al., 1983; Alaie and Papanastasiou, 1991), finite difference method (Pearson, 1971; Shah and Pearson, 1972a; Shah and Pearson, 1972b; Pearson and Shah, 1972; Kase, 1974), linearized disturbance method (Schultz and Davis, 1984), and eigenfunction expansion (Fisher and Denn, 1976). In steady state, the governing equations can be solved by Runge-Kutta method (Pearson and Shah, 1972).

In this study, as will be fully discussed later, the fourth-order Runge-Kutta method was used for the steady-state analysis, and the finite difference method together with decoupling and iterative techniques were adapted for the transient analysis. Theoretically, the results should not significantly depend on the solution methods, provided that the algorithms are correctly and precisely controlled for consistency, stability and convergence. The choices for this study were primarily based on convenience.

2.6 Summary

At the beginning of this study, there were no viscoelastic models that capture the nature of viscoelastic behavior in multi-span web handling systems. Currently existing purely elastic models could not satisfy modern industries with precise control of tension for systems with viscoelastic materials. A rigorous viscoelastic model, therefore, is needed for modeling system behavior influenced by viscoelasticity for the purpose of design, control and operation. To meet the specific requirements for web

handling systems, the desired model should include a more realistic rheological equation of state and converge to an elastic model in limiting cases. Practical difficulties are also embedded in solving the model due to complexity of the problem so that specific methods and techniques must be carefully chosen. Those situations establish the background for this study.

CHAPTER III

MODEL DEVELOPMENT

This chapter presents the development of the model of viscoelastic behavior in web handling systems. In Section 3.1, a typical web handling system is analyzed for the case of a viscoelastic material interacting with the rollers. The appropriate assumptions are stated in Section 3.2 that make the model, developed in Section 3.3, easier to solve without losing the essence of the problem. In Section 3.4, the governing equations are non-dimensionalized. In the steady-state case, the governing equations are further reduced to a single ordinary differential equation in Section 3.5. Boundary and initial conditions are given in Sections 3.3 and 3.4 for the unsteady-state case. Boundary conditions for the steady-state case are specified in Section 3.5.

3.1 System Analysis

A representative web handling system is shown in Figure 3.1. The system consists of a web line and a set of roller pairs that separate the open spans. Although the rollers do not necessarily appear as pairs as depicted in Figure 3.1, the rollers represent a means of transmitting forces to the web. Generally, the rollers are operated at different speeds so that the tension in the machine or longitudinal direction varies in the different open spans due to the drawing.

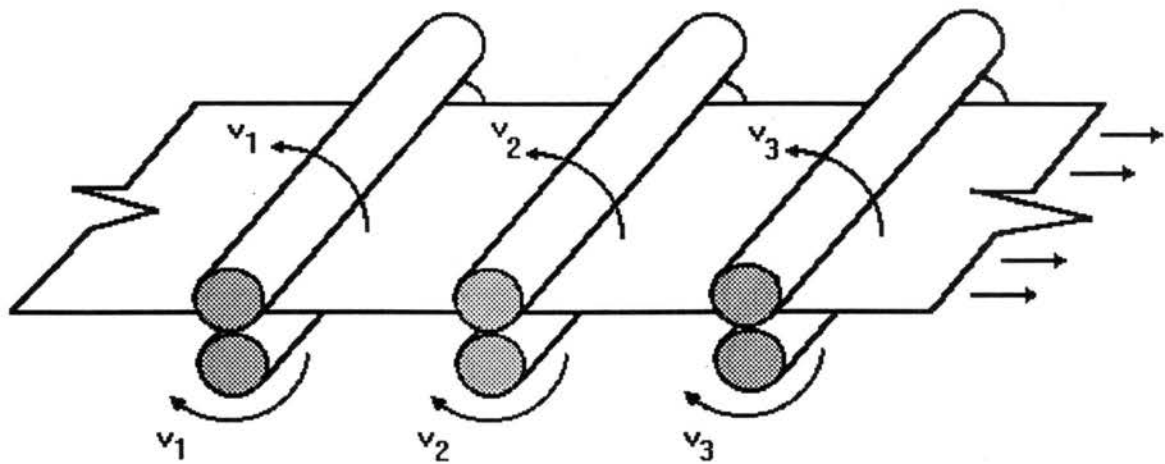


Figure 3.1 A Typical Web Handling System

In a given open span, the tension does not vary with position provided that inertial effects are neglected. When the web goes through a roller or a roller pair, the tension changes from one level in the upstream span to another in the downstream span. The tension of the current span depends on the operating condition of the two roller sets at both ends of the span, the tension level in the upstream span as well as the dynamic change across the entry roller.

Since the viscoelastic response is a function of the residence time, the viscoelastic behavior under different kinematic conditions can vary widely. There are three different time scales in the system: the time that is needed for a web particle to travel throughout the whole system, t_{system} ; the time that is needed for the particle to go through a particular open span, t_{span} ; and the time that is needed for the particle to go through a contact region of the web and a roller set, t_{roller} . For common web handling systems, the following relationship generally holds:

$$t_{system} > t_{span} > > t_{roller} \quad (3.1)$$

From Eq. (3.1), one can conclude that the Deborah number for the procedure in the contact region, De_{roller} , is quite large since t_{roller} will be several orders of magnitude smaller than the characteristic time of the material. Therefore, the viscoelastic response while in contact with the roller is negligible and elastic deformation dominates in the roller contact region. However, the Deborah number in the open span, De_{span} , is several orders of magnitude smaller than De_{roller} . There is enough time in the open span to allow for viscous deformation to occur so that the viscoelastic response is not negligible. Even though the viscoelastic response in one

open span may be not large, the viscoelastic effect will be accumulated due to the larger residence time in the whole system. Therefore, the system can be modeled as a number of viscoelastic responses in series (open spans) separated by a number of purely elastic step changes (rollers). From this point of view, the length of the contact region is not significant and can be treated as a zero-length contact since the elastic deformations are instantaneous.

The web velocities, v_i , marked in Figure 3.1 represent the velocities of the web surface at the points just before the contact regions. Consequently, the transient region at the upstream roller is included in the current span. If the contact condition is non-slip, the web surface velocity will be identical to the velocity of the roller surface in the adhesion region. In the slip case, the velocities of the web surface and roller surface are no longer identical, but the definition of the velocities, v_i , is the same. The determination of the web surface velocity at the roller contact point from a given roller velocity is difficult in the slip condition and is not the concern of this study.

Since the web line is transported downstream throughout the system, the modeling of the system behavior may be conducted span by span. However, within each span, the elastic response in the web/roller contact region and the viscoelastic response in the open span are interrelated and must be modeled simultaneously. The tension transferred from the upstream span must also be incorporated into the model. The results of the current span can serve as the input for the calculation of the next span.

Figure 3.2 shows an isolated span with a coordinate system. The Cartesian coordinate system is fixed in the space with the z-axis coinciding with the machine direction and the x-axis perpendicular to web surface. The web velocities at the upstream and downstream rollers are v_0 and v_L , respectively. The length of the span is L .

For actual web handling systems, especially operated at higher temperatures, the heat effects may be important since the temperature may affect the material properties. For high viscosity polymer materials, heat dissipation may be important during the stretching. Low thermal conductivity, typical of polymers, prohibits the heat removal from the web line. This action may result in a temperature gradient across the web (normal to the machine direction). However, most web lines are so thin that the temperature gradient is not large enough to allow the material properties to vary significantly within the cross section. Moreover, if the draw ratio is small enough, which is the most common case in commercial web handling systems, the temperature should not change significantly along the web line. Thus, the temperature may be reasonably treated as constant at least within an open span.

Exceptions may be found in cases in which a concentrated heating or cooling process takes place. In this case, the web may be considered as a number of segments that are processed at relatively constant temperatures. In this study, the open spans are considered as segments that have constant web temperatures and, therefore, the physical properties of the material are constant. However, the operating temperature may change from span to span. More severe heat effects are

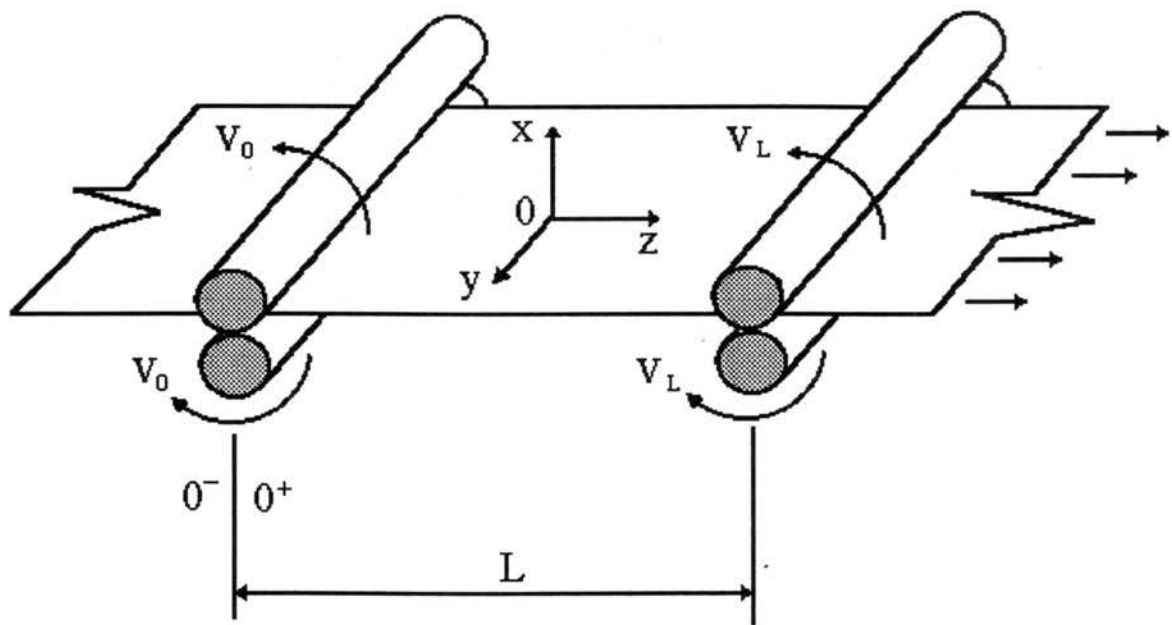


Figure 3.2 An Isolated Span with a Coordinate System

not considered in this study.

During the processing, the web material is under tension, and orientation of the polymer macromolecules or paper fibers will occur. The orientation will induce anisotropy and crystallization (for polymers), which may change the material properties. Fortunately, in most web handling systems, the draw ratios are small, making this phenomena minor.

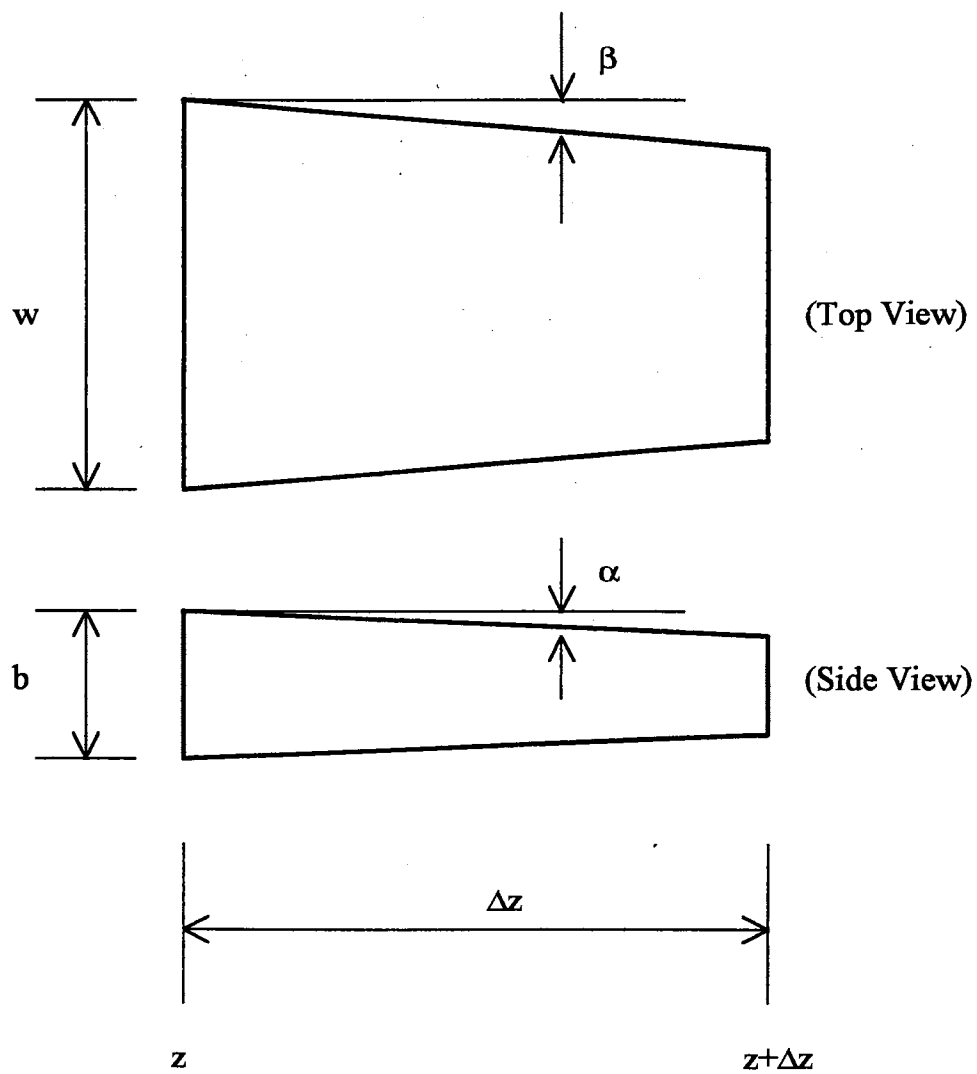
Although the longitudinal tension may induce other imperfect operating conditions such as lateral movement or wrinkling of the web line, in this study the web line is considered to be under purely uniaxial stretching. As a consequence of the small draw ratios, shearing effects are negligible.

Finally, the tension is produced only from the drawing, which is due to the velocity difference in consecutive rollers. Other forces that can potentially affect the tension such as inertial, gravitational, and air traction are excluded in this model.

3.2 Assumptions

Based on the system analysis conducted in Section 3.1, the viscoelastic behavior of the system can be modeled under the most common operating conditions encountered in the web handling industries. The conditions are reflected in the assumptions listed in this section.

To characterize the deformation, a control element cut from the web line, was considered as shown in Figure 3.3. The incline angles, α and β , result from the deformation of the web.



$$A = bw$$

Figure 3.3 A Control Volume Cut from a Web Line

Assumptions:

1. The thickness of the web, b , is much smaller than the other two length scales: width and length, w and L , respectively.
2. The web is in uniaxial extension.
3. The incline angles, α and β , are very small.
4. No shearing deformations exist in the planes perpendicular to the z -direction.
5. Inertial, gravitational and air traction forces are negligible.
6. There are no heat effects, i.e., the web temperature is constant within a span.
7. Material properties are constant within a span.
8. The length of web/roller contact region is zero.
9. The material obeys Hooke's law at the web/roller contact point.
10. The material is incompressible and isotropic.
11. Stresses and v_z are functions of z only.
12. The isotropic pressure, p , at the beginning of the open span, is given by (Han, 1976):

$$p = -\frac{1}{3}(\sigma_{xx} + \sigma_{yy} + \sigma_{zz}) \quad (3.2)$$

where σ_{ij} ($i, j = x, y, z$) are total stresses.

Assumption 10 requires the density to be constant. In practice, constant density is a common assumption in modeling viscoelastic behavior of materials such

as polymers and paper.

Assumption 12 was only used to evaluate the stress ratios at the beginning of the open spans since this relationship may not hold at every point within the span, due to the use of the White-Metzner equation.

3.3 Governing Equations

The governing equations for the free span were derived from: conservation of mass, a force balance, and the rheological equation of state.

3.3.1 Mass Conservation

A mass balance can be written for the control volume shown in Figure 3.3:

$$\begin{aligned} & \rho(z,t)A(z,t)v_z(z,t) \\ & - \rho(z+\Delta z,t)A(z+\Delta z,t)v_z(z+\Delta z,t) \\ & = [\rho(z,t+\Delta t)A(z,t+\Delta t) - \rho(z,t)A(z,t)]\frac{\Delta z}{\Delta t}. \end{aligned} \quad (3.3)$$

The left hand side of Eq. (3.3) accounts for the mass flux in and out of the control volume. The right hand side accounts for the mass accumulation rate in the control volume.

By dividing both sides of Eq. (3.3) by Δz , allowing Δz and Δt to approach zero, and applying assumption 10 ($\rho = \text{constant}$), the mass conservation equation becomes:

$$\frac{\partial A}{\partial t} + \frac{\partial(Av_z)}{\partial z} = 0. \quad (3.4)$$

3.3.2 Force Balance

By definition:

$$\sigma_{ij} = \tau_{ij} - p\delta_{ij}. \quad (3.5)$$

The two stress components of interest are:

$$\sigma_{xx} = \tau_{xx} - p, \quad (3.6)$$

and

$$\sigma_{zz} = \tau_{zz} - p. \quad (3.7)$$

Therefore,

$$\sigma_{zz} - \sigma_{xx} = \tau_{zz} - \tau_{xx}. \quad (3.8)$$

In an open span, the web is supported by rollers at the two ends.

Consideration of assumptions 2 and 11, which require the stresses to be uniformly distributed within the cross-section, allows the force balances in the x- and z-directions to be expressed as:

$$\sigma_{xx} = -p, \quad (3.9)$$

and

$$\sigma_{zz} = \frac{F}{A} - p_a, \quad (3.10)$$

where p_a denotes the ambient pressure.

By substituting Eqs. (3.9) and (3.10) into Eq. (3.8), the tension can be given as:

$$F = A(\tau_{zz} - \tau_{xx}). \quad (3.11)$$

Due to assumption 5, the tension in an open span will not be a function of position along the web line. Therefore, differentiating Eq. (3.11) with respect to z yields:

$$\frac{\partial}{\partial z}[A(\tau_{zz} - \tau_{xx})] = 0. \quad (3.12)$$

Eq. (3.12) is the needed form of the force balance.

3.3.3 The Rheological Equation of State

The White-Metzner model (White and Metzner, 1963; Bird et al., 1987) was chosen as the rheological equation of state:

$$\underline{\underline{\tau}} + \frac{\eta}{G} \underline{\underline{\dot{\tau}}}_{(1)} = \eta \underline{\underline{\dot{\gamma}}}_{(1)} \quad (3.13)$$

where,

$$\underline{\underline{\tau}}_{(1)} = \frac{D\underline{\underline{\tau}}}{Dt} - \{\underline{\underline{\tau}} \cdot \nabla \underline{\underline{v}}\}^T - \{\underline{\underline{\tau}} \cdot \nabla \underline{\underline{v}}\} \quad (3.14)$$

and

$$\frac{D\underline{\underline{\tau}}}{Dt} = \frac{\partial \underline{\underline{\tau}}}{\partial t} + \{\underline{\underline{v}} \cdot \nabla \underline{\underline{\tau}}\}. \quad (3.15)$$

Note should be made that there is no minus sign on the right hand side of the White-Metzner equation in order to be consistent with the definition of the stress tensor in Eq. (3.5).

From assumption 3 and 4, the velocity gradient tensor can be written as:

$$\nabla \underline{\underline{v}} = \begin{pmatrix} \frac{\partial v_x}{\partial x} & 0 & 0 \\ 0 & \frac{\partial v_y}{\partial y} & 0 \\ 0 & 0 & \frac{\partial v_z}{\partial z} \end{pmatrix}. \quad (3.16)$$

With assumption 4, the stress tensor can be expressed as:

$$\underline{\underline{\tau}} = \begin{pmatrix} \tau_{xx} & 0 & \tau_{xz} \\ 0 & \tau_{yy} & \tau_{yz} \\ \tau_{zx} & \tau_{zy} & \tau_{zz} \end{pmatrix}. \quad (3.17)$$

Thus,

$$\underline{\underline{\tau}} \cdot \underline{\underline{\nabla}} \underline{\underline{v}} = \begin{pmatrix} \tau_{xx} \frac{\partial v_x}{\partial x} & 0 & \tau_{xz} \frac{\partial v_z}{\partial z} \\ 0 & \tau_{yy} \frac{\partial v_y}{\partial y} & \tau_{yz} \frac{\partial v_z}{\partial z} \\ \tau_{zx} \frac{\partial v_x}{\partial x} & \tau_{zy} \frac{\partial v_y}{\partial y} & \tau_{zz} \frac{\partial v_z}{\partial z} \end{pmatrix} \quad (3.18)$$

and

$$\underline{\underline{v}} \cdot \underline{\underline{\nabla}} \underline{\underline{\tau}} = (\underline{\underline{v}} \cdot \underline{\underline{\nabla}}) \underline{\underline{\tau}} = \begin{pmatrix} v_z \frac{\partial \tau_{xx}}{\partial z} & 0 & v_z \frac{\partial \tau_{xz}}{\partial z} \\ 0 & v_z \frac{\partial \tau_{yy}}{\partial z} & v_z \frac{\partial \tau_{yz}}{\partial z} \\ v_z \frac{\partial \tau_{zx}}{\partial z} & v_z \frac{\partial \tau_{zy}}{\partial z} & v_z \frac{\partial \tau_{zz}}{\partial z} \end{pmatrix}. \quad (3.19)$$

The xx and zz components of the convected derivatives of the stress tensor can be extracted as:

$$\underline{\underline{\tau}}_{(1)xx} = \frac{\partial \tau_{xx}}{\partial t} + v_z \frac{\partial \tau_{xx}}{\partial z} - 2\tau_{xx} \frac{\partial v_x}{\partial x}, \quad (3.20)$$

and,

$$\underline{\underline{\tau}}_{(1)zz} = \frac{\partial \tau_{zz}}{\partial t} + v_z \frac{\partial \tau_{zz}}{\partial z} - 2\tau_{zz} \frac{\partial v_z}{\partial z}. \quad (3.21)$$

For an incompressible material (assumption 10):

$$\underline{\underline{\nabla}} \cdot \underline{\underline{v}} = 0. \quad (3.22)$$

From the symmetry of the deformations in the x- and y-directions:

$$\frac{\partial v_x}{\partial x} = \frac{\partial v_y}{\partial y} = -\frac{1}{2} \frac{\partial v_z}{\partial z}. \quad (3.23)$$

By definition (Bird et al., 1987), the xx, yy and zz components of the strain rate tensor can be written as:

$$\underline{\underline{\dot{\gamma}}}_{(1)xx} = 2 \frac{\partial v_x}{\partial x}, \quad (3.24)$$

$$\underline{\underline{\dot{\gamma}}}_{(1)yy} = 2 \frac{\partial v_y}{\partial y}, \quad (3.25)$$

and

$$\underline{\underline{\dot{\gamma}}}_{(1)zz} = 2 \frac{\partial v_z}{\partial z}. \quad (3.26)$$

Eq. (3.13) is a tensor equation from which the xx and zz components are of interest. From Eqs. (3.17), (3.20), (3.21), (3.24), and (3.26), the xx and zz components of Eq. (3.13) can be expressed as:

$$\tau_{xx} + \frac{\eta(\dot{\gamma})}{G} \left(\frac{\partial \tau_{xx}}{\partial t} + v_z \frac{\partial \tau_{xx}}{\partial z} - 2\tau_{xx} \frac{\partial v_x}{\partial x} \right) = 2\eta(\dot{\gamma}) \frac{\partial v_x}{\partial x}, \quad (3.27)$$

and

$$\tau_{zz} + \frac{\eta(\dot{\gamma})}{G} \left(\frac{\partial \tau_{zz}}{\partial t} + v_z \frac{\partial \tau_{zz}}{\partial z} - 2\tau_{zz} \frac{\partial v_z}{\partial z} \right) = 2\eta(\dot{\gamma}) \frac{\partial v_z}{\partial z}, \quad (3.28)$$

respectively.

Eq. (3.23) can be substituted into Eq. (3.27) to give:

$$\tau_{xx} + \frac{\eta(\dot{\gamma})}{G} \left(\frac{\partial \tau_{xx}}{\partial t} + v_z \frac{\partial \tau_{xx}}{\partial z} + \tau_{xx} \frac{\partial v_z}{\partial z} \right) = -\eta(\dot{\gamma}) \frac{\partial v_z}{\partial z}. \quad (3.29)$$

Since only one stress component normal to the transport direction is needed in the derivation of the model, σ_{xx} was arbitrarily chosen. Assumptions 2, 10 and 11 require the deformation behavior in the x- and y-directions to be identical. Thus, if σ_{yy} is chosen, the results of the model will be exactly the same. Actual cases do exist in which the deformation in the x-direction is different from that in the y-direction (Titomanlio et al., 1976). However, this effect is not within the scope of this study.

In this study, a power law expression,

$$\eta(\dot{\gamma}) = m\dot{\gamma}^{n-1}, \quad (3.30)$$

was selected for the viscosity in the White-Metzner equation. m and n are the power law coefficient and exponent, respectively. $\dot{\gamma}$ is the magnitude of the strain rate tensor, and can be obtained from Eqs. (3.23)-(3.26) and (3.31):

$$\begin{aligned} \dot{\gamma} &= \sqrt{\frac{1}{2} \underline{\underline{\gamma}}_{(1)} : \underline{\underline{\gamma}}_{(1)}} = \sqrt{\frac{1}{2} \left[\left(2 \frac{\partial v_x}{\partial x} \right)^2 + \left(2 \frac{\partial v_y}{\partial y} \right)^2 + \left(2 \frac{\partial v_z}{\partial z} \right)^2 \right]} \\ &= \sqrt{3} \left| \frac{\partial v_z}{\partial z} \right|. \end{aligned} \quad (3.31)$$

Introducing Eq. (3.31) into Eq. (3.30) yields the viscosity function:

$$\eta(\dot{\gamma}) = 3^{(n-1)/2} m \left| \frac{\partial v_z}{\partial z} \right|^{n-1}. \quad (3.32)$$

Finally, by substituting Eq. (3.32) into Eqs. (3.29) and (3.28):

$$\begin{aligned} \tau_{xx} + 3^{(n-1)/2} \left(\frac{m}{G} \right) \left| \frac{\partial v_z}{\partial z} \right|^{n-1} \left(\frac{\partial \tau_{xx}}{\partial t} + v_z \frac{\partial \tau_{xx}}{\partial z} + \tau_{xx} \frac{\partial v_z}{\partial z} \right) \\ = -3^{(n-1)/2} m \left| \frac{\partial v_z}{\partial z} \right|^{n-1} \frac{\partial v_z}{\partial z}, \end{aligned} \quad (3.33)$$

and

$$\begin{aligned} \tau_{zz} + 3^{(n-1)/2} \left(\frac{m}{G} \right) \left| \frac{\partial v_z}{\partial z} \right|^{n-1} \left(\frac{\partial \tau_{zz}}{\partial t} + v_z \frac{\partial \tau_{zz}}{\partial z} - 2\tau_{zz} \frac{\partial v_z}{\partial z} \right) \\ = 2 \cdot 3^{(n-1)/2} m \left| \frac{\partial v_z}{\partial z} \right|^{n-1} \frac{\partial v_z}{\partial z}. \end{aligned} \quad (3.34)$$

Eqs. (3.33) and (3.34) are the equations governing the rheology of an open span.

3.3.4 Strain in the Web Material

The elongational strain in the z-direction, ϵ_z , can be examined by considering three points in the web line labeled u, 1 and 2, respectively, as shown in Figure 3.4. The point u denotes the unstretched state; 1 and 2 denote any two different stretched states. Since the material is assumed to be incompressible (assumption 10), the density is constant. Mass conservation requires:

$$A_u \cdot 1 = A_1 [1 + (\epsilon_z)_1] = A_2 [1 + (\epsilon_z)_2], \quad (3.35)$$

where ϵ_z is measured relative to the unstretched state. Eq. (3.35) is a first order representation for the relation and thus can be applied to the cases with small strain, which are characteristic of web handling operations.

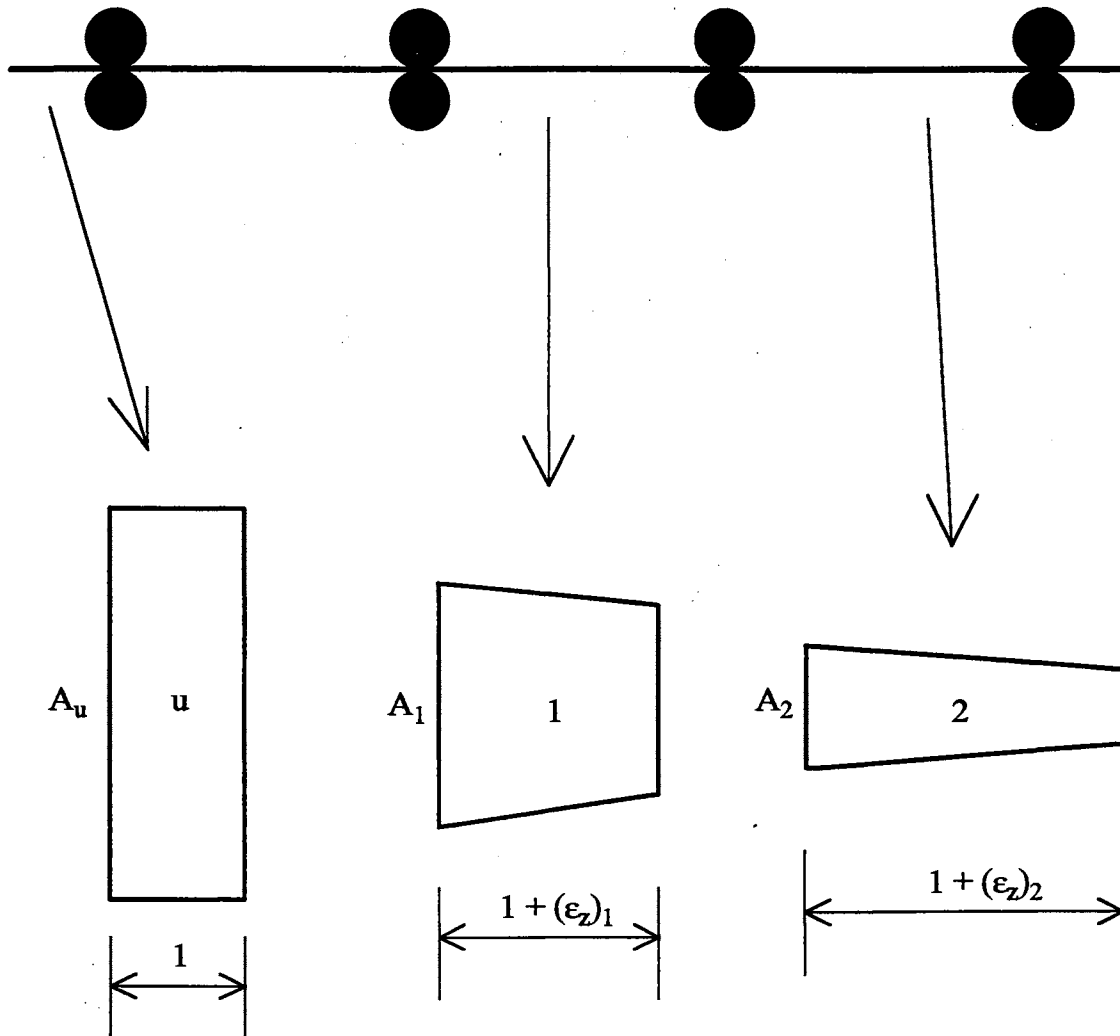


Figure 3.4 A Schematic Showing Strain at Three Different Positions

From Eq. (3.35), the strain at any time or position can be obtained from:

$$(\epsilon_z)_2 = [1 + (\epsilon_z)_1] \frac{A_1}{A_2} - 1. \quad (3.36)$$

3.3.5 Elastic Response in the Contact Region

Based on assumptions 2, 3, 4 and 9, the change in σ_{zz} and the change in ϵ_z across the contact region are related by:

$$\Delta \sigma_{zz} = E \Delta \epsilon_z, \quad (3.37)$$

where E is the Young's modulus; and $\Delta \sigma_{zz}$ and $\Delta \epsilon_z$ are defined as:

$$\Delta \sigma_{zz} = (\sigma_{zz})_{0^+} - (\sigma_{zz})_{0^-} \quad (3.38)$$

and

$$\Delta \epsilon_z = (\epsilon_z)_{0^+} - (\epsilon_z)_{0^-}. \quad (3.39)$$

In Eqs. (3.38) and (3.39), 0^- indicates the position just before the web/roller contact region, and 0^+ indicates the position just after the web/roller contact region.

From Eqs. (3.8) and (3.9),

$$\sigma_{zz} = (\tau_{zz} - \tau_{xx}) - p_a. \quad (3.40)$$

Substituting Eq. (3.40) into Eq. (3.38) yields:

$$\Delta \sigma_{zz} = (\tau_{zz} - \tau_{xx})_{0^+} - (\tau_{zz} - \tau_{xx})_{0^-}. \quad (3.41)$$

Under assumption 8, the mass cannot accumulate in the contact region.

Therefore, the mass conservation at the contact region can be expressed, with consideration of assumption 10, as:

$$(v_z)_{0^-} A_{0^-} = (v_z)_{0^+} A_{0^+}. \quad (3.42)$$

By applying Eq. (3.36) in the contact region ($1 = 0^-$, $2 = 0^+$) and taking note of Eq. (3.42), the strain at 0^+ can be written as:

$$(\epsilon_z)_{0^+} = [1 + (\epsilon_z)_{0^-}] \frac{(v_z)_{0^+}}{(v_z)_{0^-}} - 1. \quad (3.43)$$

Therefore, from Eqs. (3.39) and (3.43),

$$\Delta \epsilon_z = \left[\frac{(v_z)_{0^+}}{(v_z)_{0^-}} - 1 \right] [1 + (\epsilon_z)_{0^-}]. \quad (3.44)$$

Finally, the relationship of the stress change and the strain change across the contact region becomes:

$$(\tau_{zz} - \tau_{xx})_{0^+} = (\tau_{zz} - \tau_{xx})_{0^-} + E [1 + (\epsilon_z)_{0^-}] \left[\frac{(v_z)_{0^+}}{(v_z)_{0^-}} - 1 \right]. \quad (3.45)$$

If the conditions in the upstream span are known, and the web velocities before and after the contact region are determined, the stress difference at the beginning of the current open span can be calculated from Eq. (3.45).

Clearly, Eq. (3.45) can be considered as a relationship governing the tension transfer effect, and also serves as a link for the span to span calculations. However, the key factor that controls the tension transfer is $(v_z)_{0^+}$, and $(v_z)_{0^+}$ must be determined from the viscoelastic response in the open span, not just the elastic response in the contact region.

3.3.6 Initial and Boundary Conditions

The boundary conditions for the free span were specified as:

$$\begin{aligned} A(0^+,t) &= A_{0^+}(t), \quad v_z(0^+,t) = v_{0^+}(t), \\ (\tau_{zz} - \tau_{xx})(0^+,t) &= \tau_{0^+}(t), \end{aligned} \tag{3.46}$$

and

$$v_z(L,t) = v_L(t) \tag{3.47}$$

where L is the length of the span and the subscript L indicates the position at the end of the current span. At any time, t , the cross-sectional area, velocity and stress difference at $z = 0^+$ must be specified as functions of time. At $z = L$, only velocity needed be specified. The boundary conditions were selected based on the solution strategy that will be fully described in Chapter IV. Among the boundary conditions, only $v_L(t)$ is known prior to the solution in the case of open-loop control.

In open-loop control, the variables at the position 0^+ are initially unknown and must be determined during the solution. Determination of these variables requires a trial-and-error technique for the interaction of responses in the contact region and open span. Once $v_{0^+}(t)$ is known, $A_{0^+}(t)$ and $(\tau_{zz} - \tau_{xx})_{0^+}(t)$ can be determined from Eqs. (3.42) and (3.45).

The initial conditions for the free span were specified as:

$$\begin{aligned}
 A(z,0) &= A_{00}(z), \quad v_z(z,0) = v_{00}(z), \\
 (\tau_{zz} - \tau_{xx})(z,0) &= \tau_{00}(z),
 \end{aligned}
 \tag{3.48}$$

where subscript 00 indicates initial values. A typical start-up procedure begins with position free initial values of the variables. However, the initial values of A , v_z and $(\tau_{zz} - \tau_{xx})$ are allowed to be functions of position so that simulation of a transient procedure can be started from any initial state, for example, from a steady state.

3.3.7 Summary of the Governing Equations

Eqs. (3.4), (3.12), (3.33) and (3.34) are the governing equations for the viscoelastic response in an open span. Simultaneously solving of these nonlinear partial differential equations together with the initial and the boundary conditions, Eqs. (3.46)-(3.48), as well as the elastic response at the web/roller contact region, Eq. (3.45), can give the results for the boundary and initial value problem.

3.4 Non-Dimensionalization

The governing equations were converted to dimensionless form for general analysis. By following Fisher and Denn's example (1976), with appropriate modifications, the dimensionless variables were defined as:

$$\xi = \frac{z}{L}, \quad \phi = \frac{v_z}{(v_{zs})_{0^-}}, \quad T_{ij} = \tau_{ij} \frac{(A_s)_{0^+}}{F_s},$$

$$a = \frac{A}{(A_s)_{0^+}}, \quad \theta = \frac{(v_{zs})_{0^-}}{L} t,$$
(3.49)

where the subscript s means steady state and $ij = xx$ or zz . ξ , ϕ , T_{ij} , a and θ can be thought of as dimensionless distance, velocity, stress, area and time, respectively.

3.4.1 Dimensionless Governing Equations

By using the dimensionless variables defined above, the governing equations (3.4), (3.12), (3.33) and (3.34) become:

$$\frac{\partial a}{\partial \theta} + \frac{\partial(a\phi)}{\partial \xi} = 0, \quad (3.50)$$

$$\frac{\partial}{\partial \xi} [a(T_{zz} - T_{xx})] = 0, \quad (3.51)$$

$$T_{xx} + De \left| \frac{\partial \phi}{\partial \xi} \right|^{n-1} \left(\frac{\partial T_{xx}}{\partial \theta} + \phi \frac{\partial T_{xx}}{\partial \xi} + T_{xx} \frac{\partial \phi}{\partial \xi} \right) = -N \left| \frac{\partial \phi}{\partial \xi} \right|^{n-1} \frac{\partial \phi}{\partial \xi}, \quad (3.52)$$

and

$$T_{zz} + De \left| \frac{\partial \phi}{\partial \xi} \right|^{n-1} \left(\frac{\partial T_{zz}}{\partial \theta} + \phi \frac{\partial T_{zz}}{\partial \xi} - 2T_{zz} \frac{\partial \phi}{\partial \xi} \right) = 2N \left| \frac{\partial \phi}{\partial \xi} \right|^{n-1} \frac{\partial \phi}{\partial \xi}. \quad (3.53)$$

Two dimensionless groups naturally appear in Eqs. (3.52) and (3.53):

$$De = 3^{(n-1)/2} \left(\frac{m}{G} \right) \left[\frac{(v_{zs})_{0^+}}{L} \right]^n, \quad (3.54)$$

and

$$N = DeG \frac{(A_s)_{0^+}}{F_s}. \quad (3.55)$$

De is the Deborah number which reflects the ratio of the characteristic time of the material response to the characteristic time of the operation in steady state. N is the ratio of the characteristic viscous stress of the material to the applied tensile stress in the z-direction in steady state.

3.4.2 Initial and Boundary Conditions

The boundary and the initial conditions, Eqs. (3.46)-(3.48), were also converted to dimensionless form:

$$a(0^+, \theta) = a_{0^+}(\theta), \quad \phi(0^+, \theta) = \phi_{0^+}(\theta), \quad (3.56)$$

$$(T_{zz} - T_{xx})(0^+, \theta) = T_{0^+}(\theta),$$

$$\phi(1, \theta) = \phi_1(\theta), \quad (3.57)$$

and

$$\begin{aligned}
 a(\xi,0) &= a_{00}(\xi), \quad \phi(\xi,0) = \phi_{00}(\xi), \\
 (T_{zz} - T_{xx})(\xi,0) &= T_{00}(\xi).
 \end{aligned}
 \tag{3.58}$$

3.5 Governing Equation in Steady State

In steady state, the general governing equations can be reduced to a single ordinary differential equation with dimensionless velocity as the only independent variable. By deleting the terms that involve differentiation with respect to θ , and replacing the partial derivatives with total derivatives, Eqs. (3.4), (3.12), (3.33) and (3.34) are reduced to:

$$(a_s \phi_s)' = 0, \tag{3.59}$$

$$[a_s(T_{zss} - T_{xss})]' = 0, \tag{3.60}$$

$$T_{xss} + De|\phi_s'|^{n-1}(\phi_s T'_{xss} + \phi_s' T_{xss}) = -N|\phi_s'|^{n-1} \phi_s', \tag{3.61}$$

and

$$T_{zss} + De|\phi_s'|^{n-1}(\phi_s T'_{zss} - 2\phi_s' T_{zss}) = 2N|\phi_s'|^{n-1} \phi_s', \tag{3.62}$$

respectively, where the prime indicates differentiation with respect to ξ and the subscript s means steady state.

Expanding the derivatives in Eqs. (3.59) and (3.60) and combining the two equations yield:

$$(T_{zzs} - T_{xxs})' = \frac{\phi_s'}{\phi_s}(T_{zzs} - T_{xxs}). \quad (3.63)$$

Integrating Eq. (3.63) with respect to ξ gives:

$$T_{zzs} - T_{xxs} = c\phi_s, \quad (3.64)$$

where c is an integration constant and can be determined from the boundary conditions

$$\phi_s = (\phi_s)_{0^+}, \quad T_{zzs} - T_{xxs} = 1 \quad \text{at } \xi = 0^+, \quad (3.65)$$

yielding

$$c = \frac{1}{(\phi_s)_{0^+}}. \quad (3.66)$$

The parameter c is of particular importance since the effect of the upstream conditions on the current span enters the calculations through c . Hence, c may be thought of as a tension transfer parameter. The parameter c is also an interaction factor that reflects the link between the elastic response in the contact region and the viscoelastic response in the open span. c remains undetermined until the solution is obtained.

Subtracting Eq. (3.61) from Eq. (3.62) yields:

$$\begin{aligned} (T_{zzs} - T_{xxs}) + De|\phi_s'|^{n-1}[\phi_s(T_{zzs} - T_{xxs})' - \phi_s'(2T_{zzs} + T_{xxs})] \\ = 3N|\phi_s'|^{n-1}\phi_s'. \end{aligned} \quad (3.67)$$

By noting that $2T_{zzs} + T_{xxs} = 3T_{zzs} - (T_{zzs} - T_{xxs})$ and substituting Eq. (3.64),

Eq. (3.67) becomes:

$$c\phi_s + De|\phi_s'|^{n-1}[c\phi_s\phi_s' - \phi_s'(3T_{zss} - c\phi_s)] = 3N|\phi_s'|^{n-1}\phi_s', \quad (3.68)$$

which can be solved for T_{zss} :

$$T_{zss} = \frac{c\phi_s}{3De|\phi_s'|^{n-1}\phi_s'} + \frac{2c\phi_s}{3} - \frac{N}{De}. \quad (3.69)$$

Differentiation of T_{zss} with respect to ξ gives:

$$T'_{zss} = c \left[\frac{1}{3De|\phi_s'|^{n-1}} - \frac{\phi_s(|\phi_s'|^{n-1})'}{3De|\phi_s'|^{2n-2}\phi_s'} - \frac{\phi_s\phi_s''}{3De|\phi_s'|^{n-1}(\phi_s')^2} + \frac{2\phi_s'}{3} \right], \quad (3.70)$$

where the double prime indicates the second derivative with respect to ξ .

When $\phi_s' > 0$,

$$T'_{zss} = c \left[\frac{1}{3De(\phi_s')^{n-1}} - \frac{n\phi_s\phi_s''}{3De(\phi_s')^{n+1}} + \frac{2\phi_s'}{3} \right]. \quad (3.71)$$

When $\phi_s' < 0$,

$$T'_{zss} = c \left\{ \frac{1}{3De|\phi_s'|^{n-1}} - \frac{n\phi_s\phi_s''}{3De|\phi_s'|^{n+1}} + \frac{2\phi_s'}{3} \right\}. \quad (3.72)$$

In either case, Eqs. (3.71) and (3.72) can be written as

$$T'_{zss} = c \left\{ \frac{1}{3De|\phi_s'|^{n-1}} - \frac{n\phi_s\phi_s''}{3De|\phi_s'|^{n+1}} + \frac{2\phi_s'}{3} \right\}. \quad (3.73)$$

Eqs. (3.69) and (3.73) can be substituted into Eq. (3.62) and manipulated to

give the governing equation for the dimensionless velocity of a viscoelastic web in an open span:

$$\begin{aligned} & \phi_s - 2De^2\phi_s|\phi_s'|^{2n-2}(\phi_s')^2 \\ & + \text{sign}(\phi_s')\left[De\phi_s - \frac{3N}{c}|\phi_s'|^n - nDe\phi_s^2|\phi_s'|^{n-2}\phi_s''\right] = 0 \end{aligned} \quad (3.74)$$

where $\text{sign}(\phi')$ equals to +1, 0 or -1 when ϕ' is positive, zero or negative, respectively. Eq. (3.74) is a second-order, nonlinear ordinary differential equation.

The boundary conditions for the dimensionless governing equation in steady state are:

$$\phi_s = (\phi_s)_{0^+} \quad \text{at } \xi = 0^+, \quad (3.75)$$

and

$$\phi_s = D_{Rs} = \frac{v_{sL}}{v_{s0}} \quad \text{at } \xi = 1, \quad (3.76)$$

where D_{Rs} is the draw ratio in steady state in the span. Emphasis should be given to the fact that $(\phi_s)_{0^+}$ is unknown before the actual solution of the governing equations for the viscoelastic response in the open span and the elastic response in the contact region.

3.6 Chapter Review

In this chapter, the governing equations, in dimensionless form, were written for unsteady-state and steady-state cases. In the unsteady-state analysis, the four coupled, nonlinear partial differential equations govern the mass conservation, force

balance and rheology of the free span. The elastic step changes at web/roller contact region were also given by the relationships between stresses and strains across the contact region. The selected boundary and initial conditions were specified for the governing equations. All the governing equations must be solved simultaneously.

In steady state, the governing equations were reduced to a single, second-order, ordinary differential equation. The boundary conditions were also given for the steady-state case. Simultaneous solving of the governing equation and the elastic step change at the contact region, together with the boundary conditions will give the solution for steady state.

Since the elastic step change at web/roller contact region and the viscoelastic response in the open span are interrelated, the boundary conditions at the position of 0^+ for the viscoelastic calculations are not known prior to the solution. A special solution strategy will be used to overcome this difficulty as is fully described in the next chapter.

CHAPTER IV

NUMERICAL METHODS AND TECHNIQUES

The governing equations developed in Chapter III are sufficiently complicated that an analytical solution is not possible without significant over simplification. Numerical methods, therefore, were necessary to solve the model equations.

Since the governing equations for the steady-state and transient-state cases are different in the number of variables, classification and order, the solution methods and strategies were different. In the steady-state case, a fourth-order Runge-Kutta method was employed to solve the second-order ordinary differential equation (Section 4.1). The set of partial differential equations for the transient case was solved by using a finite difference method, which is presented in Section 4.2. The stability criteria are discussed in Section 4.3.

4.1 Steady State

The governing equation for the steady-state case, Eq. (3.74), is a second-order, nonlinear ordinary differential equation with the dimensionless velocity as the variable. Eq. (3.74) was solved by a standard fourth-order Runge-Kutta method (Gerald and Wheatley, 1989). The Runge-Kutta method is a linearization approach for solving ordinary differential equations and has been widely used in computer

solutions. For a given first-order, ordinary differential equation

$$\frac{dy}{dx} = g(x, y), \quad (4.1)$$

and boundary condition

$$y(x_0) = y_0, \quad (4.2)$$

within each step, the variable at the end of the step is evaluated based on a weighted-average combination of values of the given function estimated at four inter-points

$$y_{i+1} = y_i + \frac{1}{6}(k_1 + 2k_2 + 2k_3 + k_4). \quad (4.3)$$

In Eq. (4.3), k_i are the values of the function at the inter-points and can be expressed as

$$k_1 = hg(x_i, y_i), \quad (4.4)$$

$$k_2 = hg(x_i + \frac{1}{2}h, y_i + \frac{1}{2}k_1), \quad (4.5)$$

$$k_3 = hg(x_i + \frac{1}{2}h, y_i + \frac{1}{2}k_2), \quad (4.6)$$

$$k_4 = hg(x_i + h, y_i + k_3), \quad (4.7)$$

where $h = \Delta x$. Since the four evaluations of the function are required in each step, the fourth-order Runge-Kutta method is generally more accurate and efficient than those methods with a simple one step evaluation like the modified Euler method. The fourth-order Runge-Kutta method has a local error of $O[(\Delta x)^5]$ and a global error of

$O[(\Delta x)^4]$.

In open-loop control, roller speeds are specified at $\xi = 0$ and $\xi = 1$, which results in a boundary value problem in steady state. Two boundary conditions, Eqs. (3.75) and (3.76), are required for the solution of the governing equation, Eq. (3.74). However, the fourth-order Runge-Kutta method is based on a step-by-step procedure that needs both ϕ_s and ϕ_s' at $\xi = 0^+$ as initial values. Therefore, the boundary value problem must be transformed to an equivalent initial value problem. A shooting method (Gerald and Wheatley, 1989) was used for this purpose. In this method, an initial value of $(\phi_s')_{0^+}$ is assumed and the calculated value of $(\phi_s)_1$ based on $(\phi_s)_{0^+}$ and $(\phi_s')_{0^+}$ is compared with the specified value of $(\phi_s)_1 (= D_{Rs})$. If these two values of $(\phi_s)_1$ do not meet to within the desired precision, $(\phi_s')_{0^+}$ is reassumed and the procedure is repeated until the desired precision is achieved.

The first derivative of ϕ_s at $\xi = 0^+$, $(\phi_s')_{0^+}$, can be determined from Eq. (3.69):

$$(\phi_s')_{0^+} = \text{sign}\{[3(T_{zss})_{0^+} - 2]De + 3N\} \cdot \left| \frac{1}{[3(T_{zss})_{0^+} - 2]De + 3N} \right|^{\frac{1}{n}} \quad (4.8)$$

As shown in Eq. (4.8), the derivative can be evaluated from the initial stress, $(T_{zss})_{0^+}$, and the model parameters, De , N and n . Under assumption 12 in Chapter III, $(T_{zss})_{0^+}$ can be evaluated as below.

By considering Eqs. (3.2), (3.9) and (3.10) as well as the symmetry of σ_{xx} and σ_{yy} , the isotropic pressure at $z = 0^+$ becomes:

$$p_{0^+} = -\frac{1}{3} \frac{F}{A_{0^+}} + p_a. \quad (4.9)$$

Therefore, from Eqs. (3.7), (3.10) and (4.9), $(\tau_{zz})_{0^+}$ can be determined, in steady state, from:

$$(\tau_{zz})_{0^+} = \frac{2}{3} \frac{F_s}{(A_s)_{0^+}} \quad (4.10)$$

and, Eq. (4.8) becomes:

$$(\phi'_s)_{0^+} = \left| \frac{1}{3N} \right|^{\frac{1}{n}}. \quad (4.11)$$

However, as shown in Chapter III, the boundary condition at $\xi = 0^+$ for the viscoelastic response in the open span is unknown until the governing equations for the viscoelastic response and the elastic response in the contact region are solved simultaneously. The determination of $(\phi_s)_{0^+}$ requires that Eqs. (3.45) and (3.74) be solved by a trial-and-error technique. Once the two boundary conditions at $\xi = 0^+$ are met, $(\phi_s)_{0^+}$ is finally obtained.

To facilitate the use of the Runge-Kutta method, which is generally formulated for a first-order differential equation, Eq. (3.74) was reduced to a system of two simultaneous first-order equations:

$$\phi'_s = g(\phi_s), \quad (4.12)$$

$$\phi''_s = g'(\phi_s, \phi'_s), \quad (4.13)$$

where

$$g'(\phi_s, \phi'_s) = \left[1 - \frac{3(N/c)}{De\phi_s} + \text{sign}(\phi'_s) \left(\frac{1}{De|\phi'_s|^n} - 2De|\phi'_s|^n \right) \right] \frac{\phi_s^2}{n\phi_s}. \quad (4.14)$$

Application of the Runge-Kutta method to the system of equations, Eqs. (4.12) and (4.13), with the initial values of $(\phi_s)_{0+}$ and $(\phi'_s)_{0+}$ will give the dimensionless velocity at a set of points along the web line in an open span.

The shooting procedure is shown in Figure 4.1. The procedure is repeated from the first span to the last span in the system. The results of one span serve as the input for the next span. Within a span, the model parameters and the model variables are determined only when the specified precision is reached.

To accelerate the loop of steps (1) to (6), a searching technique was generated and a bisection technique was also used to determine the correct value of c , denoted c^* . First, guess an initial value of c , choose a step change in c , and search for c^* by marching step by step in both directions (increasing c and decreasing c). Check the deviations of $(\phi_s)_1$ from D_{Rs} at both ends of each step of c . Whenever the deviations at the two ends have different signs, c^* must be within this step. Then use the bisection to locate c^* .

4.2 Transient State

The governing equations for the transient case, Eqs. (3.50)-(3.53), are highly-coupled, nonlinear, multi-variable, partial differential equations, and must be solved simultaneously in order to get a realistic solution for the initial value and boundary

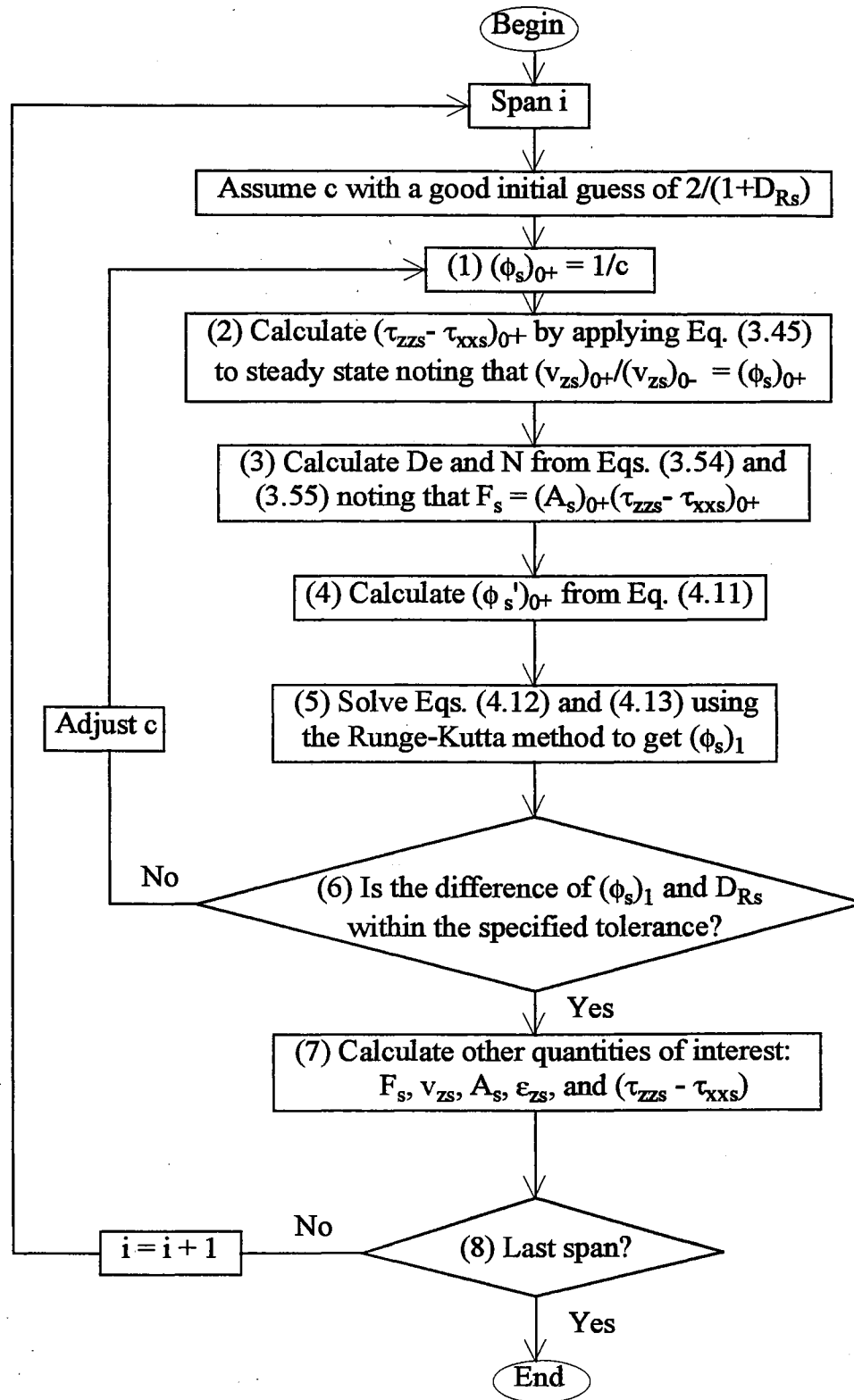


Figure 4.1 Shooting Procedure

value problem.

Since the model is one-dimensional in space, a finite difference method is suitable for the solution and preferred because of the simplicity of the method. Among the finite difference methods, MacCormack's explicit method (MacCormack, 1969; Anderson et al., 1984) was chosen in this study since the solution scheme has been widely used and is particularly useful for nonlinear partial differential equations (MacCormack, 1969; MacCormack, 1982; Anderson et al., 1984). The explicit MacCormack method provides second-order accuracy with a truncation error of $O[(\Delta\xi)^2, (\Delta\theta)^2]$. The explicit scheme was selected since the boundary conditions at both ends of the free span are not complete and the boundary conditions at the 0^+ position were determined in a trial-and-error procedure for balancing the elastic step change in the contact region and the viscoelastic deformation in the open span.

Although the explicit MacCormack method was not proposed for equations like those of the present model, the idea and the approach can be adopted for this study. The explicit approach uses a two step difference scheme and conducts the calculation explicitly from some initial point to a given point. The method can be illustrated in a simple example with a governing equation

$$\frac{\partial u}{\partial t} + c_0 \frac{\partial u}{\partial x} = 0, \quad (4.15)$$

where c_0 is a constant. At each time level, the first step of the difference involves a forward scheme and a predicting solution is obtained

Predictor

$$u_i^{\bar{j+1}} = u_i^j - c_0 \frac{\Delta t}{\Delta x} (u_{i+1}^j - u_i^j). \quad (4.16)$$

In the second step, a backward difference scheme is used to get a correcting solution based on the predicting solution

Corrector:

$$u_i^{j+1} = \frac{1}{2} \left[u_i^j + u_i^{\bar{j+1}} - c_0 \frac{\Delta t}{\Delta x} (u_i^{\bar{j+1}} - u_{i-1}^{\bar{j+1}}) \right]. \quad (4.17)$$

The predictor gives a temporary value of u at the time level $j+1$. The corrector provides the final value of u at the time level $j+1$. The discrete solution can be obtained by conducting the solution procedure throughout all time levels (j) and points in space (i). The explicit MacCormack method is conditionally stable with equation parameters limited within some given region.

Since the governing equations of the present model are highly coupled, a decoupling strategy was required for solving the set of the equations. The strategy is in two parts: (1) T_{xx} and T_{zz} are treated as independent variables in the White-Metzner model by assuming temporarily that ϕ is known; and (2) a is treated as an independent variable in the mass conservation equation by also assuming temporarily that ϕ is known. At each position step, ϕ is adjusted until the force balance is satisfied to within the required precision. Hence, the four governing equations are simultaneously solved in each step in an iteratively decoupling procedure.

4.2.1 Discretization of the Governing Equations

To facilitate the application of the MacCormack method, Eqs. (3.50)-(3.53) are reformed to (see Appendix A for details):

$$\frac{\partial a}{\partial \theta} + \phi \frac{\partial a}{\partial \xi} + \frac{\partial \phi}{\partial \xi} a = 0, \quad (4.18)$$

$$f = a(T_{zz} - T_{xx}), \quad (4.19)$$

$$\frac{\partial T_{xx}}{\partial \theta} + \phi \frac{\partial T_{xx}}{\partial \xi} + \left(\frac{\partial \phi}{\partial \xi} + \frac{1}{De} \left| \frac{\partial \phi}{\partial \xi} \right|^{1-n} \right) T_{xx} = -\frac{N}{De} \frac{\partial \phi}{\partial \xi}, \quad (4.20)$$

and

$$\frac{\partial T_{zz}}{\partial \theta} + \phi \frac{\partial T_{zz}}{\partial \xi} - \left(2 \frac{\partial \phi}{\partial \xi} - \frac{1}{De} \left| \frac{\partial \phi}{\partial \xi} \right|^{1-n} \right) T_{zz} = 2 \frac{N}{De} \frac{\partial \phi}{\partial \xi}, \quad (4.21)$$

respectively, where

$$f = \frac{F}{F_s}. \quad (4.22)$$

In the MacCormack explicit finite difference scheme, the predictor-corrector approach is achieved by:

$$\frac{\partial u}{\partial \theta} = \frac{u_i^{j+1} - u_i^j}{\Delta \theta}, \quad \frac{\partial u}{\partial \xi} = \frac{u_{i+1}^j - u_i^j}{\Delta \xi}, \quad (4.23)$$

for the predictor,

and

$$\frac{\partial u}{\partial \theta} = \frac{2\overline{u}_i^{j+1} - \overline{u}_i^{j+1} - u_i^j}{\Delta \theta}, \quad \frac{\partial u}{\partial \xi} = \frac{\overline{u}_i^{j+1} - \overline{u}_{i-1}^{j+1}}{\Delta \xi}, \quad (4.24)$$

for the corrector,

where u represents the independent variables appearing in the governing equations (a, T_{xx} or T_{zz} in this problem). The superscripts j and $j+1$ denote the time levels ($j+1$ is the current time level and j is the previous time level). The subscripts i and $i+1$ denote the position points (i is the current point and $i-1$ is the previous point). The overline indicates the predicted value.

By applying the difference approaches defined by Eqs. (4.23) and (4.24) to Eqs. (4.18) to (4.21), the finite difference formulations can be obtained as shown in Sections 4.2.1.1 to 4.2.1.4.

4.2.1.1 Discretization of Eq. (4.18)

(a) Predictor:

$$\frac{\overline{a}_i^{j+1} - a_i^j}{\Delta \theta} + \phi_i^{j+1} \frac{a_{i+1}^j - a_i^j}{\Delta \xi} + (\phi_\xi)_i^{j+1} \overline{a}_i^{j+1} = 0, \quad (4.25)$$

where $\phi_\xi = \partial \phi / \partial \xi$, which can be determined by a first-order backward difference:

$$(\phi_\xi)_i^{j+1} = \frac{\phi_i^{j+1} - \phi_{i-1}^{j+1}}{\Delta \xi}, \quad (4.26)$$

or a higher order backward difference.

Eq. (4.25) can be rearranged to:

$$a_i^{\bar{j+1}} = \left[\frac{1}{\Delta\theta} + (\phi_\xi)_i^{j+1} \right]^{-1} \left(\frac{a_i^j}{\Delta\theta} - \phi_i^{j+1} \frac{a_{i+1}^j - a_i^j}{\Delta\xi} \right). \quad (4.27)$$

(b) Corrector:

$$\frac{2a_i^{j+1} - a_i^{\bar{j+1}} - a_i^j}{\Delta\theta} + \phi_i^{j+1} \frac{a_i^{\bar{j+1}} - a_{i-1}^{\bar{j+1}}}{\Delta\xi} + (\phi_\xi)_i^{j+1} a_i^{j+1} = 0, \quad (4.28)$$

or,

$$a_i^{j+1} = \left[\frac{2}{\Delta\theta} + (\phi_\xi)_i^{j+1} \right]^{-1} \left(\frac{a_i^{\bar{j+1}} + a_i^j}{\Delta\theta} - \phi_i^{j+1} \frac{a_i^{\bar{j+1}} - a_{i-1}^{\bar{j+1}}}{\Delta\xi} \right). \quad (4.29)$$

4.2.1.2 Discretization of Eq. (4.19)

$$f = a_i^{j+1} [(T_{zz})_i^{j+1} - (T_{xx})_i^{j+1}]. \quad (4.30)$$

4.2.1.3 Discretization of Eq. (4.20)

(a) Predictor:

$$\begin{aligned} & \frac{(T_{xx})_i^{\bar{j+1}} - (T_{xx})_i^j}{\Delta\theta} + \phi_i^{j+1} \frac{(T_{xx})_{i+1}^j - (T_{xx})_i^j}{\Delta\xi} \\ & + \left[(\phi_\xi)_i^{j+1} + \frac{1}{De} |(\phi_\xi)_i^{j+1}|^{1-n} \right] (T_{xx})_i^{\bar{j+1}} = -\frac{N}{De} (\phi_\xi)_i^{j+1}, \end{aligned} \quad (4.31)$$

or,

$$(T_{xx})_i^{\bar{j}+1} = \left[\frac{1}{\Delta\theta} + (\Phi_\xi)_i^{j+1} + \frac{1}{De} |(\Phi_\xi)_i^{j+1}|^{1-n} \right]^{-1} \cdot \left[\frac{(T_{xx})_i^j}{\Delta\theta} - \Phi_i^{j+1} \frac{(T_{xx})_{i+1}^j - (T_{xx})_i^j}{\Delta\xi} - \frac{N}{De} (\Phi_\xi)_i^{j+1} \right]. \quad (4.32)$$

(b) Corrector:

$$\frac{2(T_{xx})_i^{j+1} - (T_{xx})_i^{\bar{j}+1} - (T_{xx})_i^j}{\Delta\theta} + \Phi_i^{j+1} \frac{(T_{xx})_i^{\bar{j}+1} - (T_{xx})_{i-1}^{\bar{j}+1}}{\Delta\xi} + \left[(\Phi_\xi)_i^{j+1} + \frac{1}{De} |(\Phi_\xi)_i^{j+1}|^{1-n} \right] (T_{xx})_i^{j+1} = -\frac{N}{De} (\Phi_\xi)_i^{j+1}, \quad (4.33)$$

or,

$$(T_{xx})_i^{j+1} = \left[\frac{2}{\Delta\theta} + (\Phi_\xi)_i^{j+1} + \frac{1}{De} |(\Phi_\xi)_i^{j+1}|^{1-n} \right]^{-1} \cdot \left[\frac{(T_{xx})_i^{\bar{j}+1} + (T_{xx})_i^j}{\Delta\theta} - \Phi_i^{j+1} \frac{(T_{xx})_i^{\bar{j}+1} - (T_{xx})_{i-1}^{\bar{j}+1}}{\Delta\xi} - \frac{N}{De} (\Phi_\xi)_i^{j+1} \right]. \quad (4.34)$$

4.2.1.4 Discretization of Eq. (4.21)

(a) Predictor:

$$\frac{(T_{zz})_i^{\bar{j}+1} - (T_{zz})_i^j}{\Delta\theta} + \Phi_i^{j+1} \frac{(T_{zz})_{i+1}^j - (T_{zz})_i^j}{\Delta\xi} - \left[2(\Phi_\xi)_i^{j+1} - \frac{1}{De} |(\Phi_\xi)_i^{j+1}|^{1-n} \right] (T_{zz})_i^{\bar{j}+1} = 2\frac{N}{De} (\Phi_\xi)_i^{j+1}, \quad (4.35)$$

or,

$$(T_{zz})_i^{\overline{j+1}} = \left[\frac{1}{\Delta\theta} - 2(\phi_\xi)_i^{j+1} + \frac{1}{De} |(\phi_\xi)_i^{j+1}|^{1-n} \right]^{-1} \cdot \left[\frac{(T_{zz})_i^j}{\Delta\theta} - \phi_i^{j+1} \frac{(T_{zz})_{i+1}^j - (T_{zz})_i^j}{\Delta\xi} + 2 \frac{N}{De} (\phi_\xi)_i^{j+1} \right]. \quad (4.36)$$

(b) Corrector:

$$\frac{2(T_{zz})_i^{j+1} - (T_{zz})_i^{\overline{j+1}} - (T_{zz})_i^j}{\Delta\theta} + \phi_i^{j+1} \frac{(T_{zz})_i^{\overline{j+1}} - (T_{zz})_{i-1}^{\overline{j+1}}}{\Delta\xi} - \left[2(\phi_\xi)_i^{j+1} - \frac{1}{De} |(\phi_\xi)_i^{j+1}|^{1-n} \right] (T_{zz})_i^{j+1} = 2 \frac{N}{De} (\phi_\xi)_i^{j+1}, \quad (4.37)$$

or,

$$(T_{zz})_i^{j+1} = \left[\frac{2}{\Delta\theta} - 2(\phi_\xi)_i^{j+1} + \frac{1}{De} |(\phi_\xi)_i^{j+1}|^{1-n} \right]^{-1} \cdot \left[\frac{(T_{zz})_i^{\overline{j+1}} + (T_{zz})_i^j}{\Delta\theta} - \phi_i^{j+1} \frac{(T_{zz})_i^{\overline{j+1}} - (T_{zz})_{i-1}^{\overline{j+1}}}{\Delta\xi} + 2 \frac{N}{De} (\phi_\xi)_i^{j+1} \right]. \quad (4.38)$$

4.2.2 Treatment of the Boundary Conditions

The boundary conditions for the transient analysis, Eqs. (3.56) and (3.57), are incomplete for the viscoelastic response since the stresses and the cross-sectional area at $\xi = 1$ are unknown. The variables T_{ij} , a and ϕ at $\xi = 0^+$ are also undetermined until the solution is reached. The incomplete boundary conditions make the solution of the viscoelastic response indirect. In other words, the solution for the viscoelastic response in the open span cannot be obtained from Eqs. (3.50) to (3.53) only. The

elastic step change at the web/roller contact region, Eq. (3.45), must be solved simultaneously. The use of the explicit finite difference approach together with the trial-and-error technique resulted in a solution.

The explicit approach needs only the boundary conditions at $\xi = 0^+$. As described in the beginning of Section 4.2, the decoupling strategy treats T_{xx} , T_{zz} and a as independent variables in the corresponding equations for the solution procedure. Therefore, $(T_{xx})_{0+}$, $(T_{zz})_{0+}$, and a_{0+} are required for the solution of the viscoelastic response in the open span. In the trial-and-error procedure, the viscoelastic response and the elastic step change are balanced through an iteration until ϕ_1 meets the specified value, $\phi_0 D_R$, where $D_R = v_L/v_0$, with the required precision. The three boundary conditions, $(T_{xx})_{0+}$, $(T_{zz})_{0+}$, and a_{0+} , are unknown prior to the solution, but can be temporarily estimated, during the trial and error procedure, from the elastic step change in the contact region based on the input from the upstream span. Actually, these three boundary conditions can be derived from ϕ_{0+} in each iteration, which is the adjustable parameter in the trial-and-error procedure. $(T_{xx})_{0+}$ and $(T_{zz})_{0+}$ can be separated from $(T_{zz}-T_{xx})_{0+}$ by a similar way as described in steady-state formulation (Section 4.1) based on assumption 12 in Chapter III.

In open-loop control, the tension in the span is unknown, therefore, the elastic step change in the contact region is also undetermined prior to the solution.

However, the trial-and-error method reconciles the elastic response in the contact region and the viscoelastic response in the open span. Whenever ϕ_1 reaches $\phi_0 D_R$ through the trial-and-error procedure, the corresponding ϕ_{0+} is finally determined,

and then the elastic step change can be obtained from ϕ_{0+} .

4.2.3 Solution Strategy

The solution procedure involves two major parts. One is to determine the boundary conditions at the beginning of the open span for the viscoelastic calculation. The boundary conditions are dependent upon the balance of the elastic response in the web/roller contact region and the viscoelastic response in the open span, and are not known until the two responses are balanced in the trial-and-error, iterative calculation.

The other major part is to calculate the viscoelastic response using the finite difference method for the open span. This part involves several iteration loops for getting the solution that simultaneously satisfies the mass conservation, force balance and rheological equation of state in each step.

The solution procedure is shown in Figure 4.2. The loop of steps (a) to (e) was automatically executed by a searching-bisection method similar to that in the steady-state analysis. Whereas, the loop of steps (i) to (iv) was implemented by another searching method: (1) Choose a searching range of ϕ_{0+} , denoted $[(\phi_{0+})_L, (\phi_{0+})_R]$. (2) Divide the range into two equal subranges. (3) Do steps (i) to (iv) based on the values of ϕ_{0+} at the central points of the subranges, $(\phi_{0+})_a$ and $(\phi_{0+})_b$. (4) Compare the deviations of the calculated values to the specified values of ϕ_1 at the central points and determine the larger deviation. (5) Reset the searching range to $[(\phi_{0+})_a, (\phi_{0+})_R]$ if the larger deviation occurs at the left central point, or $[(\phi_{0+})_L, (\phi_{0+})_b]$ if the larger deviation occurs at the right central point. (6) Repeat the

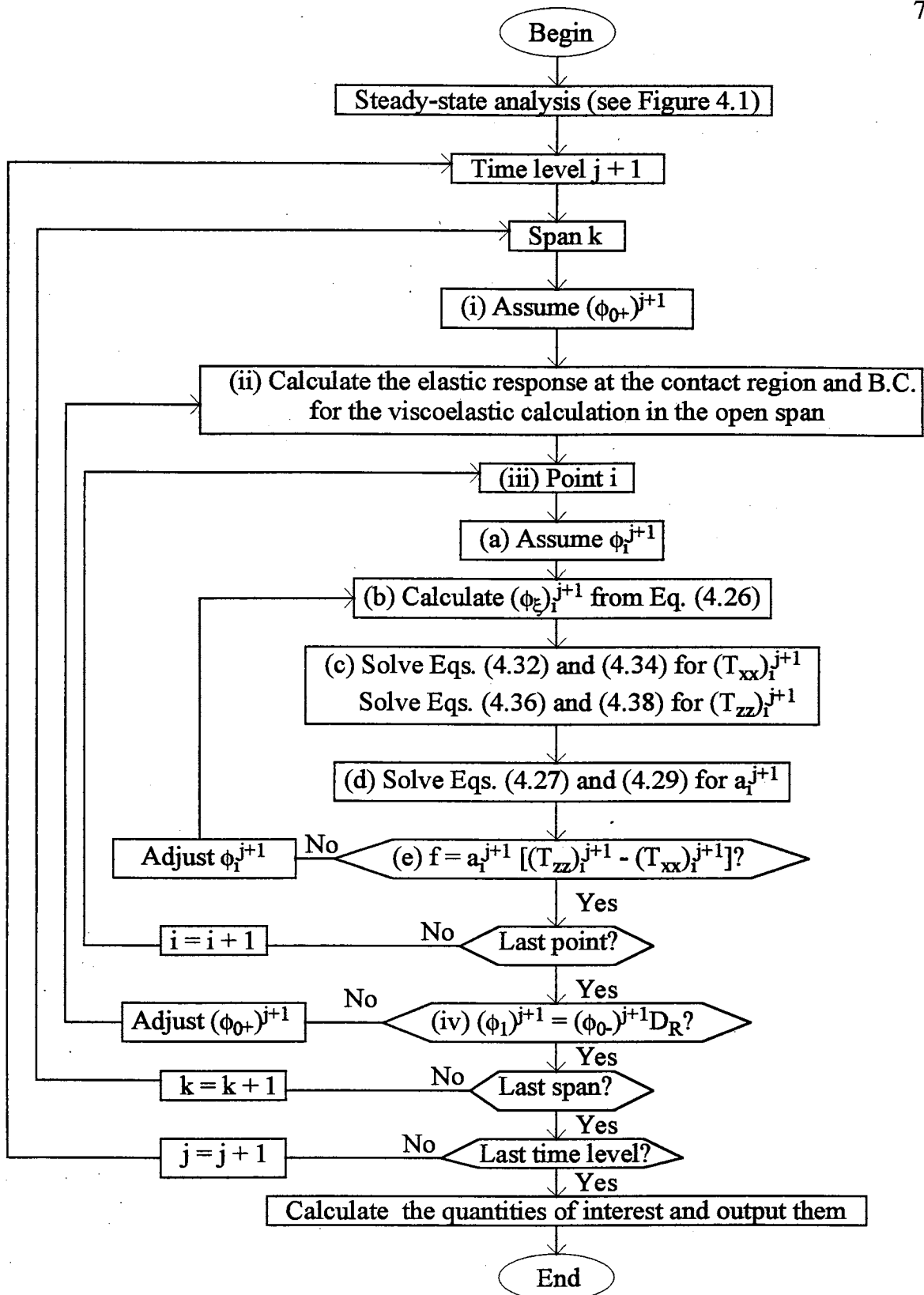


Figure 4.2 Solution Procedure

searching procedure until the larger deviation becomes smaller than the given tolerance.

4.3 Special Concerns

Generally, there are three major concerns for numerical methods: consistency, convergence and stability. These issues are of paramount importance since successful and accurate numerical solutions are critically dependent upon the simulation conditions as constrained by these requirements.

For finite difference methods, the numerical models are said to be consistent if the truncation error approach zero as the spatial and time increments go to zero; convergent if the discretization error approach zero as the spatial and time increments go to zero; and stable if the round-off error does not grow exponentially for fixed time as the spatial and time increments go to zero (Street, 1973).

In this section, these three concerns are addressed for the finite difference formulations developed in the foregoing sections. Among them, the stability is of particular interest since the numerical simulation conditions are mainly constrained by the stability criterion. Although the explicit scheme is straightforward and does not require a matrix method for the solutions, the time increment is usually bounded to prevent the solution from becoming unstable.

4.3.1 Consistency

The explicit MacCormack method is of second-order accuracy in both spatial

and time discretization meaning that the truncation error is $O[(\Delta\xi)^2, (\Delta\theta)^2]$ (MacCormack, 1969; MacCormack, 1982; Anderson et al., 1984). As $\Delta\xi$ and $\Delta\theta$ approach zero, the truncation error will go to zero with second-order accuracy. Therefore, the difference scheme is consistent.

4.3.2 Stability

A complete analysis of stability of the finite difference scheme for the governing equations is not available since the equations are nonlinear and complex making the analysis intractable. An estimation, however, was conducted in this study based on an approximate analysis for the stability criterion.

There are several available methods for analyzing stability criterion, e.g., the von Neumann method (Forsythe and Wasow, 1960; Crochet et al., 1984), matrix method (Anderson et al., 1984; Gerald and Wheatley, 1989), and energy method (Richtmyer and Morton, 1967). In this study, the von Neumann method was adopted.

Generally, inclusion of lower order terms in the governing equations will affect the stability. However, if the lower order terms do not change severely with the independent variables or have smaller coefficients resulting in bounded values, the stability criterion will be insignificantly affected or unaffected by the lower order terms (Richtmyer and Morton, 1967; Crochet et al., 1984).

In the present study, the coefficients of the first-order and zero-order terms in the governing equations are determined by the velocity derivative, $\partial\phi/\partial\xi$, as well as the model parameters, De and N . In the model, De and N remain constant and the

smooth deformation suggests that $\partial\phi/\partial\xi$ does not change significantly if the draw ratio, D_R , is small enough. Therefore, the first-order and zero-order terms can be eliminated from the equations in order to conduct an approximate analysis for the stability. Based on this analysis, the governing equations, Eqs. (4.18), (4.20) and (4.21), reduce to a common form for all of the independent variables: a , T_{xx} and T_{zz} ,

$$\frac{\partial u}{\partial \theta} + \phi \frac{\partial u}{\partial \xi} = 0, \quad (4.39)$$

where u represents a , T_{xx} or T_{zz} . The three equations represented by Eq. (4.39) are linear although the three variables are coupled implicitly by ϕ , meaning that the system behavior is nonlinear. However, if the solution strategy described in Section 4.2.3 is employed, the three equations are decoupled resulting in a linear system of equations.

The Neumann method requires constant coefficients in the linear difference equations (Crochet et al., 1984). If the coefficients are functions of independent variables, they can be treated as nearly constant within a step and the method can be applied locally (MacCormack, 1969; Crochet et al., 1984). MacCormack pointed out that if this locally linearized difference method is unstable, the general nonlinear difference equations are also expected to be unstable (MacCormack, 1969). Since the velocity distribution is smooth, ϕ can be treated locally as a constant. Thus, Eq. (4.39) can be analyzed using the Neumann method.

The stability criterion of the explicit MacCormack finite difference method for Eq. (4.39) has been investigated using the Neumann method (MacCormack, 1982;

Anderson et al., 1984):

$$\Delta\theta \leq \frac{\Delta\xi}{|\phi|}. \quad (4.40)$$

Note should be made that ϕ has been locally linearized. In a span, ϕ is changing from ϕ_{0+} to $\phi_{0-}D_R$ for the viscoelastic response. As an estimation for the global procedure, $|\phi|$ may be replaced by D_{Rs} , thus

$$\Delta\theta \leq \frac{\Delta\xi}{D_{Rs}}. \quad (4.41)$$

The relationship in Eq. (4.41) bounds the time incremental size to a value dependent on the spatial increment and draw ratio. Well controlled values of $\Delta\theta$ and $\Delta\xi$ should result in the desired accuracy and stability of the numerical solutions.

As analyzed above, Eq. (4.41) is only an estimation of the stability criterion for the explicit MacCormack finite difference formulation applied to the governing equations. Consideration of the lower order terms and the nonlinear behavior of the governing equations will modify or alter the stability criterion. If the factors are restrained to limitations mentioned above, the stability criterion should not be significantly affected.

4.3.3 Convergence

There is a definite linkage between the stability and the convergence. Lax's Equivalence Theorem (Richtmyer and Morton, 1967; Street, 1973; Anderson et al., 1984) states this relationship:

"Given a properly posed initial-value problem and a finite-difference approximation to it that satisfies the consistency condition, stability is the necessary and sufficient condition for convergence."

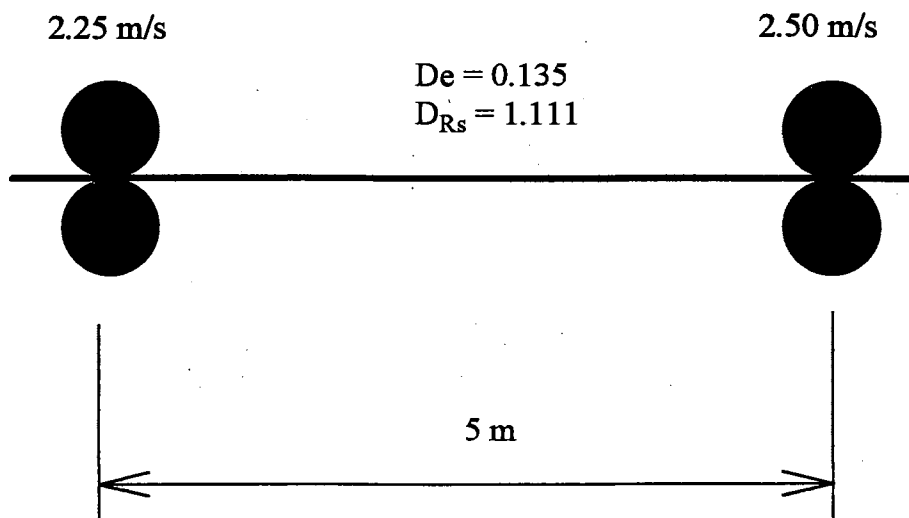
As the explicit MacCormack finite difference formulation for the governing equations has been proven to be consistent and stable (if $\Delta\theta \leq \Delta\xi/D_{RS}$, estimated), based on Lax's Equivalence Theorem, the formulation is also convergent.

The developed finite difference formulation has been shown to be consistent, convergent and conditionally stable.

4.3.4 Numerical Testing

To verify the stability criterion, Eq. (4.41), several numerical examples are given in this section. The unsteady-state cases are evaluated with emphasis on the stability. However, the steady-state cases are also investigated for the purpose of determining $\Delta\xi$. Appropriate values of spatial and time increments are suggested based on the numerical testing.

At steady state, the fourth-order Runge-Kutta method was used on a single-span system as shown in Figure 4.3. The tensions were calculated for different coordinate increments in the z -direction, $\Delta\xi$, while keeping the other conditions unchanged. The relative tolerance for the dimensionless velocity was set to be 1×10^{-5} . The tension results are shown in Table 4.1.



$G = 0.55 \times 10^9 \text{ Pa}$,
 $m = 1.65 \times 10^8 \text{ PaS}$,
 $n = 1$,
 $E = 1.65 \times 10^9 \text{ Pa}$,
 $A_0 = 1 \times 10^{-4} \text{ m}^2$,
Entry State: Unstressed.

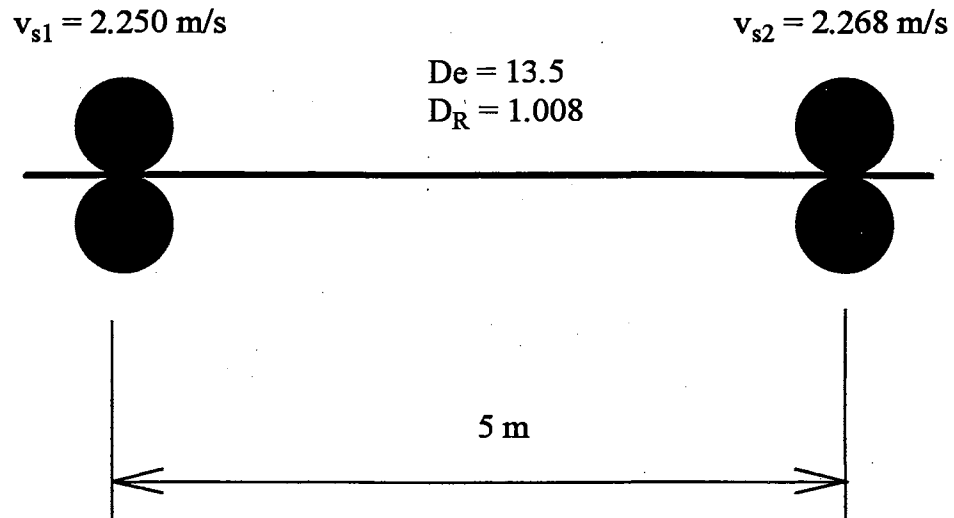
Figure 4.3 A Single-Span System at Steady State

Table 4.1 Steady-State Tensions with Different $\Delta\xi$

$\Delta\xi$	F_s (N)
0.500	2067.25868
0.333	2066.77025
0.250	2066.77025
0.200	2066.77025
0.100	2066.77025
0.050	2066.77025

Table 4.1 clearly shows that $\Delta\xi = 1/3$ is small enough for the tension calculation. Although the fourth-order Runge-Kutta method has a global error of $O[(\Delta\xi)^4]$ that requires $\Delta\xi$ to be 0.1 to achieve 10^{-4} accuracy for the dimensionless velocity, the tolerance of velocity error for the solution iteration (1×10^{-5}) made the tension saturated to five decimal places as $\Delta\xi = 1/3$. The situation was due to the fairly linear distribution of velocity in this case. Simulation has also shown that Deborah number and draw ratio could affect the requirement for the size of $\Delta\xi$ since those factors could influence the linearity of the velocity distribution. As De decreases or D_R increases, $\Delta\xi$ should be reduced to achieve the required accuracy.

The increments of $\Delta\xi$ and $\Delta\theta$ at unsteady state have also been determined from numerical experiments. To verify the relationship in Eq. (4.41), an example was examined as shown in Figure 4.4. Different sizes of $\Delta\xi$ and $\Delta\theta$ were chosen to simulate the system and the stable conditions are listed in Table 4.2.



$G = 0.55 \times 10^9 \text{ Pa},$
 $m = 1.65 \times 10^{10} \text{ PaS},$
 $n = 1,$
 $E = 1.65 \times 10^9 \text{ Pa},$
 $A_0 = 1 \times 10^{-4} \text{ m}^2,$
 Entry State: Unstressed,
 Initial State: Unstressed.

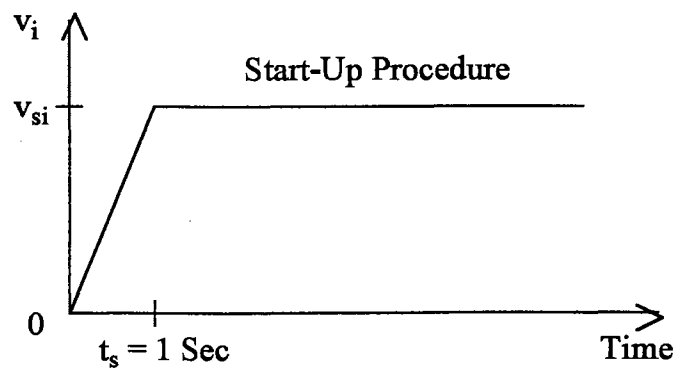


Figure 4.4 A Single-Span System Subjected to a Start-Up Procedure

Table 4.2 Stable Conditions for Different $\Delta\xi$ and $\Delta\theta$

$\Delta\theta \backslash \Delta\xi/D_{RS}$	0.0496	0.0992	0.1984
0.045	Stable	Stable	Stable
0.090	Unstable	Stable	Stable
0.180	Unstable	Unstable	Stable

A tolerance of 1×10^{-6} was used for solution iterations for both ϕ_i at each point and at $\xi = 1$ to prevent the stable condition from the disturbance due to the deviations of ϕ .

From Table 4.2, the unstable conditions really occurred when $\Delta\theta > \Delta\xi/D_{RS}$, therefore, the stability criterion was verified to be accurate and could be used in the numerical simulation in this study as a control for the increments of the coordinate and time variables.

Since the explicit MacCormack method has accuracy of $O[(\Delta\xi)^2, (\Delta\theta)^2]$, the size of $\Delta\xi$ should be smaller than that for the fourth-order Runge-Kutta method to achieve the required precision. By considering both steady-state and unsteady-state simulation, $\Delta\xi$ was chosen to be less than 0.05 for most cases in this study.

4.4 Chapter Review

In this chapter, the numerical formulations have been developed for the model equations. In steady state, two equivalent first-order differential equations were set up to replace the second order governing equation and the fourth-order Runge-Kutta

method was used to solve the system of equations. The shooting method was adopted to solve the boundary value problem with the step by step numerical scheme. The searching and bisection procedure was also created to implement the trial-and-error approach in determining the interaction of the elastic step change at web/roller contact region and the viscoelastic response in an open span.

For the unsteady-state governing equations, the finite difference formulations were developed based on the explicit MacCormack approach. The finite difference scheme was achieved by the two-step, predictor and corrector procedure. A decoupling technique was used to solve the set of governing equations simultaneously. The balance of the responses in the contact region and the open span was determined by the trial-and-error method.

Finally, the stability criterion for the finite difference scheme was estimated from an approximate analysis and an empirical study. The stability criterion requires that the time increment be constrained by the spatial increment and the draw ratio. Numerical testing for the stability criterion was also conducted and appropriate values of $\Delta\xi$ and $\Delta\theta$ were suggested.

CHAPTER V

NUMERICAL RESULTS AND DISCUSSION

In this chapter, the results of the simulation of viscoelastic behavior in common web handling systems are presented. First, the model, solution methods and program code were verified by comparison to examples from the open literature. Second, model parameters were estimated from experimental data in the literature. Steady-state operation was examined and, finally, several industrially relevant transient cases were considered.

In the steady-state case, attention was mainly paid to the effects of the viscoelasticity of materials on the operating conditions of systems. As a starting point, the viscoelastic material response within a single span was examined and compared to the response of a Hookean material and experimental observations. The viscoelastic response was characterized by the irrecoverable or permanent deformation and was correlated by the Deborah number. The effect of the power law exponent, n , on the viscoelastic response was also examined. The system response was found to be very sensitive to n . Then the study was extended to multi-span cases in which the operating conditions were shown to be very sensitive to even very small irrecoverable deformations. Tension transfer was also examined through examples with emphasis on the viscoelastic effects, and compared to Hookean results. The observed effects

were interpreted in terms of the model parameters and the draw ratio.

In order to investigate the viscoelastic behavior of web handling systems under transient conditions, various single-span and multi-span systems were simulated in start-up, the transition from one steady state to another, and a sinusoidal disturbance about a steady state. The tension variations during the transient procedures were calculated as a function of the viscoelastic properties of the web and were compared to those obtained from an elastic model based on Hooke's law. The phenomena of slackness of the web line, as well as the influence of slackness on subsequent spans were stressed in the numerical simulation. The tension interactions in multi-span systems were also examined through examples. General results showed that long time scale transitions (start-up and transition between steady states) are more readily affected by the viscoelasticity while short time scale transition (e.g. sinusoidal disturbance) does not affect the average tension but produces the short term tension variation.

5.1 Verification

There is a remarkable lack of data in the open literature concerning the operating behavior of web handling systems. However, three limiting cases are cited here for the purpose of making comparisons with the model developed in this study, VEM (which stands for "ViscoElastic Model").

Fiber spinning can be considered to be a single-span system without a step change at the entry point since the beginning of the span is taken as the point of

maximum swell. Hence, the material response is continuous across the beginning point of the span. The total deformation is due solely to the viscoelastic response in the open span.

The second case involves simulation to determine the tension in an open span using Hooke's law. In this case, the deformation is a result of the purely elastic response at the web/roller contact region. The two limiting cases represent the two major responses of viscoelastic materials that the VEM model attempts to capture.

For the unsteady-state case, a purely elastic, analytical solution was introduced to verify the transient prediction of the viscoelastic model in the limit of a purely elastic material. The transient behavior of a two-span system was examined in a start-up procedure.

The VEM model has been verified (as shown below) to be accurate in these limiting cases. The simulation results also demonstrated that the VEM model will converge to the corresponding elastic model when the model parameters were properly specified.

5.1.1 Example: Fiber Spinning

Although the geometry of fiber spinning process is different from that in a web handling system, the viscoelastic response in the open span can be characterized by the same underlying principles. Fisher and Denn (1976) modeled the viscoelastic response of a steady-state fiber spinning process using the White-Metzner rheological equation of state. The governing equation for the dimensionless velocity is identical

to that of the VEM model with $c = 1$ (no step change at web/roller contact region) and the assumption of positive tension.

To compare Fisher and Denn's model and the VEM model, simulation was carried out with the data listed below:

Material: Polystyrene at 170 °C,

$$m = 4.7 \times 10^3 \text{ PaS}^{1/3}, \quad n = 1/3,$$

$$G = 2.648 \times 10^3 \text{ Pa}, \quad (T_{zsz})_0 = 1,$$

$$D_{Rs} = 5.85, \quad (v_{zs})_0 = 0.0029 \text{ m/s},$$

$$L = 0.2 \text{ m}, \quad (A_s)_0 = 1.178 \times 10^{-5} \text{ m}^2.$$

Both models predicted the dimensionless inverse tension $N = 0.2974$ ($De = 0.3$). The dimensionless velocities simulated by the two models are shown in Figure 5.1. Good agreement can be seen in Figure 5.1, indicating that the VEM model has been properly programmed.

The viscoelastic response in processing a solid material would not be expected to be as severe as in this case, and the draw ratio in the fiber spinning case (5.85) is much larger than those in common web handling systems. Also, the stress ratio at the beginning of the span ($(T_{zsz})_0 = 1$ and $(T_{xzs})_0 = 0$ in this case) is different from the common assumptions for solid materials. However, the successful simulation of this case by the VEM model shows that the capacity and broadness of the model are sufficient for simulating the viscoelastic responses of extensional flow deformations in various applications.

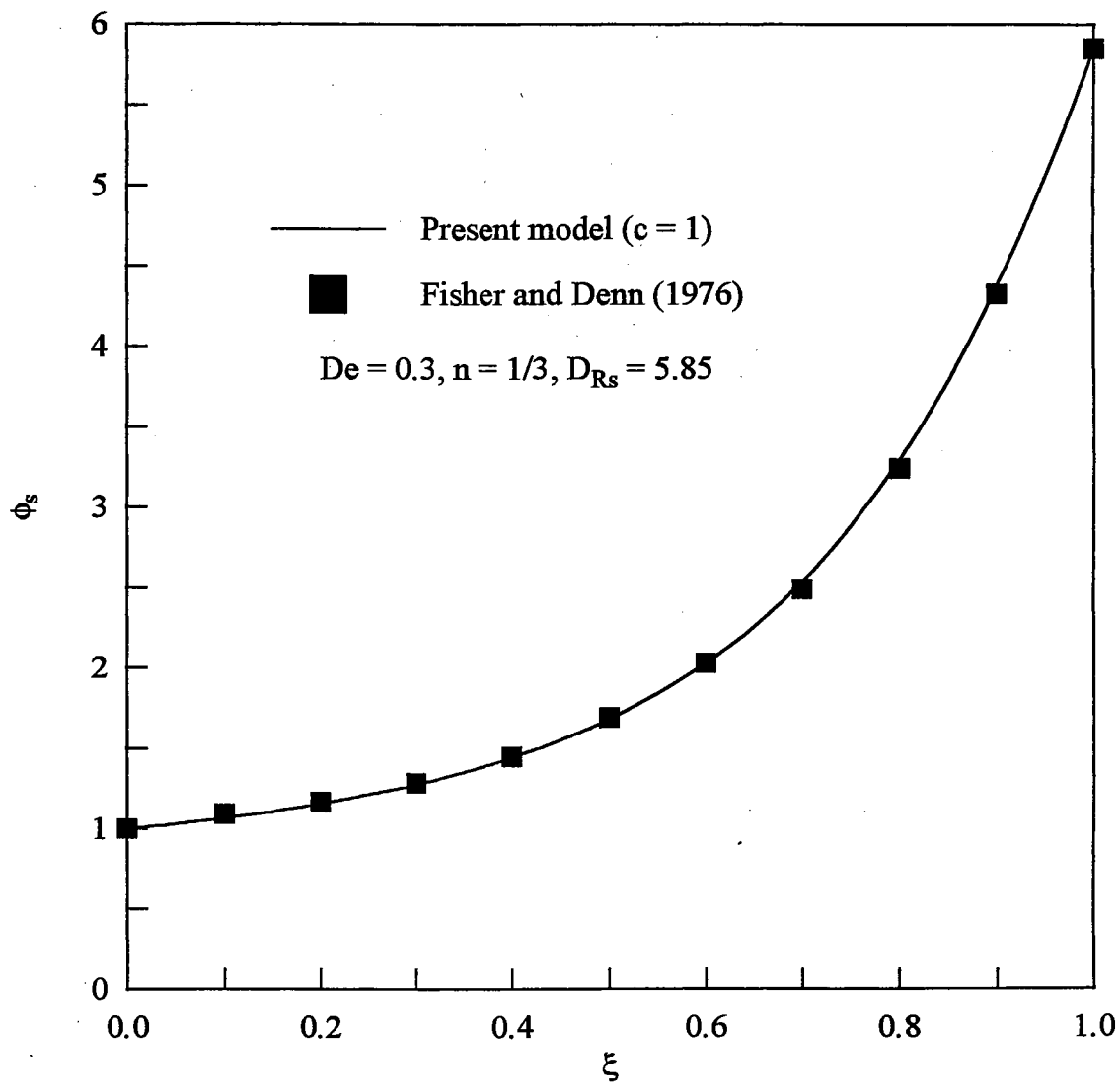


Figure 5.1 Velocity Profile for a Polystyrene Melt in a Fiber Spinning Process

5.1.2 Purely Elastic Model Case

A two-span web handling system is shown in Figure 5.2, which represents an actual industrial operation (Shin, 1991). The polypropylene film was pre-stretched before it entered the two-span system. In steady-state operation, the tension in the first span, F_{s1} , was measured to be 667.2 N. The tangential velocities of the rollers were constant at 2.301 m/s, 2.292 m/s and 2.286 m/s, respectively as shown in Figure 5.2. There was no slippage between the web and rollers and thus the tangential velocity of the roller represented the web velocity at the contact point.

To predict the tension in the second span, F_{s2} , based on a purely elastic material, the model parameter, m , was allowed to be very large. The measured data were:

$$E_1 = 7.998 \times 10^8 \text{ Pa}, \quad E_2 = 1.655 \times 10^9 \text{ Pa},$$

$$D_{Rs} = 0.9974, \quad (A_s)_{0-} = 1.016 \times 10^{-4} \text{ m}^2.$$

The other simulation data were:

$$G_2 = 5.516 \times 10^8 \text{ Pa}, \quad m = 10^{20} \text{ PaS},$$

$$n = 1, \quad (T_{zzs})_{0+} = 2/3,$$

At the end of the first span, the first normal stress difference, $(\tau_{zzs} - \tau_{xxs})_{0-}$, and strain, $(\epsilon_{zs})_{0-}$, were calculated to be:

$$(\tau_{zzs} - \tau_{xxs})_{0-} = \frac{F_{s1}}{(A_s)_{0-}} = 6.567 \times 10^6 \text{ Pa}, \quad (5.1)$$

and

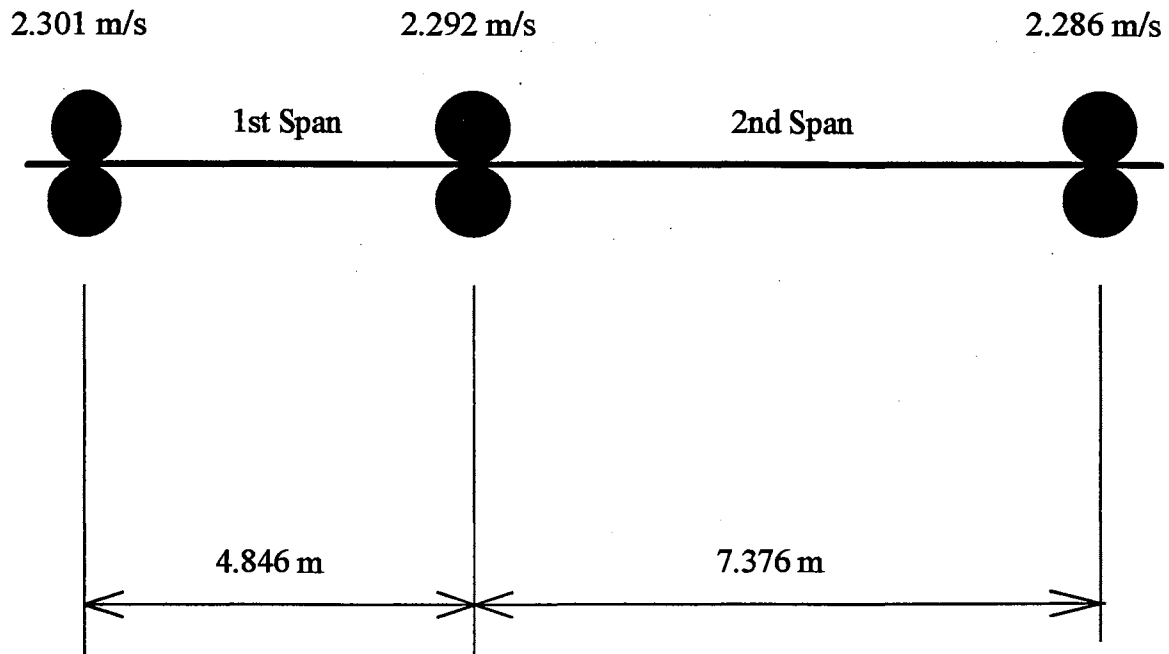


Figure 5.2 An Example in Modeling Web Handling Systems

$$(\epsilon_{zs})_0^- = \frac{(\tau_{zss} - \tau_{xss})_0^-}{E_1} = 8.211 \times 10^{-3}, \quad (5.2)$$

respectively.

Based on these data, the tension of the second span, F_{s2} , was predicted to be 224.0 N and the tension transfer parameter, c , to be 1.0026 indicating that the draw ratio was achieved at the very beginning of the span. A flat velocity profile was observed in the open span as would be expected for a purely elastic material.

An elastic model (Shin, 1991) predicted the tension of the second span to be:

$$F_{s2} = F_{s1} \frac{v_{s1}}{v_{s2}} + A_s E_2 \frac{v_{s2} - v_{s1}}{v_{s2}} = 227.6 \text{ N}. \quad (5.3)$$

The slight difference in the two predicted values of F_{s2} is due to the effect of the entry strain which is not accounted for in the elastic model.

The actual measured value of F_{s2} was 200.2 N. The model predictions are 11.9% and 13.7% higher than the measured tension for the VEM model and for Shin's model, respectively. The difference between the elastic predictions and the actual value is to be expected since the material response is not purely elastic. The operating temperature for the polypropylene film (31 °C) was much higher than the glass transition temperature, -10 °C, (Mark et al., 1984). Therefore, the viscoelasticity of the material would be expected to allow the stress to relax from the elastic level.

Although the VEM model, applied under the purely elastic restriction did not

predict the correct tension for the real system in the example, the results were in good agreement with those of Shin's model (purely elastic).

The two preceding examples have provided successful verifications for the viscoelastic model for the two limiting conditions that represent the two possible extremes in the material response.

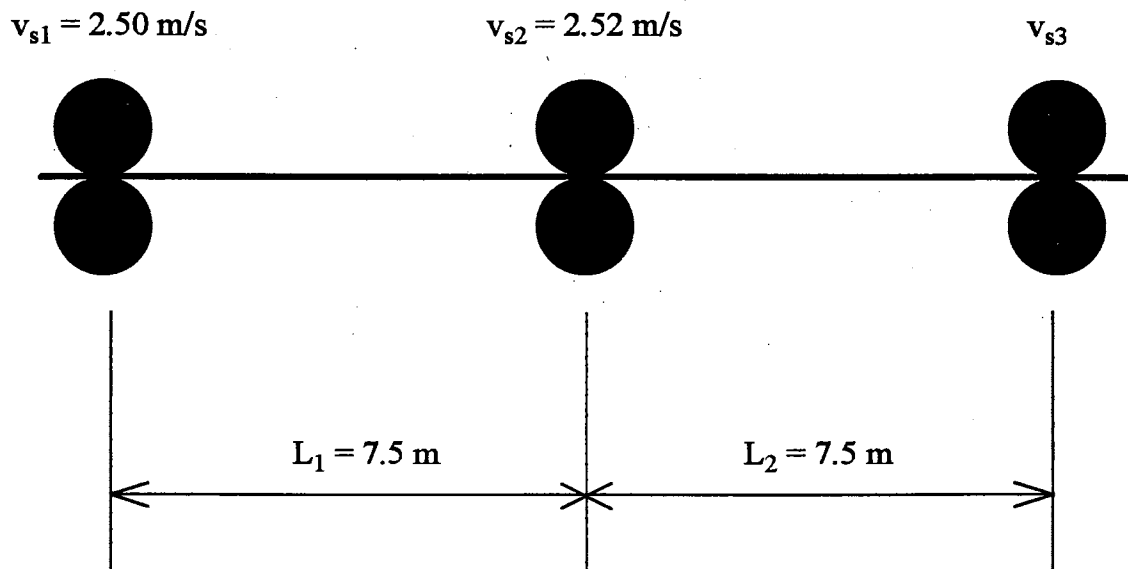
5.1.3 Transient Procedure

The prediction of the VEM model for a two-span system, during a start-up procedure and in the limit of an elastic material, is illustrated in this section and compared to an analytical solution.

The system configuration and material properties are shown in Figure 5.3. The span lengths are 7.5 m each. The web had a cross-sectional area of $1.0 \times 10^{-4} \text{ m}^2$ at the unstressed entry state and a Young's modulus of $1.65 \times 10^9 \text{ Pa}$. The initial system state was unstressed. All tangential roller velocities were linearly increased from zero to the steady-state values, 2.50 m/s, 2.52 m/s, and v_{s3} , respectively.

To simulate the purely elastic performance of the system, a very large value of m ($1 \times 10^{50} \text{ PaS}$) was provided for the viscoelastic model, resulting in an approximation of Hooke's law. Three cases were simulated with different draw ratios in the second span. The tensions in the two spans are shown in Figure 5.4 along with the analytical solutions. The analytical equations are derived in detail in Appendix B.

Perfect agreement between the VEM model predictions and the analytical solutions for different roller velocity distributions can be seen in Figure 5.4. Clearly,



$$E = 1.65 \times 10^9 \text{ Pa}$$

$$A_0 = 1.0 \times 10^{-4} \text{ m}^2$$

Entry State: Unstressed

Initial State: Unstressed

Figure 5.3 A Two-Span System with an Elastic Material Undergoing a Start-Up Procedure

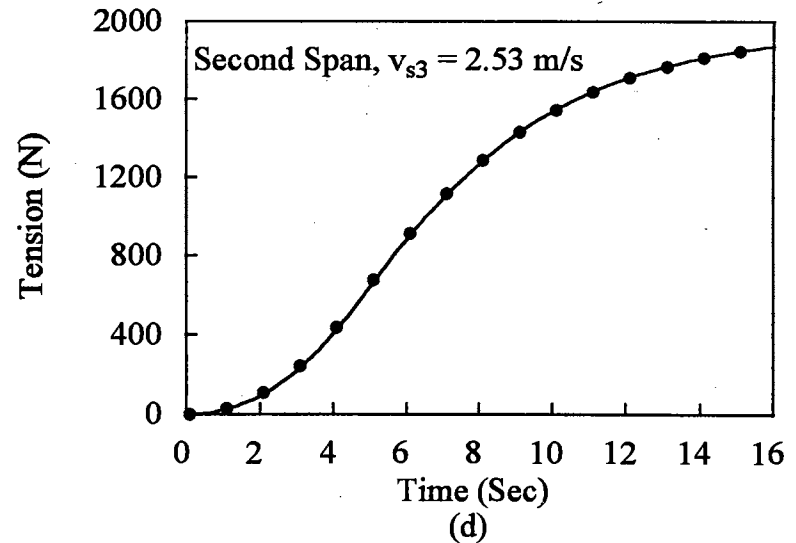
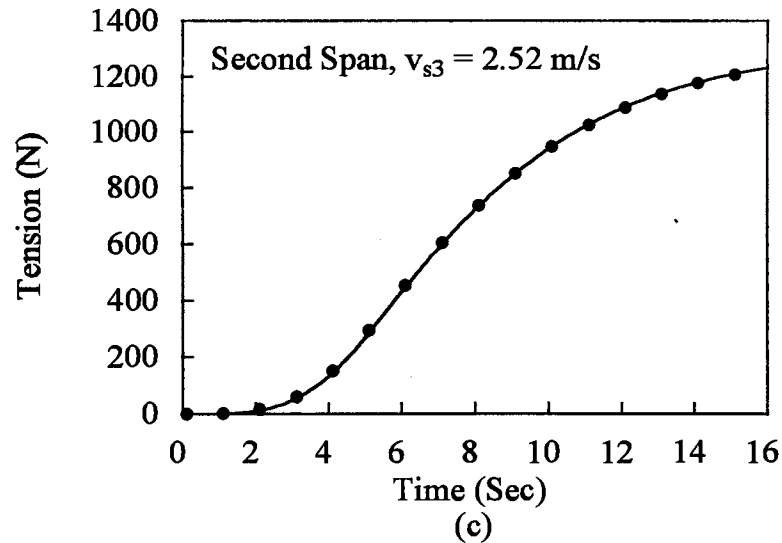
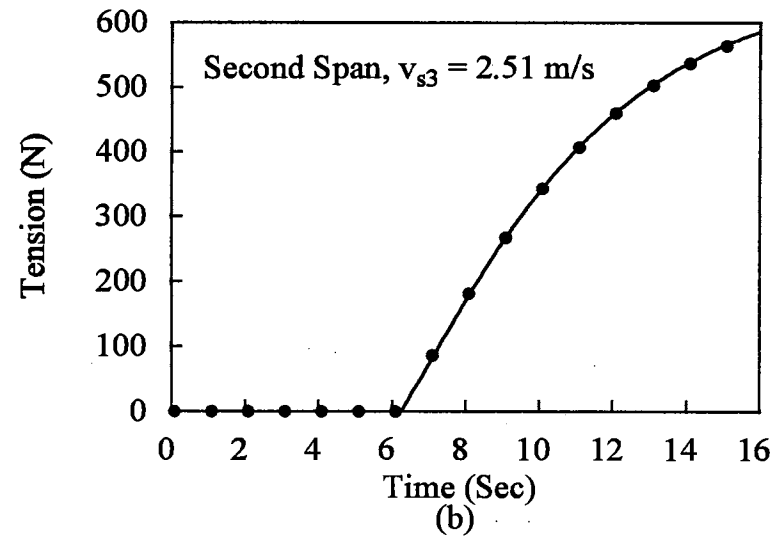
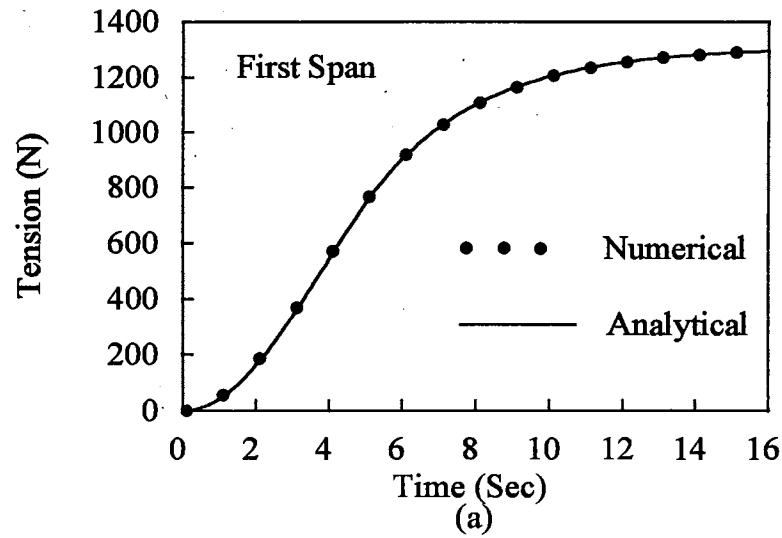


Figure 5.4 Comparison of Numerical and Analytical Simulation for the Elastic Model in the Start-Up Procedure (a) First Span, (b) Second Span with $v_{s3} = 2.51$ m/s, (c) Second Span with $v_{s3} = 2.52$ m/s, and (d) Second Span with $v_{s3} = 2.53$ m/s

from Figure 5.4, the VEM model can accurately simulate the transient responses in the elastic cases. The results of the comparison further demonstrate that a large enough value of m can make the viscoelastic model converge to an elastic model in the unsteady state.

5.2 Estimation of Model Parameters

The parameters, G , m and n , can be estimated from experimental data in the literature (Shin, 1991). Direct measurements would have been preferable. However, the appropriate instrument was not available to this study (see Section 6.2) and the estimated values were sufficient for the requirements of this work.

For the polypropylene film described in Section 5.1.2, the Young's modulus in the second span was reported to be 1.655×10^9 Pa. The tension in the second span was measured and found to be 200.2 N. The modulus, G , can be related to the Young's modulus in the limit of a deformation occurring in an infinitely small period of time. Under these conditions, the White-Metzner equation reduces to

$$\underline{\tau}_{(1)} = G\underline{\gamma}_{(1)}. \quad (5.4)$$

If the deformation is small enough, the zz component of Eq. (5.4), after integration, becomes

$$\Delta \tau_{zz} = G\Delta \gamma_{zz}. \quad (5.5)$$

Hooke's law states that, in a uniaxial deformation,

$$\Delta \sigma_{zz} = E \Delta \epsilon_z. \quad (5.6)$$

From Eqs. (3.7) and (3.9), the symmetry of σ_{xx} and σ_{yy} , as well as $p = -(\sigma_{xx} + \sigma_{yy} + \sigma_{zz})/3$, $\Delta \sigma_{zz}$ can be obtained as:

$$\Delta \sigma_{zz} = \frac{3}{2} \Delta \tau_{zz}. \quad (5.7)$$

Also, by definition: $\dot{\epsilon}_z = \partial v_z / \partial z$ and $\dot{\gamma}_{zz} = 2 \partial v_z / \partial z$, $\Delta \epsilon$ can be related to $\Delta \gamma_{zz}$:

$$\Delta \epsilon_z = \frac{\Delta \gamma_{zz}}{2}. \quad (5.8)$$

Therefore, Eq. (5.6) becomes

$$\Delta \tau_{zz} = \frac{E}{3} \Delta \gamma_{zz}. \quad (5.9)$$

By comparing Eqs. (5.5) and (5.9), G can be related to E :

$$G = \frac{E}{3}. \quad (5.10)$$

Second, m and n can also be estimated from the data on a two-span system found in Section 5.1.2 and by applying the viscoelastic model with the tension being constrained at 200.2 N. Since there is no restriction on the values of m and n other than $m > 0$, an infinite number of combinations of m and n are possible. However, the parameters may be roughly limited by intuition. For example, n should be about one with possibilities ranging from about 0.3 to 2.0. Some of the possibilities are listed in Table 5.1.

Table 5.1 Estimation of m and n

n	m (PaS ⁿ)	λ_0 (Sec)
0.3	not calculable	-
0.7	8.7×10^8	1.6
1.0	1.5×10^{10}	27.2
1.3	2.6×10^{11}	470
1.7	1.2×10^{13}	20848
2.0	2.0×10^{14}	358956

Values of m and n may vary from case to case and even from span to span in the same system since m and n are sensitive to thermal and rheological history. In polymeric materials, the orientation and crystallinity will significantly affect the material properties both in magnitude and anisotropy. Therefore, the values of G, m and n should be carefully measured. In this work, the numerical simulation was conducted based on the model parameters estimated in this Section or were taken from the range of values in Table 5.1 for trend studies.

5.3 Steady-State Analysis

The simulation has been conducted in single-span and multi-span cases in steady state. In single-span cases, the deformation behavior has been found quite different from the elastic case as demonstrated in Section 5.3.1. The viscoelastic deformation is characterized by the irrecoverable deformation and correlated by the Deborah number in Sections 5.3.2. The effect of the power law exponent, n, on the irrecoverable deformation was found to be very significant and is presented in Section 5.3.3. The model parameter N is shown in Section 5.3.4 as a function of De.

The effects of viscoelasticity on multi-span system behavior are shown in Sections 5.2.5 to 5.2.7. The operating conditions were found to be sensitive to even very small irrecoverable deformations produced in the upstream spans. As a result of the irrecoverable deformation, the spans may be in an undesirable slack condition and the slackness may further affect the operating conditions in the subsequent spans if draw ratios are small enough. Tension transfer was also studied and the simulation revealed that the amount of tension transferred was different from the elastic case.

5.3.1 Single-Span Behavior

A single-span system is shown in Figure 5.5. The stress and strain before the web enters the system were assumed to be zero and the power law exponent was set to 1.0. The tangential velocities of the rollers are v_{s0} and v_{sL} , respectively. The length of the span is L .

Figure 5.5 also shows the characteristic strain behavior which results from the simulation of an open span. The strain in the span clearly shows two parts: an instantaneous, purely elastic strain at the web/roller contact region, ϵ_e , and a viscoelastic strain developed in the open span, ϵ_{ve} . ϵ_e is recoverable. Whereas ϵ_{ve} is only partially recoverable. The total strain, ϵ_t , is the sum of ϵ_e and ϵ_{ve} . The strain ratio, ϵ_{ve}/ϵ_t , can be calculated and is shown in Table 5.2 for $D_{Rs} = 1.00667$. The relaxation time ($\lambda_0 = m/G$) is also listed in Table 5.2 for a specific case of $(v_{zs})_0 = 3$ m/s and $L = 5$ m.

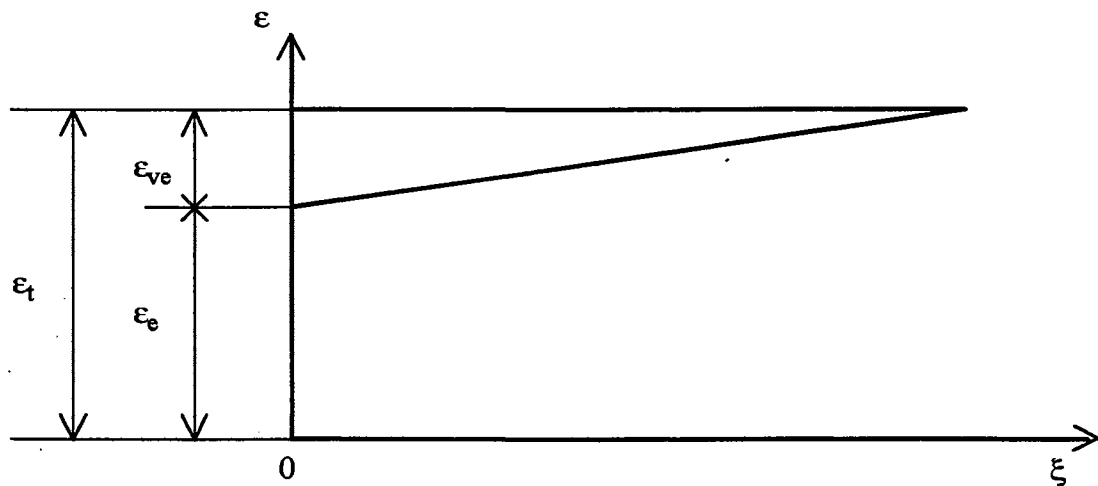
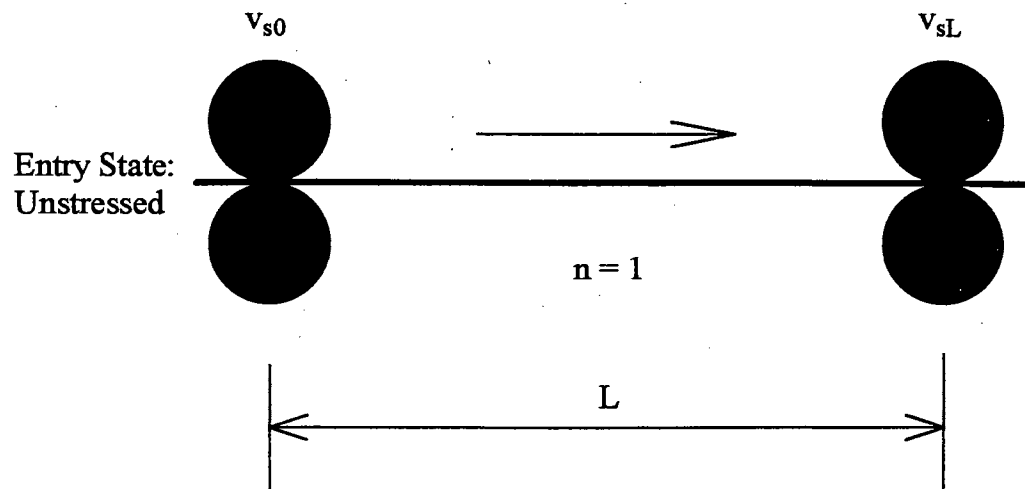


Figure 5.5 A Case Study of a Single Span

Table 5.2 Strain Ratio in a Single-Span System

De	λ_0 (Sec) ($(v_{zs})_{0-} = 3 \text{ m/s}, L = 5 \text{ m}$)	ϵ_{ve}/ϵ_t (%)
6	10	14.2
30	50	3.20
60	100	1.63
300	500	0.329
600	1000	0.166

As can be seen in Table 5.2, the strain ratio, ϵ_{ve}/ϵ_t , decreases when De or λ_0 increases. The relative contribution of the viscoelastic strain to the total strain is a strong function of the Deborah number. As the Deborah number increases to infinity, ϵ_{ve} disappears and the system behaves as a Hookean solid.

For a typical value of the relaxation time, 100 seconds, ϵ_{ve}/ϵ_t is approximately 1%. Although the viscoelastic deformation may be small in a single span, the tension distribution is very sensitive to this small amount of strain as is demonstrated in Sections 5.3.5. to 5.3.7.

The sudden change in strain upon entering a span, followed by a gradual change in strain over the span is in agreement with experimental observation (Hauptmann and Cutshall, 1977).

5.3.2 Irrecoverable Deformation

The viscoelastic deformation observed in Section 5.3.1 can be characterized by irrecoverable deformation and can be related to the Deborah number as well as the draw ratio. The irrecoverable or permanent deformation, ϵ_p , in the web material

relative to an unstressed state arises from the viscous component of the viscoelastic deformation. Generally, the irrecoverable deformation can be determined from an "unloading" procedure in which the purely elastic deformation is recovered.

To measure the relevant contribution of ϵ_p to the total strain, ϵ_t , a ratio ϵ_p/ϵ_t is obtained as (see Appendix C for details of the derivation)

$$\frac{\epsilon_p}{\epsilon_t} = \frac{cD_{Rs} \left[1 + (\epsilon_{zs})_{0^-} - \frac{1}{E}(\tau_{zzs} - \tau_{xxs})_{0^-} \right] - 1}{[1 + (\epsilon_{zs})_{0^-}]D_{Rs} - 1}. \quad (5.11)$$

In Eq. (5.11), $(\tau_{zzs} - \tau_{xxs})_{0^-}/E$ is the elastic component of the entry strain at 0.

Therefore, the quantity in the square brackets of the numerator is 1 plus the irrecoverable strain present upon entering the span.

Eq. (5.11) clearly shows that ϵ_p/ϵ_t is a function of the draw ratio, tension transfer parameter and entry state (strain and stress). Since the tension transfer parameter, c , reflects the balance of the viscoelastic response in the open span and the elastic step change at the contact region, c is a function of De . Therefore, ϵ_p/ϵ_t can be related to De when the draw ratio, power law exponent, and entry state are given. If the entry state is unstressed, i.e., $(\epsilon_{zs})_{0^-} = 0$ and $(\tau_{zzs} - \tau_{xxs})_{0^-} = 0$, Eq. (5.11) reduces to:

$$\frac{\epsilon_p}{\epsilon_t} = \frac{cD_{Rs} - 1}{D_{Rs} - 1}. \quad (5.12)$$

Figure 5.6 shows the relationship of ϵ_p/ϵ_t to De with D_{Rs} as a parameter, in a single span, if the web is initially unstressed and $n = 1$. When De approaches zero (the Newtonian fluid limit) and infinity (purely elastic solid limit), the ratio reaches

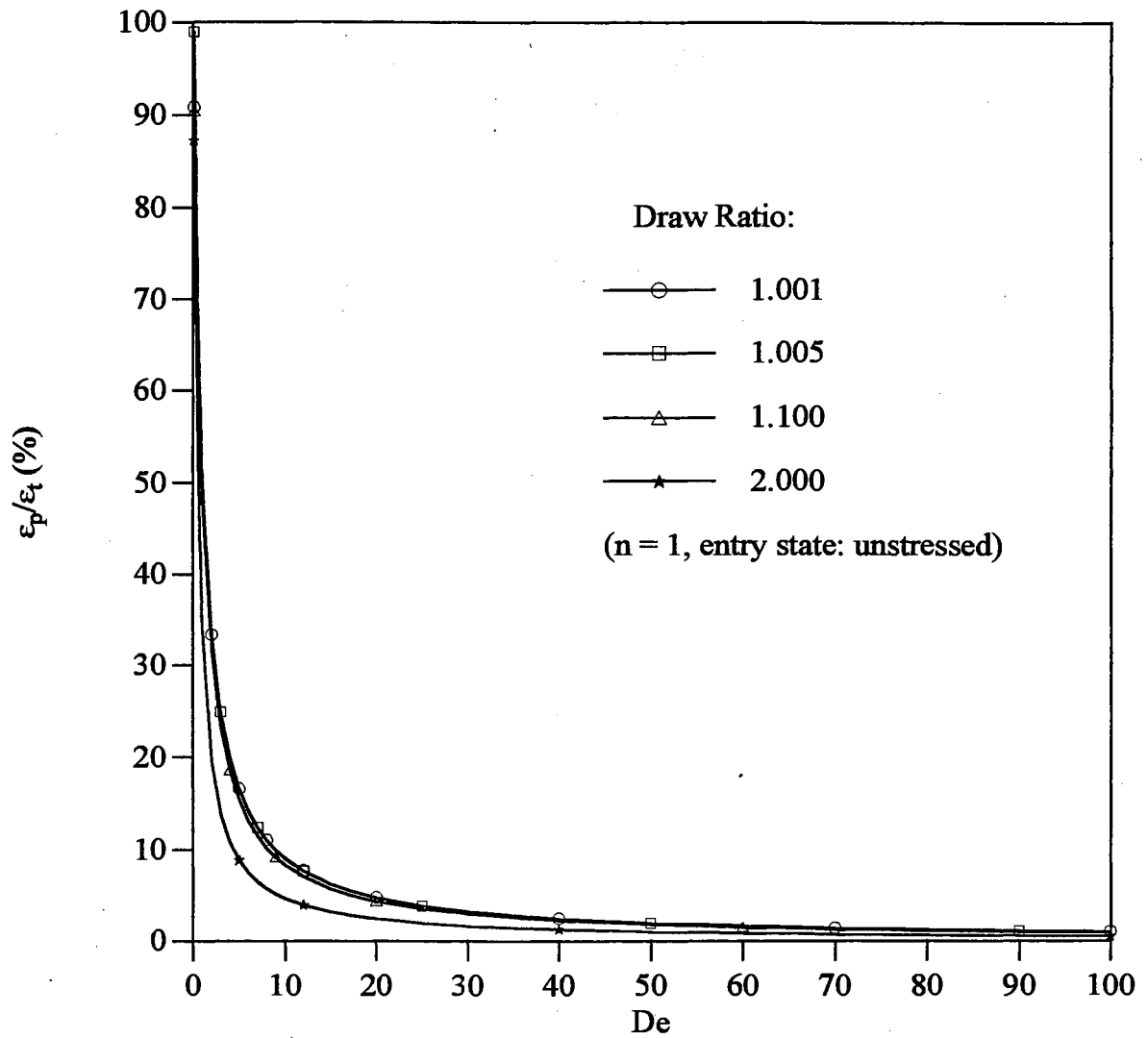


Figure 5.6 Permanent Deformation as a Function of Deborah Number with Draw Ratio as a Parameter for a Single Span

100% and zero, respectively, as would be expected. As D_{Rs} increases, the total elastic component (ϵ_e plus part of ϵ_{ve}) and ϵ_p will each increase. However, Figure 5.6 demonstrates that ϵ_p will not increase to the same extent as the elastic component.

The degree to which the material can viscoelastically respond to the tension in the span is limited by the length of time the material remains in the span. Since increasing D_{Rs} does not significantly affect t_{span} , the viscoelastic response of the material is constrained and the elastic component, which can be instantaneously achieved, must become proportionally larger to achieve the required total strain.

5.3.3 Effects of the Power Law Exponent, n

The power law exponent, n , can also affect the viscoelastic behavior of systems as illustrated in this section. n reflects the dependence of the viscosity of the material on the strain rate and also appears in the governing equation as an independent parameter. The effect of n on single-span system behavior can be examined by considering the relationship of ϵ_p/ϵ_t to De and n for a draw ratio, $D_{Rs} = 1.1$, as shown in Figure 5.7. To achieve the fixed draw ratio, 1.1 in this case, a shear thinning material ($n < 1$) responds with smaller irrecoverable deformation than a shear thickening material ($n > 1$) for constant De . This result would seem to be counter intuitive. However, the explanation follows from examination of Eq. (5.13), a working equation formed from the power law viscosity, Eq. (3.32), Eq. (3.49), and Eq. (3.54),

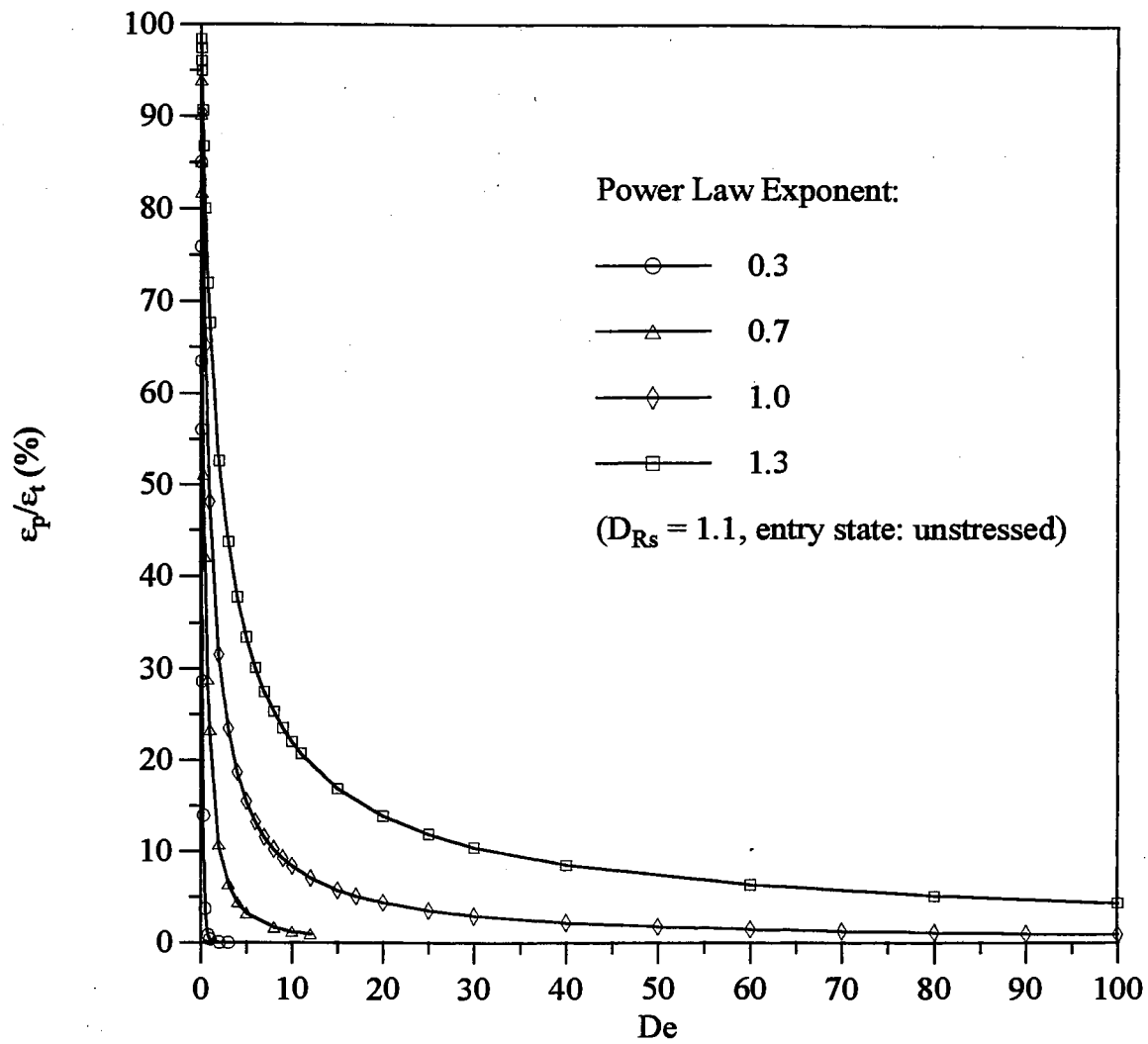


Figure 5.7 Permanent Deformation as a Function of Deborah Number with the Power Law Exponent as a Parameter

$$\eta = DeG \frac{L}{(v_{zs})_{0^-}} |\phi'_s|^{n-1}. \quad (5.13)$$

In this case, ϕ'_s is less than one due to the smaller draw ratio ($D_{Rs} = 1.1$).

Therefore, the viscosity decreases as n increases for a constant De , resulting in an easier means for the material to relax through an irrecoverable strain.

The results in this section show that the system behavior can be affected significantly by the power law exponent in the range of reasonable values (0.3 to 1.3). Further evidence of the sensitivity of the system behavior is presented in Appendix D. Therefore, the determination of the power law exponent is important. Experimental measurements of n are strongly recommended for practical applications of the model.

5.3.4 Stress Ratio

The effect of viscoelasticity on the tension level is examined in this section. The general relationship of the tension level to the viscoelasticity can be observed from the dimensionless inverse tension, N , as a function of De . A working equation for N can be derived by substituting Eq. (3.54) into Eq. (3.55),

$$N = \frac{3^{\frac{n-1}{2}} m \left[\frac{(v_{zs})_{0^-}}{L} \right]^n}{\left[\frac{F_s}{(A_s)_{0^+}} \right]}. \quad (5.14)$$

The numerator is the characteristic viscous stress of the material and reflects the relative degree of difficulty in viscously deforming the material. The denominator is

the applied tensile stress.

The relationship of N to D_e and D_{Rs} for a single span is shown in Figure 5.8 for an unstressed entry state. For a fixed D_{Rs} (fixed total strain), N increases almost linearly with D_e since the characteristic viscous stress increases due to the difficulty in the viscous deformation (see Table 5.2) while the applied tensile stress does not change as dramatically as the characteristic viscous stress. On the other hand, N decreases as D_{Rs} increases for fixed D_e (fixed characteristic viscous stress). In this case, the applied tensile stress must increase to achieve the required total deformation making N smaller.

5.3.5 Effects of Irrecoverable Deformation

In order to demonstrate the significance of the viscoelastic deformation, the system configuration shown in Figure 5.9 was considered with material parameters characteristic of a polypropylene film at room temperature. The system consists of two open spans with lengths of 7.5 m each. The web enters the first span in an unstressed state with a cross-sectional area of $1.0 \times 10^{-4} \text{ m}^2$. The material parameters are given in Figure 5.9.

The tangential velocities of the three roller sets were taken as 2.500, 2.520 and 2.501 m/s, respectively. The Deborah number of the first span, under these conditions, is 10. The draw ratio in the first span is greater than one (1.008) but, in the second span, D_{Rs2} is less than one (0.9925). The velocity distribution forces the web to stretch in the first span and then allows contraction in the second span.

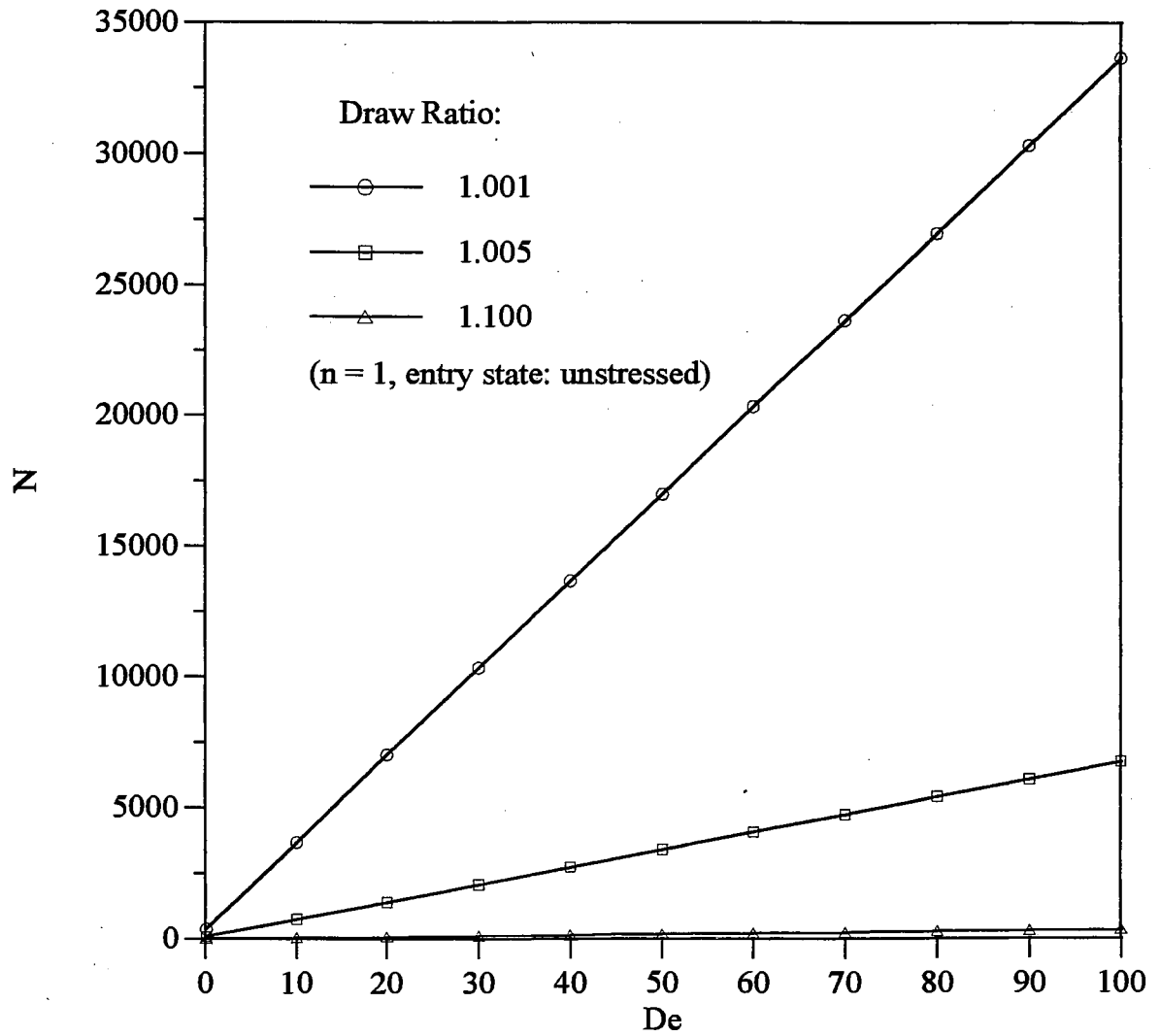
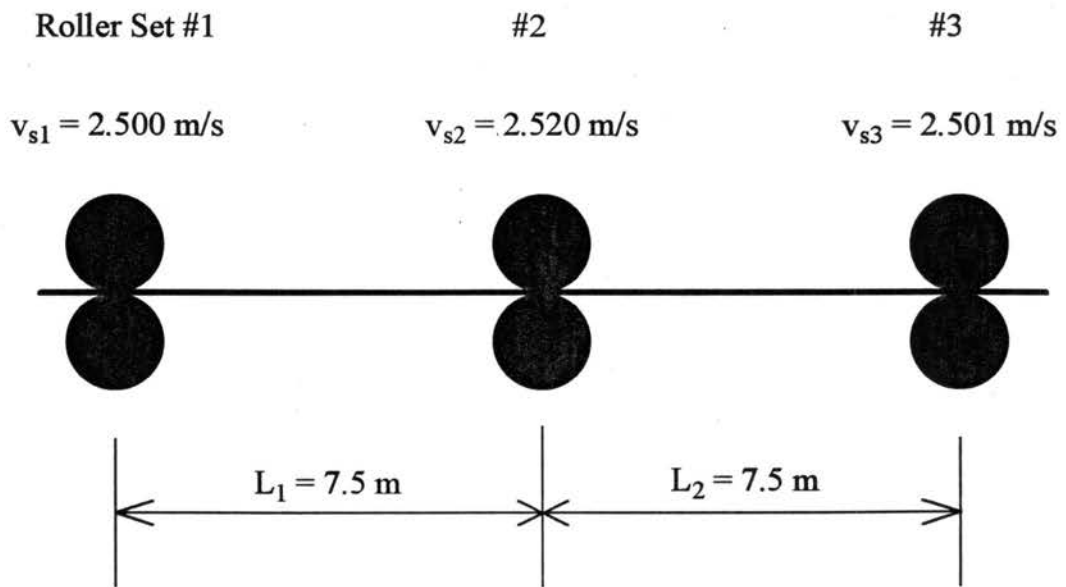


Figure 5.8 Dimensionless Inverse Tension as a Function of Deborah Number with Draw Ratio as a Parameter for a Single Span



$$A_0 = 1.0 \times 10^{-4} \text{ m}^2$$

$$G = 0.55 \times 10^9 \text{ Pa}$$

$$m = 1.65 \times 10^{10} \text{ PaS}$$

$$n = 1$$

$$E = 1.65 \times 10^9 \text{ Pa}$$

Entry state: Unstressed

No slackness if $v_{s3} > 2.5018 \text{ m/s}$

Figure 5.9 A Two-Span System Studied for the Effect of the Irrecoverable Deformation

The viscoelastic model predicted the tension in the two spans to be 1191 N and -48 N, respectively. While the model based on Hooke's law gives tensions of 1310 N and 66 N, respectively. The Hookean model predicted a tension in the first span approximately 10% greater than the viscoelastic model. This result is expected since the viscoelastic model allows for a stress relaxation mechanism which is absent from the Hookean model. However, the tensions in the second span, as predicted by the two models, are quite different. The negative tension given by the viscoelastic model indicates that the web must be compressed in order to meet the length and velocity specifications. Since a web cannot sustain a negative tension, due to the flexible nature of thin films, the second span must be in an undesirable slack or sagging state. (Note that the term "sagging" as used here does not refer to gravity since body forces have been assumed negligible.)

The slackness in the second span is due to the irrecoverable deformation produced in the first span. The web line must be operated under conditions such that the draw ratio in the second span will be greater than some minimum value that will wind up the irrecoverable part of the deformation. However, Hooke's law cannot predict the irrecoverable deformation and predicts that the velocity of the third roller need only be equal to or greater than the velocity of the first roller. In this case study, the small irrecoverable deformation in the first span due to the viscoelasticity of the material significantly affects the system behavior. The results explain the failure of some open-loop control systems that were designed with Hooke's law and clearly illustrate the need for more realistic models of the system behavior.

The minimum draw ratio required in the second span to prevent slackness, $D_{Rs2,min}$, is closely related to the irrecoverable deformation and draw ratio of the previous span. $D_{Rs2,min}$ can be expressed as (see Appendix E for details of the derivation):

$$D_{Rs2,min} = c_1 \left\{ 1 - \frac{(\tau_{zzs} - \tau_{xzs})_{10^-}}{[1 + (\epsilon_{zs})_{10^-}]E} \right\}. \quad (5.15)$$

When the entry state of the system is unstressed, the draw ratio reduces to

$$D_{Rs2,min} = c_1 = \frac{1 + \epsilon_{pl}}{D_{Rs1}}. \quad (5.16)$$

As was discussed in Section 5.3.2, c_1 is a function of De . Therefore, $D_{Rs2,min}$ can be related to De . The relationship of $D_{Rs2,min}$ to De_1 and D_{Rs1} is shown in Figure 5.10. For a fixed De_1 , $D_{Rs2,min}$ decreases as D_{Rs1} increases. Figure 5.10 shows that $De_1 = 100$ is a close approximation to the limiting case of $De_1 = \infty$, when $D_{Rs2,min} = 1/D_{Rs1}$ (purely elastic). In design, a larger De is desirable to reduce the tendency of slackness under a given set of operating conditions. Large Deborah numbers can be achieved by increasing the operating speed or reducing the span length.

In the example of Figure 5.9, the minimum draw ratio of the second span was 0.9928, while the actual draw ratio (0.9925) was within the slack region in Figure 5.10.

If the system is in a prestressed entry state, $D_{Rs2,min}$ will decrease if c_1 is the same and the minimum value will occur under the purely elastic prestressed condition, $D_{Rs2,min} = c_1/[1 + (\epsilon_{zs})_{10^-}]$. The trend can be explained by examining Eq. (5.15). (τ_{zzs}

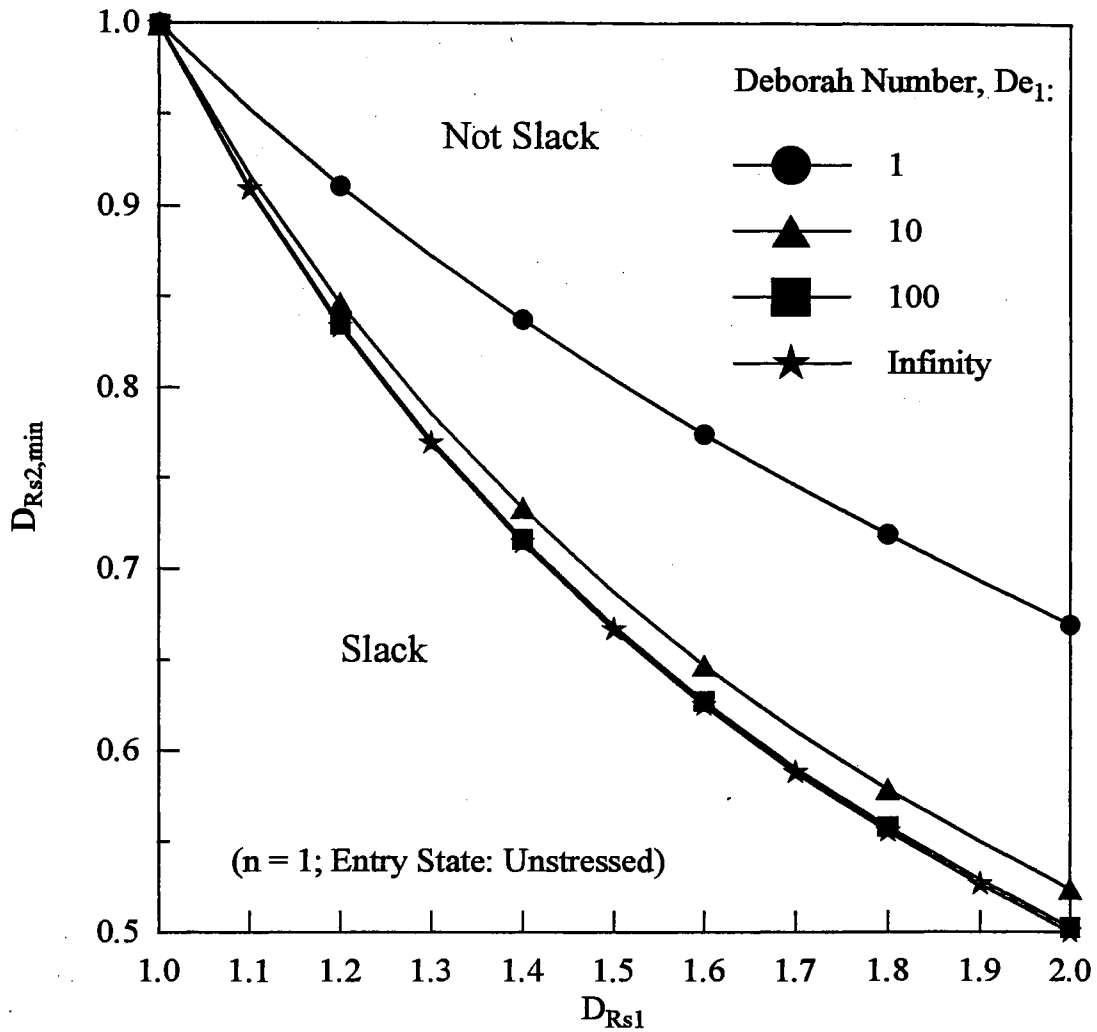


Figure 5.10 Minimum Required Draw Ratio to Prevent Slackness in the Second Span as a Function of the Draw Ratio in the First Span with Deborah Number as a Parameter

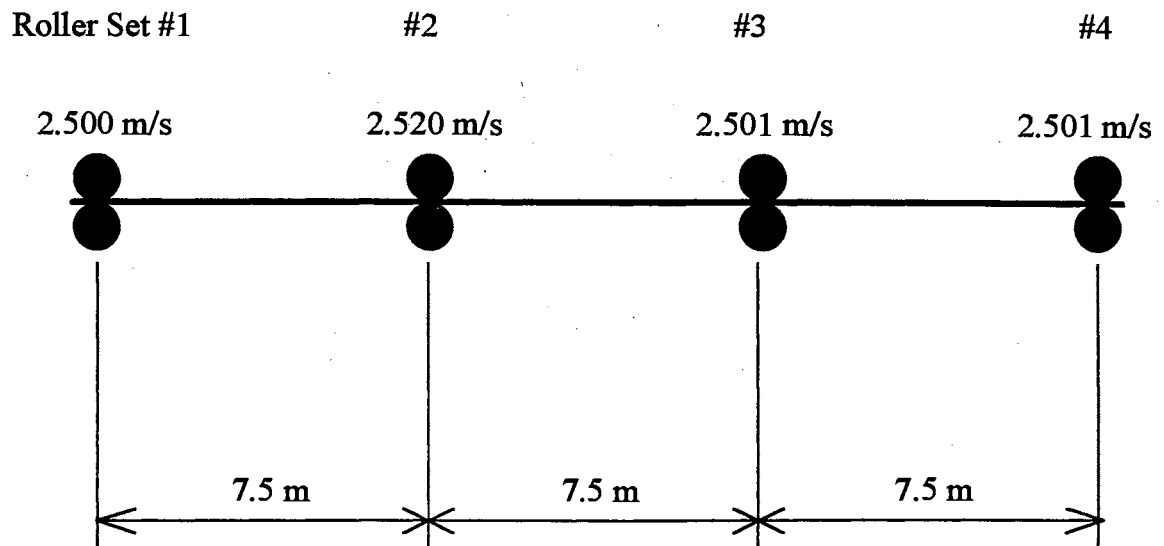
- $\tau_{xss})_{10}/E$ is the elastic component of the total entry strain, $(\epsilon_{zs})_{10}$. Therefore the term in the braces changes from 1 at the unstressed entry state to $1/[1 + (\epsilon_{zs})_{10}]$ at the purely elastic prestressed entry state. If the entry strain is completely irrecoverable (no entry stress), $D_{Rs2,min}$ is identical to the minimum draw ratio from an unstressed entry state.

For multi-span systems, a general conclusion can be drawn that the minimum draw ratio will be larger than those predicted by the purely elastic model. The difference of the two models will become greater in downstream spans since the irrecoverable strain is cumulative.

5.3.6 Effects of Slackness in Multi-Span Systems

In a multi-span system, if slackness occurs in a span due to the viscoelasticity, the operating conditions of the subsequent spans will be influenced as is illustrated in this section. The purely elastic model may not predict any such downstream effects. The difference between an elastic and viscoelastic responses can be illustrated by considering the three-span system shown in Figure 5.11. The operating conditions and material properties are given in Figure 5.11. The draw ratio in the first span is greater than one (1.008) requiring the web to stretch from the unstressed entry state. The web then contracts in the second span due to the draw ratio less than one (0.9925) in the span. The third span has a draw ratio of one and the tension level depends on the operating condition in the second span.

The tension predictions are summarized in Table 5.3.



Entry State: Unstressed

$$A_0 = 1 \times 10^{-4} \text{ m}^2$$

$$G = 0.55 \times 10^9 \text{ Pa}$$

$$m = 1.65 \times 10^{10} \text{ PaS}^n$$

$$E = 1.65 \times 10^9 \text{ Pa}$$

$$n = 1$$

Figure 5.11 A Three-Span System at Steady State

Table 5.3 Tension Predictions in the Second and Third Spans

	Viscoelastic Model	Elastic Model
2nd Span	0 (-48 N)*	66 N
3rd Span	0	66 N

(* Calculated tension is -48 N but should be treated as 0.)

The viscoelastic simulation reveals that the second span and the third span are slack (zero tension) since the draw ratios are smaller than the required minimum values. However, the purely elastic model still gives a positive tension of 66 N in each of the two spans meaning that steady-state operation is possible.

In this case, the slackness in the third span is solely due to the slackness in the second span since there is no further stretching in the third span and the tension in the third span only depends on the tension transfer (as discussed in Section 5.3.7) from the second span. If the draw ratio in the third span is kept the same ($D_{Rs3} = 1$) but v_{s3} and v_{s4} are increased by 0.001 m/s, the two spans are no longer slack with tensions of 12 N and 11 N, respectively. Therefore, the slack condition in the upstream span can propagate into the subsequent spans under certain conditions. A similar trend can be expected in systems with more open spans; especially in systems with small velocity differences. The inescapable conclusion is that even very small viscoelastic deformations may significantly affect the system operation.

5.3.7 Tension Transfer

The tension in the current span of interest is affected by the viscoelastic response of the material and the tension transferred from the previous span. Within any span, the tension must balance the elastic step change across the roller and the viscoelastic deformation within the span so that the kinematic conditions at the span ends can be met. This section shows that the tension transfer in the viscoelastic case is different from that in an elastic case.

The effect of the tension in the previous span could be examined by an example with the same system configuration and operating condition as shown in Figure 5.9 except that the tangential velocity of the third roller set is allowed to vary. Several cases are shown in Table 5.4.

Table 5.4 Tension in the Second Span

Case	v_{s3} , m/s	F_{s2} , N	
		Viscoelastic Model	Hookean Model
1	2.530	1673	1956
2	2.520	1084	1310
3	2.510	490	657
4	2.500	-108	0

In the four cases, the tensions predicted by Hook's law (i.e. $m = \infty$) in the second span are 1956 N, 1310 N, 657 N and zero, respectively. The deviations of the Hookean results from the viscoelastic results for the tension in the second span are 16.9%, 20.8%, and 34.2%, respectively in the first three cases. In the fourth case,

however, the deviation is so great that steady-state operations would not be possible based on the viscoelastic prediction but would still be possible based on the Hookean prediction.

In the first span, the tension predicted by Hooke's law is 1310 N and the deviation in tension is 9.92%. No matter how v_{s3} changes, the deviation in the second span is larger than that in the first span as long as no slackness occurs as shown in Figure 5.12. Hence, viscoelasticity is increasingly important along the web line from the beginning to the end because of the accumulation of the irrecoverable deformation.

5.3.8 Summary

The effects of viscoelasticity on system behavior in steady state have been demonstrated in Section 5.3 through numerical simulation for single-span and multi-span systems. The deformation behavior has been found quite different from that in an elastic case. The irrecoverable deformation and tension level are a strong function of Deborah number, power law exponent, and draw ratio in a single-span system. Generally, the Deborah number is a good indicator for the effect of the viscoelasticity since this dimensionless group reflects a combined contribution of material properties, operating condition and system configuration. However, the power law exponent, n , is also an independent model parameter that will affect the viscoelastic response. Although the viscoelastic deformation may be very small in the first span of a multi-span system, the effect can be dramatic in the subsequent spans. The tension in the

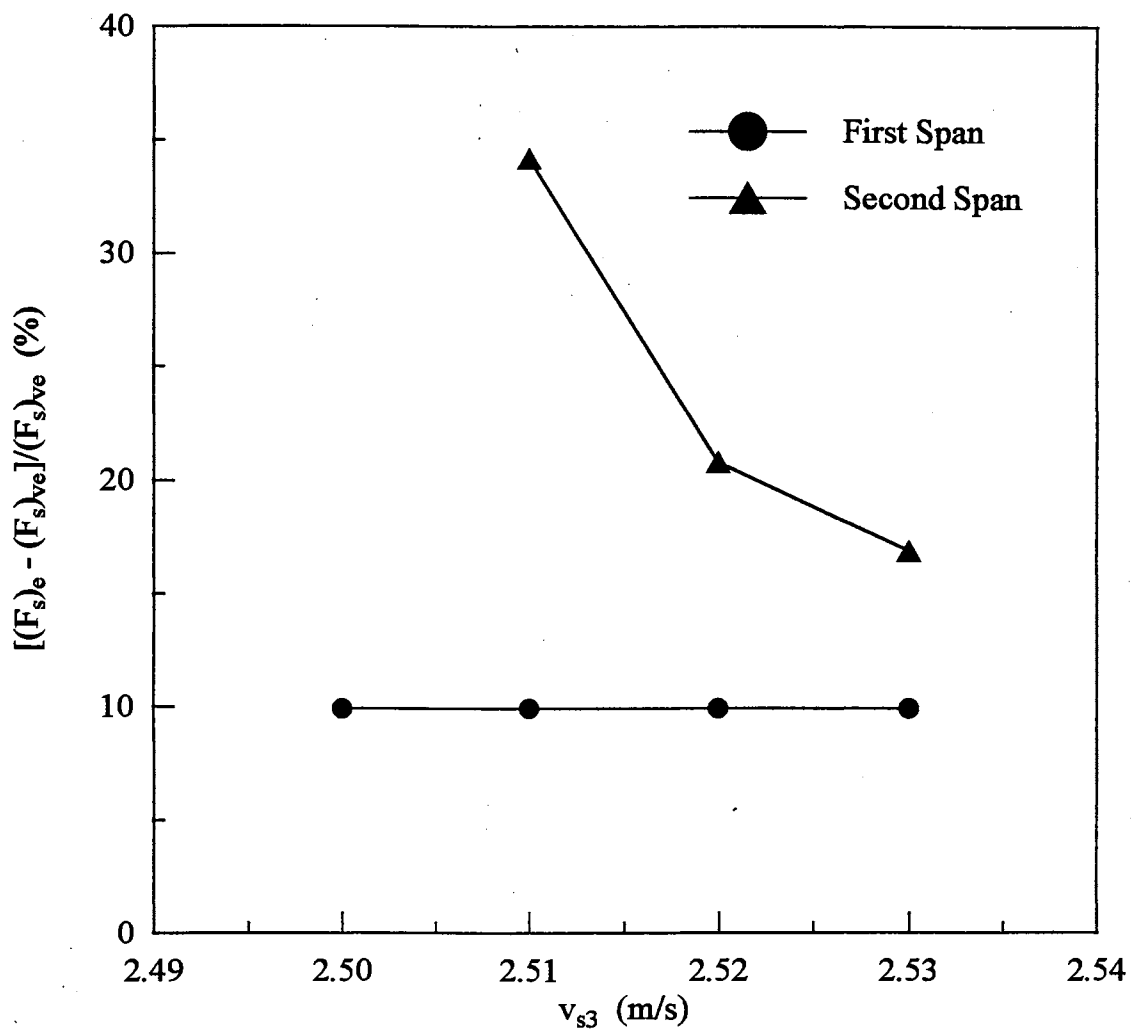


Figure 5.12 Deviations of Hookean Results from Viscoelastic Results as a Function of Roller's Velocity at the Third Roller Set of a Two-Span System

second span predicted by the viscoelastic model differs significantly from the predictions of the elastic model reflecting the fact that the transferred amount of tension deviates from that in the elastic case. A small amount of irrecoverable deformation will result in slackness in the subsequent spans under the conditions where the elastic model will still predict stable operation. To prevent slackness, the draw ratio in the second span must be greater than a minimum value determined by De . In design, larger Deborah numbers are preferred since the viscoelastic effect becomes less significant in the large Deborah number region.

5.4 Unsteady-State Analysis

In unsteady state, the deformation history of a web particle varies with time. Therefore the viscoelastic effects on the system behavior during transient procedures must differ in both magnitude and trend from those in steady state. To reveal the transient performance of the model, three common industrial procedures are simulated: start-up, transition between two steady states, and a sinusoidal disturbance about a steady state. The simulation results have shown that in long time scale events, e.g., start-up and transition between steady states, the transition time is a function of Deborah number. The short time scale disturbance does not affect the average tension but produces the short term variation (amplitude) of the tension. The amplitude of tension can be related by the Deborah number and disturbance parameters. The start-up procedure is analyzed in Section 5.4.1. The transition between steady states, as another long time scale event similar to the start-up

procedure in nature, is presented in Section 5.4.2. The short time scale disturbance is examined in Section 5.4.3.

5.4.1 Start-Up Procedure

Start-up procedures are quite different from system to system depending on the system configuration and control schemes. As an example, a linear velocity ramp and open-loop control were assumed. The velocity functions are schematically shown in Figure 5.13. The tangential velocities of all rollers were linearly increased from zero to their steady-state values over a time period t_s (or the corresponding dimensionless time period, θ_s , see Eq. (3.49)). During the start-up period, the draw ratio was kept identical to the steady-state value.

In Section 5.4.1.1, the effects of Deborah number on transition time, measured from initial state to steady state, are examined. A three-span system is simulated in Section 5.4.1.2 to examine the transition behavior of the system affected by viscoelasticity and the results are compared to the elastic simulation.

5.4.1.1 Effect of Deborah Number on Tension Variation

In this section, the dimensionless transition time of the system to a start-up procedure is correlated by the Deborah number in the following example.

A general single-span system with length L and roller velocities v_1 and v_2 is shown in Figure 5.14. The dimensionless time period, θ_s , was set to be 2.25 and the draw ratio was kept to be 1.00222. The material was taken to be initially unstressed,

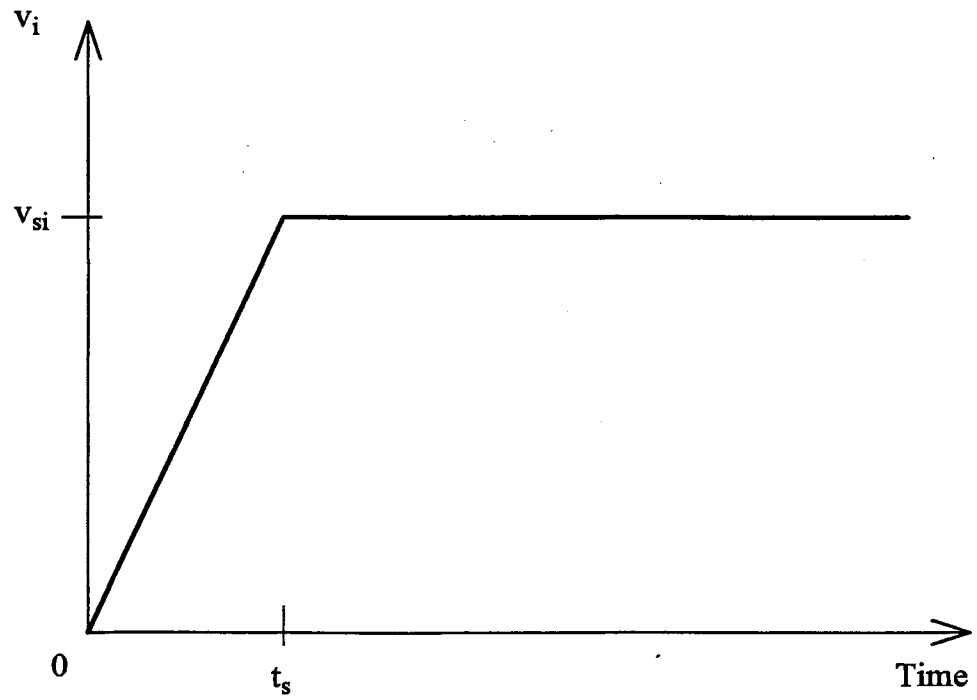
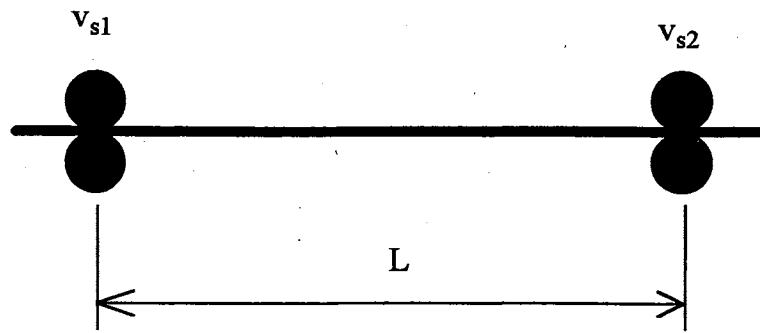


Figure 5.13 Velocity Function in the Start-Up Procedure



Velocity Function

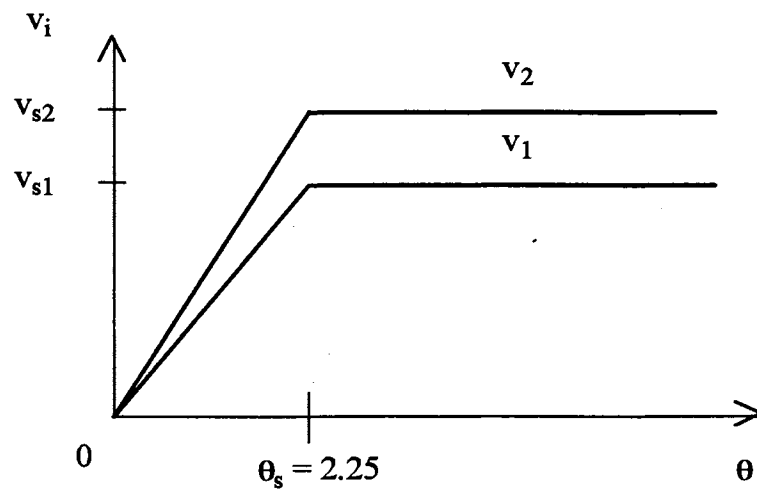


Figure 5.14 A Single-Span System Subjected to a Start-Up Procedure

and entered the span in an unstressed state. The power law exponent was set to one.

The effect of Deborah number on tension variation can be seen in the relationship between the dimensionless tension $f (= F/F_0)$ and the dimensionless time $\theta (= (v_{zs})_0/L)t$ as shown in Figure 5.15. Figure 5.15 clearly shows that the transition time of the system response decreases with decreasing Deborah number, indicating that the smaller the Deborah number is, the quicker the steady state is reached. As De decreases, the material becomes more fluid like or the residence time of a particle in the open span is longer thus the system response tends to adapt more rapidly to the current conditions. From this analysis, the longest transition time occurs when the Deborah number is infinity.

From the discussions in this section, the Deborah number has been proven to be a good indicator for viscoelastic effect on transition time during start-up procedure. No matter how the individual parameters in De change, the tension variation in the dimensionless form can be consistently correlated by the Deborah number.

5.4.1.2 Viscoelastic Behavior in a Three-Span System

The effects of viscoelasticity on multi-span systems during a start-up procedure are examined in this section by considering a three-span system. The major concerns are the influence of irrecoverable deformation on subsequent spans and tension transfer during the transition. Simulation has revealed that the tension transfer is slower than the tension response to the kinematic condition in the current span. Therefore, short time slackness in the subsequent spans may appear in the beginning

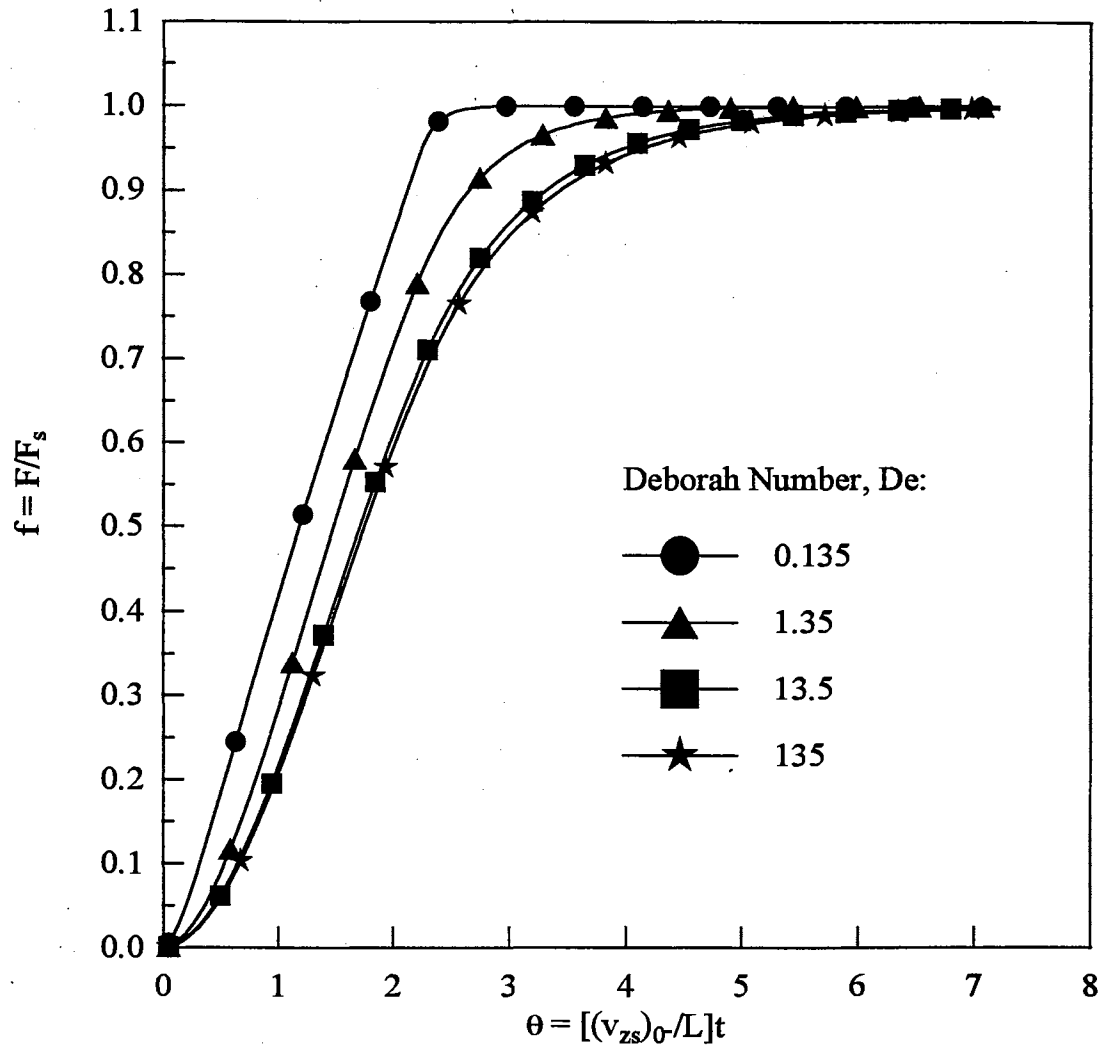


Figure 5.15 Dimensionless Tension as a Function of Dimensionless Time with De as a Parameter During Start-Up

of the procedure. If the draw ratio is smaller than the minimum required value, the slackness will persist. The slackness can also propagate to the next span if the draw ratio is small enough.

The viscoelastic behavior of a three-span system during the start-up procedure can be examined via the example shown in Figure 5.16. The initial and entry states are both unstressed. The model parameters and the entry cross-sectional area are given as:

$$G = 0.55 \times 10^9 \text{ Pa}, \quad m = 1.65 \times 10^{10} \text{ PaS}^n, \quad n = 1$$

$$E = 1.65 \times 10^9 \text{ Pa}, \quad A_0 = 1 \times 10^{-4} \text{ m}^2.$$

The steady-state values of v_1 and v_2 were 2.50 m/s and 2.52 m/s, respectively. V_{s3} and v_{s4} were allowed to vary, as specified in the following paragraphs, in order to examine the effect of the viscoelastic response of the first span on the subsequent spans. The Deborah numbers for the first two spans are 10.00 and 10.08, respectively.

The simulation results for the first two spans are shown in Figures 5.17 and 5.18 along with the purely elastic results which can be obtained either from an analytical solution (Appendix B) or from the viscoelastic model at the elastic limit (i.e. $m = \infty$).

In the first span, the tension variation follows the same general trend described in Section 5.4.1.1 since the tension in the first span is not affected by the downstream spans. The tension in the second span, however, is more sensitive to the viscoelastic response in the first span due to the tension transfer and kinematic requirement.

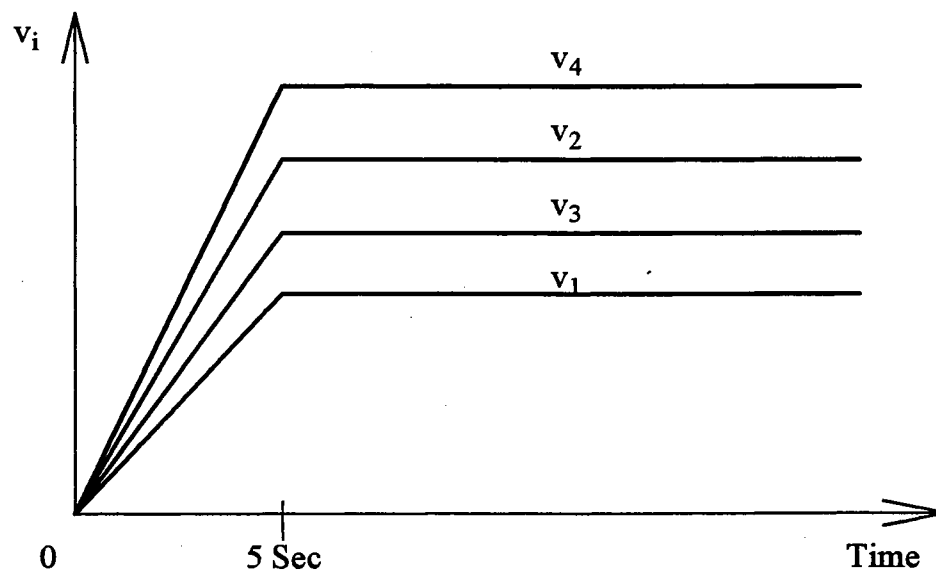
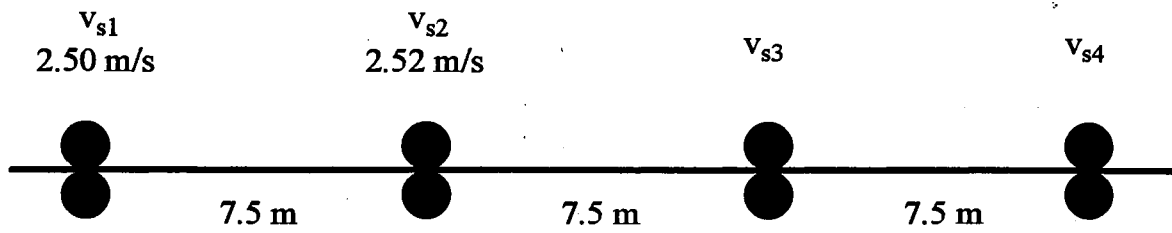


Figure 5.16 A Three-Span System Subjected to a Start-Up Procedure

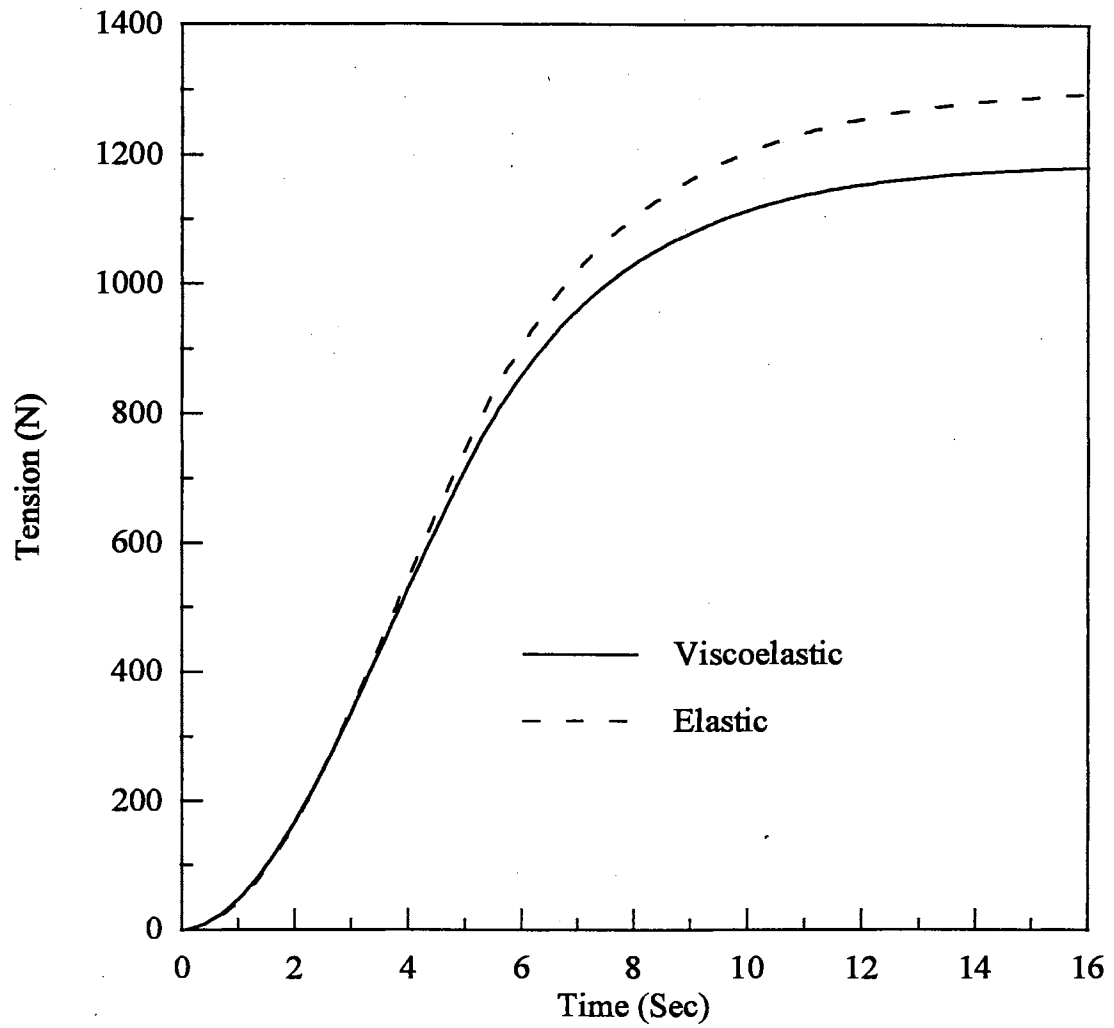
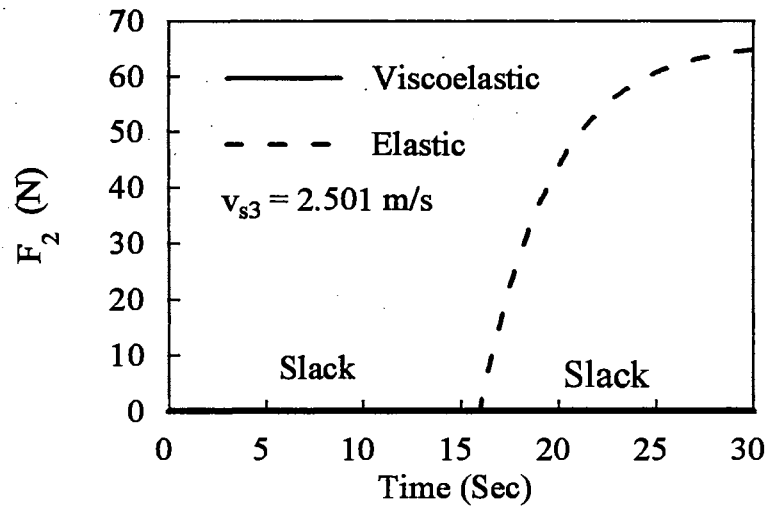
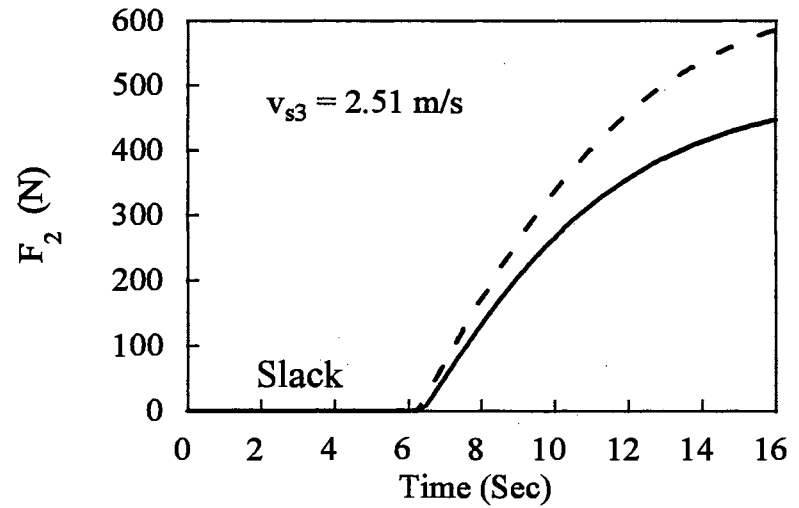


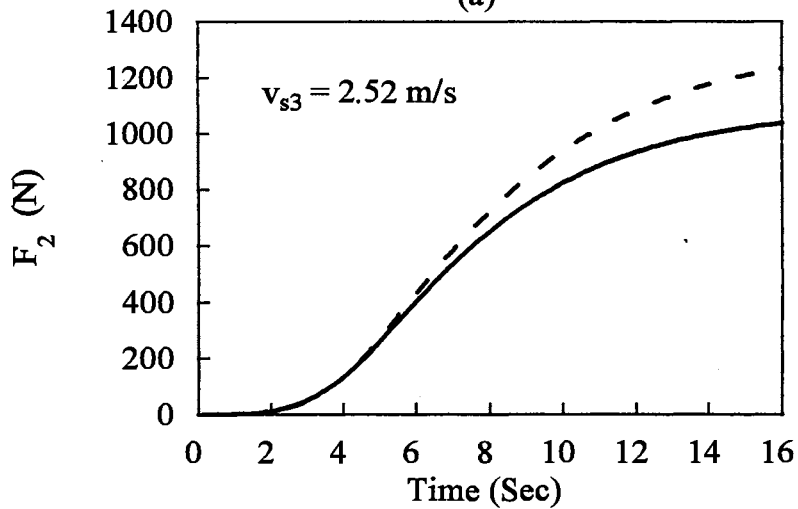
Figure 5.17 Tension in the First Span of a Three-Span System



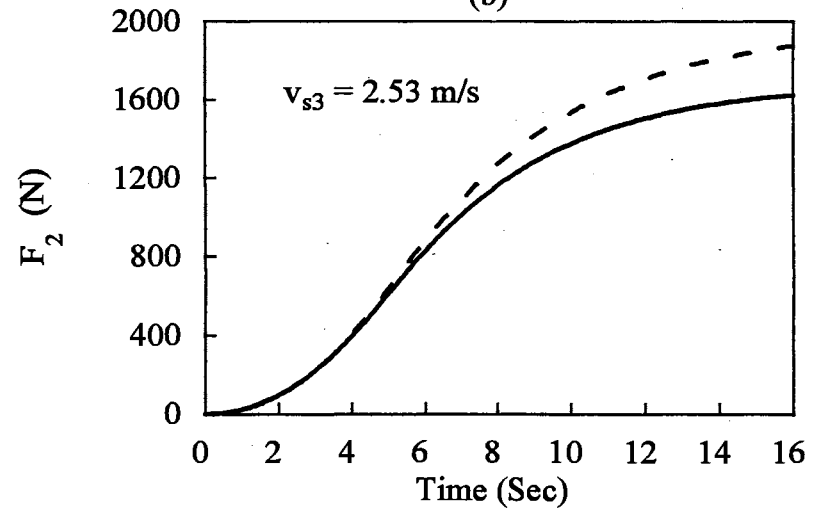
(a)



(b)



(c)



(d)

Figure 5.18 Tension in the Second Span of a Three-Span System (a) $v_{s3} = 2.501$ m/s, (b) $v_{s3} = 2.51$ m/s, (c) $v_{s3} = 2.52$ m/s, and (d) $v_{s3} = 2.53$ m/s

In the case of $v_{s3} = 2.501$ m/s, the viscoelastic model predicts slackness in the second span at all times (including $t = \infty$, see Section 5.3.5). Although the slack condition is also predicted by the elastic model during the first 16 seconds, the web is eventually tightened and reaches steady state. The persistent slackness in the viscoelastic web is due to the irrecoverable deformation in the first span. The draw ratio in the second span is always insufficient to wind up the irrecoverable deformation produced in the first span.

The period of slackness in the elastic situation, on the other hand, is due to the dynamic response of the tension transfer. As long as v_{s3} is not less than v_{s1} , the tension in the second span in steady state is positive regardless of the draw ratio in the second span. However, due to the sluggish rising of F_1 at the very beginning of the start-up period, the tension transferred to the second span cannot balance the decrease of the deformation due to the smaller draw ratio (less than one). The net effect is that the slackness lasts longer than t_s (5 seconds).

If v_{s3} is increased to 2.51 m/s, there is still slackness in both the viscoelastic and elastic predictions. However, the duration times are almost identical and much shorter (6.3 seconds) than that in the previous case. This result is attributed to the larger draw ratio in the second span. Although less than one, D_{Rs2} is still large enough to compensate for the irrecoverable deformation in the first span. In fact, D_{Rs2} is slightly larger than $D_{Rs2,min}$ in the steady-state analysis. However, D_{Rs2} is not yet sufficiently large to overcome the tension transfer resulting in the short slackness period at the beginning of the start-up procedure. After the slackness period, the

tension in the second span varies with time in a manner similar to the general trend observed in single-span systems.

As v_{s3} is increased further, the slackness disappears due to the sufficiently large draw ratio in the second span. The tensions in the second span for the cases of $v_{s3} = 2.52$ m/s and $v_{s3} = 2.53$ m/s show that the general trend is like the trend in the single-span system. The only difference in the two cases is that the tension changes slower for $v_{s3} = 2.52$ m/s than for $v_{s3} = 2.53$ m/s because no further stretching exists in the second span for $v_{s3} = 2.52$ m/s ($D_{Rs2} = 1$). The conclusion from these data is that the web material responds to the kinematic requirement in the current span more readily than the tension transfer from the upstream span in the beginning of the start-up procedure.

The operating situation in the second span can further affect the third span. In the case of v_{s3} and v_{s4} both equal to 2.51 m/s, a slackness condition also occurs in the third span during the first 6.3 seconds as shown in Figure 5.19. The draw ratio in the third span in this case is one and is larger than the minimum value required for positive tension in steady state. The tension predicted by the viscoelastic model differs from the elastic result only after the slack period. The tension variation in the third span is the same as the tension in the second span in elastic situation due to a draw ratio of unity and relaxes from F_2 in the viscoelastic analysis.

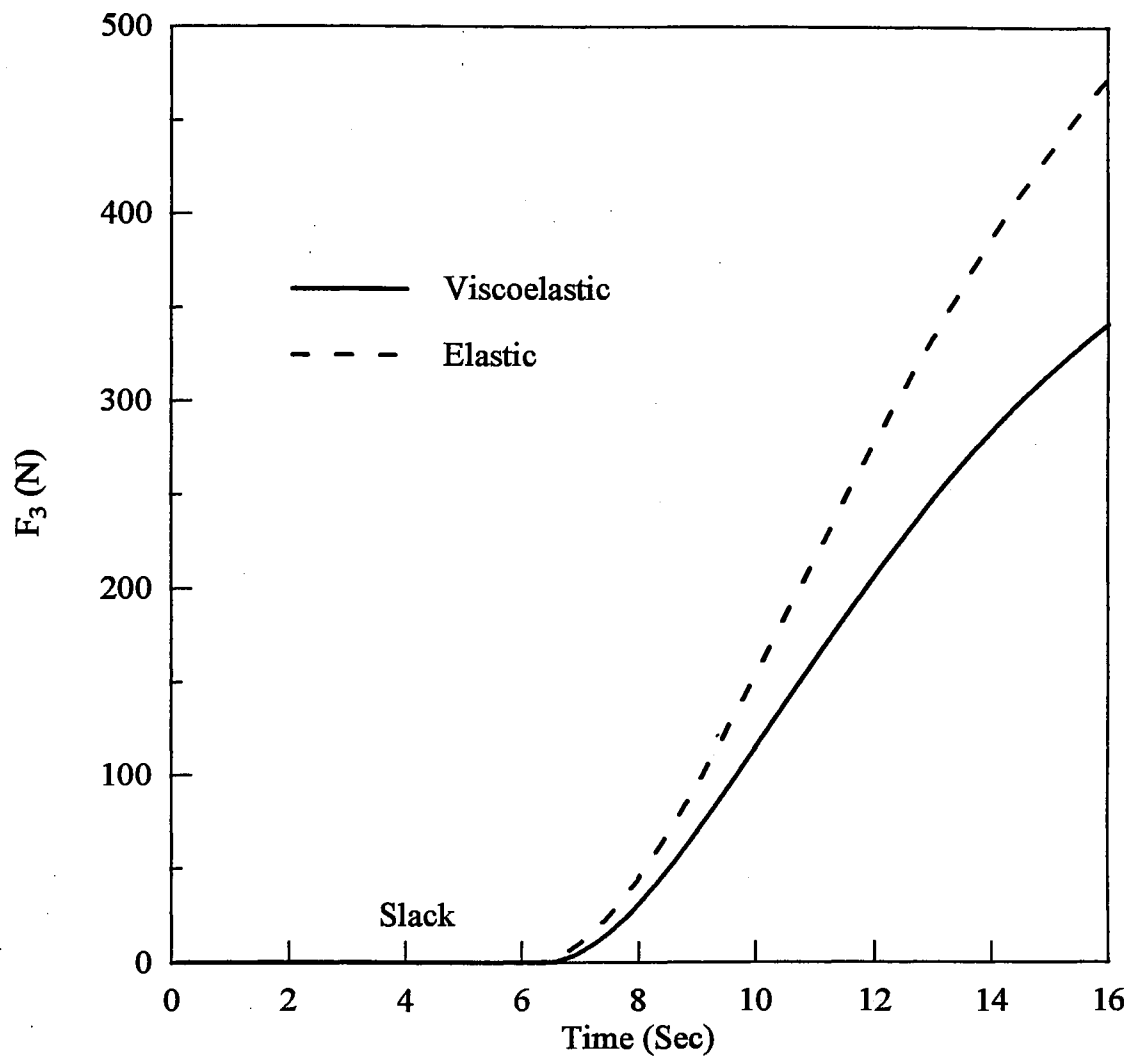


Figure 5.19 Tension in the Third Span of a Three-Span System, $v_{s3} = 2.51$ m/s

5.4.1.3 Summary

The simulation in Section 5.4.1 has demonstrated that the transition time of the system response in the start-up procedure can be correlated by the Deborah number. The smaller the Deborah number, the shorter the transition time. In multi-span systems, unfavorable slackness may occur at all times if the draw ratio is smaller than the minimum value as analyzed in the steady-state analysis. Moreover, if slackness occurs in some span, the following spans will respond to this slackness depending on their draw ratios. The larger the draw ratios are, the lower the tendency for slackness. If the tension in a span relies on the tension transferred from the previous span, the viscoelastic behavior of the current span is greatly affected by the viscoelastic history in the previous spans.

5.4.2 Transition from One Steady State to Another

The viscoelastic effect on the transient behavior of systems from one steady state to a new steady state due to velocity changes of the rollers is examined in this section. The velocity function for the transient procedure is shown in Figure 5.20. A linear change in the velocity is assumed during the time period of zero to t_s (or θ_s). If there are more than one velocities involved in the variation (i.e. more than one roller), each velocity is assumed to change proportionally from $t = \text{zero}$ to t_s (or $\theta = \text{zero}$ to θ_s).

The transition between steady states, as another long time scale transient procedure, is very similar to the start-up procedure in nature. The effects of Deborah

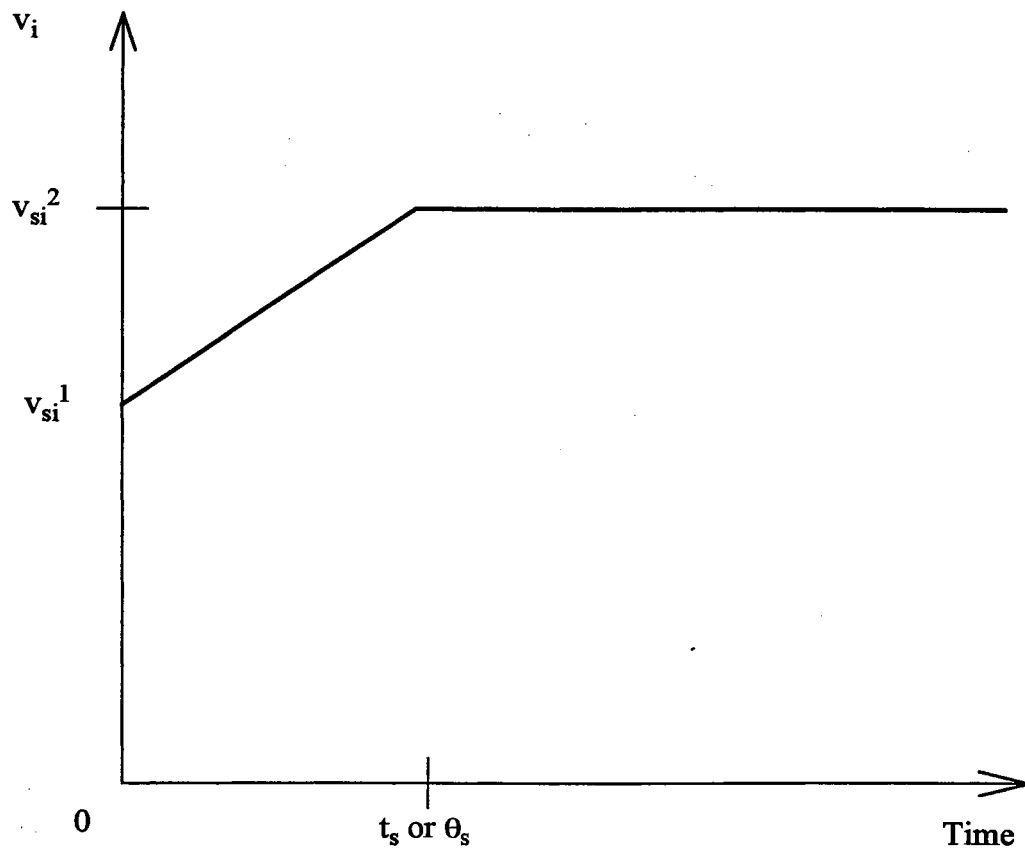


Figure 5.20 Velocity Function from One Steady State to Another

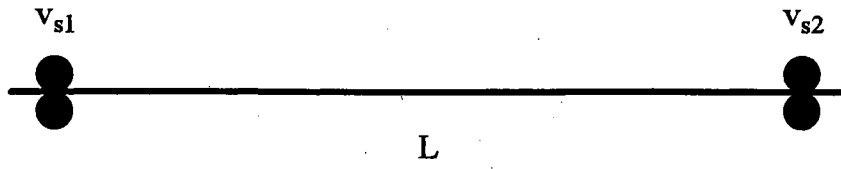
number and transient time of velocity on the transition time of systems are stressed in this section. The transition time in this case is measured between the two steady states.

The general trend of tension variation is examined in Sections 5.4.2.1 and 5.4.2.2 for single-span systems. A three-span system and a four-span system are studied in Appendix F for transient behavior during the transition.

5.4.2.1 Effect of Deborah Number on Tension Variation

The simulation has shown that tension variation during the transient period is a strong function of Deborah number, which is an indicator for the viscoelastic response of open span. The transition time of system can be correlated by De as shown in the following example.

To illustrate the effect of Deborah number on tension variation, a general single-span system, as shown in Figure 5.21, is examined. Initially the system was in steady state with a draw ratio of 1.00222. The velocity of the second roller was then allowed to increase linearly by 1.11% over a dimensionless time period of 1.35. The new draw ratio is 1.01333. The trend in tension variation, as shown in Figure 5.22, is similar to that in the start-up procedure although the draw ratio is not constant in this case. Figure 5.22 clearly shows that the system adapts to the change in the velocity much faster for a smaller Deborah number than for a larger De since the material is more fluid like or the residence time of a particle in the open span is longer in the small De region.



$n = 1$. Entry State: Unstressed.

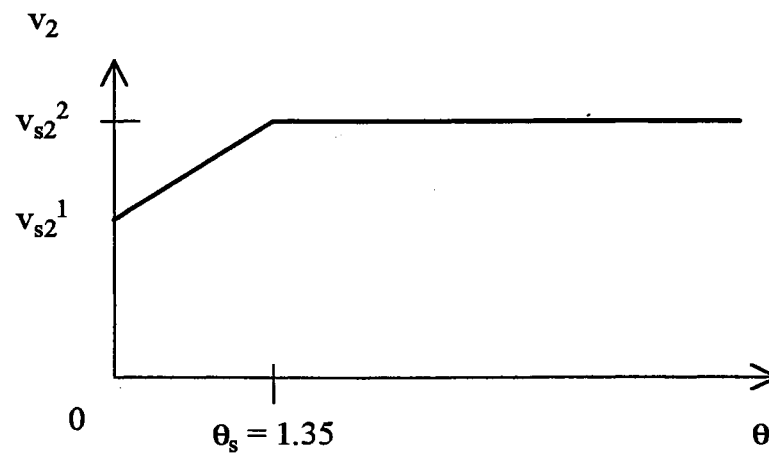


Figure 5.21 A Single-Span System Subjected to a Variation in v_2

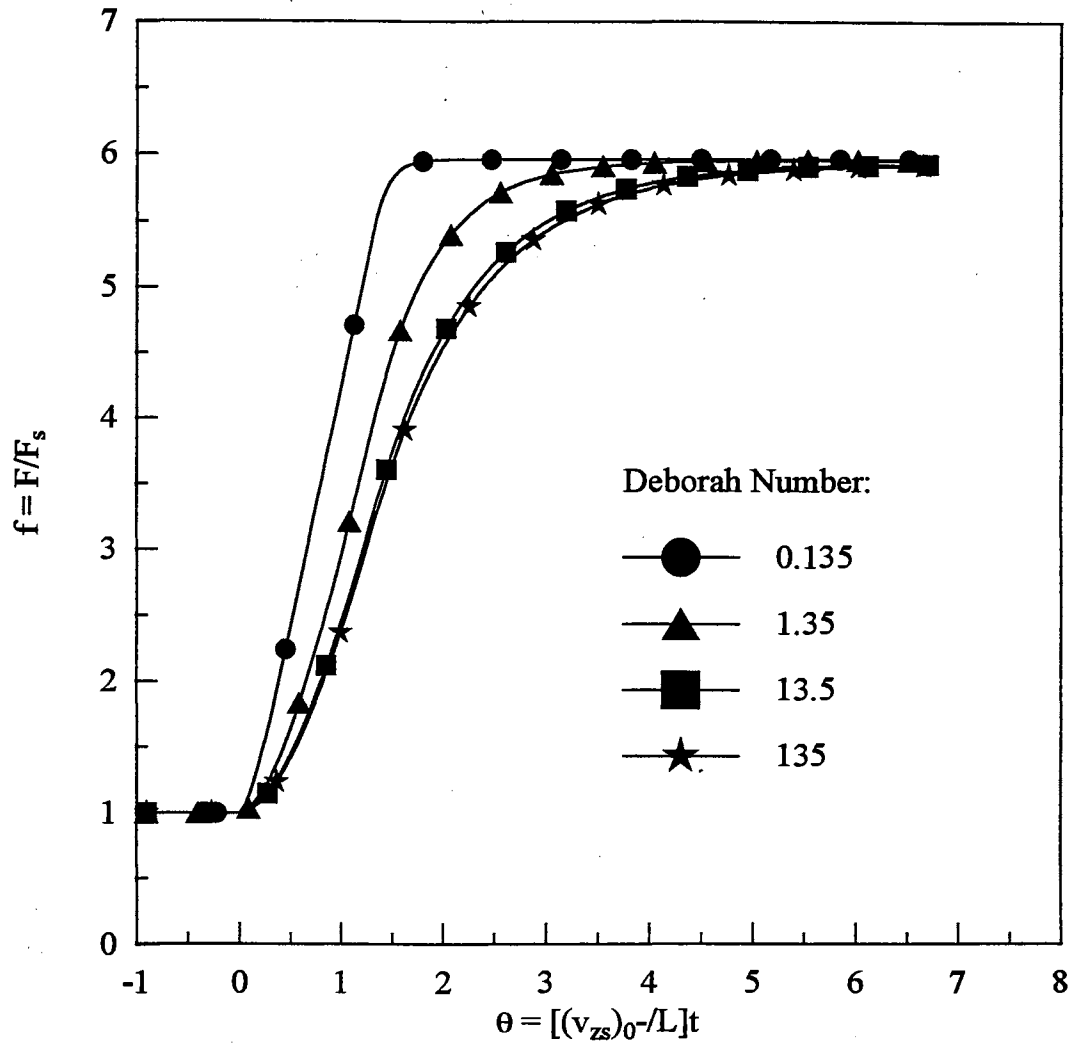


Figure 5.22 Effect of Deborah Number on Tension Variation During the Transition from One Steady State to Another

5.4.2.2 Effect of Transient Time of Velocity on Tension Variation

In addition to the Deborah number, the transient time of the velocity, θ_s , is another factor that affects the transient behavior of the system. Figure 5.23 illustrates the transition between two steady states for the same system as in Figure 5.21 with a Deborah number of 13.5 but the velocity increase (1.11%) at the ending roller is achieved in different dimensionless transient times. The transition data show that the new steady state is not affected by the transient time of the velocity. However, the response time of the system (transition time of the system) to the velocity change is very sensitive to θ_s . Even for a step change in v_2 ($\theta_s = 0$), the system cannot respond instantaneously but gradually changes to the new steady state. The elastic memory is responsible for this behavior, and therefore, based on this analysis the longest response time can be expected for the purely elastic materials for each θ_s .

5.4.2.3 Summary

In summary, the system behavior during the transition between two steady states can be significantly affected by viscoelasticity of materials and transient time of velocity. The transition time of system response during the transient procedure is highly dependent on the degree of viscoelasticity in the system and can be correlated to Deborah number. As De or the transient time of the velocity decreases, the transition time of the system decreases.

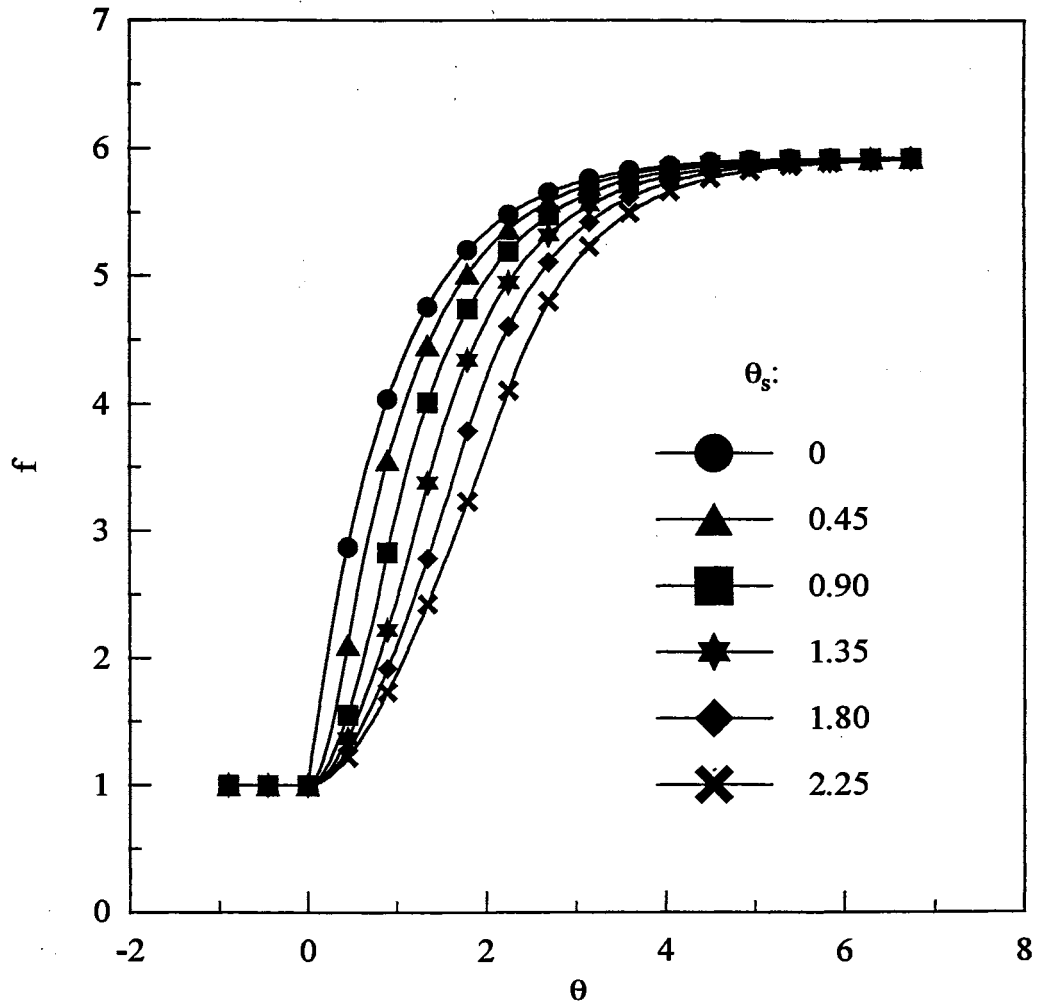


Figure 5.23 Effect of Transient Time of Velocity on Tension Variation in a Single-Span System

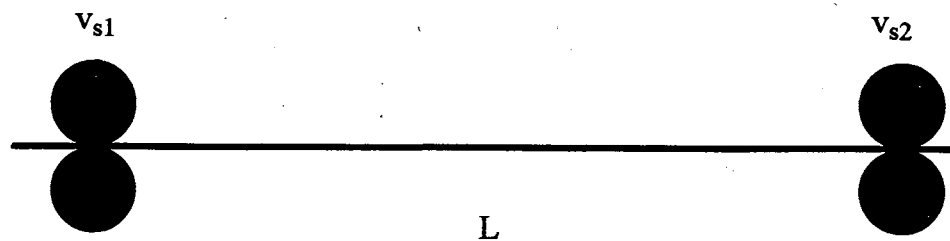
5.4.3 Sinusoidal Disturbance about a Steady State

A sinusoidal function was used to simulate the variation in the velocity of a roller. The actual situation corresponding to this kind of velocity function exists in systems with rollers eccentrically mounted on the shafts, inaccurately machined, or with imperfect surfaces.

The simulation has shown that the velocity disturbance does not affect the average tension but produces a short time scale variation. The amplitude of the tension was correlated by Deborah number and disturbance parameters. A phase angle difference exists between the tension and velocity variations due to the influence of viscoelasticity and is strongly related to the angular velocity of the disturbance. In this section, the effect of the short time scale disturbance on system behavior will be illustrated through examples. Single-span behavior is illustrated in Section 5.4.3.1 and interpreted in terms of dimensionless groups. A three-span system is analyzed in Section 5.4.3.2 through simulation with emphasis on the different behavior from elastic results and long term transitions. A numerical analysis for a four-span system can also be found in Appendix G for the tension variation in indirectly disturbed spans.

5.4.3.1 Effects of Deborah Number and Disturbance Parameters on Tension

The effects of viscoelasticity on the tension variation can be analyzed based on model and disturbance parameters. Consider a general single-span system as is shown in Figure 5.24. v_2 is changing sinusoidally about v_{s2} . The average draw ratio is



$$n = 1$$

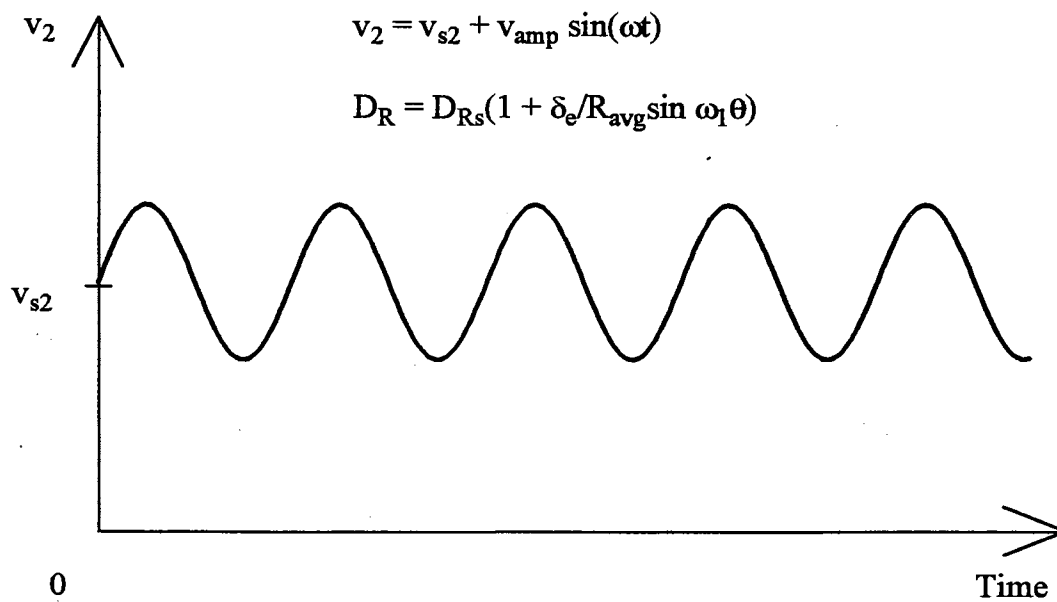


Figure 5.24 A Single-Span System with v_2 Changing Sinusoidally

specified to be 1.00222 and the power law exponent is one. The disturbed roller is assumed to be eccentrically mounted with a maximum radius, (R_{\max}), and a minimum radius, (R_{\min}), as shown in Figure 5.25. The average radius is

$$R_{avg} = \frac{(R_{\max} + R_{\min})}{2}. \quad (5.17)$$

If the surface of the roller is assumed to be perfectly circular, the center offset is

$$\delta_e = \frac{(R_{\max} - R_{\min})}{2}. \quad (5.18)$$

The tangential velocity of the second roller can be expressed as

$$v_2 = v_{s2} + v_{amp} \sin(\omega t), \quad (5.19)$$

where ω is the angular velocity,

$$v_{s2} = \omega R_{avg} \quad (5.20)$$

is the average tangential velocity, and

$$v_{amp} = \omega \delta_e \quad (5.21)$$

is the amplitude of the velocity variation.

The draw ratio can be expressed as

$$D_R = \frac{v_2}{v_{s1}} = D_{Rs} \left(1 + \frac{\delta_e}{R_{avg}} \sin \omega_1 \theta \right), \quad (5.22)$$

where $\omega_1 = [L/(v_{zs})_0] \omega$, which can be thought of as a dimensionless angular velocity.

Since the tension variation is a function of model parameter, De , and the

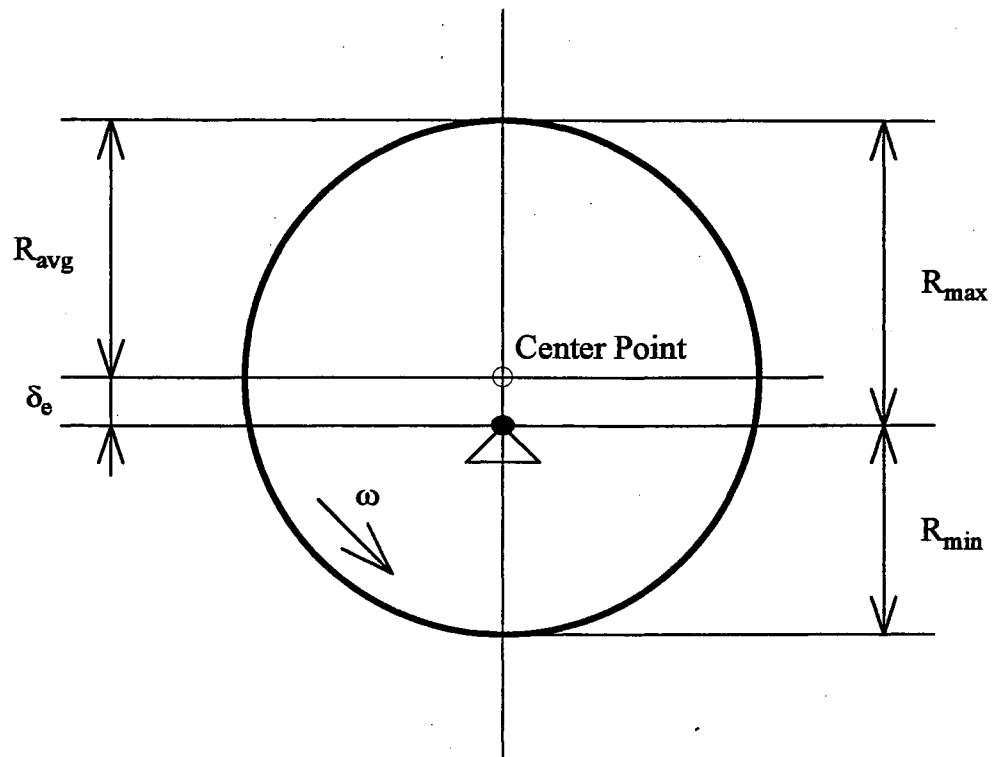


Figure 5.25 An Eccentrically Mounted Roller

boundary condition, D_R , the dimensionless tension can be correlated by the dimensionless groups of De , δ_e/R_{avg} , and ω_1 . The dimensionless group, δ_e/R_{avg} , reflects the bumpy degree of the disturbance and ω_1 reflects the frequency of the disturbance.

The dimensionless tension as a function of dimensionless time in this system is shown in Figure 5.26 with Deborah number as a parameter for $\delta_e/R_{avg} = 0.05\%$ and $\omega_1 = 10.0222$. The variation of the average tension in the beginning of Figure 5.26 should be ignored since the data were affected by the on set of the disturbance in the simulation.

Figure 5.26 shows that the average tension is unaffected by the velocity disturbance. However, the amplitude of the tension varies with Deborah number, indicating that the Deborah number has influence on the short-term tension variation.

The amplitude of tension variation is plotted in Figure 5.27 as a function of De , δ_e/R_{avg} , and ω_1 , respectively. As can be seen in Figure 5.27, the amplitude of the tension variation, Δf , decreases as De or ω_1 increases. However, Δf increases linearly with increasing δ_e/R_{avg} . As δ_e/R_{avg} increases, the bumpy effect of the disturbance is enhanced. Therefore, Δf is enlarged since the tension is more disturbed.

Another viscoelastic effect on the tension variation can be seen in Figures 5.26. The tension change is not instantly reflected in the velocity change. There is a phase angle difference, ψ , between the velocity (or draw ratio) and the tension variations. The phase angle difference increases with increasing Deborah number as

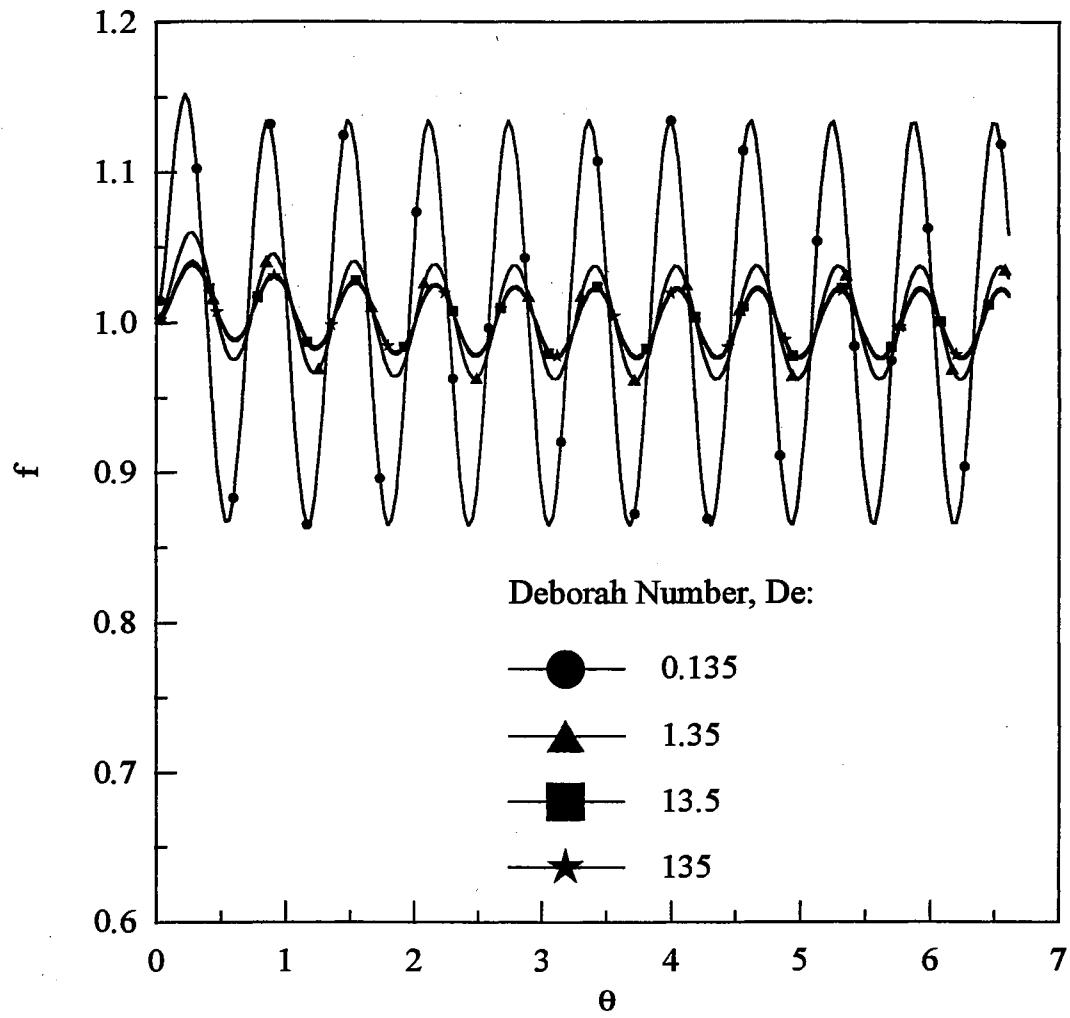


Figure 5.26 Tension Variation in a Single-Span System due to a Disturbance in v_2 , $D_{Rs} = 1.00222$, $\delta_e/R_{avg} = 0.05\%$, $\omega_1 = 10.0222$, and $n = 1$

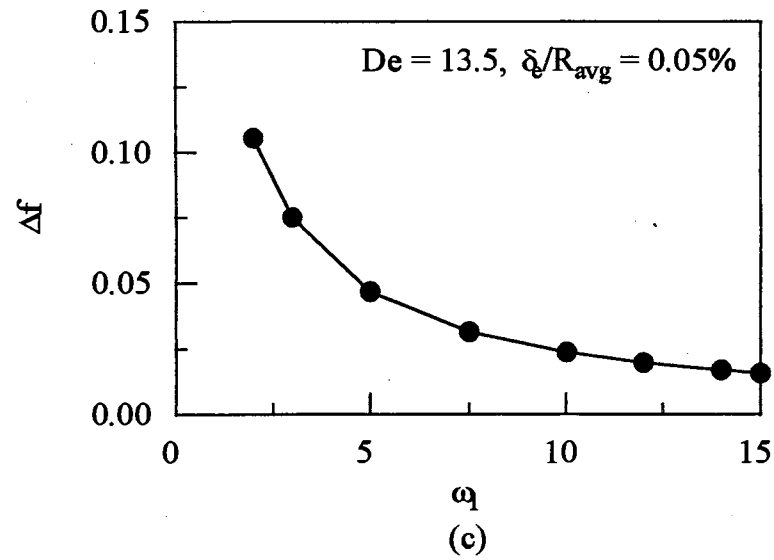
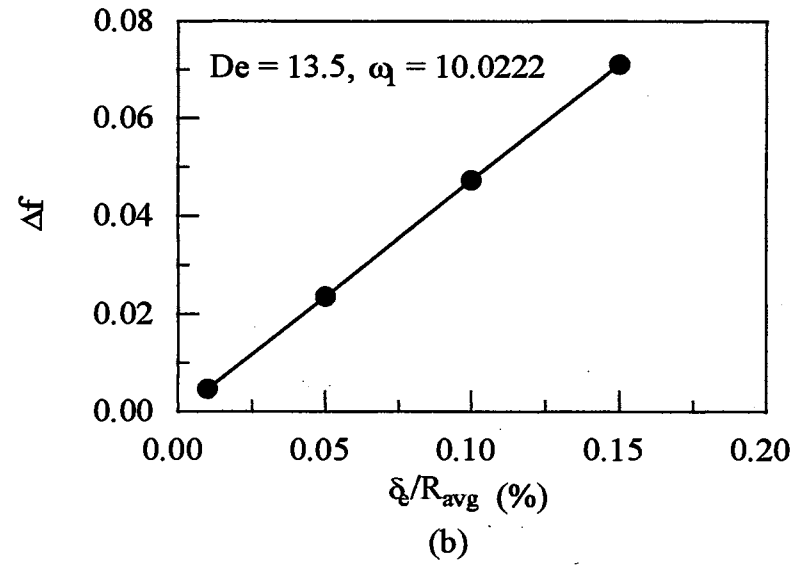
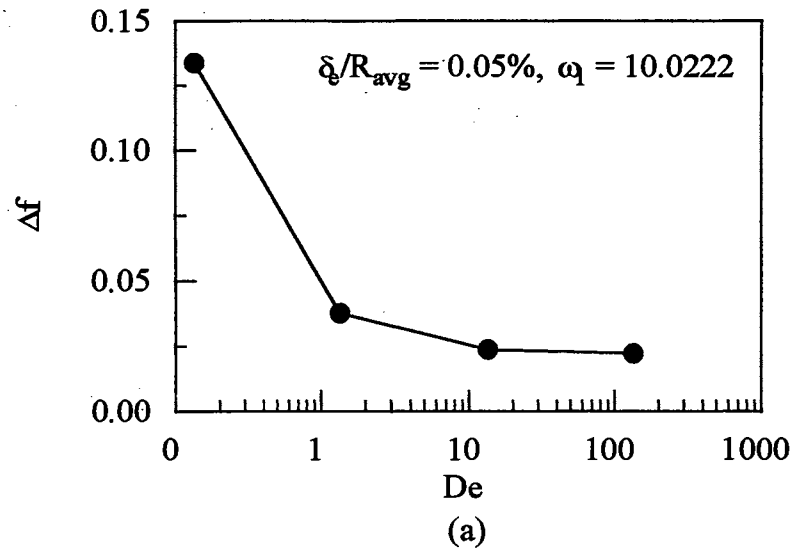


Figure 5.27 Δf as a Function of (a) De , (b) δ_g/R_{avg} , and (c) ω_1 for a Single-Span System with $D_{Rs} = 1.00222$ and $n = 1$

shown in Figure 5.28. The largest phase angle difference corresponds to the purely elastic material because the purely elastic case (infinite Deborah number) has the longest memory.

The measurement of the phase angle difference may be a potential, on-line, practical means of determining the viscoelastic properties of materials from experimental data. A strain rate variation in the open span can be linearly related to the velocity variation, $v_{\text{amp}}\sin(\omega_1\theta)$. Therefore, the tension variation, Δf , can be linearly related to the velocity variation if the strain rate is small enough:

$$\Delta f = \frac{|\eta^*(\omega_1)|}{\eta_c} \sin(\omega_1\theta - \psi), \quad (5.23)$$

where η_c is the characteristic viscosity in the open span. Eq. (5.23) can be manipulated to display the in-phase and out-of-phase parts

$$\Delta f = \frac{\eta_1(\omega_1)}{\eta_c} \sin\omega_1\theta - \frac{\eta_2(\omega_1)}{\eta_c} \cos\omega_1\theta, \quad (5.24)$$

where

$$\sqrt{\eta_1^2 + \eta_2^2} = |\eta^*|, \quad (5.25)$$

and

$$\frac{\eta_2}{\eta_1} = \tan\psi. \quad (5.26)$$

For a Newtonian fluid, η_1 is equal to the viscosity μ , and η_2 is zero (Bird et al., 1987) since the system response will be in phase ($\psi = 0$). As the Deborah number

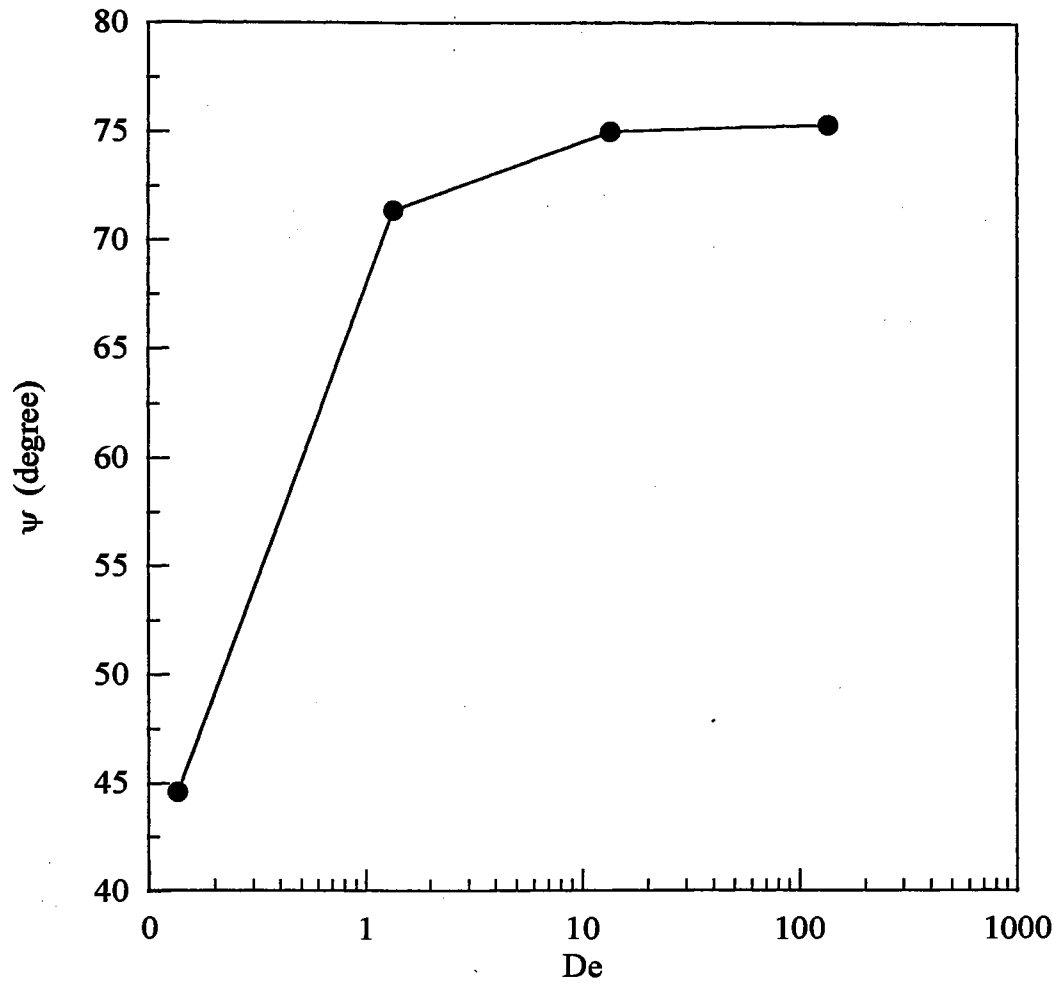


Figure 5.28 ψ as a Function of De for a Single-Span System with $D_{Rs} = 1.00222$, $\delta_e/R_{avg} = 0.05\%$, $\omega_1 = 10.0222$, and $n = 1$

increases, the simulation results revealed that ψ increases for a fixed disturbance, indicating that the ratio η_2/η_1 increases. Appropriate manipulation of experimental data will give an estimation of the viscoelastic properties of the web materials.

Generally, the complex viscosity, $|\eta^*|$ (or the phase angle difference ψ) is a function of ω_1 . The phase angle difference as a function of the dimensionless angular velocity for the system in Figure 5.24 with $De = 13.5$ and $\delta_e/R_{avg} = 0.05\%$ is shown in Figure 5.29. ψ increases deeply with increasing ω_1 at the smaller ω_1 region and decreases slightly at the larger ω_1 region. The maximum value of ψ occurs at about $\omega_1 = 10$ in this case.

5.4.3.2 Viscoelastic Behavior in a Three-Span System

If a roller is driven at a varying velocity in a multi-span system, the disturbance will affect the tensions in the two spans separated by the roller. A three-span system, shown in Figure 5.30, is studied in this section to illustrate the effect of velocity disturbance on tension transfer. The third roller was set to vary sinusoidally. The amplitude and the angular velocity of the disturbance were 0.008367 m/s and 5.02 rad/s, respectively, which corresponds to a 0.5 m radius roller with 1/600 m center offset running at an average tangential velocity of 2.51 m/s. The Deborah numbers are 10, 10.08 and 10.04, respectively, in the three spans. The material properties are listed in Figure 5.30.

The tension variations simulated for the system together with the elastic predictions are shown in Figure 5.31. As seen in Figure 5.31, the tension transfer

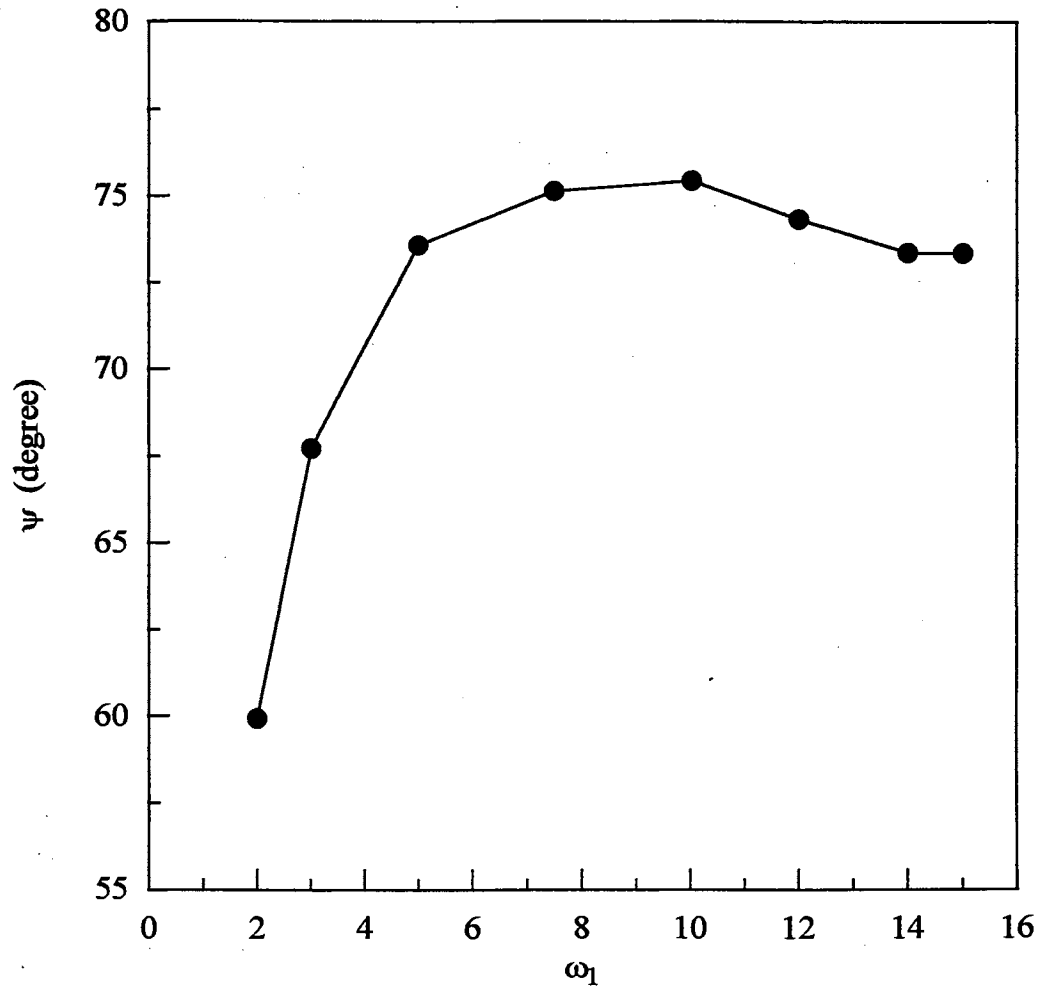
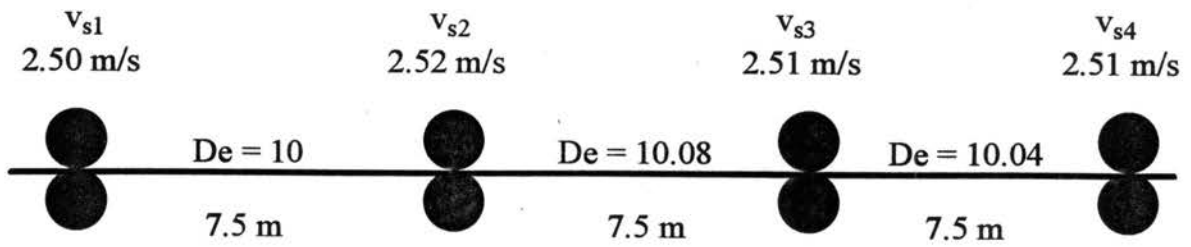


Figure 5.29 ψ as a Function of ω_1 for a Single-Span System with $D_{Rs} = 1.00222$, $De = 13.5$, $\delta_e/R_{avg} = 0.05\%$, and $n = 1$



$$\begin{aligned}
 A_0 &= 1 \times 10^{-4} \text{ m}^2 \\
 G &= 0.55 \times 10^9 \text{ Pa} \\
 m &= 1.65 \times 10^{10} \text{ PaS} \\
 n &= 1 \\
 E &= 1.65 \times 10^9 \text{ Pa}
 \end{aligned}$$

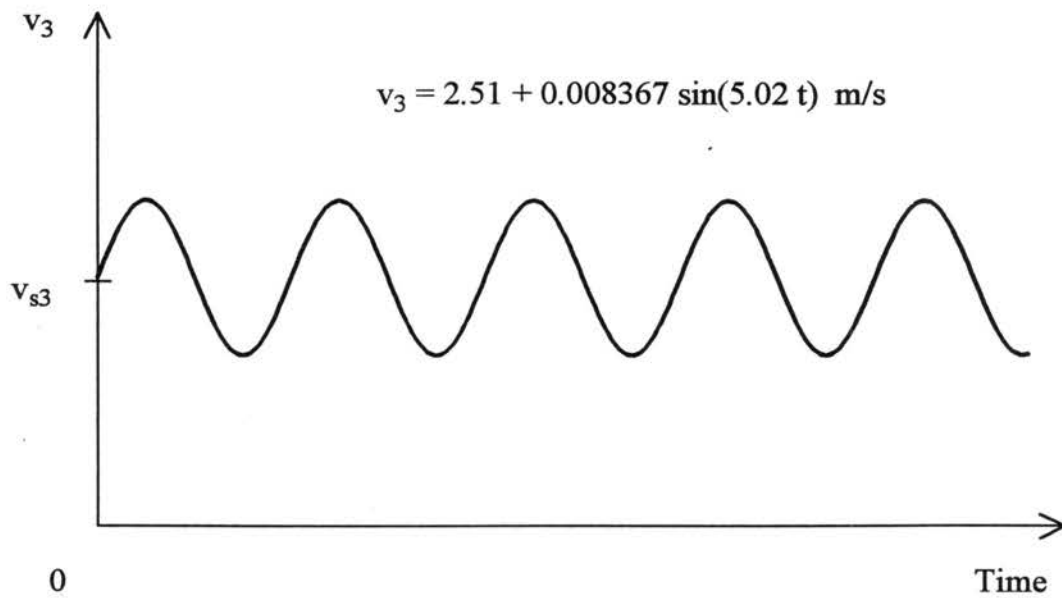
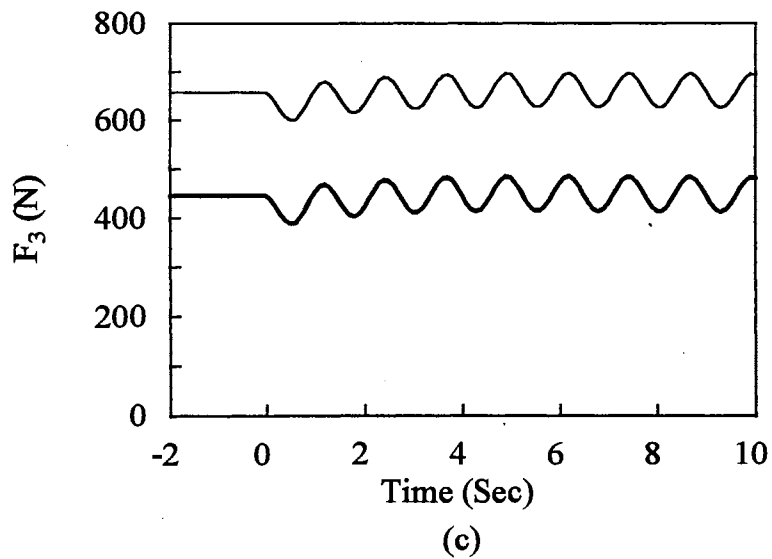
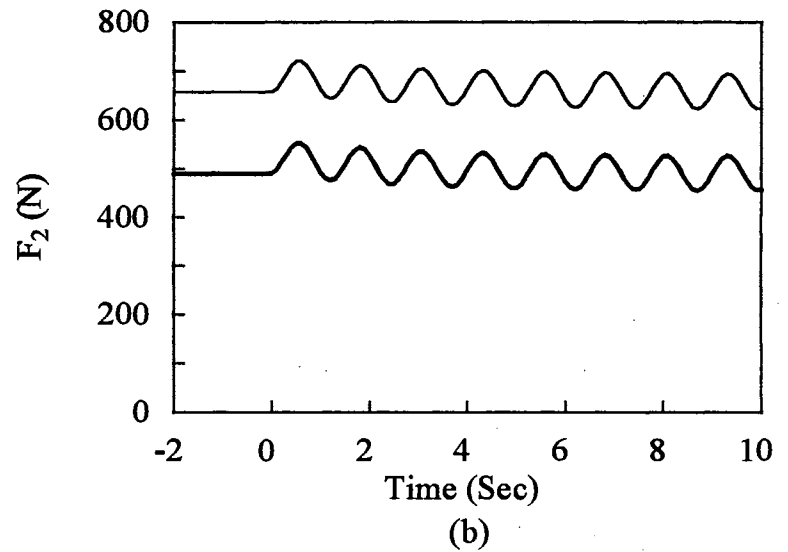
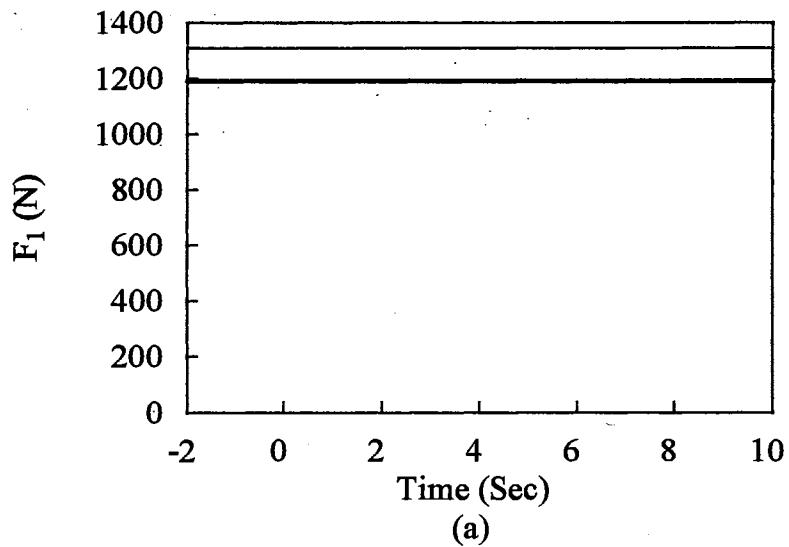


Figure 5.30 A Three-Span System with v_3 Changing Sinusoidally



— Viscoelastic
 - - - Elastic

Figure 5.31 Tension Variations in a Three-Span System due to a Disturbance in v_3 (a) First Span, (b) Second Span, and (c) Third Span

for the average level also follows the same general trend as in the undisturbed case, except for the slight variation at the beginning due to the on set of the disturbance in the simulation. Examination of the instantaneous velocity variation reveals that the draw ratio in the second span periodically falls below the minimum value to maintain positive tension (0.9928). However, no slackness occurs in the second span. While under the same draw ratio, the system with the same configuration is in a slack condition in steady state or transition between two steady states. The slack situation in the disturbance case, therefore, can be expected to occur only when the average draw ratio is less than the minimum value. The short-term variation of the disturbance does not affect the average-tension transfer since the time scale for the velocity variation is too short to allow for the viscous deformation to develop.

5.4.3.3 Summary

In summary, a disturbance in the velocity of a roller can cause variations in tension in the spans separated by the roller. The simulation has demonstrated that the average tension is not affected by the disturbance. The short-term variation of tension (amplitude) can be correlated by the Deborah number and disturbance parameters. The phase angle difference, ψ , can be related to De and is strongly affected by ω_1 . As the disturbance does not affect the average tension, tension transfer and slack condition are also not affected by the short time scale disturbance as examined in the multi-span system.

5.5 Chapter Review

In this chapter, the VEM model has been successfully verified in the limiting cases and has been used to simulate the system behavior for viscoelastic materials. The model parameters were estimated from experimental data. Viscoelastic and purely elastic simulation have been conducted in order to compare the effects of the viscoelastic properties of the materials. The effects of viscoelasticity have been correlated by the Deborah number. The viscoelastic behavior was also found to be sensitive to the power law exponent. In steady state, the simulation results have shown that the deformation distribution, tension level and tension transfer are quite different from elastic cases. The irrecoverable deformation, although is small in amount in the first span, could significantly influence the operating conditions in the subsequent spans in a multi-span system. Undesirable slackness may occur if draw ratio is smaller than a minimum value and further affect the subsequent spans. Unsteady-state simulation has also indicated that long time scale transient operations such as start up and transition between two steady states could be significantly affected by the viscoelasticity. However, the short time scale variations such as disturbance of roller velocity do not influence the average tension but induce the amplitude of the tension, which can be correlated by the Deborah number and the disturbance parameters. The phase angle difference was also related to the Deborah number and angular velocity of the disturbance.

CHAPTER VI

CONCLUSIONS AND RECOMMENDATIONS

6.1 Conclusions

This study was successful in modeling the effects of viscoelasticity on web handling system behavior. The theoretical analysis and numerical simulation provided a deeper understanding of the essence of the viscoelastic effects. The general trends of viscoelastic effects have been obtained in this study to provide guidance and suggestions for system design and operation.

The significance of this work is the determination of the relationship between the viscoelasticity of web handling systems and the Deborah number through the theoretical modeling and numerical simulation. The system behavior can be correlated by the Deborah number, which is a good indicator for the viscoelasticity of the web handling systems. The viscoelastic modeling for multi-span systems provides an accurate analysis for system behavior influenced by viscoelasticity that the currently existing purely elastic models cannot capture.

Based on the analyses, simulation and discussions conducted in the previous chapters, major conclusions can be summarized below.

1. A mathematical model, VEM, was developed to account for the effects of

viscoelasticity of the materials in web handling systems. The White-Metzner equation was chosen as the rheological equation of state with a power law function for the viscosity. The model was successfully verified in limiting cases. Model parameters were estimated from experimental data in the literature. The model can converge to the corresponding elastic model by setting the model parameter, m , to infinity.

2. The irrecoverable deformation and tension level in steady state as well as the transition time of the system in long time scale transient procedures were correlated by the Deborah number in dimensionless forms. The irrecoverable deformation was also found to be strongly sensitive to power law exponent and is cumulative throughout the system.

3. Tension transfer is affected by viscoelasticity since the stress can relax through irrecoverable deformation, making the amount of tension transferred smaller than that in an elastic case.

4. Although viscoelastic response in a single span may not be severely different from the elastic prediction, the small viscoelastic deformation produced in the first span can greatly affect the operations in subsequent spans in a multi-span system.

5. The draw ratio of a span to retain positive tension (non-slack) is larger in the viscoelastic case than in an elastic case since the extra irrecoverable deformation from the previous span must be wound up by a larger draw ratio. The minimum draw ratio was given as a function of Deborah number and operating conditions.

6. Undesirable slack condition may occur in spans with smaller draw ratios

and may further affect the subsequent spans. The irrecoverable deformation can worsen the situation compared to purely elastic cases.

7. The short time scale disturbance does not affect the average tension but can influence the amplitude of the tension, which was correlated by the Deborah number and the disturbance parameters. The phase angle difference was related to the viscoelasticity changing with De and can be significantly affected by the angular velocity.

8. This study has suggested that a viscoelastic model is necessary for simulating the system behavior with even slightly viscoelastic materials. Purely elastic models may give poor predictions in some situations. This study has demonstrated that the viscoelastic effects on the system behavior depend not only on material properties but also on system configuration and operating conditions.

6.2 Recommendations

Further investigations should be conducted on two major assumptions made in this study:

Assumption 6: There are no heat effects, i.e., the web temperature is constant within a span;

Assumption 8: The length of web/roller contact region is zero.

First, heat effects should be introduced into the present isothermal model. The main concern is the viscoelastic properties of the materials that may be significantly affected by temperature change. Two specific expectations are temperature

distribution and its influence on model parameters.

So far, the governing equations are set up only for the isothermal processes. An adequate energy equation then must be introduced into the model to account for the temperature change. Three aspects should be specifically considered: heat generation within web materials, heat transfer within web materials, and heat transfer between web surface and environment.

Second, web/roller interaction is another major concern. Until now, the model has assumed that (a) there is no slippage between web and roller surfaces, (b) the roller speeds are specified (open-loop control), and (c) the contact region is of zero length. Actual interaction between web and roller(s) is complicated. Several factors should be investigated including: slippage between web and roller surfaces, dynamic responses of rollers, and material behavior in the web/roller contact region.

In addition, other detail studies should also be conducted such as inclusion of unwinding and winding rolls and dancer subsystems. The present model does not specify the nature of rollers only that they represent a means of applying forces and providing conveyance on the web line. Although the treatment captures the essence of general rollers or rolls in real systems, specific treatments for those rollers and rolls will be helpful for industrial uses.

Experiments should be another important issue in the near future. The work involves verification of the model and evaluation of model parameters. A data bank for most common web materials should be incorporated into the model based on the experimental evaluations to facilitate industrial applications.

Finally, the inclusion of the viscoelastic model into the well-developed software package for web handling systems, WTS (Lin and Campbell, 1994), is highly recommended. The viscoelastic model will doubtlessly enhance the package in accurately simulating web handling systems for analysis and design.

REFERENCES

- Agbezuge, L. K., 1981a, "Internal Stress Levels in Xerographic Papers," *Polymer Engineering and Science*, Vol. 21, No. 9, pp. 534-537.
- Agbezuge, L. K., 1981b, "Numerical Determination of Internal Stress and Viscoelastic Parameters for Xerographic Papers," *Polymer Engineering and Science*, Vol. 21, No. 9, pp. 538-541.
- Akatsuka, M., 1990, "Models of Longitudinal Web Behavior in the Handling Process," M.S. Thesis, Oklahoma State University.
- Akker, J. A. Van Den, 1970, "Structure and Tensile Characteristics of Paper," *Tappi*, Vol. 53, No. 3, pp. 388-400.
- Aklonis, J. J., MacKnight, W. J., and Shen, M., 1972, *Introduction to Polymer Viscoelasticity*, Wiley-Interscience, New York.
- Alaie, S. M., and Papanastasiou, T. C., 1991, "Film Casting of Viscoelastic Liquid," *Polym. Eng. Sci.*, Vol. 31, No. 2, pp. 67-75.
- Anderson, D. A., Tannehill, J. C., and Pletcher, R. H., 1984, *Computational Fluid Mechanics and Heat Transfer*, Hemisphere Publishing Corporation, McGraw-Hill Book Company, New York.
- Baum, G. A., Pers, K., Shepard, D. R., and Ave'Lallemant, T. R., 1984, "Wet Straining of Paper," *Tappi Journal*, Vol. 67, No. 5, pp. 100-104.
- Bird, R. B., Armstrong, R. C., and Hassager, O., 1987, *Dynamics of Polymeric Liquids, Volume 1, Fluid Mechanics*, Second Edition, John Wiley & Sons, New York.
- Brandenburg, G., 1976, "New Mathematical Models for Web Tension and Register Error," Proc. 1, 3rd International IFAC Conf. on Instrumentation and Automation in the Paper, Rubber and Plastics Industries, Brussels, May 24-26.
- Brezinski, J. P., 1956, "The Creep Properties of Paper," *Tappi*, Vol. 39, No. 2, pp. 116-128.

- Byrd, Y. L., 1972, "Effect of Relative Humidity Changes During Creep on Handsheet Paper Properties," *Tappi*, Vol. 55, No. 2, pp. 247-252.
- Campbell, D. P., 1958, *Process Dynamics*, John Wiley & Sons, Inc., New York.
- Cogswell, F. N., 1981, *Polymer Melt Rheology*, George Godwin Limited, London, John Wiley & Sons, New York.
- Crochet, M. J., Davies, A. R., and Walters, K., 1984, *Numerical Simulation of Non-Newtonian Flow*, Elsevier, Amsterdam.
- Denn, M. M., and Marrucci, G., 1971, "Stretching of Viscoelastic Liquids," *AIChE Journal*, Vol. 17, No. 1, pp. 101-103.
- Dunn, H. S., 1969, "Equivalent Circuit Representation of Web Conveyance Systems," *Journal of Applied Mechanics*, June, pp. 316-318.
- Ericksen, J. L., 1962, "Orientation Induced by Flow," *Transactions of the Society of Rheology*, Vol. VI, pp. 275-291.
- Ferry, J. D., 1970, *Viscoelastic Properties of Polymers*, Second Edition, John Wiley & Sons, Inc., New York.
- Fisher, R. J., and Denn, M. M., 1976, "A Theory of Isothermal Melt Spinning and Draw Resonance," *AIChE Journal*, Vol. 22, No. 2, pp. 236-246.
- Forsythe, G. E., and Wasow, W. R., 1960, *Finite-Difference Methods for Partial Differential Equations*, John Wiley & Sons, Inc., New York.
- Gehlbach, L. S., Kedl, D. M., and Good, J. K., 1989, "Predicting Shear Wrinkles in Web Spans," *Tappi Journal*, August, pp. 129-134.
- Gerald, C. F., and Wheatley, P. O., 1989, *Applied Numerical Analysis*, Fourth Edition, Addison-Wesley Publishing Company, Reading, Massachusetts.
- Grenfell, K. P., 1963, "Tension Control on Paper-Making and Converting Machinery," *Proc., IEEE Ninth Annual Conference on Electrical Engineering in the Pulp and Paper Industry*, Boston, Mass., June 20-21.
- Halsey, G., White, H. J., Jr., and Eyring, H., 1945, "Mechanical Properties of Textiles, I," *Textile Research Journal*, Vol. XV, No. 9, pp. 295-311.
- Han, C. D., and Segal, L., 1970a, "A Study of Fiber Extrusion in Wet Spinning. I. Experimental Determination of Elongational Viscosity," *Journal of Applied*

- Polymer Science, Vol. 14, pp. 2973-2998.
- Han, C. D., and Segal, L., 1970b, "A Study of Fiber Extrusion in Wet Spinning. II. Effects of Spinning Conditions on Fiber Formation," *Journal of Applied Polymer Science*, Vol. 14, pp. 2999-3019.
- Han, C. D., 1976, *Rheology in Polymer Processing*, Academic Press, New York.
- Hauptmann, E. G., and Cutshall, K. A., 1977, "Dynamic Mechanical Properties of Wet Paper Webs," *Tappi*, Vol. 60, No. 10, pp. 106-108.
- Henderson, G. M., Hung, J. C., and Gooze J. M., 1979, "Automatic Tension Control for Winding Superconducting Coils," *Proc. Southeastconf. Reg. 3 Conf. Roanoke, Va. Apr. 1-4, Publ. by IEEE (Cat n 79chol432-4 Reg 3)*, pp. 148-153, New York. coden; psrccd.
- Hollmark, H., Andersson, H., and Perkins R. W., 1978, "Mechanical Properties of Low Density Sheets," *Tappi*, Vol. 61, No. 9, pp. 69-72.
- Horst, R. L., and Negin, M., 1992, "Vision System for High-Resolution Dimensional Measurements and On-Line SPC: Web Process Application," *IEEE Transactions on Industry Applications*, Vol. 28, No. 4, pp. 993-997.
- Kalker, J. J., 1991, "Viscoelastic Multilayered Cylinders Rolling with Dry Friction," *Journal of Applied Mechanics*, Vol. 58, pp. 666-679.
- Kase, S., and Matsuo, T., 1965, "Studies on Melt Spinning. I. Fundamental Equations on the Dynamics of Melt Spinning," *Journal of Polymer Science: Part A*, Vol. 3, pp. 2541-2554.
- Kase, S., 1974, "Studies on Melt Spinning. IV. On the Stability of Melt Spinning," *Journal of Applied Polymer Science*, Vol. 18, pp. 3279-3304.
- Kase, S., and Katsui, J., 1985, "Analysis of Melt Spinning Transients in Lagrangian Coordinates," *Rheol Acta*, Vol. 24, pp. 34-43.
- Keunings, R., Crochet, M. J., and Denn, M. M., 1983, "Profile Development in Continuous Drawing of Viscoelastic Liquids," *Ind. Eng. Chem. Fundam.*, Vol. 22, pp. 347-355.
- Lin, J. Y., and Westmann, R. A., 1989, "Viscoelastic Winding Mechanics," *Journal of Applied Mechanics*, Vol. 56, pp. 821-827.
- Lin, K. C., and Campbell, M. K., 1994, "WTS 6.0 - A Computer-Based Analysis

Program for Multi-Span Web Transport Systems," Web Handling Research Center, Oklahoma State University, June.

- Lockett, F. J., 1972, *Nonlinear Viscoelastic Solids*, Academic Press, London.
- MacCormack, R. W., 1969, "The Effect of Viscosity in Hypervelocity Impact Cratering," AIAA Paper, No. 69-354, pp. 1-7.
- MacCormack, R. W., 1982, "A Numerical Method for Solving the Equations of Compressible Viscous Flow," AIAA Journal, Vol. 20, No. 9, pp. 1275-1281.
- Mark, J. E., Eisenberg, A., Graessley, W. W., Mandelkern, L., and Koenig, J. L., 1984, *Physical Properties of Polymers*, American Chemical Society, Washington, D.C.
- Martin, J. R., 1973, "Tension Control for Web-Offset," *The Penrose Graphic Arts and International Annual*, Vol. 66, pp. 209-214.
- Matovich, M. A., and Pearson, J. R. A., 1969, "Spinning a Molten Threadline," *I&EC Fundamentals*, Vol. 8, No. 3, pp. 512-520.
- McHugh, A. J., Tree, D. A., Pornnimit, B., and Ehrenstein, G. W., 1991, "Flow-Induced Crystallization and Self-Reinforcement During Extrusion," *Intern. Polymer Processing*, Vol. VI, No. 3, pp. 208-211.
- McHugh, A. J., Guy, R. K., and Tree, D. A., 1992, "Extensional Flow-Induced Crystallization of a Polyethylene Melt," submitted to *Colloid & Polymer Science*.
- Mukherjee, S., 1974, "Time Base Errors in Video Tape Packs," *Journal of Applied Mechanics*, September, pp. 625-630.
- Nissan, A. H., 1977, "The Effects of Water on Young's Modulus of Paper," *Tappi*, Vol. 60, No. 10, pp. 98-101.
- Page, D. H., Seth, R. S., and Grace, J. H. De, 1979, "The Elastic Modulus of Paper I. The Controlling Mechanisms," Vol. 62, No. 9, pp. 99-102
- Parant, F., Coeffier, C., and Lung, C., 1992, "Modeling of Web Tension in a Continuous Annealing Line," *Iron and Steel Engineer*, November, pp. 46-49.
- Pearson, J. R. A., 1971, "The Stability of Fiber Drawing Processes," *Ind. Eng. Chem. Fundam.*, Vol. 10, No. 3, pp. 534-535.

- Pearson, J. R. A., and Shah, Y. T., 1972, "Stability Analysis of the Fiber Spinning Process," *Transactions of the Society of Rheology*, Vol. 16, No. 3, pp. 519-533.
- Pecht, M., Johnson M. W., Jr., and Rowlands, R. E., 1984, "Constitutive Equations for the Creep of Paper," *Tappi Journal*, Vol. 67, No. 5, pp. 106-108.
- Pecht, M. G., and Johnson, M. W., Jr., 1985, "The Strain Response of Paper under Various Constant Regain States," *Tappi Journal*, Vol. 68, No. 1, pp. 90-93.
- Perez, M., 1970, "A Model for the Stress-Strain Properties of Paper," *Tappi*, Vol. 53, No. 12, pp. 2237-2242.
- Perkins, W. G, and Porter, R., 1977, "Review Solid-State Deformation of Polyethylene and Nylon and Its Effects on Their Structure and Morphology," *Journal of Materials Science*, Vol. 12, pp. 2355-2388.
- Pfeiffer, J. D., 1966, "Internal Pressures in a Wound Roll of Paper," *Tappi*, Vol. 49, No. 8, pp. 342-347.
- Pfeiffer, J. D., 1968, "Mechanics of a Rolling Nip on Paper Webs," *Tappi*, Vol. 51, No. 8, pp. 77A-85A.
- Pfeiffer, J. D., 1977, "Nip Forces and Their Effect on Wound-in Tension," *Tappi*, Vol. 60, No. 2, pp. 115-117.
- Rance, H. F., 1956, "The Formulation of Methods and Objectives Appropriate to the Rheological Study of Paper," *Tappi*, Vol. 39, No. 2, pp. 104-115.
- Rand, T., and Eriksson, L. G., 1973, "Physical Properties of Newsprint Rolls During Winding," *Tappi*, Vol. 56, No. 6, pp. 153-156.
- Reid, K. N., and Lin, K.-C., 1993, "Control of Longitudinal Tension in Multi-Span Web Transport System During Start Up," *Proceedings of the Second International Conference on Web Handling*, Stillwater, Oklahoma.
- Rendell, R. W., Ngai, K. L., Fong, G. R., Yee, A. F., and Bankert, R. J., 1987, "Nonlinear Viscoelasticity and Yield: Application of a Coupling Model," *Polymer Engineering and Science*, Vol. 27, No. 1, pp. 2-15.
- Richtmyer, R. D., and Morton, K. W., 1967, *Difference Methods for Initial-Value Problems*, Interscience Publishers, New York.
- Roylance, D., McElroy, P., and McGarry, F., 1980, "Viscoelastic Properties of

- Paper," *Fiber Science and Technology*, Vol. 13, pp. 411-421.
- Sanborn, I. B., 1962, "A Study of Irrecoverable, Stress-Induced Changes in the Macrostructure of Paper," *Tappi*, Vol. 45, No. 6, pp. 465-474.
- Schultz, W. W., and Davis, S. H., 1984, "Effects of Boundary Conditions on the Stability of Slender Viscous Fibers," *Journal of Applied Mechanics*, Vol. 51, March, pp. 1-5.
- Schulz, J. H., 1961, "The Effect of Straining During Drying on the Mechanical and Viscoelastic Behavior of Paper," *Tappi*, Vol. 44, No. 10, pp. 736-744.
- Shah, Y. T., and Pearson, J. R. A., 1972a, "On the Stability of Nonisothermal Fiber Spinning," *Ind. Eng. Chem. Fundam.*, Vol. 11, No. 2, pp. 145-149.
- Shah, Y. T., and Pearson, J. R. A., 1972b, "On the Stability of Nonisothermal Fiber Spinning-General Case," *Ind. Eng. Chem. Fundam.*, Vol. 11, No. 2, pp. 150-153.
- Shelton, J. J., and Reid, K. N., 1971a, "Lateral Dynamics of a Real Moving Web," *Journal of Dynamic Systems, Measurement, and Control*, Sept., pp. 180-186.
- Shelton, J. J., and Reid, K. N., 1971b, "Lateral Dynamics of an Idealized Moving Web," *Journal of Dynamic Systems, Measurement, and Control*, Sept., pp. 187-192.
- Shin, K.-H., 1991, "Distributed Control of Tension in Multi-Span Web Transport Systems," *Doctoral Thesis*, Oklahoma State University.
- Smith, T. L., 1973, "Physical Properties of Polymers-An Introductory Discussion," *Polymer Engineering and Science*, Vol. 13, No. 3, pp. 161-175.
- Soong, T.-C., and Li, C., 1979, "An Elastic Analysis of Multiroll Endless Web Systems," *Journal of Dynamic Systems, Measurement, and Control*, Vol. 101, pp. 308-313.
- Spearot, J. A., and Metzner, A. B., 1972, "Isothermal Spinning of Molten Polyethylenes," *Transactions of the Society of Rheology*, Vol. 16, No. 3, pp. 495-518.
- Spielbauer, T. M., and Walker, T. J., 1993, "Theory and Application of Draw Control for Elastic Webs with Nipped Pull Rollers," *Proceedings of the Second International Conference on Web Handling*, Stillwater, Oklahoma.

- Spriggs, T. W., Huppler, J. D., and Bird, R. B., 1966, "An Experimental Appraisal of Viscoelastic Models," *Transactions of the Society of Rheology*, Vol. 10, No. 1, pp. 191-213.
- Street, R. L., 1973, *The Analysis and Solution of Partial Differential Equations*, Brooks/Cole Publishing Company, Monterey.
- Taguchi, T., Morimoto, K., Terada, Y., and Sakamoto, Y., 1985, "Web Behavior on Newspaper Web Rotary Presses," *Technical Review*, Mitsubishi Heavy Industries, Ltd., Tokyo, Japan.
- Tanner, R. I., 1983, "Recent Progress in Rheology," *Journal of Applied Mechanics*, Vol. 50, pp. 1181-1190.
- Titomanlio, G., Anshus, B. E., Astarita, G., and Metzner, A. B., 1976, "The Rheology of Solid Polymers Subjected to Large Deformations," *Transaction of the Society of Rheology*, Vol. 20, No. 4, pp. 527-543.
- Tramposch, H., 1967, "Anisotropic Relaxation of Internal Forces in a Wound Reel of Magnetic Tape," *Journal of Applied Mechanics*, December, pp. 888-894.
- Tree, D. A., 1990, *Crystallization Kinetics of Polymer Melts in Extensional Flow*, Ph.D. Thesis, University of Illinois at Urbana-Champaign, Urbana, Illinois.
- Veits, V. L., Beilin, I. S., and Merkin, V. M., 1981, "Mathematical Models of an Elastic Strip in Mechanisms with Flexible Couplings," *Soviet Applied Mechanics*, Vol. 19, No. 8, pp. 721-726.
- Ward, I. M., 1983, *Mechanical Properties of Solid Polymers*, Second Edition, John Wiley & Sons, Chichester.
- White, J. L., and Metzner, A. B., 1963, "Development of Constitutive Equations for Polymeric Melts and Solutions," *Journal of Applied Polymer Science*, Vol. 7, pp. 1867-1889.
- Whitworth, D. P. D., and Harrison, M. C., 1983, "Tension Variations in Pliable Material in Production Machinery," *Appl. Math. Modelling*, Vol. 7, June, 189-196.
- Williams, D. G., 1983, "A Fiber Network Model Theory for the Wet Web Strength of Paper," *Tappi Journal*, March, pp. 159-162.
- Young, G. E., Shelton, J. J., and Feng, B., 1989, "Interaction of Web Spans: Part I-Statics," *Journal of Dynamic Systems, Measurement, and Control*, Vol. 111,

pp. 490-496.

Young, G. E., Shelton, J. J., and Kardamilas, C., 1989, "Modeling and Control of Multiple Web Spans Using State Estimation," *Journal of Dynamic Systems, Measurement, and Control*, Vol. 111, pp. 505-510.

APPENDIXES

APPENDIX A

TRANSFORMATION OF EQS. (3.50)-(3.53) TO EQS. (4.18)-(4.21)

Eqs. (3.50) to (3.53) are rewritten as below:

$$\frac{\partial a}{\partial \theta} + \frac{\partial(a\phi)}{\partial \xi} = 0, \quad (3.50)$$

$$\frac{\partial}{\partial \xi} [a(T_{zz} - T_{xx})] = 0, \quad (3.51)$$

$$T_{xx} + De \left| \frac{\partial \phi}{\partial \xi} \right|^{n-1} \left(\frac{\partial T_{xx}}{\partial \theta} + \phi \frac{\partial T_{xx}}{\partial \xi} + T_{xx} \frac{\partial \phi}{\partial \xi} \right) = -N \left| \frac{\partial \phi}{\partial \xi} \right|^{n-1} \frac{\partial \phi}{\partial \xi}, \quad (3.52)$$

and

$$T_{zz} + De \left| \frac{\partial \phi}{\partial \xi} \right|^{n-1} \left(\frac{\partial T_{zz}}{\partial \theta} + \phi \frac{\partial T_{zz}}{\partial \xi} - 2T_{zz} \frac{\partial \phi}{\partial \xi} \right) = 2N \left| \frac{\partial \phi}{\partial \xi} \right|^{n-1} \frac{\partial \phi}{\partial \xi}. \quad (3.53)$$

First, by expanding the derivative in the second term of the left hand side of Eq. (3.50), Eq. (4.18) can be obtained

$$\frac{\partial a}{\partial \theta} + \phi \frac{\partial a}{\partial \xi} + \frac{\partial \phi}{\partial \xi} a = 0. \quad (4.18)$$

Eq. (4.19) can be derived by directly non-dimensionalizing Eq. (3.11), an equivalent of Eq. (3.51). Introducing the dimensionless variables, a and T_{ij} , in Eq. (3.49) into Eq. (3.11) and denoting $f = F/F_s$ yield Eq. (4.19)

$$f = a(T_{zz} - T_{xx}), \quad (4.19)$$

For Eqs. (3.52) and (3.53), both sides of the equations are divided by $De|\partial\phi/\partial\xi|^{n-1}$ assuming $\partial\phi/\partial\xi$ to be non-zero. Then the left hand sides of the two equations are rearranged by collecting terms based on $\partial T_{ij}/\partial\theta$, $\partial T_{ij}/\partial\xi$, and T_{ij} . The final forms of the two equations are Eqs. (4.20) and (4.21):

$$\frac{\partial T_{xx}}{\partial\theta} + \phi \frac{\partial T_{xx}}{\partial\xi} + \left(\frac{\partial\phi}{\partial\xi} + \frac{1}{De} \left| \frac{\partial\phi}{\partial\xi} \right|^{1-n} \right) T_{xx} = -\frac{N}{De} \frac{\partial\phi}{\partial\xi}, \quad (4.20)$$

and

$$\frac{\partial T_{zz}}{\partial\theta} + \phi \frac{\partial T_{zz}}{\partial\xi} - \left(2 \frac{\partial\phi}{\partial\xi} - \frac{1}{De} \left| \frac{\partial\phi}{\partial\xi} \right|^{1-n} \right) T_{zz} = 2 \frac{N}{De} \frac{\partial\phi}{\partial\xi}, \quad (4.21)$$

respectively.

APPENDIX B

AN ANALYTICAL SOLUTION OF THE PURELY ELASTIC MODEL

The governing equation for the purely elastic analysis can be written as (Shin, 1991):

$$L_i \frac{d\varepsilon_i}{dt} = -v_i + v_{i+1} + \varepsilon_{i-1}v_i - \varepsilon_i v_{i+1}, \quad (\text{B.1})$$

where the subscript i indicates the current span. The subscript z for indicating the z -direction has been dropped for convenience.

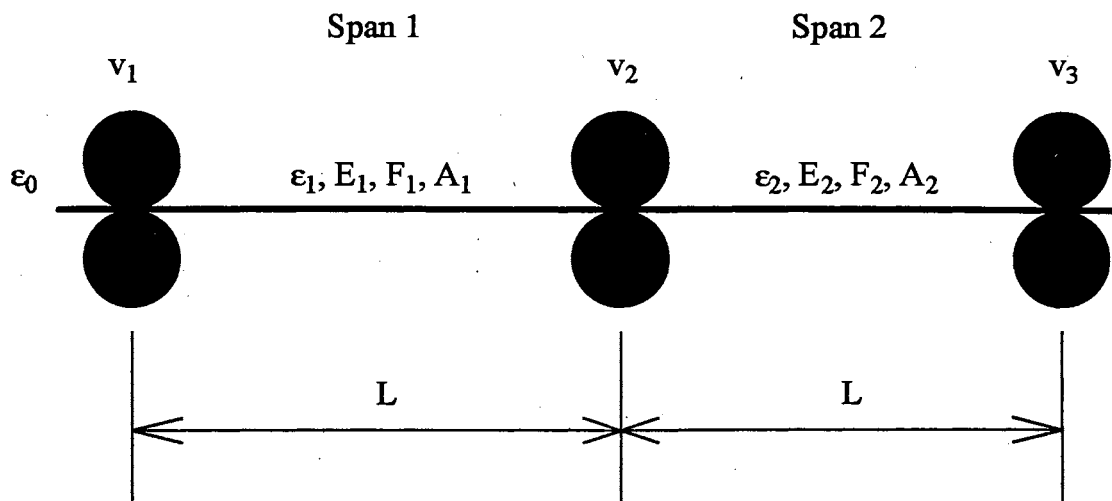
Consider a two-span system shown in Figure B.1 for an example. The lengths of the two spans are the same and are denoted by L . The system is subjected to a start-up procedure from an unstressed initial state

$$\varepsilon_i(t = 0) = 0, \quad \text{Initial Condition}, \quad (\text{B.2})$$

and an unstressed entry state

$$\varepsilon_0(z = 0) = 0, \quad \text{Boundary Condition}. \quad (\text{B.3})$$

The tangential velocities of the three rollers are linearly increased from zero to their steady-state values. The velocity functions are given as:



B.C.: $\epsilon_0(z=0) = 0$,

I.C.: $\epsilon_i(t=0) = 0$.

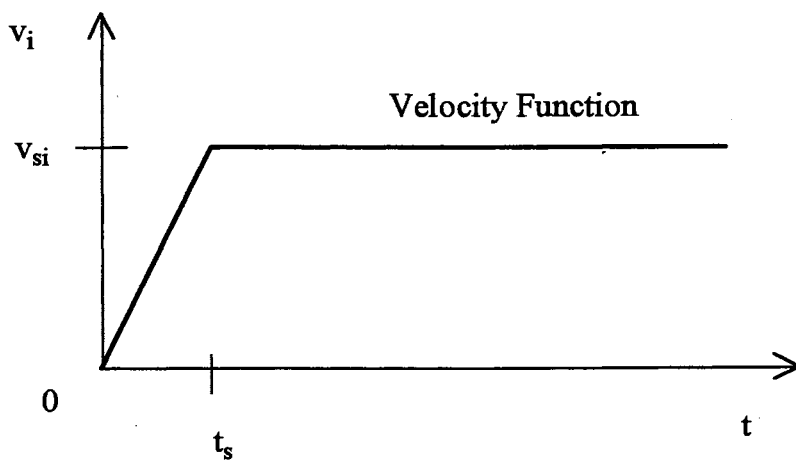


Figure B.1 A Two-Span System with Purely Elastic Material Properties Subjected to a Start-Up Procedure

$$v_i = \frac{v_{si}t}{t_s}, \quad t \leq t_s, \quad (\text{B.4})$$

$$v_i = v_{si}, \quad t > t_s. \quad (\text{B.5})$$

Application of Eq. (B.1) to the two spans gives:

$$L \frac{d\epsilon_1}{dt} = -v_1 + v_2 + \epsilon_0 v_1 - \epsilon_1 v_2, \quad (\text{B.6})$$

$$L \frac{d\epsilon_2}{dt} = -v_2 + v_3 + \epsilon_1 v_2 - \epsilon_2 v_3. \quad (\text{B.7})$$

(1) For $t \leq t_s$

Introducing the velocity function, Eq. (B.4), into Eqs. (B.6) and (B.7) and noting the unstressed entry state give:

$$\frac{d\epsilon_1}{dt} + \frac{v_{s2}t}{Lt_s} \epsilon_1 = \frac{v_{s2} - v_{s1}t}{Lt_s}, \quad (\text{B.8})$$

$$\frac{d\epsilon_2}{dt} + \frac{v_{s3}t}{Lt_s} \epsilon_2 = \frac{v_{s3} - v_{s2}t}{Lt_s} + \frac{v_{s2}t}{Lt_s} \epsilon_1. \quad (\text{B.9})$$

Eq. (B.8) can be integrated to:

$$\epsilon_1 = \frac{v_{s2} - v_{s1}}{v_{s2}} + C_1 e^{-\frac{v_{s2}t^2}{2Lt_s}}, \quad (\text{B.10})$$

where C_1 is an integration constant. From the initial condition, Eq. (B.2), C_1 is determined as

$$C_1 = -\frac{v_{s2} - v_{s1}}{v_{s2}}. \quad (\text{B.11})$$

Thus Eq. (B.10) becomes

$$\epsilon_1 = \frac{v_{s2} - v_{s1}}{v_{s2}} \left(1 - e^{-\frac{v_{s2}}{2L_t} t^2} \right). \quad (\text{B.12})$$

Further, by introducing Eq. (B.12), Eq. (B.9) can be integrated as

$$\epsilon_2 = \frac{v_{s3} - v_{s1}}{v_{s3}} - \frac{v_{s2} - v_{s1}}{v_{s3} - v_{s2}} e^{-\frac{v_{s2}}{2L_t} t^2} + C_2 e^{-\frac{v_{s3}}{2L_t} t^2}. \quad (\text{B.13})$$

The integration constant, C_2 , can be evaluated from the initial condition as

$$C_2 = -\frac{v_{s3} - v_{s1}}{v_{s3}} + \frac{v_{s2} - v_{s1}}{v_{s3} - v_{s2}}. \quad (\text{B.14})$$

Therefore, Eq. (B.13) becomes

$$\epsilon_2 = \frac{v_{s3} - v_{s1}}{v_{s3}} \left(1 - e^{-\frac{v_{s3}}{2L_t} t^2} \right) - \frac{v_{s2} - v_{s1}}{v_{s3} - v_{s2}} e^{-\frac{v_{s2}}{2L_t} t^2} \left(1 - e^{-\frac{v_{s3} - v_{s2}}{2L_t} t^2} \right). \quad (\text{B.15})$$

In the case that v_{s2} and v_{s3} are identical, Eq. (B.15) becomes nonsense.

However, reintegration of Eq. (B.9) without including the term in that $(v_{s3} - v_{s2})$ is

yields another expression for ϵ_2 :

$$\epsilon_2 = \frac{v_{s2} - v_{s1}}{v_{s2}} \left(1 - e^{-\frac{v_{s2}}{2L_t} t^2} \right) - \frac{v_{s2} - v_{s1}}{2L_t} t^2 e^{-\frac{v_{s2}}{2L_t} t^2}. \quad (\text{B.16})$$

(2) For $t > t_s$

By considering Eq. (B.5), Eqs. (B.6) and (B.7) can be simplified to

$$\frac{d\epsilon_1}{dt} + \frac{v_{s2}}{L}\epsilon_1 = \frac{v_{s3} - v_{s1}}{L}, \quad (\text{B.17})$$

$$\frac{d\epsilon_2}{dt} + \frac{v_{s3}}{L}\epsilon_2 = \frac{v_{s3} - v_{s2}}{L} + \frac{v_{s2}}{L}\epsilon_1. \quad (\text{B.18})$$

Integration of Eq. (B.17) yields

$$\epsilon_1 = \frac{v_{s2} - v_{s1}}{v_{s2}} + C_3 e^{-\frac{v_{s2}}{L}t}. \quad (\text{B.19})$$

C_3 can be evaluated from the continuity of the strain at $t = t_s$,

$$C_3 = \left(\epsilon_{1T} - \frac{v_{s2} - v_{s1}}{v_{s2}} \right) e^{\frac{v_{s2}}{L}t_s}, \quad (\text{B.20})$$

where ϵ_{1T} can be obtained from Eq. (B.12) at $t = t_s$. Then, Eq. (B.19) becomes

$$\epsilon_1 = \epsilon_{1T} e^{-\frac{v_{s2}}{L}(t - t_s)} + \frac{v_{s2} - v_{s1}}{v_{s2}} \left[1 - e^{-\frac{v_{s2}}{L}(t - t_s)} \right]. \quad (\text{B.21})$$

With the similar procedure, the strain in the second span can be also obtained

as

$$\begin{aligned} \epsilon_2 = & \epsilon_{2T} e^{-\frac{v_{s3}}{L}(t-t_s)} + \frac{v_{s3} - v_{s1}}{v_{s3}} \left(1 - e^{-\frac{v_{s3}}{L}(t-t_s)} \right) \\ & + \frac{v_{s2} \epsilon_{1T} - v_{s2} + v_{s1}}{v_{s3} - v_{s2}} \left(e^{-\frac{v_{s2}}{L}(t-t_s)} - e^{-\frac{v_{s3}}{L}(t-t_s)} \right), \end{aligned} \quad (\text{B.22})$$

where ϵ_{2T} can be evaluated from Eq. (B.15) or (B.16) at $t = t_s$.

The nonsense will also arise when $v_{s2} = v_{s3}$. The strain function for the second span in this situation, however, can be obtained from the integration of Eq. (B.18) without including the term in that $(v_{s3} - v_{s2})$ is

$$\begin{aligned} \epsilon_2 = & \epsilon_{2T} e^{-\frac{v_{s2}}{L}(t-t_s)} + \frac{v_{s2} - v_{s1}}{v_{s2}} \left(1 - e^{-\frac{v_{s2}}{L}(t-t_s)} \right) \\ & + \frac{v_{s2} \epsilon_{1T} - v_{s2} + v_{s1}}{L} e^{-\frac{v_{s2}}{L}(t-t_s)}. \end{aligned} \quad (\text{B.23})$$

Once the strain function is obtained, tension can be calculated by

$$F_i = A_i E_i \epsilon_p \quad (\text{B.24})$$

where A_i and E_i are the cross-sectional area and Young's modulus in the i th span, respectively.

APPENDIX C

IRRECOVERABLE DEFORMATION

The irrecoverable deformation can be determined from an "unloading" procedure in which the purely elastic deformation is recovered.

In a span, a particle of the web experiences a deformation history under a tension from the beginning to the end of the span. The deformation of the particle is accumulated throughout the span from its entry state. At the end of the span, the irrecoverable strain, ϵ_p , is evaluated by

$$\epsilon_p = \epsilon_t - \Delta\epsilon_e \quad (\text{C.1})$$

where $\Delta\epsilon_e$ is the recovered elastic strain. If the unloading is assumed linear and to obey Hooke's law, $\Delta\epsilon_e$ can be written as

$$\Delta\epsilon_e = \frac{F_s}{(A_s)_L E} \quad (\text{C.2})$$

where $(A_s)_L$ is the cross-sectional area at the end of the span.

To measure the relative contribution of ϵ_p to the total strain, ϵ_t , a ratio, ϵ_p/ϵ_t , is introduced.

From Eqs. (3.49), (3.59), (3.66) and (3.76),

$$\frac{(A_s)_{0^+}}{(A_s)_{0^-}} = \frac{1}{(\phi_s)_{0^+}} = c, \quad (\text{C.3})$$

$$\frac{(A_s)_L}{(A_s)_{0^-}} = \frac{1}{D_{Rs}}. \quad (\text{C.4})$$

By substituting $F_s = (A_s)_{0^+}(\tau_{zzs} - \tau_{xxs})_{0^+}$ together with Eqs. (C.3) and (C.4), $\Delta\epsilon_e$ can be obtained as

$$\Delta\epsilon_e = \frac{cD_{Rs}}{E}(\tau_{zzs} - \tau_{xxs})_{0^+}. \quad (\text{C.5})$$

By substituting Eq. (3.45) in steady state and noting that $(v_{zs})_{0^+}/(v_{zs})_{0^-} = (\phi_s)_{0^+} = 1/c$, Eq. (C.5) becomes

$$\Delta\epsilon_e = \frac{cD_{Rs}}{E} \left\{ E[1 + (\epsilon_{zs})_{0^-}] \left(\frac{1}{c} - 1 \right) + (\tau_{zzs} - \tau_{xxs})_{0^-} \right\}. \quad (\text{C.6})$$

Eq. (C.6) gives an appropriate expression for finding $\Delta\epsilon_e$.

ϵ_t can be found by applying Eq. (3.36) at $z = 0^-$ and $z = L$ (for 1 and 2, respectively) in steady state, and then substituting Eq. (C.4),

$$\epsilon_t = [1 + (\epsilon_{zs})_{0^-}]D_{Rs} - 1. \quad (\text{C.7})$$

Finally ϵ_p/ϵ_t is obtained as

$$\frac{\epsilon_p}{\epsilon_t} = 1 - \frac{\Delta\epsilon_e}{\epsilon_t} = \frac{cD_{Rs} \left[1 + (\epsilon_{zs})_{0^-} - \frac{1}{E}(\tau_{zzs} - \tau_{xxs})_{0^-} \right] - 1}{[1 + (\epsilon_{zs})_{0^-}]D_{Rs} - 1}. \quad (\text{C.8})$$

APPENDIX D

EFFECT OF n ON ϵ_p/ϵ_t AT VERY HIGH D_{Rs}

In Section 5.3.3, the effect of the power law exponent, n , on ϵ_p/ϵ_t at $D_{Rs} = 1.1$ has been described. As D_{Rs} increases, the situation is different depending on the Deborah number. For larger De , the elastic step change dominates the deformation so that ϕ_s' (see Eq. (5.13)) is smaller due to the smaller viscous deformation rate for a given draw ratio. As long as ϕ_s' is less than one, the relationship between ϵ_p/ϵ_t and n for a given De is in the same trend as in Figure 5.7. Figure D.1 shows the relationship between ϵ_p/ϵ_t and n for $De = 10$. The simulation for the case with $De = 10$ reveals that ϕ_s' is always less than one for D_{Rs} up to 10. On the other hand, if De is small enough, ϕ_s' may be larger than one, resulting in an opposite trend of the relationship as shown in Figure D.2 for $De = 1$. In Figure D.2, the trend is reversed for $D_{Rs} = 5.0$ and 10.0 compared to that for $D_{Rs} = 1.1$ and 2.0 since ϕ_s' becomes larger than one in the cases of larger D_{Rs} . The reason that ϕ_s' becomes larger in this case is due to the larger viscous component of deformation, which results in a larger deformation rate. Thus, as n increases, the viscosity increases making the viscous deformation more difficult.

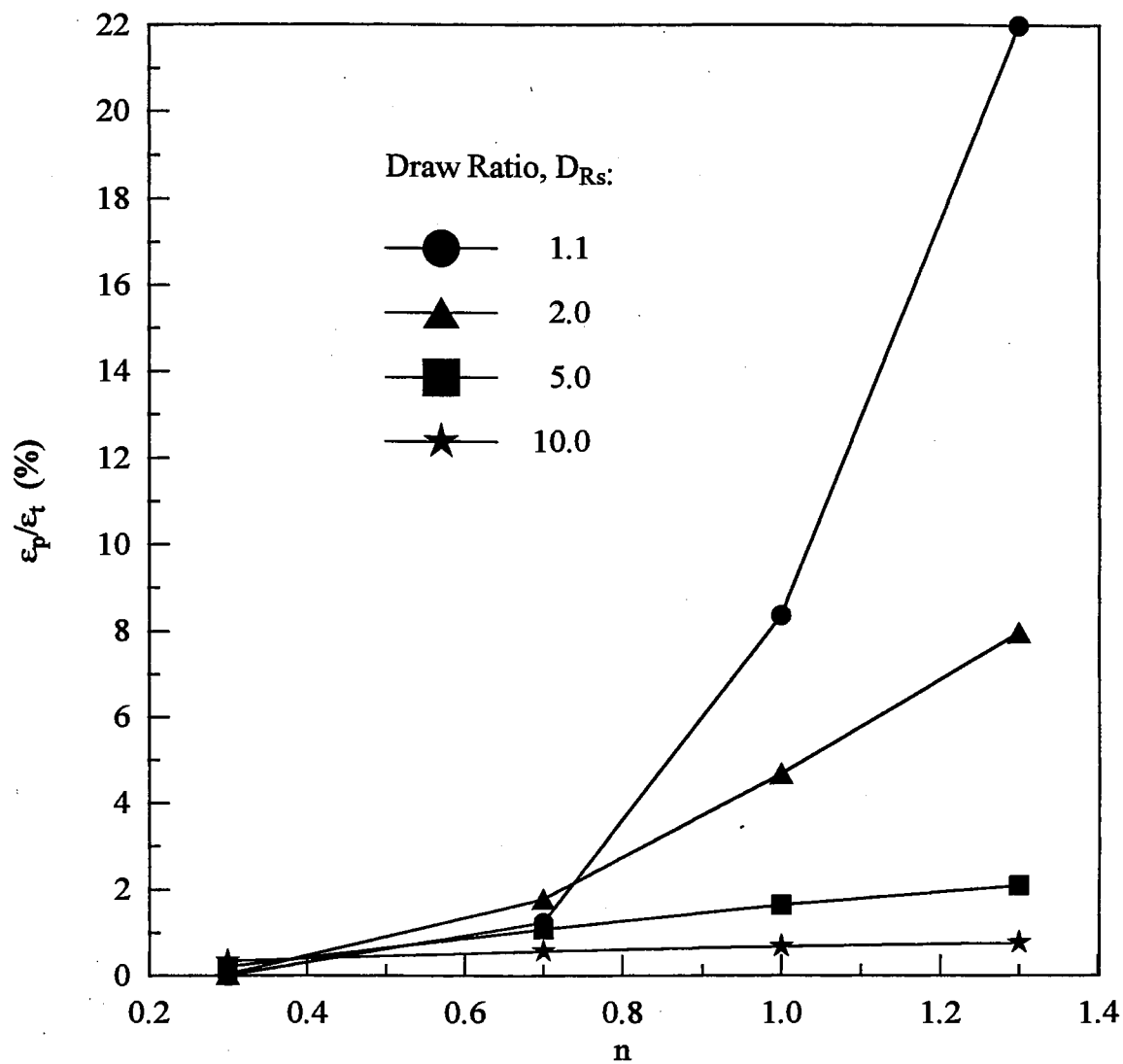


Figure D.1 ϵ_p/ϵ_t as a Function of n with D_{Rs} as a Parameter (for $De = 10$)

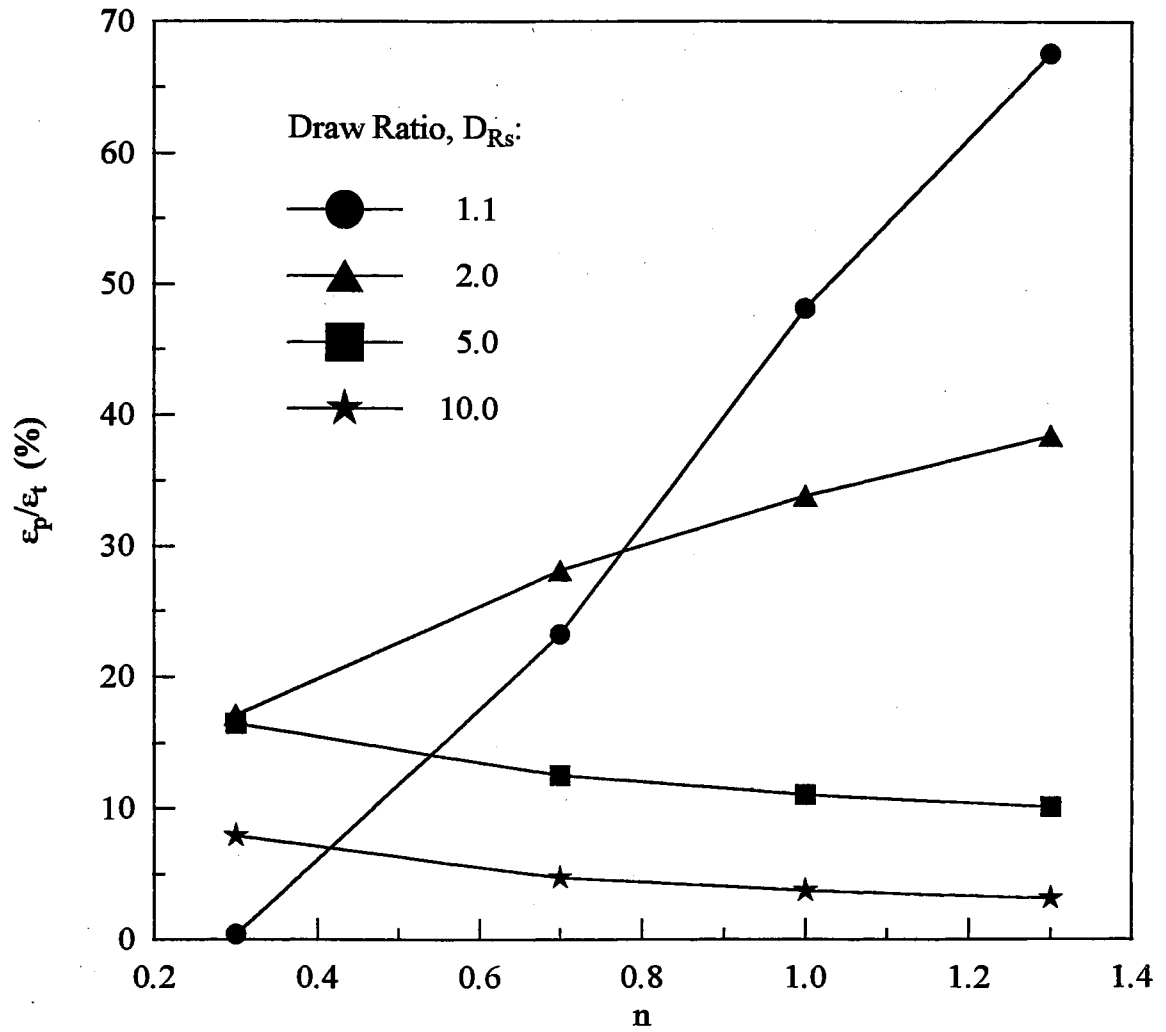


Figure D.2 ϵ_p/ϵ_t as a Function of n with D_{Rs} as a Parameter (for $De = 1$)

APPENDIX E

MINIMUM REQUIRED DRAW RATIO

In a two-span system, the minimum draw ratio required in the second span to prevent slackness, $D_{Rs2,min}$, is closely related to the irrecoverable deformation and draw ratio of the previous span. If the draw ratio in the second span is less than the minimum draw ratio, $D_{Rs2,min}$, the tension in the second span, by definition, is zero resulting in

$$(\tau_{zzs} - \tau_{xzs})_{20^+} = 0. \quad (\text{E.1})$$

Zero tension in the second span also indicates that the dimensionless velocity, ϕ_s , is always equal to the draw ratio, $D_{Rs2,min}$, after $\xi = 0^+$ in the second span. Hence, from Eqs. (E.1) and (3.45) (applied in the second span at steady state) and by recalling that $(\phi_s)_{20^+} = (v_{zs})_{20^+}/(v_{zs})_{20^-}$, the minimum draw ratio can be found:

$$D_{Rs2,min} = 1 - \frac{(\tau_{zzs} - \tau_{xzs})_{20^-}}{[1 + (\epsilon_{zs})_{20^-}]E}. \quad (\text{E.2})$$

Since the term $(\tau_{zzs} - \tau_{xzs})_{20^-}/E$ corresponds to the elastic component of the total strain at the end of the first span,

$$\frac{(\tau_{zss} - \tau_{xss})_{20^-}}{E} = (\epsilon_{zs})_{20^-} - \epsilon_{pI}. \quad (\text{E.3})$$

Therefore,

$$D_{Rs2,\min} = \frac{1 + \epsilon_{pI}}{1 + (\epsilon_{zs})_{20^-}}. \quad (\text{E.4})$$

By applying Eq. (C.7) in the first span (ϵ_t is identical to $(\epsilon_{zs})_{20^-}$), $D_{Rs2,\min}$ can be obtained as

$$D_{Rs2,\min} = \frac{1 + \epsilon_{pI}}{[1 + (\epsilon_{zs})_{10^-}]D_{Rs1}}. \quad (\text{E.5})$$

Another form of $D_{Rs2,\min}$ can be found by referring to Eq. (C.8),

$$D_{Rs2,\min} = c_1 \left\{ 1 - \frac{(\tau_{zss} - \tau_{xss})_{10^-}}{[1 + (\epsilon_{zs})_{10^-}]E} \right\}. \quad (\text{E.6})$$

APPENDIX F

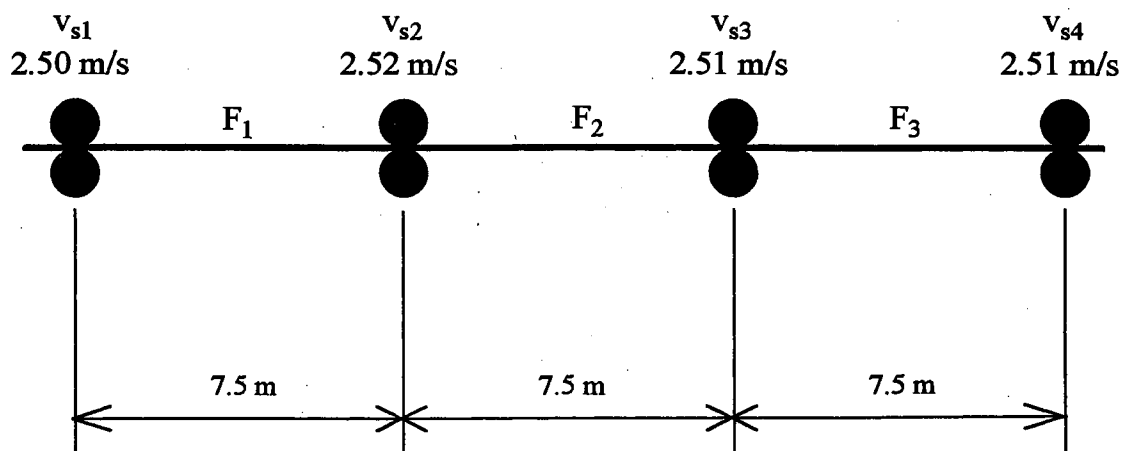
SIMULATION FOR MULTI-SPAN SYSTEMS IN TRANSITION BETWEEN TWO STEADY STATES

F.1 Viscoelastic Behavior in a Three-Span System

If a roller in a multi-span system experiences a velocity change, not only the immediate upstream span is affected but also the downstream spans. Since the draw ratios in the two spans separated by the roller are changed, the tension variations will respond to the velocity change and the viscoelastic behavior will be different from the elastic result due to the deformation history as demonstrated in this section.

Consider the three-span system in Figure F.1. Initially the system was in steady-state operation with tangential velocities of rollers being 2.50 m/s, 2.52 m/s, 2.51 m/s and 2.51 m/s, respectively. The velocity of the third roller then was linearly decreased by 0.009 m/s in 1 second. The system response due to the velocity change is simulated and shown in Figure F.2.

The tension in the first span, as expected, experiences no change confirming that effects do not propagate upstream. The tension in the second span, however, is reduced from the initial steady-state level. Since the new draw ratio (0.9925) in the second span is less than the minimum required value for take up of the slack



Entry State: Unstressed
 Initial State: Unstressed
 $A_0 = 1 \times 10^{-4} \text{ m}^2$
 $G = 0.55 \times 10^9 \text{ Pa}$
 $m = 1.65 \times 10^{10} \text{ PaS}^n$
 $n = 1$
 $E = 1.65 \times 10^9 \text{ Pa}$

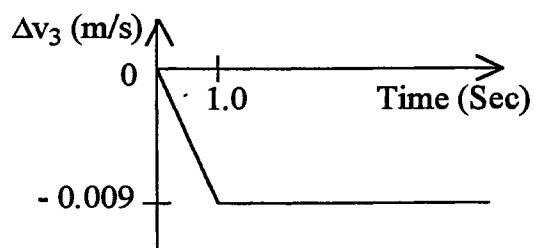
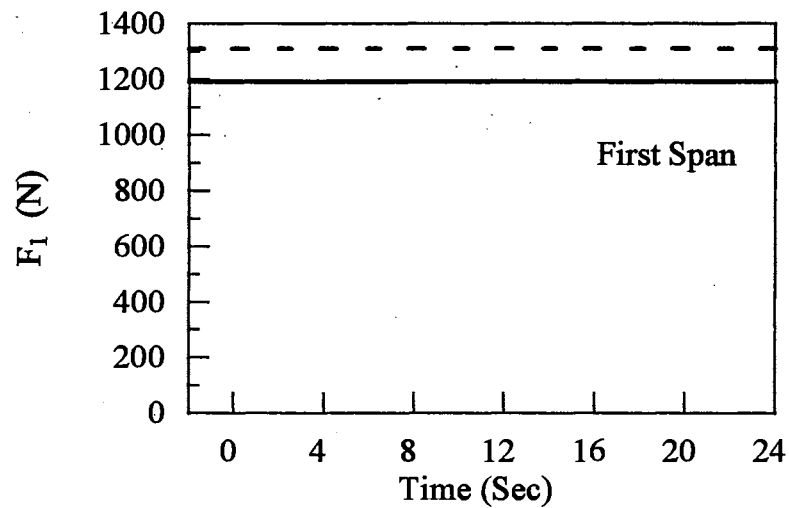
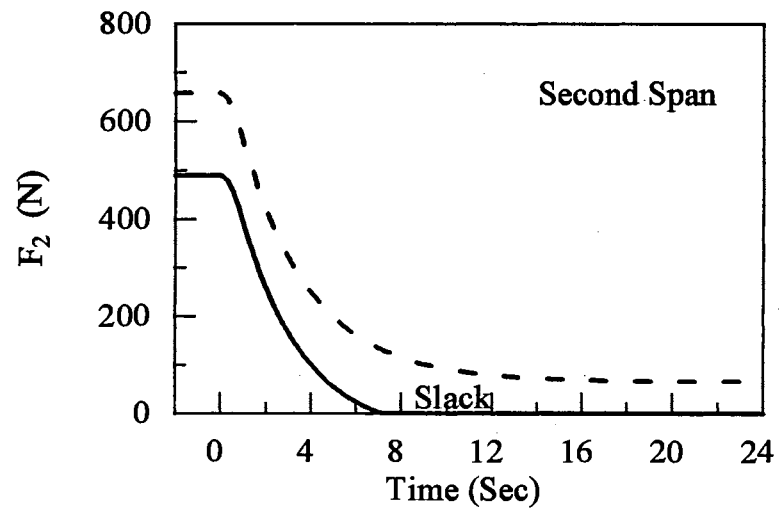


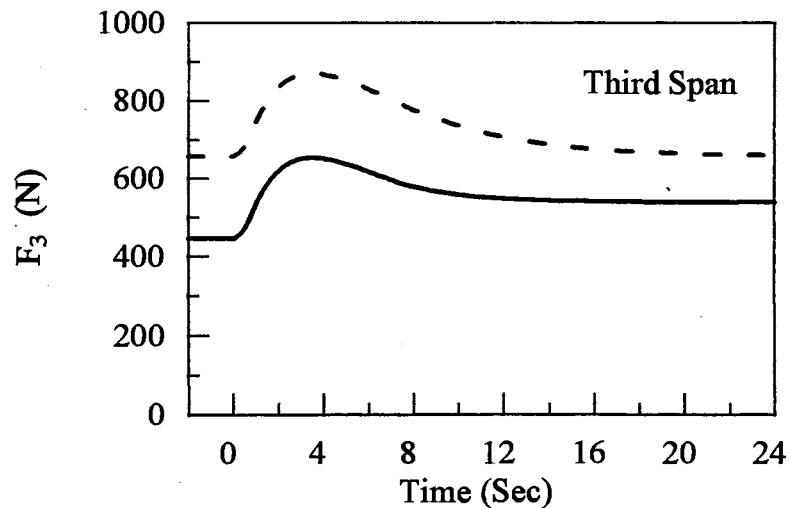
Figure F.1 A Three-Span System Subjected to a Variation in v_3



(a)



(b)



(c)

— Viscoelastic
 - - - Elastic

Figure F.2 Tension in a Three-Span System During the Transition between Two Steady States due to the Variation in v_3
 (a) First Span, (b) Second Span, and
 (c) Third Span

(0.9928), the span is slack when the transition is finished. However, the elastic result indicates no slackness.

In the third span, the tension based on the purely elastic simulation eventually returns to the initial level after the dynamic response (overshooting) to the velocity change. In the new steady state, even though the new draw ratio is greater than the initial draw ratio in the old steady state, the tension transfer from the second span compensates for the effect of increasing the draw ratio on tension. The phenomenon can be explained by considering the fact that Δv_3 results in a decrease in F_2 and an increase in F_3 at the new steady state. However, the increasing amount in F_3 just balances the deduction in tension transferred from F_2 since the total draw ratio in the second and the third span, v_{s4}/v_{s2} , does not change. The history independence of the elastic response secures the net effect of tension change in this case. The same conclusion can be drawn for the case of increasing v_3 . Similar phenomena have also been examined by Shin (1991).

The overshooting of F_3 during the transition results in the slower response to tension transfer from the second span than the response to the change of draw ratio in the third span. The elastic memory is responsible for the dynamic variation in tension. In theory, a purely viscous material exhibits no dynamic response and purely elastic material has the largest response.

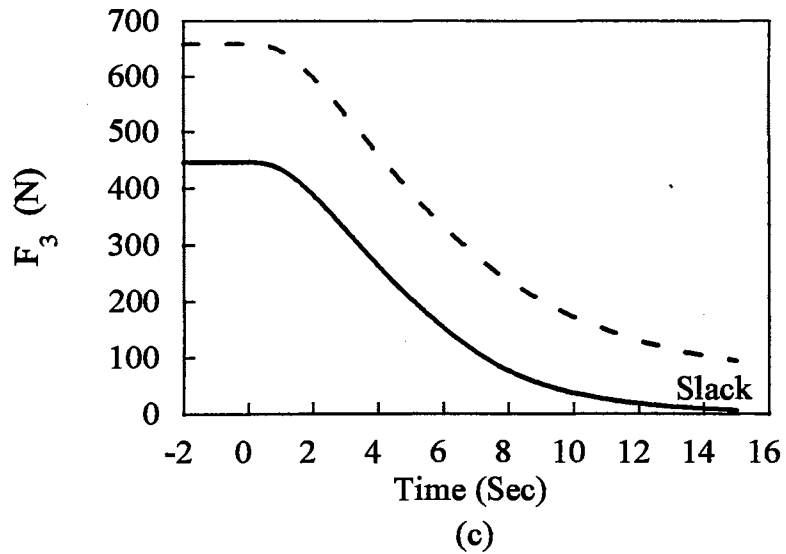
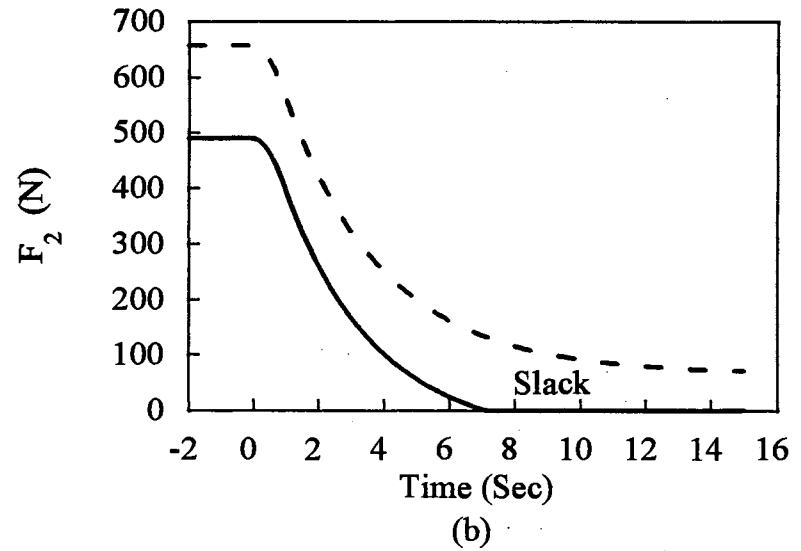
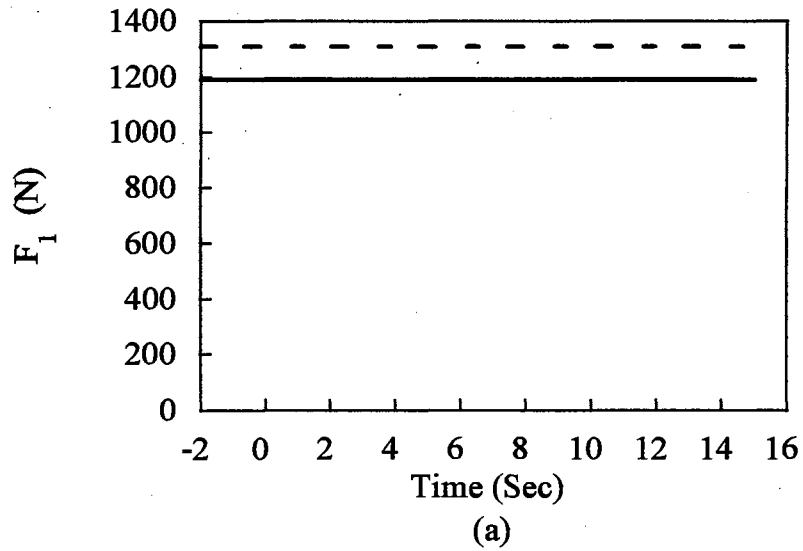
The viscoelastic response in the third span, however, is different from the elastic result. Although the tension variation follows the same qualitative tendency as for the elastic analysis, the tension does not return to the initial value after the

transition since no tension is transferred from the second span due to the slackness. The tension in the new steady state is greater than the initial value because of the higher draw ratio in the third span. Generally, even if the second span is not slack, tension in the third span in the new steady state will not remain unaffected since the irrecoverable deformation will influence the tension level.

The viscoelastic effect on the system controlled by the progress set-point coordination scheme (Shin 1991) was also examined. In the set-point coordination scheme, the change of the roller velocity will be automatically propagated to the rollers in downstream spans. If some roller has a change in velocity during a transient procedure, all rollers downstream will be adjusted to adapt to this velocity change. In this case, both v_3 and v_4 were lowered by 0.009 m/s so that the draw ratio in the third span was always one. This trend in velocity change can be thought of as a progress set-point coordination scheme with v_4 adapting v_3 during the transition. As no further stretching exists in the third span at any time, the tension in the third span will totally depend on the tension transferred from the second span in the elastic case or allow for relaxation in the viscoelastic case. However, in the case of slackness in the second span, the third span eventually goes to a slack condition after the transition as is shown in Figure F.3. The third span, as predicted by the elastic model, however, is still under tension since v_4 is larger than v_1 .

F.2 Transition between Two Steady States in a Four-Span System

In this section, a propagation of dynamic response of tension to the subsequent



— Viscoelastic
 - - - Elastic

Figure F.3 Tension in a Three-Span System During the Transition between Two Steady States due to the Variations in v_3 and v_4
 (a) First Span, (b) Second Span, and
 (c) Third Span

spans during the transition is studied. The dynamic response is initiated by a variation in the velocity of a given roller. A four-span system is examined for this purpose as shown in Figure F.4 with material properties: $G = 0.55 \times 10^9$ Pa, $m = 1.65 \times 10^{10}$ PaS, $n = 1$ and $E = 1.65 \times 10^9$ Pa. From steady state, v_3 was increased to 2.525 m/s within 5 seconds to reach a new steady state.

In the elastic analysis ($m = \infty$), as shown in Figure F.5, the increase in v_3 causes an increase in F_2 . The subsequent spans, not only the third span that is immediately affected by the draw ratio but also the fourth span, experience variations of tension due to tension transfer. However, F_3 and F_4 eventually return to the initial values in the new steady state meaning that v_3 does not permanently affect the subsequent spans after a short disturbance.

On the other hand, in the viscoelastic case, shown in Figure F.6, the results are different. In addition to the different tension levels, F_3 and F_4 cannot reach the initial values after the transition. The increase in F_2 causes more irrecoverable deformation in the second span, which makes F_3 and F_4 lower than the initial values. This effect can be expected to propagate throughout the whole system as long as all of the subsequent spans are not slack.

F.3 Summary

During the transition between two steady states, undesirable slackness may occur and propagate throughout a multi-span system if the system is operated under smaller draw ratios in the spans after a slack span. Those situations cannot be

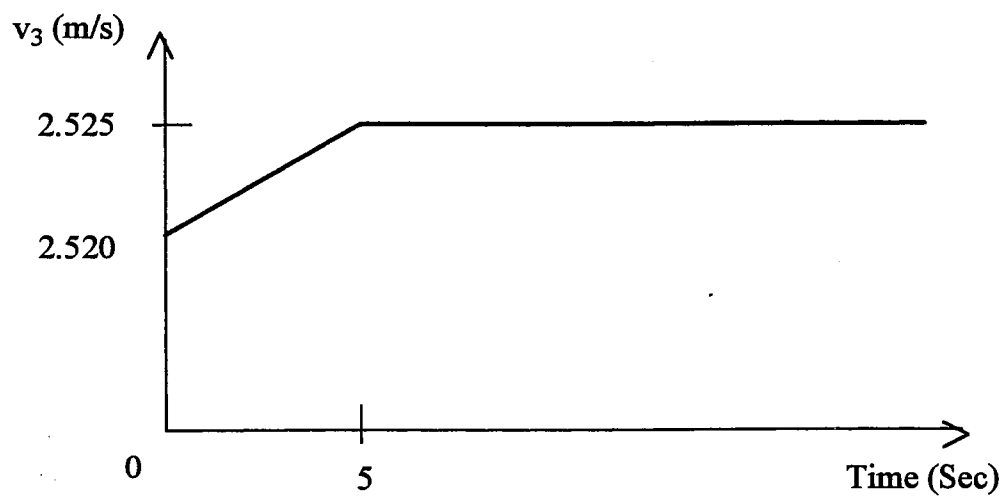
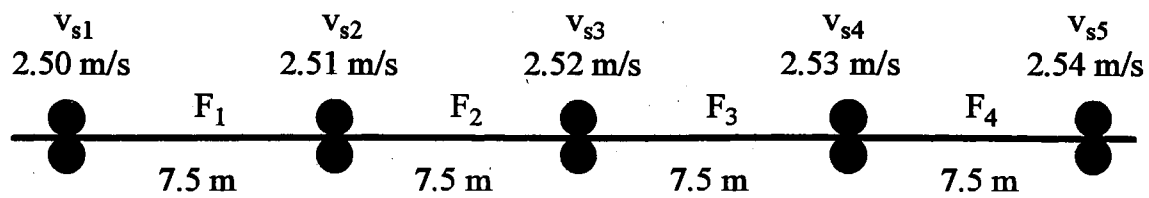


Figure F.4 A Four-Span System Subjected to a Variation in v_3

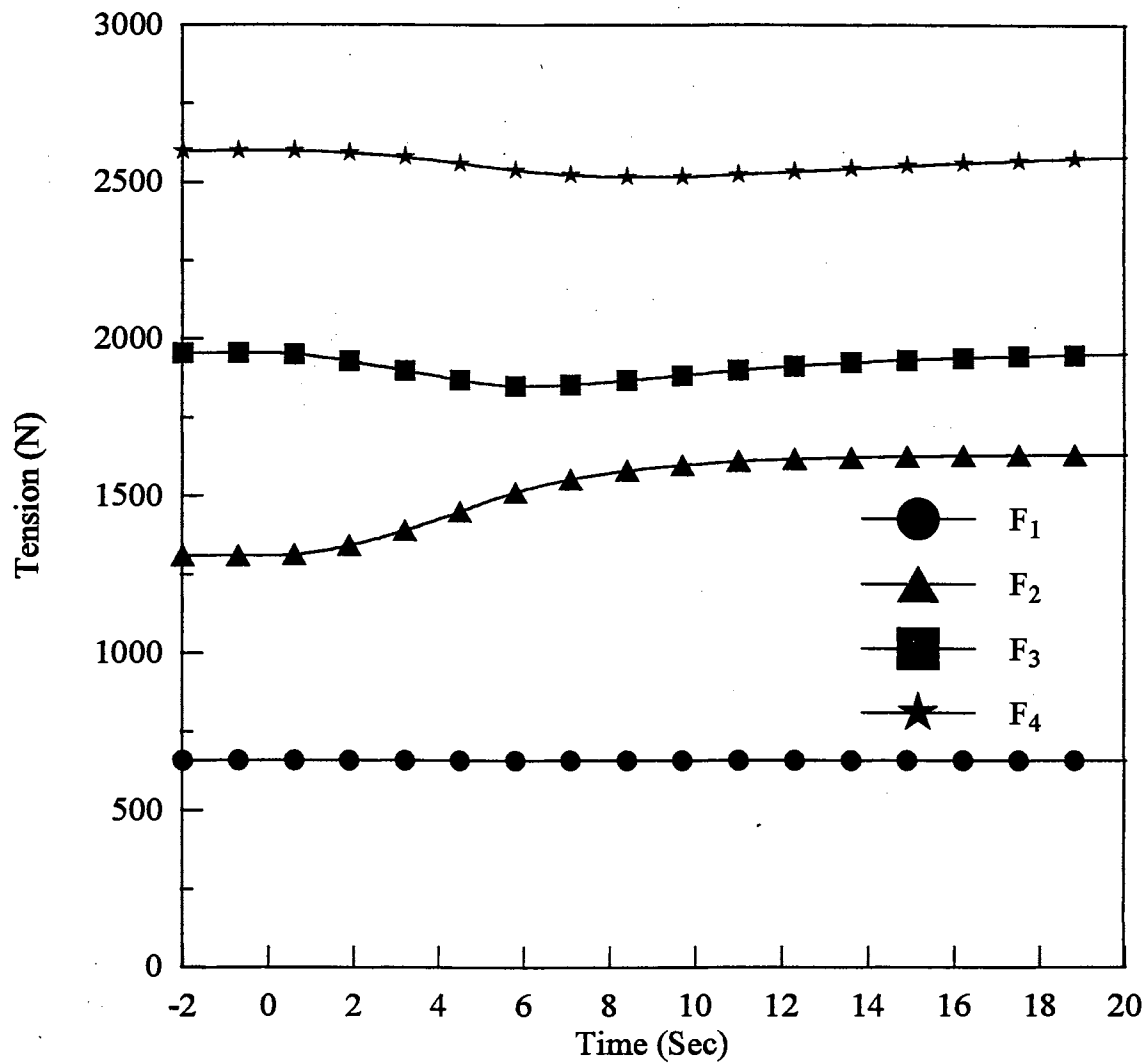


Figure F.5 Tension in a Four-Span System Subjected to a Variation in v_3 , Simulated by the Elastic Model

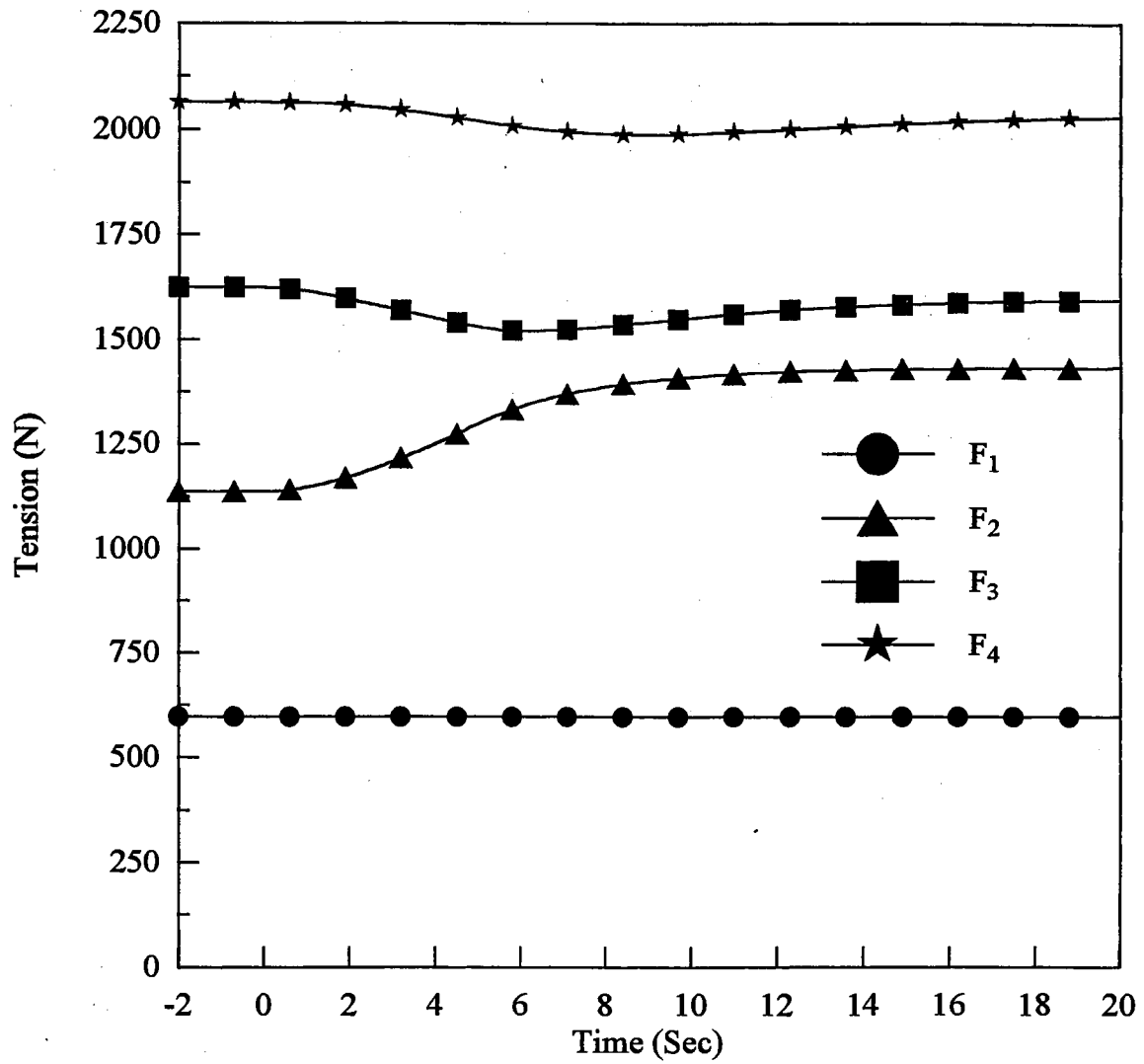


Figure F.6 Tension in a Four-Span System Subjected to a Variation in v_3 , Simulated by the Viscoelastic Model

predicted by the elastic model.

APPENDIX G

ADDITIONAL SIMULATION FOR SINUSOIDAL DISTURBANCE CASES

G.1 Sinusoidal Disturbance in a Single-Span System

In a single-span system, if the disturbance occurs at the entry roller, the analysis can be conducted similarly to that for the ending roller being disturbed but the Deborah number should be evaluated by the average velocity of the entry roller.

Figure G.1 shows the tension variation due to the velocity disturbance at the entry roller or ending roller for the same Deborah number (13.5) for the system in Figure 5.24. The simulation data were specified as:

$$v_{s1} = 2.250 \text{ m/s}, \quad v_{s2} = 2.255 \text{ m/s}, \quad L = 5 \text{ m},$$

$$A_0 = 1 \times 10^{-4} \text{ m}^2, \quad n = 1, \quad v_{\text{amp}} = 0.001128 \text{ m/s},$$

$$\omega = 4.51 \text{ rad/s}.$$

As shown in Figure G.1, the amplitudes and the average levels of the tensions in the two cases are almost the same. However, the variations of the tensions are always opposite in sign.

G.2 Sinusoidal Disturbance in a Four-Span System

A four-span system, sketched in Figure G.2, is studied in this section to

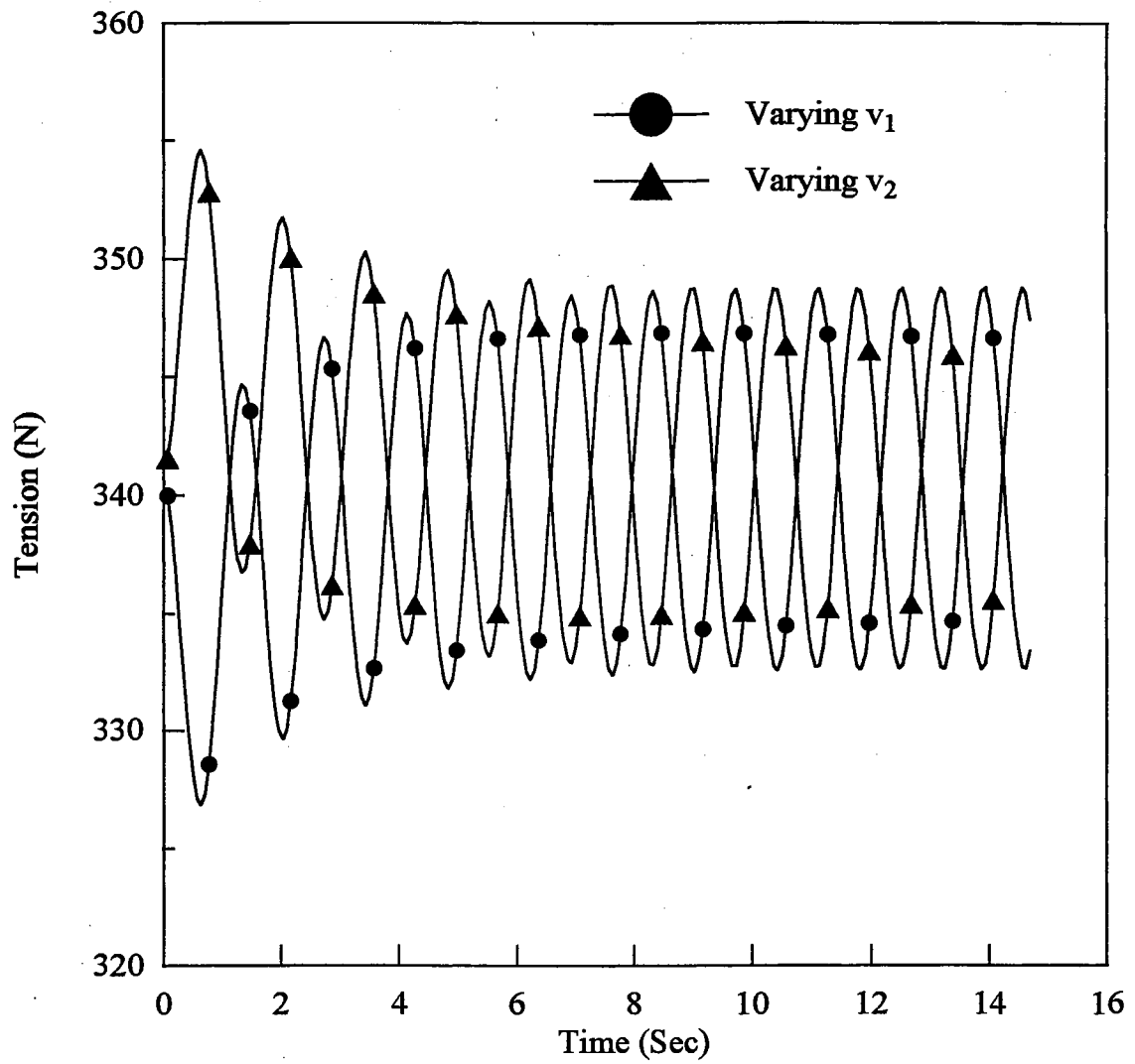
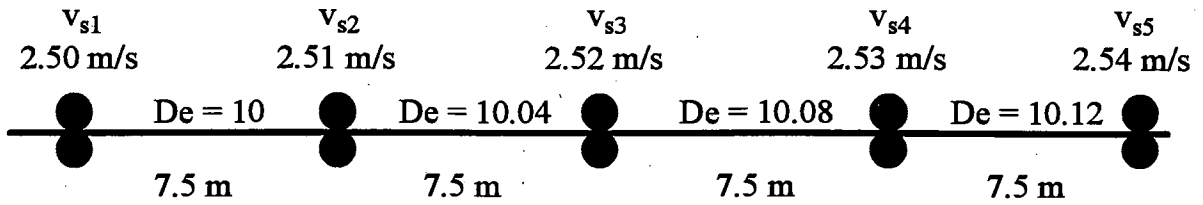


Figure G.1 Tension Variations in a Single-Span System with $De = 13.5$ by Changing v_1 or v_2



$$A_0 = 1 \times 10^{-4} \text{ m}^2$$

$$G = 0.55 \times 10^9 \text{ Pa}$$

$$m = 1.65 \times 10^{10} \text{ PaS}$$

$$n = 1$$

$$E = 1.65 \times 10^9 \text{ Pa}$$

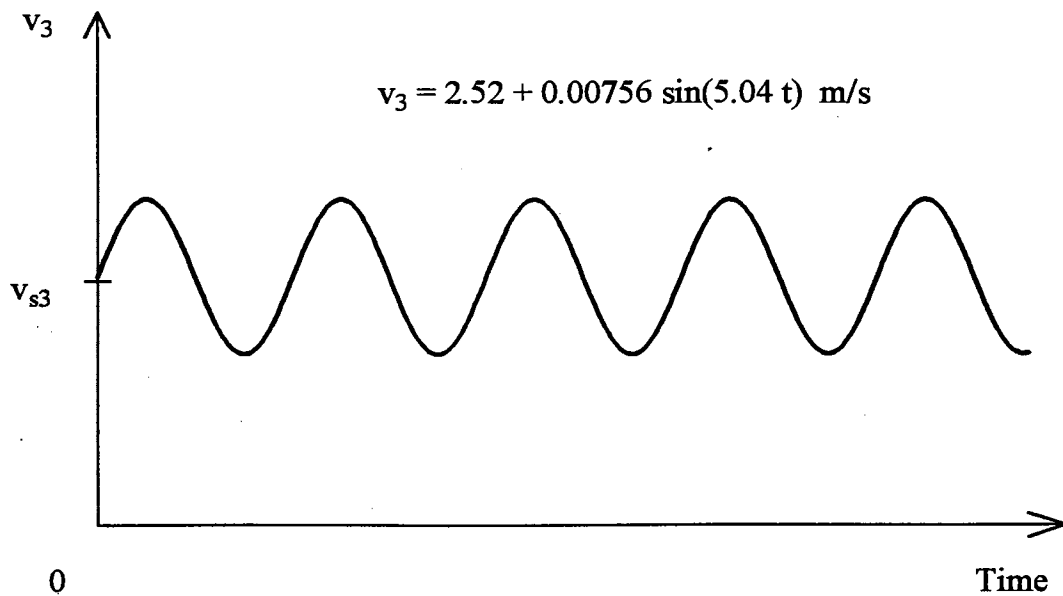


Figure G.2 A Four-Span System with v_3 Changing Sinusoidally

examine the tension transfer in the spans after the disturbed span during a sinusoidal disturbance. The third roller is subjected to a sinusoidal disturbance about the steady state. The amplitude of the velocity is 0.00756 m/s and the angular velocity is 5.04 rad/s, which can be achieved by an eccentric roller with 0.5 m radius and 0.0015 m center offset. The Deborah numbers are 10, 10.04, 10.08 and 10.12, respectively.

The viscoelastic simulation for the system shows, as illustrated in Figure G.3, that in the fourth span the tension is almost unaffected by the disturbance. The amplitude of F_4 is so small as to be negligible. Unlike the transition between two steady states, the disturbance is too fast to allow for the viscous deformation to occur. Therefore, the tension variations in the second and the third spans almost each other counteract with a very small difference that is transferred to the fourth span. The small amplitude of F_4 is due to the elastic memory from the disturbance and the phase angle difference is between those of the tension variations in the second and the third spans. Figure G.4 shows that F_4 , simulated for the elastic material ($m = \infty$), varies almost in the same way as in the viscoelastic situation (De is 10.12 in the fourth span).

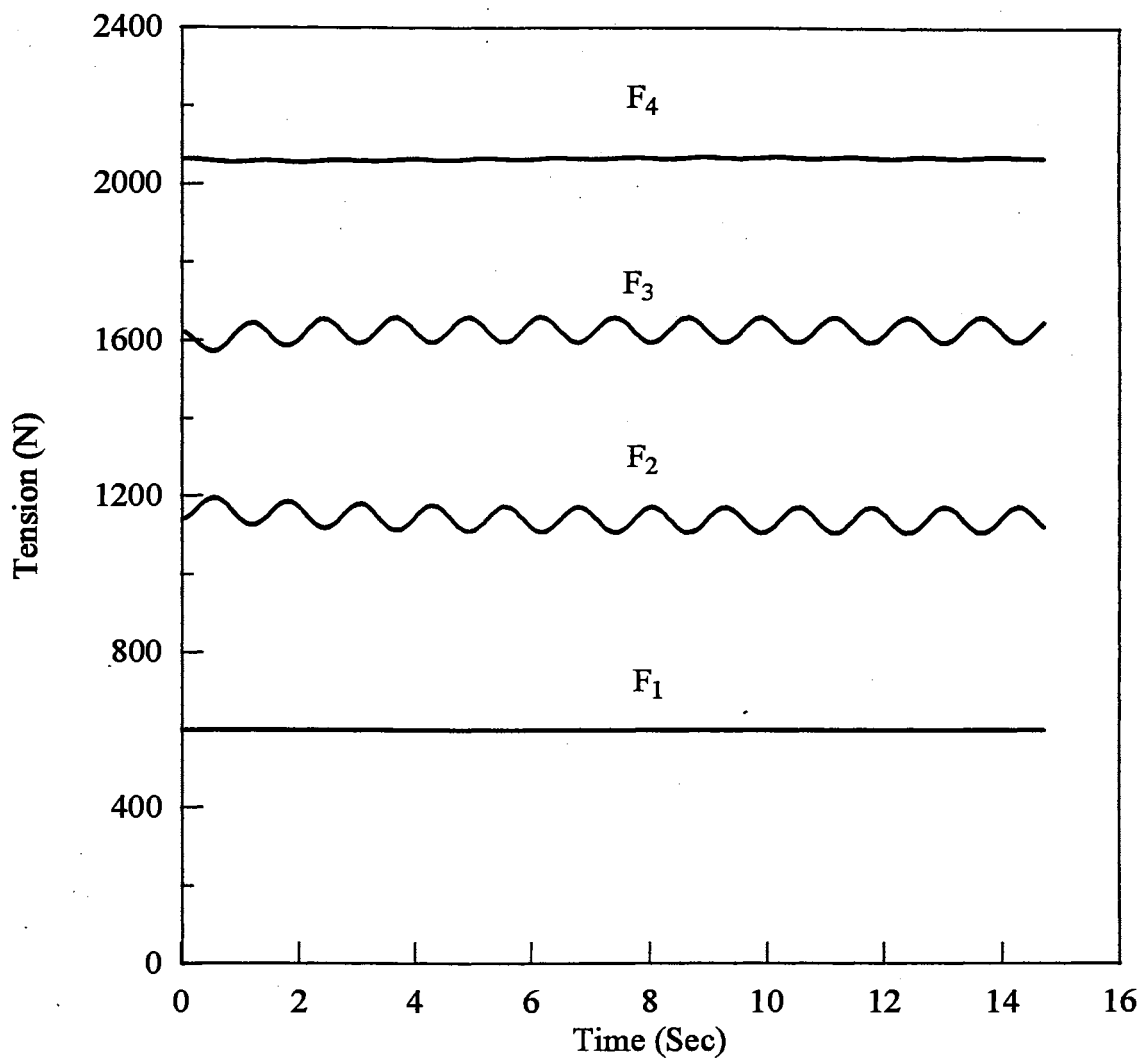


Figure G.3 Tension Variations in a Four-Span System Subjected to a Disturbance in v_3 (Viscoelastic Simulation)

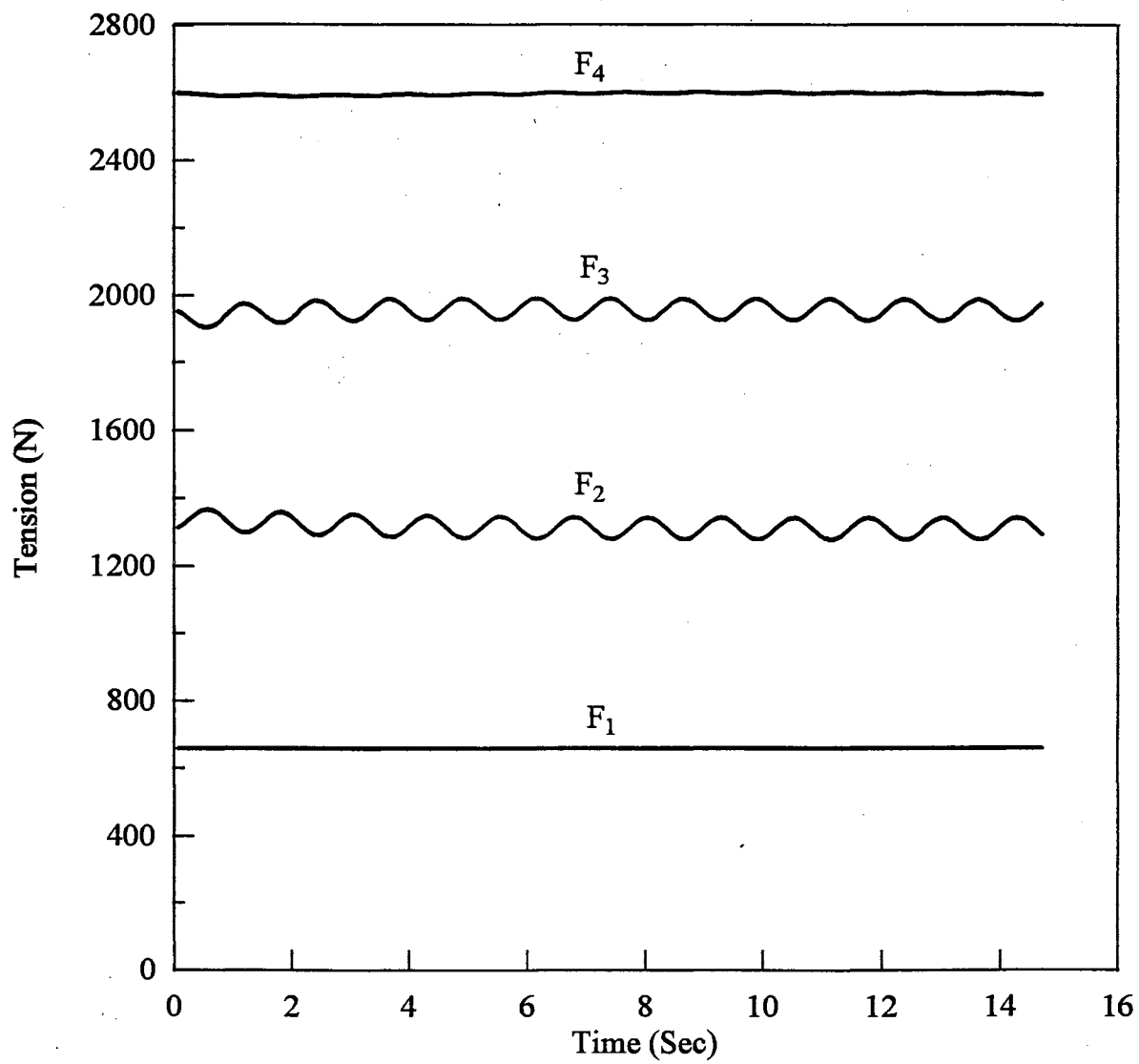


Figure G.4 Tension Variations in a Four-Span System Subjected to a Disturbance in v_3 (Elastic Simulation)

APPENDIX H

COMPUTER CODES

A typical computer program for the numerical simulation of steady-state and unsteady-state cases is listed in this appendix. The program was designed in a functional structure and coded in FORTRAN language. The algorithms and solution strategy of the program were described in Chapter IV in detail.

Subroutines are explained as below:

- MAIN - Control the computation.
- INPUT - Input data from a data file.
- SSA - Steady-state calculation.
- USSA - Unsteady-state calculation.
- SRHBSC - Searching and bisection procedure.
- RKSYS - Fourth-order Runge-Kutta procedure.
- FUNC_RKS - Functions solved by the fourth-order Runge-Kutta method.
- FDM - Finite difference procedure.
- OUTPUT - Output the results to a file.
- FRCBLC - Check force balance at a point in space.

The input data are described as below:

Line 1 - G, PWM, PWN, E:

G - Elastic modulus, G,

PWM - Power law coefficient, m,

PWN - Power law exponent, n,

E - Young's modulus, E.

Line 2 - A00, EPS00, SIG00:

A00 - Initial cross-sectional area, A_{00} ,

EPS00 - Initial strain in the z-direction, $(\epsilon_z)_{00}$,

SIG00 - Initial stress difference, $(\tau_{zz} - \tau_{xx})_{00}$.

In the start-up procedure, the values of variables at entry state were treated as the same as at the initial state. If the two states are different, user can introduce other variables to define the data for the entry state.

Line 3 - NSPAN,NTIME,NMAX,NSRCH,NBISC,NSTEP,

NSHOOT,NFDM:

NSPAN - Number of spans,

NTIME - Number of time levels,

NMAX - Number of points from $\xi = 0$ to $\xi = 1$,

NSRCH - Number of iterations for searching,

NBISC - Number of iterations for bisection,

NSTEP - Number of steps for determining step length of searching,

NSHOOT - Number of iterations for shooting,

NFDM - Number of iterations for ϕ_i .

Line 4 - VS(IS),IS=1,NSPAN+1:

VS(IS) - Steady-state values of tangential
velocities of rollers.

Line 5 - ALENG(IS),IS=1,NSPAN:

ALENG(IS) - Lengths of spans.

Line 6 - TTOTAL,TS,TOLDR,TOLPHI:

TTOTAL - Total time,

TS - The time period over which the velocity changes linearly
with time,

TOLDR - Tolerance for ϕ_1 ,

TOLPHI - Tolerance for ϕ_i .

The code listed in this appendix was used for start-up procedures. However, user can slightly modify the subroutine USSA to change the velocity function for other transient procedures such as transition between two steady states or disturbance about a steady state. Of course, communications of different subroutines should also be adjusted based on the modification. The INPUT subroutine should be implemented to accommodate the new variables if necessary.

Special thanks should be given to Dr. Guohai Liu for his ideas of coding the Runge-Kutta method.

The program code is listed as follows:

C PROGRAM WVE62.FOR, APRIL 19, 1994. UPDATED OCTOBER 5,
 C 1994.
 C STEADY-STATE AND UNSTEADY-STATE ANALYSES FOR WEB
 HANDLING C SYSTEMS.
 C STEADY STATE: FOURTH-ORDER RUNGE-KUTTA METHOD.
 C UNSTEADY STATE: EXPLICIT MacCormack FINITE DIFFERENCE.
 C VARIABLES:
 C T-TIME
 C V0T-V0(T)
 C V0L-VL(T),
 C A - AREA (NON-D)
 C R - TAUXX (NON-D)
 C S - TAUZZ (NON-D),
 C PHI - VELOCITY (NON-D)
 C RPVS - TAUXX (AT PREVIOUS TIME LEVEL)
 C SPVS - TAUZZ (AT PREVIOUS TIME LEVEL)
 C APVS - A (AT PREVIOUS TIME LEVEL)
 C PHIITR - PHI (IN LAST ITER. STEP)
 C FT - TENSION (N-D, AT U.S.S.)
 C VS - ROLLER SPEED (AT S.S.)
 C ALENG - LENGTHS OF THE SPANS
 C A00 - (1) ENTRY CROSS-SECTIONAL AREA
 C (2) INITIAL C-S AREA IN THE WHOLE SYSTEM
 C EPS00 - ENTRY STRAIN(Z)
 C SIG00 - (1) ENTRY (TAUZZ-TAUXX)
 C (2) INITIAL (TAUZZ-TAUXX) IN THE WHOLE SYSTEM
 C A0M - A0(-)
 C EPS0M - EPS0(-)
 C SIG0M - (TAUZZ-TAUXX)0(-)
 C SIG0P - (TAUZZ-TAUXX)0(+)
 C P - PHI0P, OR PHI0(+)
 C PHI0M - PHI0(-)
 C AS0P - A (AT S.S)
 C FS - TENSION (AT S.S.)
 C NSPAN - # OF SPANS
 C NTIME - # OF TIME LEVELS
 C NMAX - # OF COORD. STEPS
 C NSRCH - # OF SEARCHES
 C NBISC - # OF BISECTIONS
 C NSTEP - # OF SUBREGIONS
 C NSHOOT - # OF ITERATIONS FOR SHOOTING PHI0P IN USSA
 C NFDM - # OF ITERATIONS FOR SYSTEM EQS. IN FDM

```

C   G, PWM, PWN, E - PHYSICAL PROPERTIES
C   TOLDR - TOLERANCE FOR CONVERGENCE OF PHI1-DR
C   TOLPHI - TOLERANCE FOR CONVERGENCE OF PHI AT EVERY STEP
C           OF POSITION
C   DES - DEBORAH NUMBER (AT S.S.)
C   ANS - RECIPROCAL TENSION (AT S.S.)
C   YW, RK, YV, FRK - USED IN R-K METHOD FOR S.S. ANALYSIS
C   TTOTAL - TOTAL TIME OF THE U.S.S. ANALYSIS
C   RATIO - SPECIFY THE RANGE OF PHI0(+)
C   RSTP - RATIO STEP
C
C*****
C
C MAIN PROGRAM
C
C   IMPLICIT REAL*8(A-H, O-Z), INTEGER*4(I-N)
C   PARAMETER (NL=1001, NS=5, NT=1000)
C   COMMON /C1/ T(NT),DT,TS,IS,IT,DXI,DTHETA,V0T,VLT,PHI0M
COMMON /C2/ A(NL),R(NL),S(NL),PHI(NL),
$   RPVS(NS,NL),SPVS(NS,NL),APVS(NS,NL)
COMMON /C3/ FT(NS,NT)
COMMON /C4/ VS(NS),ALENG(NS),A00,A0M,A0P,
$   EPS00,EPS0M,SIG00,SIG0M,SIG0P,
$   P,AS0P(NS),FS(NS),PS(NS)
COMMON /C5/ NSPAN,NTIME,NMAX,NSRCH,NBISC,
$   NSTEP,NSHOOT,NFDM
COMMON /C6/ G,PWM,PWN,E,TOLDR,TOLPHI,DES(NS),ANS(NS)
COMMON /C7/ YW(NL,2),RK(4,NL),YV(2),FRK(2)
C
C   OPEN(20,FILE='wve6.out')
C INPUT DATA
C   CALL INPUT
C STEADY-STATE ANALYSIS
C   CALL SSA
C UNSTEADY-STATE ANALYSIS
C   CALL USSA
C OUTPUT
C   CALL OUTPUT
C   CLOSE(20)
C
C   STOP
C   END
C
C*****C

```

```

SUBROUTINE INPUT
IMPLICIT REAL*8(A-H, O-Z), INTEGER*4(I-N)
PARAMETER (NL=1001, NS=5, NT=1000)
COMMON /C1/ T(NT),DT,TS,IS,IT,DXI,DTHETA,VOT,VLT,PHIOM
COMMON /C2/ A(NL),R(NL),S(NL),PHI(NL),RPVS(NS,NL),
$      SPVS(NS,NL), APVS(NS,NL)
COMMON /C3/ FT(NS,NT)
COMMON /C4/ VS(NS),ALENG(NS),A00,A0M,A0P,
$      EPS00,EPS0M,SIG00,SIG0M,SIG0P,P,
$      ASOP(NS),FS(NS),PS(NS)
COMMON /C5/ NSPAN,NTIME,NMAX,NSRCH,NBISC,
$      NSTEP,NSHOOT,NFDM
COMMON /C6/ G,PWM,PWN,E,TOLDR,TOLPHI,
$      DES(NS),ANS(NS)
COMMON /C7/ YW(NL,2),RK(4,NL),YV(2),FRK(2)
C
OPEN(10,FILE='wve6.dat')
C THE UNITS OF THE DATA SHOULD BE CONSISTENT.
READ(10,*) G,PWM,PWN,E
WRITE(20,'(1X,A,2E15.9,F10.5,E15.9)') 'G,m,n,E = ',      $
G,PWM,PWN,E
READ(10,*) A00,EPS00,SIG00
WRITE(20,'(1X,A,3E15.9)') 'A00,EPS00,SIG00 =          $
',A00,EPS00,SIG00
C IN UNSTEADY-STATE ANALYSIS, THE ENTRY VALUES AND INITIAL
C VALUES OF THE VARIABLES MAY BE DIFFERENT. IF SO,
C MODIFICATIONS ARE NEEDED.
READ(10,*) NSPAN,NTIME,NMAX,NSRCH,NBISC,NSTEP,
$      NSHOOT,NFDM
WRITE(20,'(1X,A,/1X,8I8)') 'NSPAN,NTIME,NMAX,
$      NSRCH,NBISC,NSTEP,NSHOOT,NFDM =
$      ',NSPAN,NTIME,NMAX,NSRCH,NBISC,
$      NSTEP,NSHOOT,NFDM
READ(10,*) (VS(IS),IS=1,NSPAN+1)
WRITE(20,'(1X,A)') 'VS(IS) = '
WRITE(20,'((1X,I4,F20.9))') (IS,VS(IS), IS=1,NSPAN+1)      READ(10,*)
(ALENG(IS),IS=1,NSPAN)
WRITE(20,'(1X,A)') 'L(IS) = '
WRITE(20,'((1X,I4,F20.9))') (IS,ALENG(IS), IS=1,NSPAN)
READ(10,*) TTOTAL,TS,TOLDR,TOLPHI
WRITE(20,'(1X,A,/1X,2F15.9,2E15.9)')
$      'Ttotal,Ts,TOLDR,TOLPHI = ',
$      TTOTAL,TS,TOLDR,TOLPHI
C

```

```

C TIME AND COOR INCREMENTS
  DT = TTOTAL/NTIME
  DXI = 1.0/(NMAX-1)
  WRITE(20,'(1X,A,2F20.9)') 'DT,DXI = ', DT,DXI
C STEADY-STATE DRAW RATIOS
  WRITE(20,'(1X,A)') 'DR(IS) = '
  DO 100 IS=1,NSPAN
    DRS = VS(IS+1)/VS(IS)
    WRITE(20,'(1X,I4,F20.15)') IS,DRS
  100 CONTINUE
C
  CLOSE(10)
  RETURN
  END
C
C*****C
SUBROUTINE SSA
  IMPLICIT REAL*8(A-H, O-Z), INTEGER*4(I-N)
  PARAMETER (NL=1001, NS=5, NT=1000)
  COMMON /C1/ T(NT),DT,TS,IS,IT,DXI,DTHETA,V0T,VLT,PHI0M
COMMON /C2/ A(NL),R(NL),S(NL),PHI(NL),
  $      RPVS(NS,NL),SPVS(NS,NL),APVS(NS,NL)
COMMON /C3/ FT(NS,NT)
COMMON /C4/ VS(NS),ALENG(NS),A00,A0M,A0P,
  $      EPS00,EPS0M,SIG00,SIG0M,SIG0P,
  $      P,AS0P(NS),FS(NS),PS(NS)
COMMON /C5/ NSPAN,NTIME,NMAX,NSRCH,NBISC,
  $      NSTEP,NSHOOT,NFDM
  COMMON /C6/ G,PWM,PWN,E,TOLDR,TOLPHI,DES(NS),ANS(NS)
COMMON /C7/ YW(NL,2),RK(4,NL),YV(2),FRK(2)
C
C ENTRY STATE: AREA, STRAIN AND STRESS
  A0M = A00
  SIG0M = SIG00
  EPS0M = EPS00
C
  DO 900 IS=1,NSPAN
C DEBORAH NUMBER AND DRAW RATIO FOR THE CURRENT SPAN
  DES(IS) = 3.0**((PWN-1.0)/2.0)*PWM/G
  $      *(VS(IS)/ALENG(IS))**PWN
  DR = VS(IS+1)/VS(IS)
C SEARCHING FOR PHI0P
  CALL SRHBSC(YW(NMAX,2),DR)
C CALCULATE VARIABLES FOR NEXT SPAN AS WELL AS FOR U.S.S.A.

```

```

ASOP(IS) = A0M/P
  FS(IS) = SIGOP*ASOP(IS)
  EPSOM = (1.0+EPSOM)*YW(NMAX,2)-1.0
  A0M = A0M/YW(NMAX,2)
  SIGOM = FS(IS)/A0M
900 CONTINUE

C OUTPUT THE GENERAL INFORMATION OF THE SYSTEM
  WRITE(20,'(1X,A)') 'DES(I)='
  WRITE(20,'((1X,I4,F20.9))') (I,DES(I), I=1,NSPAN)
  WRITE(20,'(1X,A)') 'ANS(I)='
  WRITE(20,'((1X,I4,F20.5))') (I,ANS(I), I=1,NSPAN)
WRITE(20,'(1X,A)') 'FS(I)='
  WRITE(20,'((1X,I4,F20.5))') (I,FS(I), I=1,NSPAN)
  WRITE(20,'(1X,A)') 'ASOP(I)='
  WRITE(20,'((1X,I4,F20.12))') (I,ASOP(I), I=1,NSPAN)

C
  RETURN
  END

C
C*****C
  SUBROUTINE USSA
  IMPLICIT REAL*8(A-H, O-Z), INTEGER*4(I-N)
  PARAMETER (NL=1001, NS=5, NT=1000)
  COMMON /C1/ T(NT),DT,TS,IS,IT,DXI,DTHETA,V0T,VLT,PHI0M
COMMON /C2/ A(NL),R(NL),S(NL),PHI(NL),
  $          RPVS(NS,NL),SPVS(NS,NL),APVS(NS,NL)
COMMON /C3/ FT(NS,NT)
COMMON /C4/ VS(NS),ALENG(NS),A00,A0M,A0P,
  $          EPS00,EPSOM,SIG00,SIGOM,SIGOP,
  $          P,ASOP(NS),FS(NS),PS(NS)
COMMON /C5/ NSPAN,NTIME,NMAX,NSRCH,NBISC,
  $          NSTEP,NSHOOT,NFDM
  COMMON /C6/ G,PWM,PWN,E,TOLDR,TOLPHI,DES(NS),ANS(NS)
COMMON /C7/ YW(NL,2),RK(4,NL),YV(2),FRK(2)
COMMON /C8/ R1,S1,AA1
  DIMENSION RATIO(NS),RSTP(NS)

C
C INITIAL CONDITIONS (NON-D)
  DO 50 IS=1,NSPAN
  DO 50 J=1,NMAX
    APVS(IS,J) = A00/ASOP(IS)
    RPVS(IS,J) = -1.0/3.0*SIG00*ASOP(IS)/FS(IS)
    SPVS(IS,J) = -2.0*RPVS(IS,J)

```

```

50 CONTINUE
C
C INPUT RATIO STEP FROM KEYBOARD. THE RATIO STEP IS USED TO C
HELP NARROW THE RANGE IN WHICH PHI0(+) IS LOCATED.
  WRITE(*,*) 'RATIO STEP (IS) = '
  DO 22 IS=1,NSPAN
    READ(*,*) RSTP(IS)
22  RATIO(IS) = RSTP(IS)
C
C ITERATION FOR ALL TIME LEVELS
  DO 1000 IT=1,NTIME
    WRITE(*,*) '          TIME LEVEL=',IT          T(IT) = IT*DT
C ENTRY STATE
  A0M = A00
  SIG0M = SIG00
  EPS0M = EPS00
C
C ITERATION FOR ALL SPANS
  DO 900 IS=1,NSPAN
    WRITE(*,*) '          # OF TIME,          $SPAN = ', IT,IS
C ASSUME THAT ALL ROLLER SPEEDS ARE LINEARLY INCREASED TO
C THE STEADY-STATE VALUES WITHIN TS IN THE START-UP
C PROCEDURE. USER CAN REDEFINE THIS PART FOR OTHER
C PROCEDURES
    IF(T(IT) .LE. TS) THEN
      V0T = VS(IS)*T(IT)/TS
      VLT = VS(IS+1)*T(IT)/TS
    ELSE
      V0T = VS(IS)
      VLT = VS(IS+1)
    ENDIF
    DR = VLT/V0T
    PHI0M = V0T/VS(IS)
    DTHETA = DT*VS(IS)/ALENG(IS)
C
    RATIO(IS) = RATIO(IS)-RSTP(IS)
C SHOOTING FOR PHI0P.
C RATIO IS INCREASED BY THE RATIO STEP WHENEVER PHI0(+) IS
C ABSENT IN THE RANGE
123  RATIO(IS) = RATIO(IS)+RSTP(IS)
    IF(RATIO(IS) .GT. 5.0) THEN
      WRITE(*,*) 'FDM FAILED: RATIO(IS)>5.0 <<<?>>>'
      STOP
    ENDIF

```



```

C SET UP THE SHOOTING RANGE FOR PHI0P. SEVERAL DIFFERENT
C CONDITIONS ARE CONSIDERED SEPARATELY: (1) DR = 1, (2) DR
C <> 1. THE RANGE IS LABELED BY [BLEFT, BRIGHT].
  IF(DR .LE. 1.0) THEN
    BLEFT = PHI0M
    IF(DR .EQ. 1.0) THEN
      SCALE = PS(IS)-1.0
    ELSE
      SCALE = DR-1.0
    ENDIF
    BRIGHT = PHI0M*(1.0+RATIO(IS)*SCALE)
    IF(DR .EQ. 1 .AND. PS(IS) .EQ. 1) THEN
      BLEFT = PHI0M*(1.0-RATIO(IS))
      BRIGHT = PHI0M*(1.0+RATIO(IS))
    ENDIF
  ELSE
    BLEFT = PHI0M*(1.0-RATIO(IS)*(DR-1.0))
    BRIGHT = PHI0M*(1.0+RATIO(IS)*(DR-1.0))
  ENDIF
C ITERATIONS FOR SHOOTING
  DO 300 I=1,NSHOOT
C IN LEFT SUBRANGE
  BMID = (BLEFT+BRIGHT)/2.0
  P = (BLEFT+BMID)/2.0
  CALL FDM(PHI0M*DR,ERROR,IRT)
  ERR1 = ERROR
C   WRITE(*,*)'I,PL,ERR1=',I,P,ERR1
  IF(IRT .EQ. 0) THEN
    WRITE(*,*) 'IT,IS,LAST $RATIO(IS)=' ,IT,IS,RATIO(IS),' RETRY'

C ADJUST THE RANGE AND REDO THE PROCEDURE
  GOTO 123
  ENDIF
  IF(ERR1 .LE. TOLDR) THEN
C   WRITE(20,'(1X,A,2F20.15)') 'P, ERROR=' ,P,ERR1
    WRITE(*,*) 'USSA SHOOTING SUCCESSFUL!'
    GOTO 400
  ENDIF
  BNL = P
C IN RIGHT SUBRANGE
  P = (BMID+BRIGHT)/2.0
  CALL FDM(PHI0M*DR,ERROR,IRT)
  ERR2 = ERROR
C   WRITE(*,*)'I,PR,ERR2=',I,P,ERR2

```

```

IF(IRT .EQ. 0) THEN
  WRITE(*,*) 'IT,IS,LAST $RATIO(IS)=' ,IT,IS,RATIO(IS),' RETRY'
C ADJUST THE RANGE AND REDO THE PROCEDURE
  GOTO 123
ENDIF
IF(ERR2 .LE. TOLDR) THEN
C   WRITE(20,'(1X,A,2F20.15)') 'P, ERROR=' ,P,ERR2
  WRITE(*,*) 'USSA SHOOTING SUCCESSFUL!'
  GOTO 400
ENDIF
BNR = P
IF(ERR2 .LE. ERR1) THEN
  BLEFT = BNL
ELSE
  BRIGHT = BNR
ENDIF
300 CONTINUE
  WRITE(*,*) 'USSA SHOOTING FAILED'
  WRITE(*,*) 'IT,IS,LAST RATIO(IS)=' ,IT,IS,RATIO(IS),' $RETRY'
C ADJUST THE RANGE AND REDO THE PROCEDURE
  GOTO 123
400 CONTINUE
C MEMORIZE VARIABLES AS THE PREVIOUS VALUES FOR NEXT TIME
C LEVEL. SPECIAL CONSIDERATIONS ARE TAKEN IN NAGTIVE
C TENSION CASES (SLACK). IF THE SPAN IS SLACK, THE PROGRAM C
C MUST MEMORIZE THE SLACK CONDITION UNTIL THE SPAN BECOMES
C TIGHT AGAIN.
  IF(IS .EQ. 1) THEN
    FPRE = SIG00*A00
  ELSE
    FPRE = FT(IS-1,IT)*FS(IS-1)
  ENDIF
  IF(FPRE .LE. 0.0) THEN FPRE = 0.0
  EPSCUR = EPS0M-FPRE/(E*A0M)
  A0MNXT = A00/(1.0+EPSCUR)
  IF(IT .EQ. 1) THEN
    FPSUD1 = SIG00*A00
  ELSE
    FPSUD1 = FT(IS,IT-1)*FS(IS)
  ENDIF
  FPSUD2 = FT(IS,IT)*FS(IS)
  IF(FPSUD1 .LT. 0.0 .AND. FPSUD2 .GE. 0.0) THEN
    DO 460 I=1,NMAX
      RPVS(IS,I) = 0.0

```

```

        SPVS(IS,I) = 0.0
        APVS(IS,I) = A0MNXT/ASOP(IS)
460    CONTINUE
        RATIO(IS) = RSTP(IS)
        ELSE
        DO 500 I=1,NMAX
        RPVS(IS,I) = R(I)
        SPVS(IS,I) = S(I)
        APVS(IS,I) = A(I)
500    CONTINUE
        ENDIF
C CALCULATE VARIABLES FOR NEXT SPAN AT THE SAME TIME LEVEL.
C SET UP THE ENTRY VALUES FOR THE NEXT SPAN.
        IF(FPSUD2 .LE. 0.0) THEN
        A0M = A0MNXT
        EPS0M = EPSCUR
        SIG0M = 0.0
        ELSE
        A0M = A(NMAX)*ASOP(IS)
        EPS0M = A00/A0M-1.0
        SIG0M = (S(NMAX)-R(NMAX))*FS(IS)/ASOP(IS)
        ENDIF
C
C AT THE LAST TIME LEVEL, OUTPUT THE VARIABLES (OPTIONAL)
        IF(IT .EQ. NTIME) THEN
        WRITE(20,'(1X,A,I4)') 'SPAN = ',IS
        WRITE(20,'(1X,A)') '      a          Phi          $          Txx
Tzz'
        DO 444 I=1,NMAX
        WRITE(20,'(1X,4F19.14)') A(I),PHI(I),R(I),S(I)
444    CONTINUE
        ENDIF
900    CONTINUE
1000 CONTINUE
C
        RETURN
        END
C
C*****C
SUBROUTINE SRHBSC(PHI1,DR)
IMPLICIT REAL*8(A-H, O-Z), INTEGER*4(I-N)
PARAMETER (NL=1001, NS=5, NT=1000)
COMMON /C1/ T(NT),DT,TS,IS,IT,DXI,DTHETA,V0T,VLT,PHI0M
COMMON /C2/ A(NL),R(NL),S(NL),PHI(NL),

```

```

$          RPVS(NS,NL),SPVS(NS,NL),APVS(NS,NL)
COMMON /C3/ FT(NS,NT)
COMMON /C4/ VS(NS),ALENG(NS),A00,A0M,A0P,
$          EPS00,EPS0M,SIG00,SIG0M,SIG0P,
$          P,AS0P(NS),FS(NS),PS(NS)
COMMON /C5/ NSPAN,NTIME,NMAX,NSRCH,NBISC,
$          NSTEP,NSHOOT,NFDM
COMMON /C6/ G,PWM,PWN,E,TOLDR,TOLPHI,DES(NS),ANS(NS)
COMMON /C7/ YW(NL,2),RK(4,NL),YV(2),FRK(2)
C
C REFERENCE VALUE: CENTRAL POINT IN [1, DR]
P0 = (1.0+DR)/2.0
P = P0
C CALCULATE DEVIATION (ERROR) AS THE REFERENCE.
CALL RKSYS
ERROR0 = (PHI1-DR)/DR
IF(DABS(ERROR0) .LE. TOLDR) THEN
WRITE(*,*) 'SSA SEARCHING SUCCESSFUL!'
WRITE(20,'(1X,A,I4,F20.15)') 'IS, P = ',IS,P
WRITE(*,*) 'FINAL P=',P
PS(IS) = P
GOTO 1000
ENDIF
P1 = P0
P2 = P0
C CALCULATE THE SEARCHING LENGTH.
IF(P0 .NE. 1.0) THEN
SEARCH = (P0-1.0)/NSTEP
ELSE
SEARCH = 0.00005*P0
ENDIF
C ITERATIONS FOR SEARCHING PHI0(+)
DO 200 I=1,NSRCH
WRITE(*,*) 'SSA SEARCH: (# OF SPAN, ITERATION)= $
',IS,I
C LEFT SEARCHING.
P = P1-SEARCH
WRITE(*,*) 'PL= ',P
CALL RKSYS
ERROR1 = (PHI1-DR)/DR
IF(DABS(ERROR1) .LE. TOLDR) THEN
WRITE(*,*) 'SSA SEARCHING SUCCESSFUL!'
WRITE(20,'(1X,A,I4,F20.15)') 'IS, P = ',IS,P
WRITE(*,*) 'FINAL P=',P

```

```

    PS(IS) = P
    GOTO 1000
ENDIF
IF(ERROR1/ERROR0 .LT. 0.0) THEN
    PL = P1-SEARCH
    PR = P1
    ERRORL = ERROR1
    ERRORR = ERROR0
    GOTO 700
ELSE
    P1 = P1-SEARCH
ENDIF
C RIGHT SEARCHING.
P = P2+SEARCH
WRITE(*,*) 'PR= ',P
CALL RKSYS
ERROR2 = (PHI1-DR)/DR
IF(DABS(ERROR2) .LE. TOLDR) THEN
    WRITE(*,*) 'SSA SEARCHING SUCCESSFUL!'
    WRITE(20,'(1X,A,I4,F20.15)') 'IS, P = ',IS,P
    WRITE(*,*) 'FINAL P=',P
    PS(IS) = P
    GOTO 1000
ENDIF
IF(ERROR2/ERROR0 .LT. 0.0) THEN
    PL = P2
    PR = P2+SEARCH
    ERRORL = ERROR0
    ERRORR = ERROR2
    GOTO 700
ELSE
    P2 = P2+SEARCH
ENDIF
200 CONTINUE
WRITE(*,*) 'SSA SEARCHING FAILED'
STOP
700 CONTINUE
WRITE(*,*) 'SSA SEARCHING SUCCESSFUL!'
C BISECTION PROCEDURE.
DO 800 I=1,NBISC
    WRITE(*,*) 'SSA BISECTION:      # OF SPAN, ITERATION      $='
    ,IS,I
    P = (PL+PR)/2.0
    CALL RKSYS

```

```

ERROR = (PHI1-DR)/DR
IF(DABS(ERROR) .LE. TOLDR) THEN
  WRITE(*,*) 'SSA BISECTION SUCCESSFUL! '
  WRITE(20,'(1X,A,I4,F20.9)') 'IS, P=',IS,P
  WRITE(*,*) 'FINAL P=',P
  PS(IS) = P
  GOTO 1000
ELSE IF(ERROR/ERRORL .LT. 0.0) THEN
  PR = P
ELSE
  PL = P
ENDIF
800 CONTINUE
  WRITE(*,*) 'SSA BISECTION FAILED'
  STOP
1000 CONTINUE
C
  RETURN
  END
C
C*****C
  SUBROUTINE RKSYS
  IMPLICIT REAL*8(A-H, O-Z), INTEGER*4(I-N)
  PARAMETER (NL=1001, NS=5, NT=1000)
  COMMON /C1/ T(NT),DT,TS,IS,IT,DXI,DTHETA,V0T,VLT,PHI0M
  COMMON /C2/ A(NL),R(NL),S(NL),PHI(NL),
    $          RPVS(NS,NL),SPVS(NS,NL),APVS(NS,NL)
  COMMON /C3/ FT(NS,NT)
  COMMON /C4/ VS(NS),ALENG(NS),A00,A0M,A0P,
    $          EPS00,EPS0M,SIG00,SIG0M,SIG0P,
    $          P,AS0P(NS),FS(NS),PS(NS)
  COMMON /C5/ NSPAN,NTIME,NMAX,NSRCH,NBISC,
    $          NSTEP,NSHOOT,NFDM
  COMMON /C6/ G,PWM,PWN,E,TOLDR,TOLPHI,DES(NS),ANS(NS)
  COMMON /C7/ YW(NL,2),RK(4,NL),YV(2),FRK(2)
C
  EPS0P = (1.0+EPS0M)*P-1.0
  SIG0P = SIG0M+E*(EPS0P-EPS0M)
  ANS(IS) = DES(IS)*G/SIG0P
  TINL = 2.0/3.0
  W3 = (3.0*TINL-2.0)*DES(IS)+3.0*ANS(IS)
  IF(W3 .LT. 0.0) THEN
    YW(1,1) = -1.0/DABS(W3)**(1.0/PWN)
  ELSE

```

```

      YW(1,1) = 1.0/W3**(1.0/PWN)
      ENDIF
      YW(1,2) = P
      DO 10 I=2,NMAX
        DO 25 K=1,2
25      YV(K) = YW(I-1,K)
          CALL FUNC_RKS
          DO 30 J=1,2
30      RK(1,J) = DXI*FRK(J)
          DO 35 K=1,2
35      YV(K) = YW(I-1,K)+0.5*RK(1,K)
          CALL FUNC_RKS
          DO 40 J=1,2
40      RK(2,J) = DXI*FRK(J)
          DO 45 K=1,2
45      YV(K) = YW(I-1,K)+0.5*RK(2,K)
          CALL FUNC_RKS
          DO 50 J=1,2
50      RK(3,J) = DXI*FRK(J)
          DO 55 K=1,2
55      YV(K) = YW(I-1,K)+RK(3,K)
          CALL FUNC_RKS
          DO 60 J=1,2
60      RK(4,J) = DXI*FRK(J)
          DO 70 J=1,2
            SUMK = RK(1,J)+2.0*RK(2,J)+2.0*RK(3,J)+RK(4,J)
            YW(I,J) = YW(I-1,J)+SUMK/6.0
70      CONTINUE
10     CONTINUE
      C
      RETURN
      END
      C
      C*****C
      SUBROUTINE FUNC_RKS
      IMPLICIT REAL*8(A-H, O-Z), INTEGER*4(I-N)
      PARAMETER (NL=1001, NS=5, NT=1000)
      COMMON /C1/ T(NT),DT,TS,IS,IT,DXI,DTHETA,V0T,VLT,PHI0M
      COMMON /C2/ A(NL),R(NL),S(NL),PHI(NL),
      $           RPVS(NS,NL),SPVS(NS,NL),APVS(NS,NL)
      COMMON /C3/ FT(NS,NT)
      COMMON /C4/ VS(NS),ALENG(NS),A00,A0M,A0P,
      $           EPS00,EPS0M,SIG00,SIG0M,SIG0P,
      $           P,AS0P(NS),FS(NS),PS(NS)

```

```

COMMON /C5/ NSPAN,NTIME,NMAX,NSRCH,NBISC,
$           NSTEP,NSHOOT,NFDM
COMMON /C6/ G,PWM,PWN,E,TOLDR,TOLPHI,DES(NS),ANS(NS)
COMMON /C7/ YW(NL,2),RK(4,NL),YV(2),FRK(2)
C
W1 = DES(IS)*DABS(YV(1))**PWN
W2 =DES(IS)*YV(2)
IF(YV(1) .LT. 0.0) THEN
  ISIGN = -1
ELSE
  ISIGN = 1
ENDIF
FRK(1) = (1.0-3.0*ANS(IS)*P/W2+ISIGN*(1.0/W1-2.0*W1))  $
*YV(1)**2.0/(PWN*YV(2))
FRK(2) = YV(1)
C
RETURN
END
C
C*****C
SUBROUTINE FDM(DR,ERROR,IRT)
IMPLICIT REAL*8(A-H, O-Z), INTEGER*4(I-N)
PARAMETER (NL=1001, NS=5, NT=1000)
COMMON /C1/ T(NT),DT,TS,IS,IT,DXI,DTHETA,V0T,VLT,PHI0M
COMMON /C2/ A(NL),R(NL),S(NL),PHI(NL),
$           RPVS(NS,NL),SPVS(NS,NL),APVS(NS,NL)
COMMON /C3/ FT(NS,NT)
COMMON /C4/ VS(NS),ALENG(NS),A00,A0M,A0P,
$           EPS00,EPS0M,SIG00,SIG0M,SIG0P,
$           P,AS0P(NS),FS(NS),PS(NS)
COMMON /C5/ NSPAN,NTIME,NMAX,NSRCH,NBISC,
$           NSTEP,NSHOOT,NFDM
COMMON /C6/ G,PWM,PWN,E,TOLDR,TOLPHI,DES(NS),ANS(NS)
COMMON /C7/ YW(NL,2),RK(4,NL),YV(2),FRK(2)
COMMON /C8/ R1,S1,AA1
C
C (1) STEP CHANGES AT ROLLER; (2) SET B.C.
SIG0P = SIG0M+E*(P/PHI0M-1.0)*(1.0+EPS0M)
A0P = A0M*PHI0M/P
A(1) = A0P/AS0P(IS)
FT(IS,IT) = A0P*SIG0P/FS(IS)
R(1) = -1.0/3.0*SIG0P*AS0P(IS)/FS(IS)
S(1) = -2.0*R(1)
C WRITE(*,*)'A0P,SIG0P=',A0P,SIG0P

```



```
PHI(1) = P
C
DO 1000 I=2,NMAX
C ITERATION FOR PHI(I) WITHIN THE ITH STEP:
PT = 1.0105*PHI(I-1)
CALL FRCBLC(I,PT,EFB)
ER0 = EFB
IF(DABS(ER0) .LE. TOLPHI) THEN
PHI(I) = PT
GOTO 1000
ENDIF
SP = 0.002*PHI(I-1)
PT1 = PT
PT2 = PT
DO 100 K=1,NFDM
C LEFT SEARCHING FOR PHI(I):
PT = PT1-SP
CALL FRCBLC(I,PT,EFB)
ER1 = EFB
IF(DABS(ER1) .LE. TOLPHI) THEN
PHI(I) = PT
GOTO 1000
ENDIF
IF(ER1/ER0 .LT. 0.0) THEN
PTL = PT1-SP
PTR = PT1
ERL = ER1
ERR = ER0
GOTO 666
ELSE
PT1 = PT1-SP
ENDIF
C RIGHT SEARCHING FOR PHI(I):
PT = PT2+SP
CALL FRCBLC(I,PT,EFB)
ER2 = EFB
IF(DABS(ER2) .LE. TOLPHI) THEN
PHI(I) = PT
GOTO 1000
ENDIF
IF(ER2/ER0 .LT. 0.0) THEN
PTL = PT2
PTR = PT2+SP
ERL = ER0
```

```

        ERR = ER2
        GOTO 666
    ELSE
        PT2 = PT2+SP
    ENDIF
100  CONTINUE
    WRITE(*,*)'PHI(I) SEARCHING FAILED AT I=',I
    IRT = 0
    RETURN
C  BISECTION FOR PHI(I)
666  CONTINUE
    DO 200 K=1,NFDM
        PT = (PTL+PTR)/2.0
        CALL FRCBLC(I,PT,EFB)
        ER = EFB
        IF(DABS(ER) .LE. TOLPHI) THEN
            PHI(I) = PT
            GOTO 1000
        ELSE IF(ER/ERL .LT. 0.0) THEN
            PTR = PT
        ELSE
            PTL = PT
        ENDIF
200  CONTINUE
    WRITE(*,*)'PHI(I) BISECTION FAILED AT I=',I
    IRT = 0
    WRITE(*,*) 'IT,IS,I = ',IT,IS,I
    RETURN
1000 CONTINUE
    IRT = 1
1100 ERROR = DABS((PHI(NMAX)-DR)/DR)
C      WRITE(*,*)'PHI(1),PHI(NMAX),ERROR',
    $          PHI(1),PHI(NMAX),ERROR
C
    RETURN
    END
C
C*****C
    SUBROUTINE OUTPUT
    IMPLICIT REAL*8(A-H, O-Z), INTEGER*4(I-N)
    PARAMETER (NL=1001, NS=5, NT=1000)
    COMMON /C1/ T(NT),DT,TS,IS,IT,DXI,DTHETA,V0T,VLT,PHI0M
COMMON /C2/ A(NL),R(NL),S(NL),PHI(NL),
    $          RPVS(NS,NL),SPVS(NS,NL),APVS(NS,NL)

```

```

COMMON /C3/ FT(NS,NT)
COMMON /C4/ VS(NS),ALENG(NS),A00,A0M,A0P,
$           EPS00,EPS0M,SIG00,SIG0M,SIG0P,
$           P,AS0P(NS),FS(NS),PS(NS)
COMMON /C5/ NSPAN,NTIME,NMAX,NSRCH,NBISC,
$           NSTEP,NSHOOT,NFDM
COMMON /C6/ G,PWM,PWN,E,TOLDR,TOLPHI,DES(NS),ANS(NS)
COMMON /C7/ YW(NL,2),RK(4,NL),YV(2),FRK(2)
C
DO 100 K=1,NSPAN
WRITE(20,'(1X,A,I4)') 'SPAN = ',K
WRITE(20,'(1X,A)') ' No.      Time          $Tension (N-D)    Tension
(D)'
DO 50 J=1,NTIME
IF(FT(K,J)*FS(K) .GE. 0.0) THEN
  FNON = FT(K,J)
  FD = FNON*FS(K)
ELSE
  FNON = 0.0
  FD = 0.0
ENDIF
WRITE(20,'(1X,I4,1X,F15.6,2X,F20.15,2X,F20.6)')
$           J,T(J),fnon,fd
50 CONTINUE
100 CONTINUE
RETURN
END
C
C*****C
SUBROUTINE FRCBLC(I,PT,EFB)
IMPLICIT REAL*8(A-H, O-Z), INTEGER*4(I-N)
PARAMETER (NL=1001, NS=5, NT=1000)
COMMON /C1/ T(NT),DT,TS,IS,IT,DXI,DTHETA,V0T,VLT,PHI0M
COMMON /C2/ A(NL),R(NL),S(NL),PHI(NL),
$           RPVS(NS,NL),SPVS(NS,NL),APVS(NS,NL)
COMMON /C3/ FT(NS,NT)
COMMON /C4/ VS(NS),ALENG(NS),A00,A0M,A0P,
$           EPS00,EPS0M,SIG00,SIG0M,SIG0P,
$           P,AS0P(NS),FS(NS),PS(NS)
COMMON /C5/ NSPAN,NTIME,NMAX,NSRCH,NBISC,
$           NSTEP,NSHOOT,NFDM
COMMON /C6/ G,PWM,PWN,E,TOLDR,TOLPHI,DES(NS),ANS(NS)
COMMON /C7/ YW(NL,2),RK(4,NL),YV(2),FRK(2)
COMMON /C8/ R1,S1,AA1

```

C

```

IF(I .EQ. 2) THEN
  R1 = R(1)
  S1 = S(1)
  AA1 = A(1)
ENDIF
PHIDRV = (PT-PHI(I-1))/DXI
IF(I .EQ. NMAX) THEN
  RDRV = (RPVS(IS,NMAX)-RPVS(IS,NMAX-1))/DXI
  SDRV = (SPVS(IS,NMAX)-SPVS(IS,NMAX-1))/DXI
  ADRV = (APVS(IS,NMAX)-APVS(IS,NMAX-1))/DXI
ELSE
  RDRV = (RPVS(IS,I+1)-RPVS(IS,I))/DXI
  SDRV = (SPVS(IS,I+1)-SPVS(IS,I))/DXI
  ADRV = (APVS(IS,I+1)-APVS(IS,I))/DXI
ENDIF
W1 = 1.0/(1.0/DTHETA+PHIDRV+DABS(PHIDRV)**(1.0-
PWN)/DES(IS))
W2 = 1.0/(2.0/DTHETA+PHIDRV
$      +DABS(PHIDRV)**(1.0-PWN)/DES(IS))
W3 = ANS(IS)*PHIDRV/DES(IS)
C PREDICTOR FOR TAU XX:
R2 = W1*(RPVS(IS,I)/DTHETA-PT*RDRV-W3)
C CORRECTOR FOR TAUXX:
R(I) = W2*((R2+RPVS(IS,I))/DTHETA-PT*(R2-R1)/DXI-W3)
W1 = 1.0/(1.0/DTHETA-2.0*PHIDRV
$      +DABS(PHIDRV)**(1.0-PWN)/DES(IS))
W2 = 1.0/(2.0/DTHETA-2.0*PHIDRV
$      +DABS(PHIDRV)**(1.0-PWN)/DES(IS))
C PREDICTOR FOR TAU ZZ:
S2 = W1*(SPVS(IS,I)/DTHETA-PT*SDRV+2.0*W3)
C CORRECTOR FOR TAU ZZ:
S(I) = W2*((S2+SPVS(IS,I))/DTHETA
$      -PT*(S2-S1)/DXI+2.0*W3)
C CALCULATE A FROM MASS CONSERVATION:
C PREDICTOR:
AA2 = 1.0/(1.0/DTHETA+PHIDRV)
$      *(APVS(IS,I)/DTHETA-PT*ADRV)
C CORRECTOR:
A(I) = 1.0/(2.0/DTHETA+PHIDRV)
$      *((AA2+APVS(IS,I))/DTHETA
$      -PT*(AA2-AA1)/DXI)
C CHECK IF a(Tzz-Txx) = f ?
EFB = (A(I)*(S(I)-R(I))-FT(IS,IT))/FT(IS,IT)

```

```
C
IF(DABS(EFB) .LE. TOLPHI) THEN
  R1 = R2
  S1 = S2
  AA1 = AA2
ENDIF
C
RETURN
END
```

APPENDIX I

AN EXAMPLE PROBLEM

A solution procedure for a start-up process is illustrated in this appendix. The simulated case is a single-span system with $L = 5$ m, $v_{s1} = 2.250$ m/s, and $v_{s2} = 2.255$ m/s. The entry and initial states are both unstressed. The material properties are listed as below:

$$G = 0.55 \times 10^9 \text{ Pa}, m = 1.65 \times 10^{10} \text{ PaS},$$

$$n = 1, E = 1.65 \times 10^9 \text{ Pa}.$$

The roller tangential velocities were linearly increased from zero to their steady-state values over five seconds. The total time simulated is 16 seconds. The increments for time and space, $\Delta\theta$ and $\Delta\xi$, are 0.045 and 0.05, respectively. The tolerances for both ϕ_1 and ϕ_i were set to be 1×10^{-6} .

By following the instruction in Appendix H, the input file, "wve6.dat", can be generated as:

```
-----wve6.dat-----  
0.55e9, 1.65e10, 1.0, 1.65e9  
1.0e-4, 0.0, 0.0  
1, 160, 21, 50, 50, 5, 60, 100  
2.25, 2.255
```

5.0

16.0, 5.0, 1.0e-6, 1.0e-6

The execution was done on RS6000 using the executable code, wve62, in about 10 minutes. The controlling factor, "Ratio Step (IS)", was set to be 0.02 at the beginning of the unsteady-state computation.

The output file, "wve6.out", is listed as below. The description for the symbols in the output file can be found in Appendix H.

-----wve6.out-----

G,m,n,E =
 .550000000E+09 .165000000E+11 1.00000 .165000000E+10

A00,EPS00,SIG00 =
 .100000000E-03 .000000000E+00 .000000000E+00

NSPAN,NTIME,NMAX,NSRCH,NBISC,NSTEP,NSHOOT,NFDM =
 1 160 21 50 50 5 60 100

VS(IS) =
 1 2.250000000
 2 2.255000000

L(IS) =
 1 5.000000000

Ttotal,Ts,TOLDR,TOLPHI =
 16.000000000 5.000000000 .100000000E-05 .100000000E-05

DT,DXI = .100000000 .050000000

DR(IS) =
 1 1.002222222222222

IS,P= 1 1.002069444

DES(I)=
1 13.500000000

ANS(I)=
1 2174.49664

FS(I)=
1 340.75316

ASOP(I)=
1 .000099793483

SPAN = 1

a	Phi	Txx	Tzz
1.00000386964	1.00206556680	-.33270875699	.66541751398
.99999623629	1.00207344845	-.33270603291	.66542767665
.99998860273	1.00208133017	-.33270337712	.66543793876
.99998096945	1.00208921195	-.33270083172	.66544835749
.99997333878	1.00209709379	-.33269800810	.66545819981
.99996570805	1.00210497569	-.33269536288	.66546833622
.99995807532	1.00211286530	-.33269319314	.66547939963
.99995044651	1.00212074732	-.33269056161	.66548950213
.99994281995	1.00212862941	-.33268775380	.66549918313
.99993519301	1.00213651156	-.33268518022	.66550930209
.99992756689	1.00214439377	-.33268264383	.66551949606
.99991994195	1.00215227605	-.33268010934	.66552968366
.99991231805	1.00216015838	-.33267762724	.66553993098
.99990469547	1.00216804078	-.33267516009	.66555014866
.99989707464	1.00217592324	-.33267263422	.66556021484
.99988945544	1.00218380576	-.33267006955	.66557020392
.99988183662	1.00219168835	-.33266766926	.66558053547
.99987421967	1.00219957099	-.33266523042	.66559078201
.99986660521	1.00220745370	-.33266268799	.66560078613
.99985899346	1.00221533647	-.33266000878	.66561047280
.99985138248	1.00222321930	-.33265752170	.66562052058

SPAN = 1

No.	Time	Tension (N-D)	Tension (D)
1	.100000	.000964037680396	.328499
2	.200000	.002885538386188	.983256
3	.300000	.005757361759988	1.961839
4	.400000	.009566486680851	3.259811
5	.500000	.014294995587837	4.871065
6	.600000	.019933444689306	6.792384

7	.700000	.026460075554364	9.016354
8	.800000	.033853276089448	11.535611
9	.900000	.042091056176905	14.342661
10	1.000000	.051140133576479	17.426162
11	1.100000	.060988957569664	20.782180
12	1.200000	.071593111169883	24.395579
13	1.300000	.082929089112996	28.258349
14	1.400000	.094975259791373	32.363120
15	1.500000	.107691630283712	36.696264
16	1.600000	.121032440059620	41.242187
17	1.700000	.134981451564769	45.995357
18	1.800000	.149481701640989	50.936363
19	1.900000	.164518537249411	56.060212
20	2.000000	.180046132865865	61.351289
21	2.100000	.196022499125377	66.795287
22	2.200000	.212412111017261	72.380099
23	2.300000	.229162806190463	78.087951
24	2.400000	.246259185240264	83.913596
25	2.500000	.263651901470147	89.840220
26	2.600000	.281289321815626	95.850226
27	2.700000	.299165872134782	101.941717
28	2.800000	.317203027448654	108.087935
29	2.900000	.335390904993051	114.285512
30	3.000000	.353704221646196	120.525833
31	3.100000	.372074982089681	126.785727
32	3.200000	.390502623572286	133.065004
33	3.300000	.408938976369308	139.347250
34	3.400000	.427323770764927	145.611927
35	3.500000	.445674584536576	151.865025
36	3.600000	.463916483203514	158.081009
37	3.700000	.482045809621382	164.258635
38	3.800000	.500051180465464	170.394022
39	3.900000	.517866834278797	176.464762
40	4.000000	.535482823274815	182.467466
41	4.100000	.552890599782596	188.399221
42	4.200000	.570085761110858	194.258527
43	4.300000	.587017441552609	200.028050
44	4.400000	.603672849142959	205.703433
45	4.500000	.620033375353641	211.278334
46	4.600000	.636059907506463	216.739426
47	4.700000	.651753985091623	222.087232
48	4.800000	.667142098493928	227.330781
49	4.900000	.682160753102183	232.448435
50	5.000000	.696844374961658	237.451925

51	5.100000	.710824136029821	242.215573
52	5.200000	.724162420774536	246.760636
53	5.300000	.736903440828575	251.102179
54	5.400000	.749029822401479	255.234282
55	5.500000	.760625279882228	259.185470
56	5.600000	.771687895463468	262.955092
57	5.700000	.782236201333646	266.549460
58	5.800000	.792299984262241	269.978726
59	5.900000	.801895075585907	273.248284
60	6.000000	.811016948903818	276.356591
61	6.100000	.819751181661714	279.332809
62	6.200000	.828058191777213	282.163448
63	6.300000	.835978124083370	284.862190
64	6.400000	.843529750104055	287.435431
65	6.500000	.850729247999306	289.888683
66	6.600000	.857597378335979	292.229020
67	6.700000	.864183395758970	294.473226
68	6.800000	.870462018764134	296.612687
69	6.900000	.876449728228733	298.653018
70	7.000000	.882155097065188	300.597140
71	7.100000	.887571357253270	302.442748
72	7.200000	.892738065997250	304.203320
73	7.300000	.897683199113608	305.888390
74	7.400000	.902409060816770	307.498742
75	7.500000	.906918375907740	309.035306
76	7.600000	.911217928883387	310.500392
77	7.700000	.915328224574947	311.900988
78	7.800000	.919210682707606	313.223948
79	7.900000	.922952305479675	314.498918
80	8.000000	.926512840670504	315.712182
81	8.100000	.929913883611876	316.871098
82	8.200000	.933128406124181	317.966456
83	8.300000	.936192912635112	319.010697
84	8.400000	.939146875708833	320.017269
85	8.500000	.941933897203706	320.966955
86	8.600000	.944600639585029	321.875656
87	8.700000	.947167888185578	322.750454
88	8.800000	.949612933007652	323.583611
89	8.900000	.951939148681306	324.376276
90	9.000000	.954159636587821	325.132915
91	9.100000	.956248840962252	325.844818
92	9.200000	.958271450605845	326.534028
93	9.300000	.960169620941832	327.180836
94	9.400000	.962009966041575	327.807939

95	9.500000	.963734194072352	328.395475
96	9.600000	.965384348629256	328.957771
97	9.700000	.966982159574580	329.502230
98	9.800000	.968516200401008	330.024959
99	9.900000	.969944044341862	330.511502
100	10.000000	.971337552627003	330.986344
101	10.100000	.972669014956684	331.440044
102	10.200000	.973930927667507	331.870045
103	10.300000	.975114490401523	332.273347
104	10.400000	.976232345777157	332.654260
105	10.500000	.977302219202291	333.018823
106	10.600000	.978329225421814	333.368779
107	10.700000	.979301849792012	333.700203
108	10.800000	.980261464508569	334.027195
109	10.900000	.981175049905112	334.338502
110	11.000000	.982053198389934	334.637734
111	11.100000	.982888568227358	334.922389
112	11.200000	.983655577207819	335.183750
113	11.300000	.984419378441258	335.444018
114	11.400000	.985118546102146	335.682261
115	11.500000	.985776691372482	335.906526
116	11.600000	.986434875335227	336.130804
117	11.700000	.987064756201609	336.345438
118	11.800000	.987665877775508	336.550272
119	11.900000	.988211154178148	336.736077
120	12.000000	.988732104366407	336.913593
121	12.100000	.989252754785609	337.091006
122	12.200000	.989724596533404	337.251787
123	12.300000	.990172495711414	337.404410
124	12.400000	.990598289882118	337.549501
125	12.500000	.991004121017893	337.687789
126	12.600000	.991428732913952	337.832477
127	12.700000	.991829780883639	337.969136
128	12.800000	.992206262079940	338.097423
129	12.900000	.992537834812079	338.210407
130	13.000000	.992889678634671	338.330299
131	13.100000	.993192446191170	338.433468
132	13.200000	.993484192335011	338.532882
133	13.300000	.993793084128814	338.638137
134	13.400000	.994048014453535	338.725006
135	13.500000	.994322695545015	338.818604
136	13.600000	.994591141184036	338.910078
137	13.700000	.994819269340581	338.987813
138	13.800000	.995059830502271	339.069785

139	13.900000	.995257739780850	339.137223
140	14.000000	.995454954340102	339.204425
141	14.100000	.995669592395014	339.277564
142	14.200000	.995874315083122	339.347323
143	14.300000	.996064959339045	339.412286
144	14.400000	.996246533623501	339.474158
145	14.500000	.996394071282445	339.524432
146	14.600000	.996538210435266	339.573548
147	14.700000	.996673151295946	339.619529
148	14.800000	.996827138517214	339.672001
149	14.900000	.996975196198090	339.722452
150	15.000000	.997119335004228	339.771568
151	15.100000	.997225416038669	339.807715
152	15.200000	.997333289770847	339.844474
153	15.300000	.997435328555546	339.879244
154	15.400000	.997556983780669	339.920698
155	15.500000	.997672139414622	339.959938
156	15.600000	.997748977334258	339.986120
157	15.700000	.997853662327407	340.021792
158	15.800000	.997959073824787	340.057712
159	15.900000	.998029026906794	340.081548
160	16.000000	.998130103627435	340.115990

VITA

Xiaofeng Guan

Candidate for the Degree of

Doctor of Philosophy

Thesis: MODELING OF VISCOELASTIC EFFECTS
ON WEB HANDLING SYSTEM BEHAVIOR

Major Field: Chemical Engineering

Biographical:

Personal Data: Born in Shenyang, Liaoning, the People's Republic of China (PRC), on October 28, 1957, the son of Zuo Guan and Shuhua Wang.

Education: Graduated from the Seventh High School, Dalian, Liaoning, PRC in July 1975; received Bachelor of Science degree in Chemical Engineering Machinery from Dalian University of Technology, Dalian, PRC in January 1982; received Master of Science degree in Chemical Engineering Machinery from Dalian University of Technology in December 1984; completed the requirements for the Doctor of Philosophy degree at Oklahoma State University in May 1995.

Experience: Employed as a full-time teaching assistant, assistant professor by Dalian University of Technology, PRC, 1984 to 1991; employed as a research assistant by Oklahoma State University, School of Chemical Engineering, January 1992 to present.

Professional Membership: American Institute of Chemical Engineers.